The Impact of Macrophage Inflammatory Protein-3 Alpha and Other Innate Immune Markers on Susceptibility/Resistance to HIV Infection in the Female Genital Tract Mucosa using Cellular and *Ex Vivo* Tissue Models

Student Details:

Dr Sengeziwe Sibeko

Wolfson College

University of Oxford

Research Supervisors:

Professor Sarah Rowland-Jones

Professor Robin Shattock

A thesis submitted for the degree of

Doctor of Philosophy

Michaelmas 2016

This thesis is submitted to the Nuffield Department of Clinical Medicine, University of Oxford, in partial fulfilment of the requirements for the degree of Doctor of Philosophy.

This thesis is entirely my own work, and except where otherwise stated, describes my own research.

ABSTRACT

The distinctive feature of the Human Immunodeficiency Virus (HIV) epidemic in the 21st century is the burden it places on women. Scientists believe that the best opportunities for successful interventions to prevent sexual HIV transmission lie in the initial stages of infection at the portal of entry, the genital tract (GT), which offers the greatest host advantages and viral vulnerabilities. However, understanding of the correlates of protection/vulnerability and innate immunity at the portal of entry is poor. First and foremost, there is no agreement about which GT sub-compartment is the primary site of HIV/SIV infection. Second, the epithelium, previously studied solely for its function as a barrier, has hardly been investigated for its role in innate immunity in the context of SIV/HIV infection. MIP-3α, a chemokine secreted by epithelial cells, was previously proposed to have a role in amplifying the early Simian Immunodeficiency Virus (SIV) infection events in the GT of female macaques. Specifically, MIP-3α was shown to be secreted by epithelial cells of the endocervix, accumulating subepithelially within the first 24 hours post exposure, following deposition of an intravaginal inoculum of SIV. Similar studies in humans have not been reported. We hence undertook to study MIP-3α for its role in early HIV infection events in the endocervix of humans. In order to achieve this, we first characterised MIP-3α constitutive secretion patterns in different sub-compartments of the GT before proceeding to determine its induced secretion patterns, stimulating with HIV-1 and various Toll-like receptor ligands. For completeness we determined constitutive and induced secretion patterns of multiple soluble proteins (SPs) and antimicrobial peptides (AMPs) in the endocervices of humans and macaques**.** The GT being an immunohormonal system, we further studied the influence of endogenous hormonal changes on the stability of MIP-3α and that of other innate immune markers. We quantified MIP-3α with a sandwich Elisa, and SPs and AMPs with the Luminex multiplex bead assay. Our results showed that the GT is a rich source of MIP-3α with its levels being among those of the highest SPs in the GT. Constitutive levels were highest in the endocervical sub-compartment of all the sub-compartments studied. Further, the GT is an inflammatory environment, which would explain the high levels of MIP-3α. The primary driver of MIP-3α levels appears to be inflammation rather than hormonal levels. MIP-3α levels are significantly higher in the GT of humans than in macaques. There was no evidence that MIP-3α levels are elevated on exposure to HIV and SIV in humans and macaques, respectively. We therefore concluded that since the endocervix is unlikely to respond to HIV/SIV by secreting MIP-3α *in vivo*, contrary to the previous reports, MIP-3α is hence not a key player in amplifying early events in infection. And as such, it should not be a prime target for preventive therapy. Further, the human GT having a pre-existing inflammatory profile may explain the high rates of HIV sexual transmission. Lastly, we concluded that the infection mechanisms described in the macaque model (i.e. the 'outside-in' signaling) are likely not required for human infection.

ACKNOWLEDGEMENTS

First and foremost, my appreciation goes to the Almighty Lord, the Alpha and the Omega of my life, without whom none of this would have happened. Thank you Lord for being there, providing and seeing me through the course of this DPhil.

To my supervisor Professor Robin Shattock at the Imperial College London: I am absolutely grateful for your generosity of heart and spirit. Thank you for giving me a chance. I don't know many who would have taken me on at the stage at which you did. Thank you for many hours dedicated to this project. It has been an honour to be your student these past years.

To my supervisor Professor Sarah Rowland-Jones at the University of Oxford: thank you for your reassurance, enthusiasm for my project, and your commitment to seeing me through. I wouldn't have come to the University of Oxford if you had not given me a chance in the first instance.

To my mentor Professor Bongani Mayosi at the University of Cape Town (UCT): thank you for your prayers, for believing in me and standing with me amid all the hardships I have experienced over the past few years. University of Oxford would not have even been a possibility without your guidance and your support.

To Professors Slim and Quarraisha Abdool Karim, Jack Moodley, Malegapuru Makgoba, Thandinkosi Madiba and the late Alan Berkman: you prepared me well for the journey ahead. I salute you and thank you.

To Professor Stephen Kennedy, Head of the Nuffield Department of Obstetrics and Gynecology: thank you for seeing me from the starting point to the finishing line. I would not have had any specimens to carry out this work without your support. I smile on the benefit of the doubt that you have afforded me.

To Professor Richard Cornall, the former DGS in the Nuffield Department of Medicine at the University of Oxford: my warm appreciation goes to you for ensuring that I accomplish the mission at hand. I bow to you for giving me a start.

To Dr Julia Makinde, my laboratory supervisor at the Imperial College London: you worked with me when my laboratory skills were zero. You took me from nowhere to where I am at today. Thank you for your kindness and patience.

To the many great colleagues I have walked and worked with over the years: Professors Koleka Mlisana and Thumbi N'dungu from UKZN, Professors Ntobeko Ntusi and Jo-Ann Passmore from UCT, thank you for inspiration and support.

To my College (Wolfson) at the University of Oxford: you were there for me when I was at my weakest point. Thank you for your immense support.

To the Trustees of the Nuffield Dominions Trust: thank you for giving me a first and a second chance. You showed faith in me by generously giving me much-needed extra support at the most difficult of times.

I would not have been able to take time off work, study full-time, and pursue my academic goals without generous financial support from the Oppenheimer Memorial Trust, the South African Medical Research Council, the Discovery Foundation, the Nuffield Department of Medicine, the HIV Research Trust, the British HIV Association, Professor Sarah Rowland-Jones and her sponsors.

Dr Carolina Herrera, Dr Jamie Mann, Dr Suzanne Campion, Dr Carolina Arancibia, Dr Agnes Gwela, Dr Sunanda Dhar, and Dr Ane Ogbe: I am full of gratitude to you for giving me a kick-start when I terribly needed one.

To faculty at Imperial College London, Mucosal Infection and Immunity unit: Dr Alethea Cope, Dr Jacqueline McDonald, Natalia Olejniczak, Yoann Aldeon, Abbey Evans, Guillermo Barinaga, Sven Kratochvil, and Hephzibah Akpovwa: your support has not gone without notice, thank you for accommodating me.

Group members of the Viral Immunology laboratory at the University of Oxford: Drs Louis-Marie Yindom, Sophie Andrews, Katherine James, Glenn Wong and Shmona Simpson: I bow down to you for your love and support.

To the many dedicated prayer warriors who have committed many hours of intercession to see me through this DPhil: my sister Morapedi Sibeko, my mother Ivy Sibeko, my dad Eric Sibeko, my sister Lindani Mufhadi, my sister Evangelist Lindiwe Mbebe, my church leader Monica Webley, Angela Webley, Xoliswa Dangala, Sis Thandi, Bagcinile Xulu, Joyce Mpundu, Nokuthula Bavu, Zandile Ndimande, Wilfride Kamdoum, Laura Riach, Stephanie, Karl, Illyas, Kristina, Mathilda, Hyacinth, Julian, Lydia, Sandra, Ashley, Emilie and the ECC Gloucester ladies, thank you for love and for standing in the gap. To God be all Glory.

To the ministers of the word and their churches who have supported me in this challenging period: Apostle LV Mahlangu of KEI, Pastor Chim of CAPRO, Pastor K and Mrs Masuku of GOH, Apostle V and Pastor K Loate of ECC, Pastor B and Mrs M Mwaisoloka and Rev M Munyaneza: thank you. May God richly reward you.

To Kareni, Mashiko, Des and Valli: deep appreciation for your warm friendship.
To all women participating in my research projects: a big thank you to you.

PUBLICATIONS

i. Ngcapu S, Masson L, **Sibeko S**, Lise Werner L, McKinnon LR, Mlisana K, Shey M, Natasha Samsunder N, Salim Abdool Karima S, Abdool Karim Q, Passmore JS: Lower concentrations of chemotactic cytokines and soluble innate factors in the lower female genital tract associated with the use of injectable hormonal contraceptive: Journal of Reproductive Immunology, Volume 110, pg14-21, August 2015

ii. Rafferty H, **Sibeko S**, Rowland-Jones S. How can we design better vaccines to prevent HIV infection in women? Frontiers in Microbiology, Volume 5, Article 572, pg 1-10, November 2014

iii. **Sibeko S,** Makvandi-Nejad S: From laboratory sciences to clinical trials and back again: lessons from HIV prevention trials. American Journal of Reproductive Immunology, Volume 28, Supplement 1, pg 106-115, February 2013

CONFERENCE PROCEEDINGS

i. **S Sibeko,** J Makinde, C Herrera, N Olejniczak, Y Aldonn, A Evans, C Jones, S Rowland-Jones, R Shattock: Understanding HIV-1 epithelial responses in the human female genital tract: the endocervical epithelium demonstrates differential signatures in response to TLR ligands and HIV-1 constructs. Poster presentation at the Early Career Scientist South African Medical Research Council Conference held in Cape Town, South Africa on 19 to 20 October 2016

ii. **Sibeko S,** Makinde J, Rowland-Jones S, and Shattock R: HIV-1 constructs do not trigger macrophage inflammatory protein - 3 alpha secretion in human genital epithelial cell models: Poster presentation at the 21st AIDS International Conference held in Durban, South Africa on 18 to 22 July 2016. Abstract # TUPEA018

iii. **Sibeko S,** Makinde J, Rowland-Jones S, and Shattock R: MIP-3α is detectable constitutively in female genital tract tissues; however, endogenous hormonal fluctuations do not impact on its levels. Oral presentation at the HIV and Women Workshop 2016 held on 20 to 21 February in Boston, Masachussettes. Abstract #14

iv. **Sibeko S,** Makinde J, Jones C, Rowland-Jones S, and Shattock R: From clinical trials to laboratory sciences: does timing of specimen collection in relation to the menstrual cycle affect innate immune markers? Guided tour poster presentation at the HIV and Women Workshop 2015 in Seattle held on 21 to 22 February. Abstract #19

v. **Sibeko S,** Makinde J, Rowland-Jones S, Shattock R: Constitutive MIP-3α levels in five matrices of the female genital tract (FGT). Oral presentation at the Mucosal Surfaces Workshop in Cape Town, South Africa on 21 to 24 January 2015

TABLE OF CONTENTS

ABSTRACT III
PUBLICATIONS VI
CONFERENCE PROCEEDINGS VI
TABLE OF CONTENTS VII
LIST OF ABBREVIATIONS X

CHAPTER ONE 1

INTRODUCTION and BACKGROUND 1

SECTION 1: HUMAN IMMUNODEFICIENCY VIRUS INFECTION 1
What is HIV: 1
Structure of HIV: 5
Lifecycle of HIV: 7
Epidemiology of HIV infection: 9
Epidemiology of HIV infection in women: 13
Why focus on women: 14
SECTION 2: BIOLOGY OF FEMALE GENITAL TRACT IN THE CONTEXT OF HIV INFECTION 15
Anatomy and structure of the FGT: 15
Structure of the FGT endocrine system: 17
Structure of the FGT immune system: 18
"Window" of HIV infection: 21
SECTION 3: MUCOSAL HIV TRANSMISSION 22
SECTION 4: FGT EPITHELIUM IN HIV INFECTION 23
SECTION 5: MACROPHAGE INFLAMMATORY PROTEIN 3 ALPHA 28
SECTION 6: HYPOTHESES AND STUDY AIMS 30
Research questions: 31
Research aims: 31
Specific aim 1: 32
Specific aim 2: 32
Specific aim 3: 33
Specific aim 4: 33
Specific aim 5: 34

CHAPTER TWO 36

MATERIALS and METHODS 36

STUDY DESIGN: 36
COLLECTION OF SAMPLES: 38
Human genital tract tissues: 38
Macaque genital tract tissues: 39
Cervicovaginal fluid: 39
CELLULAR BIOLOGY AND TISSUE CULTURE: 40
Epithelial models: 40
CELL STAINING: SURFACE AND INTRACELLULAR MARKERS: 45
IMMUNOSTIMULANTS: 47
IMMUNOASSAYS: 48
Sandwich MIP-3α Elisa: 48
Luminex multiplex bead assay: 49
Flow cytometry: 52
MOLECULAR BIOLOGICAL TECHNIQUES: 53

SIV preparations: *53*
HIV-1 preparations: *53*
DATA MANAGEMENT and STATISTICAL ANALYSES: **56**

CHAPTER THREE **58**

CONSTITUTIVE BASELINE EXPRESSION OF MIP-3α IN SIX BIOLOGICAL MATRICES **58**

SUMMARY 58
INTRODUCTION 60
MATERIALS and METHODS 63
RESULTS 76
DISCUSSION 86
CONCLUSION 92

CHAPTER FOUR **93**

STIMULATED LEVELS OF MIP-3α, STIMULATING WITH ENVELOPE AND NON ENVELOPE HIV-1 PREPARATIONS **93**

SUMMARY 93
INTRODUCTION 95
MATERIALS and METHODS 98
RESULTS 108
DISCUSSION 125
CONCLUSION 132

CHAPTER FIVE **133**

MIP-3α IN THE CONTEXT OF OTHER SOLUBLE MARKERS AND ANTIMICROBIAL PEPTIDES IN THE HUMAN FEMALE GENITAL TRACT **133**

SUMMARY 133
INTRODUCTION 135
MATERIALS and METHODS 140
RESULTS 145
DISCUSSION 159
CONCLUSION 166

CHAPTER SIX **167**

INTERPLAY BETWEEN ENDOCRINE AND IMMUNE SYSTEMS: IMPACT OF CHANGES IN MENSTRUAL CYCLE PHASES ON LEVELS OF MIP-3α AND OTHER SOLUBLE MARKERS **167**

SUMMARY 167
INTRODUCTION 169
MATERIALS and METHODS 173
RESULTS 181
DISCUSSION 205
CONCLUSION 212

CHAPTER SEVEN **214**

MIP-3α RESPONSES IN THE ENDOCERVIX OF MACAQUES **214**

SUMMARY 214

INTRODUCTION 215
MATERIALS and METHODS 220
RESULTS 225
DISCUSSION 240
CONCLUSION 247

CHAPTER EIGHT 248

DISCUSSION and SUMMARY 248

SECTION A: THESIS BACKGROUND CONCEPTS 249
SECTION B: BACKGROUND RESEARCH AND CONCEPTS THIS THESIS HAS BUILT UPON 253
SECTION C: EXPERIMENTAL METHOD CONCEPTS 256
SECTION D: CONTEXT OF RESULTS AND THEMES THAT EMERGED FROM THIS THESIS 264
SECTION E: LIMITATIONS AND FUTURE PERSPECTIVES 270

REFERENCES 272

LIST OF ABBREVIATIONS

AIDS	Acquired immunodeficiency syndrome
AMPs	Antimicrobial peptides
ART	Antiretroviral therapy
CCL20	CC chemokine ligand 20
CM	Cynomolgus macaque
CSPG	Chondroitin sulphate proteoglycan
CVF	Cervocivaginal fluid
CVL	Cervicovaginal lavage
DC-SIGN	Dendritic cell-specific ICAM-grabbing non-integrin
DC-SIGNR	DC-SIGN related
DMPA	Depot medroxyprogesterone acetate
DNA	Deoxyribonucleic acid
ECET	Ectocervical explant tissue
ET	Explant tissue
ECL	Epithelial cell line
EET	Endocervical explant tissue
EMPECs	Endometrial primary epithelial cells
EPECs	Endocervical primary epithelial cells
FACS	Fluorescence-activated cell sorting
FGT	Female genital tract
G-CSF	Granulocyte-colony stimulating factor three
GalCer	Galactosylceramide
GI	Gastrointestinal
GIT	Gastrointestinal tract
GML	Glycerol monolaurate
GM-CSF	Granulocyte-macrophage colony-stimulating factor
gp	Glycoprotein
HBD	Human beta defensin
HDV	High dose virus
HIV	Human immunodeficiency virus
HNP	Human neutrophil peptides
HSPG	Heparan sulphate proteoglycans
ICAM-1	Intercellular adhesion molecule 1
IL	Interleukin
HTLV	Human T-lymphotropic virus
IFN	Interferon
IP-10	Interferon gamma-induced protein 10

K-SFM	Keratinocyte-serum free medium
LARC	Liver- and activation- regulated chemokine
LDV	Low dose virus
LGT	Lower genital tract
LPS	Lipopolysaccharide
LFA-1	Lymphocyte function-associated antigen 1
MIP-1β	Macrophage inflammatory protein 1 beta
MIP-3α	Macrophage inflammatory protein 3 alpha
MCP	Monocyte chemotactic protein 1
MIG	Monokine induced by gamma-interferon
NHP	Non-human primate
OD	Optical density
PIC	Poly I:C
PM	Pigtail macaque
PrEP	Pre-exposure prophylaxis
PRR	Pattern recognition receptor
RANTES	Regulated on activation, normal T cell expressed and secreted
RNA	Ribonucleic acid
RM	Rhesus macaque
RT	Reverse transcriptase
SDF-1β	Stromal cell-derived factor 1 beta
SHIV	Simian–human immunodeficiency virus
SIV	Simian immunodeficiency virus
SIVcpz	SIVs from chimpanzees (SIVcpz)
SIVmac	SIV from macaques
SIVsm	SIVs from Sooty Mangabees
SLPI	Secretory leukocyte protease inhibitor
SP	Seminal plasma
SPs	Soluble proteins
Th	T helper
TLR	Toll-like receptor
TNF-α	Tissue necrosis factor alpha
TGF-β	Transforming growth factor beta
UGT	Upper genital tract
UNAIDS	Joint United Nations Programme on HIV/AIDS
VLPs	Virus-like particles
WHO	World Health Organisation

CHAPTER ONE INTRODUCTION and BACKGROUND

SECTION 1: HUMAN IMMUNODEFICIENCY VIRUS INFECTION

What is HIV:

HIV is an acronym for Human Immunodeficiency Virus. It was first discovered in 1983 by French investigators at the Pasteur Institute in Paris following investigation of tissues from a Caucasian patient presenting with signs and symptoms that often precede the acquired immune deficiency syndrome (AIDS) [11]. This was after a task force had been set up in the United States of America (US) to undertake surveillance and investigate the escalating number of cases of immune deficiency in various countries since June 1981 [12].

HIV is a ribonucleic acid (RNA) virus belonging to the family of retroviruses. Retroviruses are a type of RNA virus that contain the enzyme reverse transcriptase (RT), which allows their genetic information to be transcribed first into deoxyribonucleic acid (DNA) rather than the other way around, thereby going against conventional viral transcription processes. Retroviruses have a genome consisting of two identical copies of single positive-strand RNA molecules from which they code for DNA. They are approximately 100 nanometres (nm) in diameter. Retroviruses form by budding off of the cell membrane of host cells and thus have an outer covering called the envelope. They are hence described as enveloped viruses. Further, retroviruses are categorised into exogenous and endogenous based on whether they are transmitted horizontally or vertically. Endogenous retroviruses are transmitted vertically through the germ-line and represent footprints of previous retroviral infection while the exogenous subclass of

retroviruses consists of infectious RNA-containing viruses horizontally-transmitted from human-to-human. HIV is categorised as an exogenous retrovirus.
In man, there are at least three exogenous retroviruses, each associated with disease: (i) Human T-lymphotropic virus type-1 (HTLV-1) which is associated with adult T-cell leukemia and tropical spastic paraparesis; (ii) HTLV-2 which is associated with hairy cell leukemia; and (iii) HIV which is associated with AIDS.

Retroviruses were originally classified into three subfamilies including the oncoviruses, lentiviruses, spumaviruses, even though nowadays they are classified into various classes comprising at least seven genera. HIV is a human retrovirus of the lentivirus genus. Infections with lentiviruses typically show a chronic course of disease, a long period of clinical latency, persistent viral replication and involvement of the central nervous system, and they affect both man and mammals. The primate lentiviruses, of which HIV is one, are distinguished by the use of the CD4 protein as a receptor.

HIV has two major antigenic types: HIV-1 and HIV-2, even though most people typically refer to HIV-1 in the context of HIV, as it is far more prevalent and more pathogenic. HIV-1 and HIV-2 are very similar and share many traits including mode of transmission, genomic organisation, pathological processes and the development into AIDS. However, they differ in their zoonotic origins and epidemiology, and demonstrate genetic diversity, particularly in their *env* genes. HIV-1 and HIV-2 are thought to have originated from zoonotic transmissions of simian immunodeficiency virus (SIV)-infected non-human primates (NHP) [13, 14]. SIVs from chimpanzees (SIVcpz) cluster phylogenetically with HIV-1 [13] and hence, the HIV-1 epidemic is thought likely to have originated from chimpanzees.

On the other hand, HIV-2 is a zoonosis from the sooty mangabey and hence HIV-2 and SIVsm (SIV from sooty mangabeys) have similar genomic organisation, geographical overlap and demonstrate phylogenetic relatedness [15, 16].

HIV-1 infection, the epicentre of which was once thought to be in East Africa, extends worldwide while HIV-2 is restricted primarily to West Africa. Although human HIV-1 infection is responsible for most of the global AIDS pandemic, HIV-2 is an important cause of disease in a number of regions of the world. HIV-2 was first described in a Senegalese cohort in 1985 [17] and was isolated from West African patients in Guinea-Bissau and Cape Verde in 1986 [18], where it remains endemic although prevalence is declining. HIV-1 on the other hand was first discovered in the Unites States in 1981 [19-21] and subsequently isolated in 1983 [11].

The genomic organization of HIV-1, HIV-2, and SIV is similar and all three of them comprise the subgenus ‘lentiviruses’. HIV-1 and SIVcpz encode a vpu gene, while HIV-2 and SIVsm have a vpx gene in its place. They are also largely distinguishable by antibody reactivity to envelope glycoproteins. There is a high degree of genetic diversity between their *env* genes. However, major differences include reduced pathogenicity of HIV-2 relative to HIV-1, enhanced immune control of HIV-2 infection and some degree of CD4-independence for many HIV-2 isolates. For the purposes of this thesis, we have only studied HIV-1 and hence from this point forward we will discuss only HIV-1.

Each HIV type is divided into groups, and each group is divided into sub-types and circulating recombinant forms (CRFs). HIV-1 is further classified into four groups:

M (the major group), N (the new group), O (the outlier group), and P. These three groups may represent three separate introductions of SIV into humans. More than 90% of HIV-1 infections belong to HIV-1 group M. Group O appears to be restricted to west-central Africa and group N, discovered in 1998 in Cameroon, is extremely rare. Within group M, based on nucleotide sequence analyses of the *env* and gag genes, there are known to be at least nine genetically distinct sub-types of HIV-1, namely sub-types A, B, C, D, F, G, H, J and K. The major one in North America, Latin America and the Caribbean, Europe, Japan and Australia is sub-type B. Most sub-types are found in sub-Saharan Africa, with A and D found at the highest rates in central and eastern Africa and C in southern Africa. Type C is also the predominant form in India and Nepal, and this sub-type has caused the most infections worldwide. Type E, now renamed CRF01 AE, is found in Thailand and central Africa, type F in Brazil and Romania, type G in Russia and Gabon, while type H is found in Zaire and in Cameroon. Sub-type K is found in the Congo and Cameroon. Sub-type I was a name given to an apparent sub-type found in Cyprus but the name is no longer used. This former sub-type I is a CRF that is a recombinant of sub-types A, G, H and K.

There is some evidence from laboratory studies that different HIV-1 sub-types can be transmitted by different routes. For example, sub-type B found in western countries, may be transmitted more effectively by homosexual intercourse and via blood (as in intra-venous drug use) whereas types C and E may be transmitted more efficiently via the heterosexual route [22]. This could be because sub-types C and E replicate better in Langerhans' cells found in the mucosa of the cervix, vagina and penis while sub-type B replicates better in the rectal mucosa. It also appears that sub-type E is more readily transmitted between sexual partners than

type B. Sub-type D seems to be more virulent than sub-type A, and as such infected persons progress to overt disease more rapidly. In addition sub-types D and C seem to be transmitted more effectively from mother to child than sub-type A. In this thesis we have made use of group M viruses mostly of the C sub-type, and BaL, which is clade B.

Structure of HIV:

HIV is a roughly spherical virus of around 120 nm in diameter that consists of a cylindrically shaped nucleoid enclosed in a lipid (fatty) envelope. It essentially comprises two main parts: the viral membrane and the inner core (*Figure 1.1*). The viral membrane encloses the particle, and has about nine or ten gp160 spikes (viral envelope glycoproteins, gp) embedded in it, which are involved in binding and membrane fusion when the virus particle attaches to a cell. The envelope protein is found on the surface of the virus particle. It has two parts: gp120 (surface glycoprotein) and gp41 (transmembrane glycoprotein). gp120 is the cap-like structure found outside the virus particle; it is the first part to make contact with receptors on the target cell. gp41 spans the viral membrane, anchors the gp120 in place, and causes the fusion of virus and cell membranes during the entry stage of infection. A thin bi-layer of fatty material, the viral membrane, encloses the contents of the virus particle, the inner viral core. The matrix is a layer beneath the viral membrane that consists of the protein p17, protease and p6. Protease is an enzyme that cuts long strands of HIV protein into the smaller components that make up the mature virus particle. P6 is a small viral protein that recruits host cell proteins that pinch off the viral bud. The capsid is the cone-shaped core of the virus, which consists of the protein p24. The capsid contains the genetic

information and enzymes needed for the virus to replicate. Encased within the capsid are nucleocapsid, reverse transcriptase and viral RNA. The nucleocapsid is a protein found within the capsid that coats the viral RNA. Integrase is an enzyme found within the capsid that causes the viral DNA to integrate, or insert, into the DNA of the host cell. Finally, RT is an enzyme found within the capsid that is needed to make viral DNA by copying the sequence of the viral RNA.

The inner core consists essentially of three genes: *env* for the viral envelope protein, *gag* for the RNA-containing core, and *pol* for the viral enzymes protease, reverse transcriptase, and RNase H. Other genes code for small proteins that are involved in the regulation of gene expression. The genetic material of HIV, a retrovirus, takes the form of RNA rather than the DNA (deoxyribonucleic acid) of human cells. In order for HIV to replicate, its enzyme reverse transcriptase, which consists of polymerase and ribonuclease, must first produce a DNA version using the RNA as a template. In this stepwise process the polymerase transcribes the viral genome into DNA, the ribonuclease digests the original RNA strand, and the polymerase produces a complementary strand of DNA. The viral DNA produced in this way now migrates to the nucleus of the host cell and is inserted into the human genome with the aid of the enzyme integrase. Subsequently it is replicated with each cell division. Capsids form around the viral genomes and proteins before they are budded from the cell membrane, further encapsulating the material into envelopes.

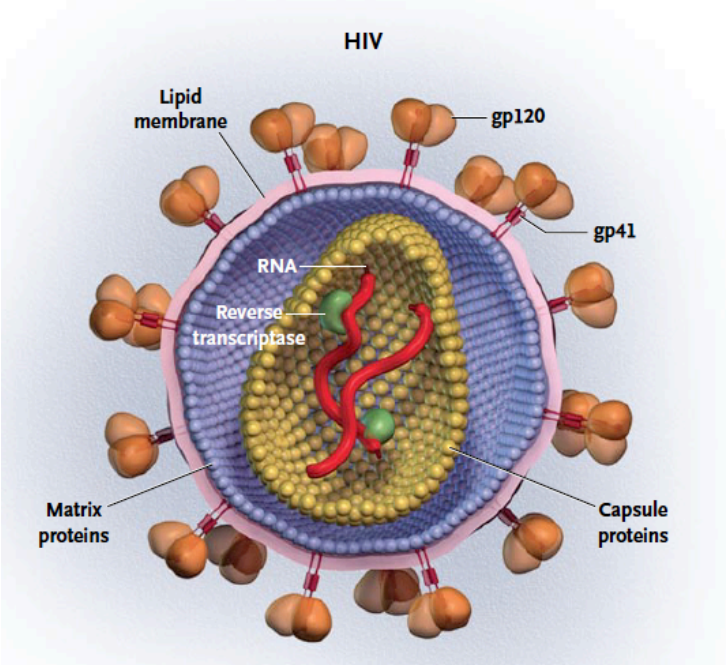

Figure 1.1: Structure of HIV. Source: [7]

Lifecycle of HIV:

The HIV-1 replication cycle can be divided into an early and a late phase. The early phase encompasses the events that occur from virus binding to the surface of the host cell until the integration of the viral DNA into the host cell genome. These early events include virus binding to cell surface receptors; fusion of virus membrane to host cell membrane, cell entry; reverse transcription of the viral RNA to DNA; uncoating of the viral capsid; nuclear import of viral DNA; and DNA integration.

Binding: Binding of HIV to CD4+ cells begins when trimeric gp120 interacts with the host cell CD4+ receptors and either CCR5 or CXCR4 receptors. Gp120 binds to the CCR5 or CXCR4 co-receptors causing conformational changes to gp120, exposing the hydrophobic N-terminal fusion peptide of gp41, and then inserts itself

into the target cell membrane.

Fusion: The extraviral portion of gp41contains triple heptad repeats 1 and 2, which bind to each other, causing gp41 to fold in a hairpin configuration, drawing the viral and host-cell membranes together and promoting fusion and virus entry into the host cell. Nucleocapsid core proteins are removed, releasing the viral genome and enzymes into the host cell's cytoplasm.

Reverse transcription: RT transcribes viral RNA into single-strand DNA. The single-strand DNA complement is then synthesised by RT to form double-strand viral DNA.

Integration: HIV integrase cleaves two terminal nucleotides off each viral DNA copy in a process called 3'-processing. Integrase DNA complex is transported into the host-cell nucleus, where integrase catalyses the insertion of viral DNA into the host genome, forming provirus.

The late phase refers to the events that occur from gene expression to the release and maturation of new virions, and includes the transcription of viral genes; export of the viral RNAs from the nucleus to the cytoplasm; translation of viral RNAs to produce the Gag polyprotein precursor (also known as Pr55Gag), the GagPol polyprotein precursor, the viral envelope glycoproteins (Env glycoproteins), and the regulatory and accessory viral proteins; trafficking of the Gag and GagPol precursors and of the Env glycoproteins to the plasma membrane; assembly of the Gag and GagPol polyproteins at the plasma membrane; encapsidation of the viral RNA genome by the assembling Gag lattice; incorporation of the viral Env glycoproteins; budding of the new virions from the infected cell; and particle particle maturation [23].

Transcription: Proviral DNA may lie dormant until cellular transcription factors stimulate RNA polymerase to replicate proviral DNA into short strands of viral messenger RNA (mRNA) and longer strands of viral RNA.

Translation: Viral mRNA is catalysed and synthesised by host cell ribosomes into precursor proteins. Envelope proteins are synthesised in the cell and cleaved into gp120 and gp140.

Assembly: Viral RNA, viral precursor proteins, and gp41 and gp120 complexes assemble at the host-cell surface in preparation for budding.

Budding and maturation: HIV protease cleaves polyproteins into functional viral enzymes and proteins, which reorganise to form a mature viral particle ready to infect other cells.

Epidemiology of HIV infection:

From mid 1981 groups of previously healthy gay men in parts of the US presented with a rare lung infection called *Pneumocystis carinii* pneumonia [21] while simultaneously others in other parts of the US were found to present with an aggressive cancer named Kaposi's Sarcoma [24]. These patients had common features, which were suggestive of immune deficiency. By the end of 1982, these features were collectively referred to by the Centers for Disease Control (CDC) as AIDS [25]. Meanwhile, this clinical picture of immune deficiency had spread to other countries in Europe [26-28] and Africa [29], and to other patient profiles including haemophiliacs [30] and people who injected drugs [31]. Even though HIV was first thought to be horizontally transmitted amongst men who have sex with men [32], it was subsequently discovered to be also vertically [33] and heterosexually transmitted [34], hence affecting men, women and children alike.

From this point, the epidemic grew at alarming rates, affecting various populations and regions of the world differentially, before starting to decline in the late 1990s with regards to rates of new infections. Consequently, the face of the HIV epidemic has been evolving over time. With the advent of antiretroviral therapy in the 1990s, the face of the epidemic has changed even further with substantial falls in the numbers of new infections in different parts of the world.

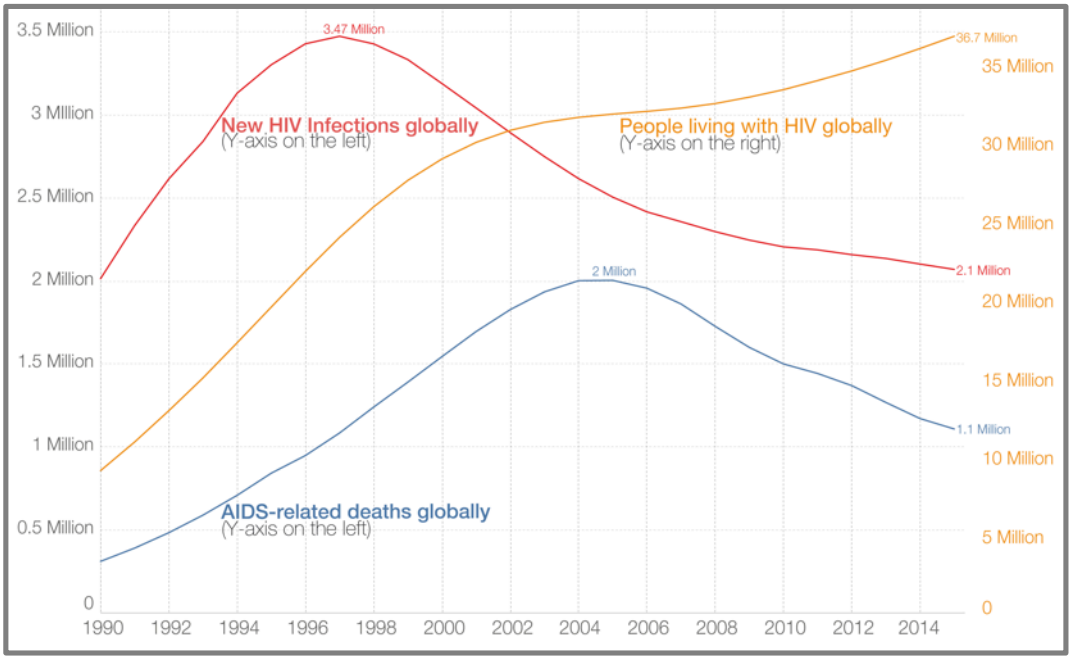

Figure 1.2: Global number of AIDS-related deaths, new HIV Infections, and People living with HIV. Source: [5]

Since the beginning of the epidemic, more than 70 million people have been infected with the HIV virus and about 35 million people have died of HIV [4]. The 1990s saw a substantial increase in the number of people infected with HIV and dying of AIDS (*Figure 1.2*) [5]. In 1997, almost 3.5 million people were diagnosed with HIV per year. After 1997, the number of new diagnoses began to decline and by 2015 it was reduced to 2.1 million per year. The number of AIDS-related deaths

increased throughout the 1990s and reached a peak in 2004 and 2005, when in both years 2 million people died. Since then the annual number of deaths from AIDS has declined, and a decade later it had almost halved when 1.1 million people died in 2015 [5]. The same chart also shows the continuing increase in the number of people living with HIV. The rate of increase has slowed down compared to the 1990s but the absolute number reached a peak in 2015.

Globally, an estimated 36.7 million people were living with HIV at the end of 2015 [3]. This was translated to an estimated 0.8% of adults aged 15–49 years worldwide living with HIV. Sub-Saharan Africa remains the most severely affected region, with nearly 1 in every 25 adults (4.4%) living with HIV and accounting for

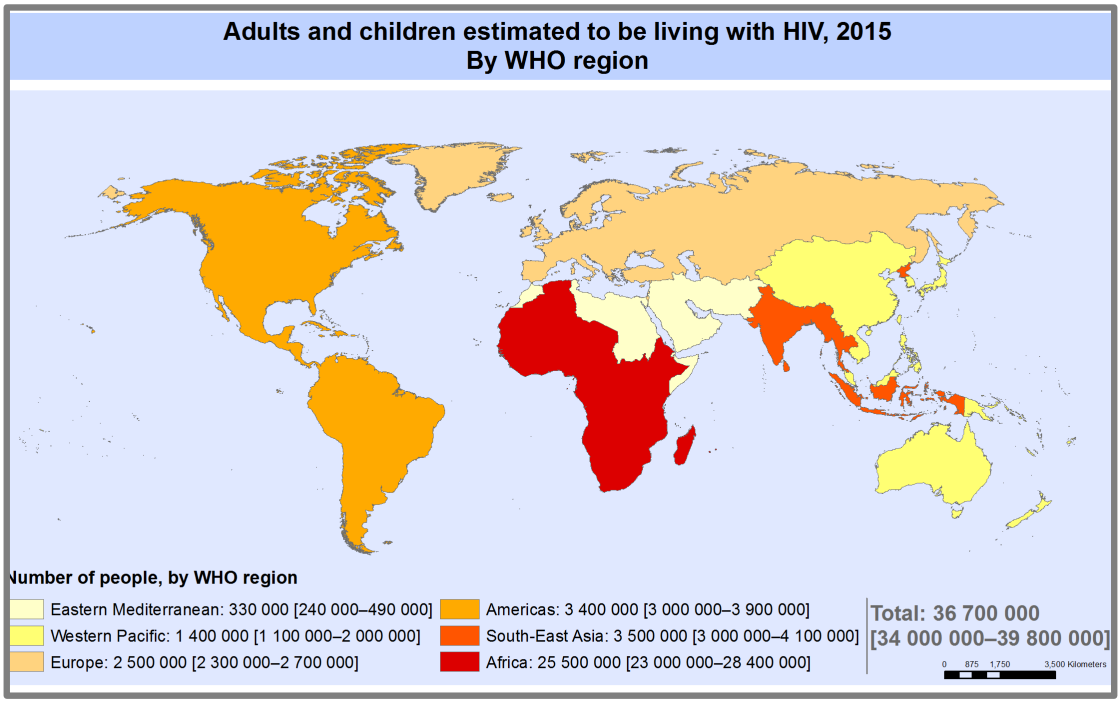

Figure 1.3: Global state of the HIV/AIDS epidemic. Source: [4]

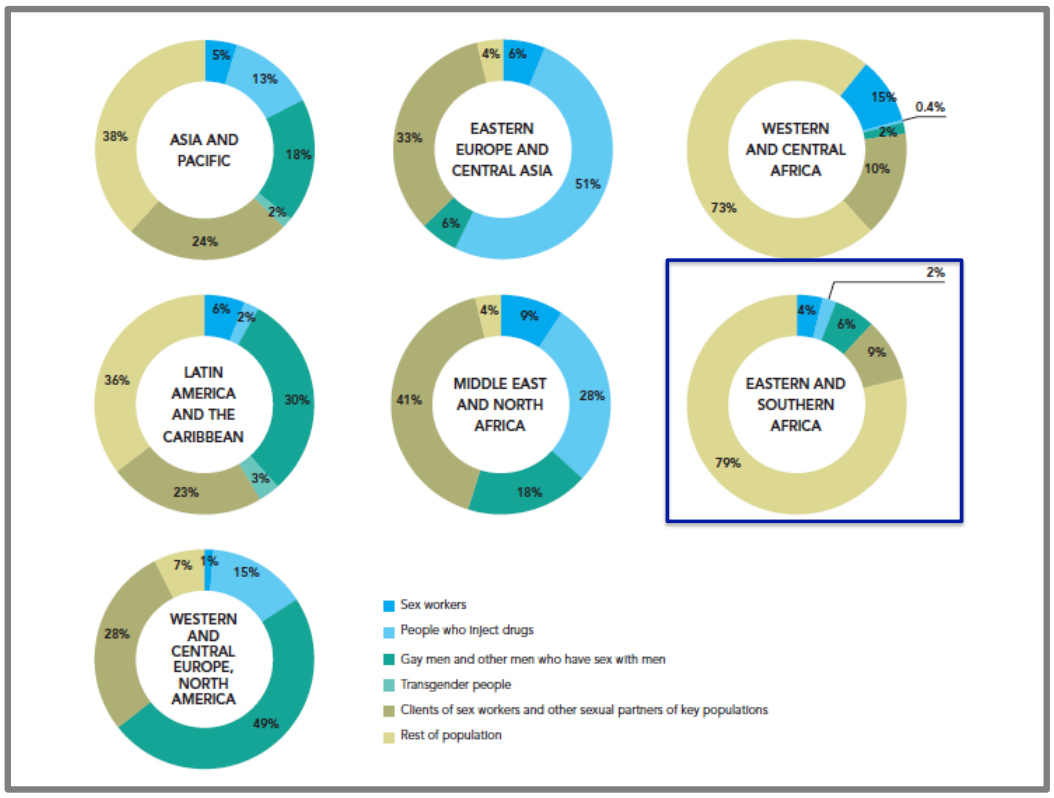

Figure 1.4: Distribution of new HIV infections among various populations by region in 2015. Source: [2]

nearly 70% of the people living with HIV worldwide (*Figure 1.3*). Again in 2015, 2.1 million people became newly infected with HIV although the burden of the epidemic continues to vary considerably between countries and regions (*Figure 1.4*). Sub-Saharan Africa had a distinct picture with the majority of the people (>70%) newly affected not falling in any of the previously-specified risk categories [2]. Looking closely at this region, the majority of the affected people are women, and particularly girls between the ages of 15 and 24 (*Figure 1.5*).

Epidemiology of HIV infection in women:

Currently, the distinctive feature of the HIV epidemic in the 21st century is its increasing burden in women, and particularly young women aged between 15 and 24 [35]. Whereas the first diagnosed cases of HIV infection in the 1980s were in men [36], there has been a steady escalation of incident infections in women [37]. Women now account for about one-half of all people living with HIV globally [2]. Whereas globally an estimated 50% of new HIV infections were in women in 2015, in sub-Saharan Africa alone an estimated 57% new HIV infections were in women, with 25% being in young girls between the ages of 15 and 24 years [2] (*Figure 1.5*). Heterosexual transmission is understood to be the most common risk factor

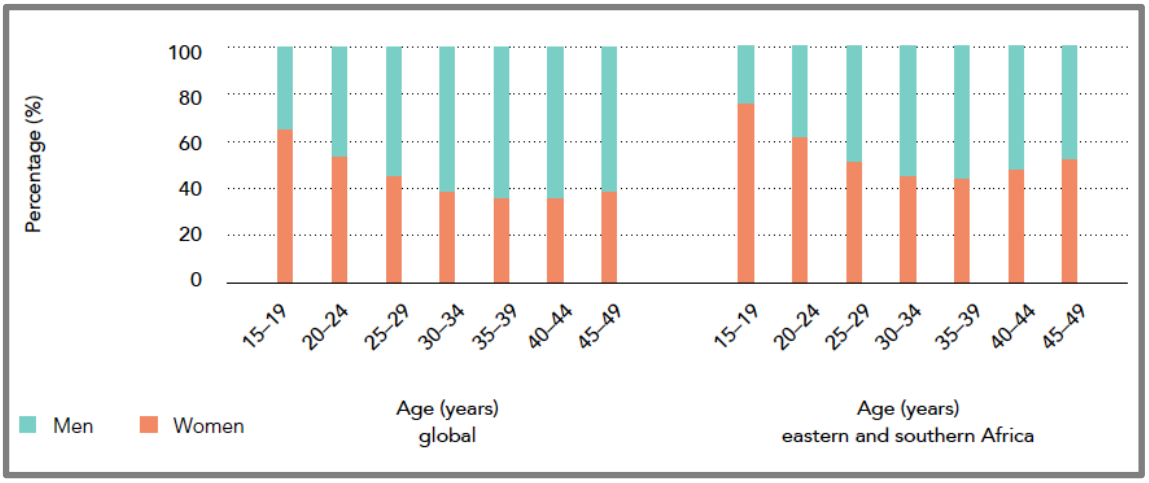

Figure 1.5: Proportion of new HIV infections by sex, global and eastern and southern Africa, 2015. Source: [3]

for acquisition of HIV-1 in women, overtaking other modes of transmission such as injection drug use. In sub-Saharan Africa, where heterosexual transmission is the primary driver of the epidemic, women are twice as likely as male counterparts to become newly infected [35]. Hence the literature describes the “feminisation” of the

AIDS pandemic, referring to the dominance of HIV infection in women over men [38].

Why focus on women:

Increased vulnerability in women is multifactorial, ranging from behavioural to sociocultural and biological causes. Stein argued that women in sub-Saharan Africa, where feminisation of HIV-1 is at its worst, are not able to negotiate safer sexual practices and hence biomedical preventive strategies that women can control might hold better hope for this group [39]. Abstinence from sexual activity, female and male condoms, and antiretroviral therapy (ART) use or voluntary male medical circumcision by their partners, are all available strategies, however, they depend on male partner co-operation. Development of biomedical preventive strategies that women can initiate and control has been hindered by poor understanding of correlates of protection in the female genital tract (FGT) [40]. Further, of all the successful biomedical preventive strategies tested to date, only one can be primarily used and controlled by women, i.e. Tenofovir based oral pre-exposure prophylaxis (PrEP) [41]. This is only available in some countries, having only been approved and adopted by the World Health Organisation (WHO) late in 2015. Even for this strategy, its implementation has been limited despite tremendous promise as a female-controlled HIV prevention strategy, it is thought in part because of disparate efficacy results from randomised trials in the populations where it was tested [42]. Women adhered poorly to this strategy in clinical trials, thereby compromising its effectiveness. Of the remaining potential strategies women could use, clinical trial results have been conflicting and perplexing [43]. Moreover, biological reasons for conflicting results remain unknown. Conversely,

understanding of natural correlates of protection that would enhance and expedite formulation of biomedical HIV preventive strategies is incomplete [44]. Significant biological factors at the level of the mucosa are, however, understood to include immature [45] or broken epithelium [46], structural and biochemical changes due to fluctuation in hormone levels, as with menstrual changes and exogenous hormone administration [47, 48], and co-prevalent reproductive tract infections [49]. In view of the burden of HIV infection in women in the 21st century, this thesis has therefore focused solely on addressing issues around HIV in the female genital tract.

SECTION 2: BIOLOGY OF FEMALE GENITAL TRACT IN THE CONTEXT OF HIV INFECTION

Anatomy and structure of the FGT:

The FGT is one of the organs of the body that connect the internal to the external environments, and hence, it comprises a sequence of cavities. The external vulva leads into the vagina, which connects in succession to the uterine cervix, the endometrium, and then to the fallopian tubes (*Figure 1.6*). The lumen of the lower genital tract (LGT) is lined with pluristratified squamous epithelium, which is composed of superficial, intermediate and basal epithelial cells, whereas the upper genital tract (UGT) is lined with a single-layer columnar epithelium. The transformation zone is where the columnar epithelium of the UGT meets the squamous epithelium of the LGT. It is divided into two distinct regions: the LGT consisting of vagina and ectocervix, with the endocervix, uterus and fallopian tubes comprising the upper genital tract.

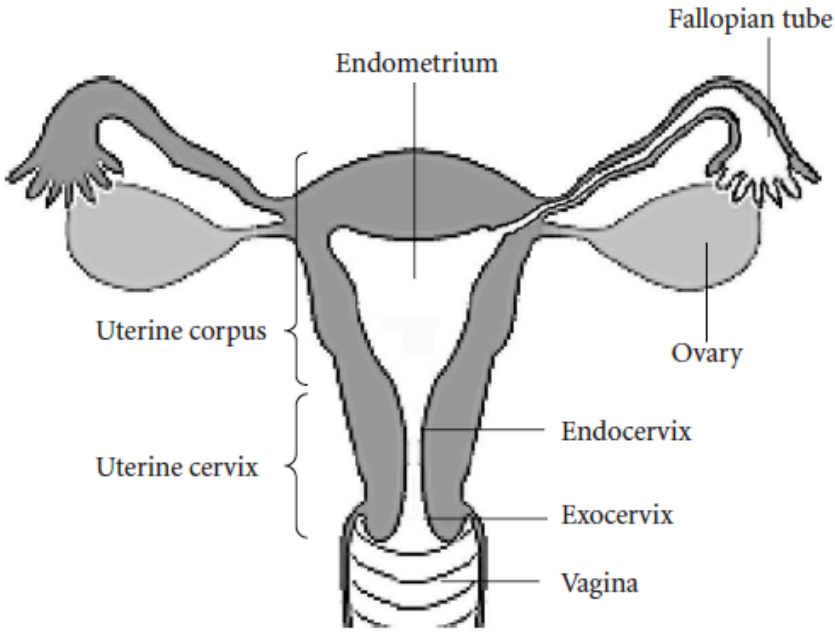

Figure 1.6: Anatomical structure of the female genital tract. Source: [9]

The FGT is lined by mucosal surfaces. The mucosal surfaces, which separate the external from the internal environments, form the innermost layer of the FGT, surrounding its luminal centre. The mucosa is made up of three layers: (i) the epithelium which is the innermost layer and thus the first layer to be in contact with incoming pathogens, (ii) the lamina propria which is a layer of loose connective tissue that hosts a large cell population, consisting of fibroblasts and other immune cells such as T cells, B cells, natural killer (NK) cells, macrophages, neutrophils and dendritic cells and (iii) the muscularis mucosae which is a thin layer of smooth muscle lining the submucosa. The transformation zone contains a particularly high number of immune cells compared with the rest of the FGT. Overlying the epithelial surface in the LGT and endocervix is mucus, the consistency of which changes across the cycle, becoming thick and viscous in the secretory phase. Also present is a dynamic population of bacteria, primarily composed of lactobacilli in most women that acidify the lumen of the LGT.

Structure of the FGT endocrine system:

Epithelial and stromal cells of the mucosa possess endocrine as well as immune and microbial receptors. Consequently, most aspects of the immune system in the FGT are hormonally regulated [50]. The immunohormonal system of the FGT is organised such as to optimise the prospect of successful fertilisation, implantation, and pregnancy while minimising the chances of rejection of the conceptus. Various studies, from as early as the 1960s, have clearly defined the changing pattern of sex hormones in blood over the menstrual cycle and the consequences that these changes have throughout the female reproductive tract. The length of the menstrual cycle in humans is estimated to be 28 days on average, while that of female macaques can be up to 32 days on average (*Figure 1.7*). The menstrual cycle is calculated beginning from the first day of menses. The first half of the menstrual cycle (follicular/proliferative phase) is under oestradiol predominance while the second half after ovulation (luteal/secretory phase) is under progesterone predominance. Under the influence of the hypothalamic–pituitary-ovarian axis, oestradiol levels during the proliferative phase rise and peak 2–3 days before ovulation, after which oestradiol levels transiently decline before increasing along with progesterone for 7–10 days before menses during the secretory phase. Thereafter, both progesterone and oestradiol levels decline to initiate menstruation in the absence of fertilisation. However, should unprotected sexual exposure occur, these hormonal changes prepare the vagina and cervix for sperm propagation into the Fallopian tube, while they prepare the uterus for subsequent implantation. There is, however, evidence that these hormonal variations are accompanied by biophysiological, structural and immune changes throughout the FGT, changes which are likely to favour HIV acquisition and transmission.

Structure of the FGT immune system:

Contrary to the gastrointestinal (GI) and respiratory tracts, which are also lined by

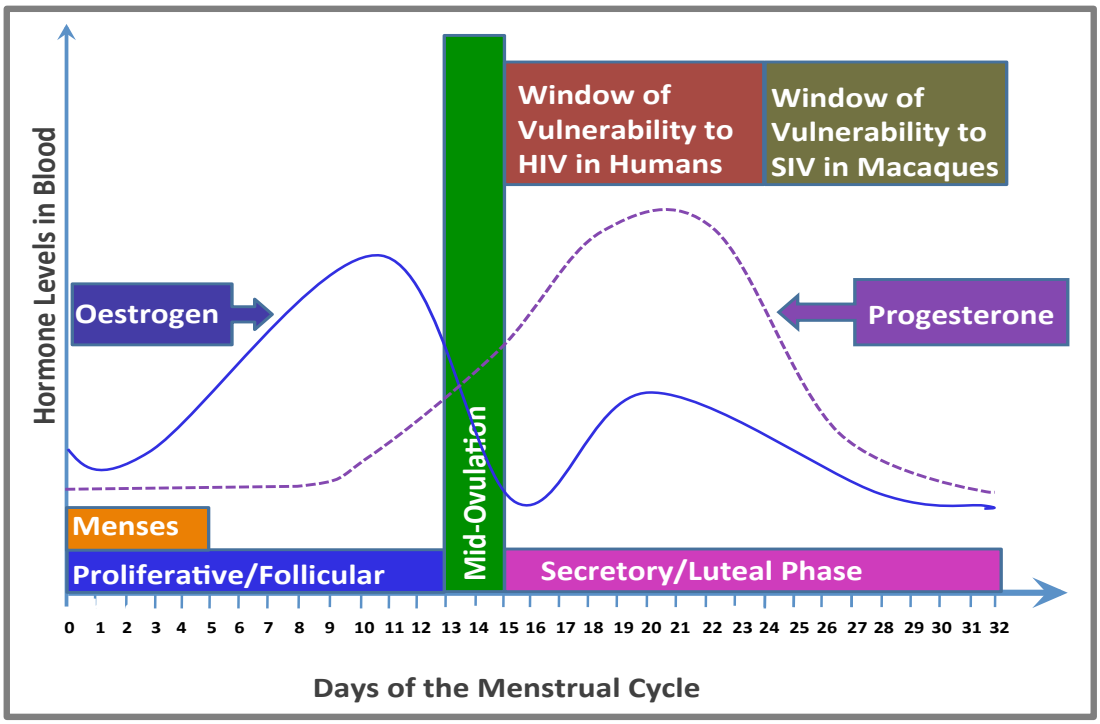

Figure 1.7: Hormonal fluctuations during the phases of the menstrual cycle in the female reproductive tract of humans and macaques. "Window" of vulnerability to HIV and SIV in humans and macaques, respectively.

mucosal surfaces, the function of the immune system of the FGT has a distinct and critical role to balance protection against sexually transmitted infections with allowing the survival of foreign sperm and allogeneic embryo. The FGT is somewhat unique among mucosal surfaces in that it lacks organised lymphoid elements, possessing instead small numbers of mononuclear cells scattered throughout the subepithelial stroma in the uterus [51]. These structures, which consist of a B cell core surrounded by CD8+ T cells and macrophages, are hormonally regulated in pre-menopausal women, and are absent from post-

menopausal women. They reach a peak size around ovulation and during the secretory phase of the cycle. This contrasts sharply with the resident immune system of the intestinal mucosa that consists of the Peyer's patches, submucosal lymphocytes, and a large population of intraepithelial lymphocytes poised between crypt epithelial cells to defend the integrity of the mucosal barrier [52]. The absence of a rudimentary follicular structure means an immune inductive site responsible for initiating an immune response to infection or vaccines cannot clearly be identified. Therefore induction of immunity to genital pathogens is assumed to occur outside the genital tract, followed by recruitment of re-circulating cells into infected sites. This has important implications for GT homing.

The FGT possesses both innate and adaptive components of the immune system, the architectural structure of which is unique to this site. The FGT mucosal innate system consists principally of mechanical, chemical, and cellular components. The first of these, the mechanical component, primarily carries out the physical barrier function of the mucosa, but also includes physiological functions such as cilial action, motility, desquamation, and mucus secretion. The second component, the chemical component, responsible for orchestration of the immune responses, can be further sub-divided into three: soluble or cell-associated pattern recognition molecules, proteins, and peptides. The third component of the innate immune system is the cellular component, which includes epithelial cells, stromal fibroblasts, and various inflammatory leucocytes.

The humoral system of the GT comprises antibodies that are unique to this mucosal surface; they mainly comprise the immunoglobulin (Ig) A and G isotypes.

Uniquely in the FGT Ig levels and isotypes display strong hormone-dependent variations, which are not as pronounced in other external secretions [53]. Further, in human cervical mucus, there are higher levels of IgG than of IgA; this contrasts with other typical external secretions, such as saliva, tears, milk, and intestinal fluids, in which secretory IgA (S-IgA) is the dominant isotype. Studies of the origin of Igs in genital secretions revealed that approximately half of the Igs are produced locally by plasma cells present in genital tract mucosa; the remaining Igs are derived from the circulation [54]. IgA is synthesised locally by subepithelial plasma cells as a polymeric J chain-containing molecule, secreted and then selectively bound to the secretory component (SC), which is expressed on the basolateral surface of epithelial cells. IgA is an antibody that has two classes: IgA1 and IgA2; and it exists in two forms: the monomeric and the dimeric forms, whereas IgG exists only in the monomeric form. More than 90% of serum IgA is present in monomeric form whereas mucosal secretions contain S-IgA [55].

20% of the total cells in the human FGT are leucocytes, with more leucocytes being present in the UGT than in the LGT [56]. Most leucocyte subsets have a preferential distribution within the different sub-compartments in the FGT; for example, T cells (CD3+), which are the most abundant leucocyte subset in the FGT, have higher proportions in the lower than in the upper tract, whereas granulocytes (CD66b+) and natural killer (NK) cells are more abundant in the upper tract than in the lower tract [57]. T lymphocytes are a major constituent (30-60%) of leucocytes from all tissues but concentrate mainly in the cervix. Data from Pudney *et al* showed that the endocervix had a high concentration of intraepithelial lymphocytes [58]. Furthermore, the cervix, especially the transformation zone, is

thought to be the major inductive and effector site for cell-mediated immunity in the lower FGT.

"Window" of HIV infection:

There is evidence that the innate immune system is suppressed in the luteal/secretory phase in order to optimise conditions for fertilisation and implantation, thereby enhancing chances of a successful pregnancy. Consequently it is postulated that HIV exploits this period of immunosuppression to establish successful infection. Several studies have supported and reported on the concept of a "window" for HIV and SIV infection. In humans, it is postulated based on studies of the patterns of distribution of endocrine receptors, distribution and density of immune target cells, and secretory patterns of molecules in different sub-compartments over the menstrual cycle that there is a "window" of heightened vulnerability to HIV infection in the luteal phase of the menstrual cycle (*Figure 1.7*) [59]. In NHP, Vishwanathan *et al* estimated that susceptibility to vaginal SHIV infection was significantly elevated in the second half of the menstrual cycle, between days 24 and 31, when progesterone levels were high and when local immunity might be low, which they postulated could be reason for higher susceptibility to HIV in women during other progesterone dominated periods including pregnancy and contraceptive use [60]. Saba *et al* observed that the menstrual cycle phases of the donors at the time of hysterectomy strongly affected virus production; only cervical explant tissues obtained in the progesterone dominant phase sustained productive virus replication [61]. Repeated vaginal exposure of pigtail macaques to low doses of simian–human immunodeficiency virus (SHIV) during normal menstrual cycles showed that the majority of macaques first showed signs of viraemia in the proliferative phase. Taking into account a viral

eclipse phase of 7–14 days before viraemia could be detected, these studies estimated a window of most frequent virus transmission between days 24 and 31 of the menstrual cycle (the late secretory phase) [62].

SECTION 3: MUCOSAL HIV TRANSMISSION

Mucosal surfaces constitute the major portal of entry and transmission route for HIV infection. Of the estimated 33 million infections, more than 90% gain entry into the body through gastrointestinal and genital tracts, with the FGT alone comprising almost 40% [63]. The study of the SIV/Rhesus macaque animal model has provided valuable information into understanding early HIV infection events via the

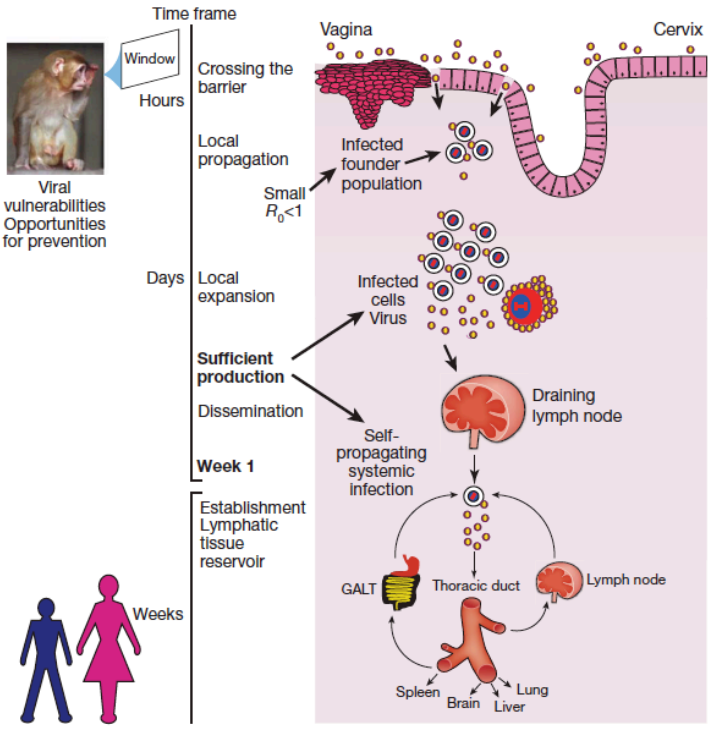

Figure 1.8: *Time frame, sites and major events in vaginal transmission*. The male (blue) and female (pink) figures at the lower left are positioned in the time frame marked weeks, after systemic infection has been established. Source: [10]

mucosal surfaces of the FGT. According to Haase *et al*, there is a window through which to view early infection and to intervene to halt the mucosal spread of HIV infection [10]. HIV-1 infection is first clinically manifest some weeks after exposure to the virus-containing inoculum, and hence, there is a need for the animal model to view sexual mucosal transmission and the earlier stages of infection. Within hours,virus in the inoculum may gain access through breaks in the mucosal epithelial barrier to susceptible target cells. The small focal infected founder population is initially composed mainly of infected resting CD4+ T cells lacking conventional markers of activation. The founder population expands locally in these 'resting' and in activated CD4+ T cells. Local expansion is necessary to disseminate infection to the draining lymph node, and subsequently through the bloodstream to establish a self-propagating infection in secondary lymphoid organs. Crossing the barrier, establishing these small founder populations, and local expansion are all periods of potential vulnerability for the virus in week 1 of infection. These vulnerabilities create opportunities for prevention targeting this critical stage of infection.

SECTION 4: FGT EPITHELIUM IN HIV INFECTION

Epithelial cells form the topmost layer of the mucosal surface, hence, on entry to the FGT HIV interacts with epithelial cells, making use of epithelial signalling mechanisms and trafficking pathways of the host cell to establish infection. However, epithelial cells have attributes that limit microbial access and the establishment of infection, and these include their architectural structure, which includes tight intercellular junctions; production of mucus; and secretion of innate immune mediators.

A single layer of simple columnar cells lines the UGT while multilayered pluristratified squamous cells line the LGT. The multilayered pluristratified epithelial layer contains a single layer of basal cells (stratum basale) and overlying layers of spinous cells (stratum spinosum) and granular cells (stratum granulosum) [64]. These distinct anatomical regions undergo morphological changes during the menstrual cycle fluctuations in levels of oestradiol and progesterone. Oestradiol induces proliferation, complete maturation, and desquamation of all layers of the squamous epithelium of the cervix, whereas progesterone causes thickening of intermediate layers [57].

Simple epithelial cells are polarised having a plasma membrane that is separated by tight junctions into two clearly distinct domains: the apical domain that faces the tract lumen, and the basolateral surface that faces the serosal side (*Figure 1.9*). Actin and microtubules participate in the establishment and maintenance of cell polarity. The simple epithelial cells have polarised endocytic pathways which are responsible for the selective and rapid transcellular vesicular transport from one pole of the epithelium to the opposite one, referred to as transcytosis. Transcytosis works in both directions and controls epithelial barrier function. Contrary to the simple columnar epithelial layer, the multilayered pluristratified epithelial layer does not have a polarised plasma membrane or tight junctions. Owing to this lack of tight junctions, extracellular molecules or other cell types are free to diffuse between cells using paracellular pathways [8].

Secretions containing a mucosal protective armour coat the epithelium. These secretions not only house an array of immunomodulatory proteins but also house

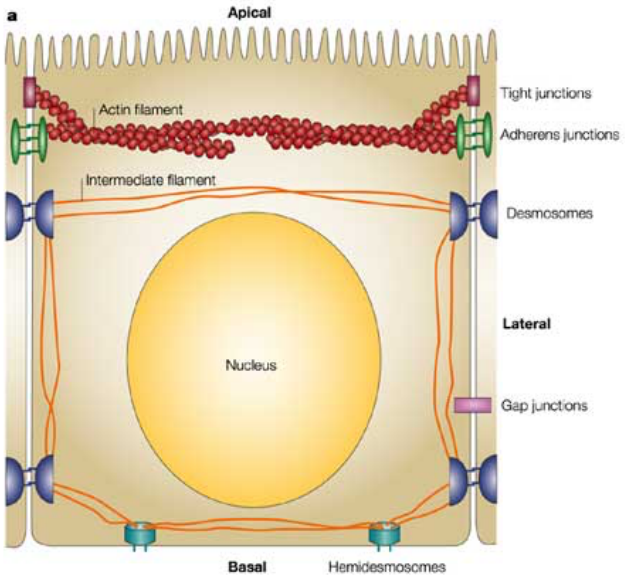

Figure 1.9: A schematic representation of a simple polarised epithelial columnar cell. Source: [8]

an array of antimicrobial molecules and form a physical protective barrier against external environmental challenges [65]. Thick mucus secretions with immune cells and immunoglobulins are typically found in the endocervical canal overlying its epithelium while cervicovaginal fluid coats the LGT. The endocervical surface is also highly convoluted and contains numerous goblet cells that are continually producing more mucus. Antibodies that are capable of neutralising the virus coat the columnar epithelium of the endocervix, thus enhancing its protective role. Further, they have been shown to trap the virus thus limiting the chances of being transmitted across the epithelium [66].

The epithelium is efficient in: (i) regulating viral passage across the epithelium and mucosa, (ii) responding directly to the presence of the virus, and (iii) relaying signals to the underlying cells of the innate and adaptive immune system. For

instance, despite its high prevalence, sexual HIV-1 transmission is relatively inefficient; male-to-female transmission incidence has been estimated to be 0.002% to 0.02% for each sexual act, thereby suggesting that the genital epithelium serves as a major barrier against HIV-1 [46]. It is, however, not entirely clear by what mechanism viral transmission across the epithelium occurs. It is postulated that transmission mechanisms vary for different HIV-1 presentations including direct infection of epithelial cells, transcytosis through epithelial cells, epithelial transmigration of infected donor cells, or circumvention of the epithelial barrier through physical breaches. Whether free or cell-associated HIV-1 is more prone to overcome the multiple barriers that defend the FGT from HIV-1 transmission remains to be elucidated. Free virus seems to diffuse where water diffuses. Unlike cell-free HIV-1 particles, which move passively, cells are capable of active locomotion through epithelial barriers [67].

Genital epithelial cells lack CD4 [68], thus cell-free HIV-1 has to utilise unconventional mechanisms to cross primary genital epithelial cell layers. However, several other receptors have been reported to facilitate HIV-1 entry into CD4-negative cells. Specifically, galactosylceramide (GalCer), adhesion molecules such as intercellular adhesion molecule 1 (ICAM-1) and lymphocyte function-associated antigen 1 (LFA-1), C-type lectins such as dendritic cell-specific ICAM-grabbing non-integrin (DC-SIGN), DC-SIGN related (DC-SIGNR), langerin, and the mannose receptor, and proteoglycans such as chondroitin sulphate (CSPGs) and heparan sulphate proteoglycans (HSPGs) [69] have all been shown to promote HIV-1 attachment and/or entry into cells that lack CD4.

The distinctive role of the epithelium includes the detection of harmful stimuli

through pattern recognition receptors (PRRs) and then to relay this information to the adaptive immune system through secretion and up-regulation of various cytokines and chemokines [70]. These cytokines and chemokines have immunomodulatory functions. They are also capable of impeding HIV replication and recruiting relevant cells from underlying tissues to the site of infection. The secretion of these molecules may be constitutive or induced by stimuli such as the virus itself or the presence of inflammation. The epithelial function of the secretion of proteins is stimulated when infectious agents attach to the membrane via receptors or other molecules, or via autocrine/paracrine functions [70]. However, the mechanisms by which innate immune factors, and particularly effector molecules, modulate HIV susceptibility and resistance have not been fully elucidated [71].

Some of the antimicrobial peptides (AMPs) detected in cervical mucus include the following: human defensins which are small cationic AMPs and include the α-defensins, the so-called human neutrophil peptides 1 to 3 (HNP1-3) that are released from the neutrophils, and the β-defensins, the so-called human β-defensins 1 to 4 (HBD-1-4) secreted by epithelial cells [72]. Secretory leukocyte protease inhibitor (SLPI) is an antimicrobial polypeptide already known to be in a high concentration in the cervical mucus plug [73]. Lysozyme and lactoferrin are known antimicrobial components of epithelial secretions, which include cervical mucus [74]. AMPs thus form an extra protective layer of the endocervix and exert their effect by disrupting microbial membranes and the metabolic processes of microbes.

Over and above having innate immune antimicrobial functions, mucosal epithelial

cells also have the ability to modulate the recruitment and activity of immune cells of both the innate and adaptive immune systems. By secreting antimicrobial factors, such as SLPI and human β-defensins, epithelial cells are able to eliminate potential pathogens [75]. By secreting chemokines such as interleukin-8 (IL-8), monocyte chemoattractant protein (MCP-1), and RANTES (regulated upon activation, normal, T-cell- expressed and secreted), epithelial cells are able to recruit immune cells to the sites of infection [76-78]. In addition, by secreting cytokines such as IL-6 and IL-1β, epithelial cells are able to activate and regulate the inflammatory and immune responses of both the innate and adaptive immune systems [79, 80]. However, despite the important role that the genital tract mucosa plays in immune defence, little is known about the mechanism of cell activation by pathogens and the secondary mediators involved in this regulated response.

SECTION 5: MACROPHAGE INFLAMMATORY PROTEIN 3 ALPHA

Macrophage inflammatory protein 3 alpha (MIP-3α) is another product of the epithelial cells. It is a chemokine that belongs to the CC chemokine group of molecules [81]. MIP-3α is also designated as liver- and activation- regulated chemokine (LARC) [82], exodus-1 [83] or CC chemokine ligand 20 (CCL20) [81]. It is a 70 aa, 8 kDa protein that is the sole ligand for the receptor CCR6 which is expressed on immature dendritic cells and T lymphocytes, particularly memory T cells [84]. Its functions range from chemoattraction to linking the innate and adaptive immune systems, and having antimicrobial activities [85]. It is a small pro-inflammatory peptide, which functions to attract leucocyte populations to sites of inflammation [86]. It tends to be distributed in mucosal and inflamed sites. It is distributed widely in tissues including lymph nodes, appendix, skin, and intestinal

tissues. It is secreted by epithelial cells [87] and its secretion and expression is induced by inflammation. It is categorised as a chemokine whose secretion is otherwise either constitutive or stimulated [88], and its secretion pattern is specific for both tissue type and inducing agent [89]. Pro-inflammatory mediators and chemical compounds such as phorbol myristate acetate (PMA), ionomycin, tumour necrosis factor (TNF) - α, and lipopolysaccharide (LPS) up-regulate its secretion, while it is down-regulated by interleukin-10 (IL-10) [90].

MIP-3α was first discovered through bioinformatics in 1997 [90]. Thereafter Dieu-Nosjean *et al* showed that immature dendritic cells (DCs) were attracted by MIP-3α to the epithelial crypts of tonsillar tissue [87]. Initial investigators studied it widely for its association with dermatological and gastrointestinal diseases [91, 92]. MIP-3α was subsequently studied in the FGT from the early 2000s when various investigators studied its constitutive and induced secretion patterns in various epithelial cell line models and primary epithelial cell models of the endometrium and vagina [93-95]. Data from Wira *et al* subsequently showed that MIP-3α has antimicrobial activity, and particularly anti-HIV-1 activity in the FGT [85].

A recent landmark study looking at the SIV/Rhesus macaque model highlighted the role of the endocervix, the epithelium, and MIP-3α simultaneously in early SIV infection. In this study they noted that the accumulation of SIV RNA+ CD4+ T cells post exposure to virus in a SIV/Rhesus macaque model was preceded by a subepithelial influx of plasmacytoid dendritic cells (pDCs) in the endocervix one day post inoculation (d.p.i.), an effect that was not replicated in the vagina and transformation zone sub compartments [96]. They subsequently showed that this accumulation of pDCs was associated with increased expression of MIP-3α.

Through a series of experiments they concluded that the exposure and binding of SIV to epithelial cells in the FGT induced an “outside-in” signalling cascade i.e. exposure of endocervical epithelium to the viral inoculum increases the expression of MIP-3α, which in turn recruits pDCs, thereby commencing the sequence of events leading to productive infection. This group, in a quest to identify potential microbicide agents, showed in further studies that glycerol monolaurate (GML), a general anti-inflammatory compound, reversed MIP-3α secretion and dampened local inflammation, thus reversing infection events in female macaques [97]. Because these findings had not been replicated in humans and the secretion of MIP-3α by the endocervix on exposure to virus had not been investigated in humans, we embarked on a project that looks at the role of MIP-3α in early HIV infection in humans. Further, none of these or other groups has studied secretion of MIP-3α by the human cervix, in the form of either the cervical epithelial lines or the cervical explant models. We therefore designed a study to primarily focus on the secretion of this molecule, MIP-3α, by the endocervical epithelial models.

SECTION 6: HYPOTHESES AND STUDY AIMS

More than three decades into the HIV epidemic women bear the brunt of HIV infection and yet there are hardly any strategies they can use to protect themselves against HIV infection. To date, results of clinical trials looking at biomedical preventive strategies to reduce sexual transmission of HIV infection in women have been conflicting and perplexing. Inherent to these contradictory findings in clinical trials, scientists believe that identifying and understanding mucosal defences at the portal of entry in the context of heterosexual transmission should be a priority in order to inform successful development of HIV preventive strategies including

vaccines. Specifically there have been calls to define the sequence of events required to establish infection and to elucidate acute mucosal events that need to be prevented by HIV biomedical preventive strategies, which this thesis has responded to.

Research questions:

Given that the endocervix, recently proposed as the primary site of infection, has not been studied extensively in the context of HIV in humans, unlike in macaques, this study undertakes to address the question of whether there is any evidence for triggering of epithelial response to HIV exposure based on the expression of MIP-3α and a wider multiplex array of immunological and antimicrobial biomarkers in the human FGT with a particular focus on the endocervix. It also seeks to answer the questions of what the likely viral (envelope) triggering factor is for MIP-3α secretion, whether there is any influence of menstrual cycle variations on MIP-3α secretion patterns, and whether there are any differences between the endocervices of macaques and humans with regards to MIP-3α secretion patterns.

Research aims:

The overall study aim of this thesis is to determine the physiological relevance of the “outside-in” signalling mechanism of MIP-3α secretion in humans and its potential as a target for intervention to prevent or reduce HIV transmission. The specific study aims are as follows:

Specific aim 1:

To quantify constitutive levels of MIP-3 alpha in various matrices of the FGT using cellular epithelial models and validating with explant tissues models, with particular focus on the endocervix

Rationale: MIP-3α secretion has been shown to be both constitutive and inducible but dependent on the cell tissue type; but MIP-3α secretion has never previously been studied in the endocervical sub-compartment. Further, the FGT functions in a compartmentalised fashion and hence it is not feasible to infer the secretion pattern of one sub-compartment from studying other sub-compartments.

Hypothesis: the endocervix, being immunologically distinct from other FGT sub-compartments and implicated in primary SIV infection, will have the highest concentration of MIP-3α in epithelial cell and tissue models versus endometrium and vagina, and that this concentration will be more pronounced in the explant tissues versus the cellular models.

Specific aim 2:

To determine stimulated levels of MIP-3α in various human FGT sub-compartments using various HIV-1 preparations in cellular and explant tissues models.

Rationale: a landmark study showed that exposure of the FGT to SIV in the endocervix of macaques triggered secretion of MIP-3α by epithelial cells.

Hypothesis: MIP-3α secretion is up-regulated in the endocervical sub-compartment of humans following HIV exposure, when the viral envelope proteins interact with the apical epithelial surface.

Specific aim 3:

To explore up-regulation and/or down-regulation of various soluble proteins and antimicrobial peptides following stimulation with HIV-1 in the human endocervix using explant tissues models.

Rationale: Explant tissues comprise epithelium embedded on the underlying lamina propria. Cells in the lamina propria have been shown to have paracrine effects that contribute to the regulation and functioning of the cells of the epithelium. Further, MIP-3α is unlikely to be the sole role player in the events determining early infection. We hence wanted to understand the role of MIP-3α in early HIV infection in near normal physiological conditions as we see *in vivo*.

Hypothesis: FGT mucosal layer secretes various cytokines and chemokines that regulate resistance and/or susceptibility to HIV infection in the FGT. On the other hand it secretes AMPs that possess antiviral activity and hence the resulting responses of the epithelial-HIV interaction are a result of the balance between the two. We hence hypothesised that exposure of the endocervical epithelium to HIV-1 dampens the secretion of SPs and AMPs with antiviral activity.

Specific aim 4:

To determine the interplay between the endocrine and immune systems by

assessing the impact that fluctuation of endogenous hormones levels during the menstrual cycle has on the secretion pattern of MIP-3α and that of other cytokines in the FGT and serum of women at low risk of HIV infection.

Rationale: Most aspects of the immune system in the FGT are hormonally regulated, responding differentially to changing levels of endogenous hormones throughout the menstrual cycle. The literature describes a 'window' of heightened vulnerability to HIV/SIV infection in the luteal/secretory phase of the menstrual cycle.

Hypothesis: the levels MIP-3α are highest in the FGT during the luteal/secretory phase of the menstrual cycle when they contribute to the heightened risk of HIV acquisition in the secretory phase.

Specific aim 5:

To compare and contrast early epithelial responses in the endocervix of humans to those in macaques with regards to MIP-3α secretion and to identify other factors that might be an equivalent of MIP-3α in the initial HIV infection events in humans.

Rationale: much of our understanding of the early events in HIV infection comes from studies in female macaque monkeys exposed to SIV via the genital mucosa and yet humans do not always behave in the same manner as macaques with regards to immunogenetics and responses to immunostimulants. In view of a landmark study in an SIV/Rhesus macaque model highlighting the significance of an "outside-in" signalling mechanism involving the triggering of MIP-3α secretion by endocervical epithelium on exposure to virus, we decided to extend these studies

in humans. Identifying these factors and comparing responses in macaque and human tissues will make a major contribution towards understanding these important early events in SIV/HIV infection.

Hypothesis: human epithelial cells sense and respond to retroviral exposure differently from the way in which macaque cells appear to do. They may secrete different factors that recruit susceptible viral target cells into the mucosa, as MIP-3α appears to do in the macaques.

CHAPTER TWO MATERIALS and METHODS

STUDY DESIGN:

Four of the five projects in this thesis were designed as cross-sectional laboratory-based studies entailing the use of *in vitro* and *ex vivo* assays. Epithelial cellular and tissue models were prepared from biological specimens collected from either humans or macaques. The fifth project was designed as a prospective cohort study in which cervicovaginal secretions and serum from women (humans) were collected at various successive time points before being analysed in the laboratory.

Study cohorts:

Three cohorts were included in this thesis:

1. John Radcliffe Hospital, Women's Centre cohort
2. St George's Hospital, CASHIR[1] study cohort
3. Public Health England, macaque cohort

Study setting:

The entire study was conducted in the United Kingdom (UK) and the experimental work was divided equally between the laboratories in the University of Oxford in Oxford and the Imperial College London in London.

Study population:

[1] CASHIR is an acronym for characterisation of the activity and stability of anti-HIV-1 agents in the presence of female genital secretions and establishing methods to measure immune responses

Humans[2]*:* UK women between the ages of 18 and 55 were recruited into these studies if they were HIV uninfected and at low risk for HIV infection. They were recruited only if they gave informed consent to participate.

1. Women's Centre cohort: we collected hysterectomy samples from this cohort. Women were eligible to participate if they were scheduled for a hysterectomy for their own health. The indication for a hysterectomy was a non-cancerous lesion and in the majority of cases this was for abnormal uterine bleeding.

2. CASHIR study cohort: Dr Clifford Jones and the clinical study team at St George's hospital collected cervicovaginal secretions and serum from this cohort. Women were eligible to participate only if they had regular monthly menstrual cycles with an average 28-day cycle.

Macaques: Simian Immunodeficiency Virus (SIV) uninfected rhesus macaques of around 14 years of age who had been involved in a bacille Calmette-Guerin (BCG) aerosol vaccination study were included in this study. A further group of SIV and simian retrovirus (RSV) uninfected cynomolgus macaques around the mean age of 10 years was also included in this study.

Sample size:

Seven women were recruited into the Women's Centre cohort while 31 women were recruited into the CASHIR study cohort. Only six and 11 samples, respectively, were subsequently eligible for inclusion into this analysis. Samples

[2] Additional human genital tract tissue samples were obtained from the St Mary's, Imperial College London cohort through a unit wide tissue study that enables access to tissues for the whole unit focusing on mucosal immunity to HIV infection.

from three rhesus macaques and three cynomolgus macaques were included in this analysis.

Ethical consent:

Ethical, and Research and Development committees in the Oxford and London NHS Trusts approved the studies. Specifically the John Radcliffe Hospital study was approved through the Bloomsbury Research Ethics Committee while the St George's Hospital study was approved through the St George's healthcare NHS Trust Clinical Ethics Committee. Further, the University of Oxford's clinical trials and research governance unit (CTRG), Oxford University hospitals research and development unit and Oxford Centre for Histopathology Research (OCHRE) approved the John Radcliffe Hospital study. Informed consent was sought and obtained from all study participants at screening and prior to recruitment into the respective studies.

COLLECTION OF SAMPLES:

Human genital tract tissues:

We prepared endocervical explant tissues (EET) and endocervical primary epithelial cells (EPECs) from hysterectomy specimens. Hysterectomy specimens were received intact in theatre by the study investigator, and prior to immersion in formalin. The endocervix was subsequently resected and immediately transported to the laboratory. EET were prepared and experiments commenced on the same day of hysterectomy, particularly within two to four hours of womb resection from the body. Blocks of tissue were frozen down and EPECs prepared and experiments performed at a later date.

Macaque genital tract tissues:

We prepared EET from post-mortem hysterectomy specimens. The hysterectomy was performed at Public Health England immediately at the time of culling the macaques and the womb complete with uterus, endocervix and vagina was subsequently shipped intact on the day of womb resection to the Oxford laboratory. Blocks of tissue from rhesus macaques were used to prepare EET and were used fresh i.e. within 8 hours of womb resection while blocks of tissue from cynomolgus macaques were frozen down and EET prepared and experiments performed at a later date[3].

Transport medium:

Female genital tract (FGT) tissues from both humans and macaques were immediately immersed in cold RPMI-1640 medium (Sigma-Aldrich®, UK) complete with 10% heat inactivated foetal bovine serum (FBS) (Life Technologies, Gibco®, UK), 2 μM L-glutamine (Life Technologies, Gibco®, UK), and antibiotics (100 units/ml penicillin/streptomycin (Life Technologies, Gibco®, UK), 1μg/mL fungizone (Life Technologies, Gibco®, UK), and 10μg/mL gentamycin (Life Technologies, Gibco®, UK). They were packaged and shipped to us on ice at 4^0C.

Cervicovaginal fluid:

Cervicovaginal fluid (CVF) secretions were collected using the Instead softcup™**,** a vaginal cup used originally as a menstrual cup. A concentrate of CVF was collected longitudinally at three time points corresponding to the oestrogenic (D5–8), mid-ovulatory (D14–16), and progestogenic (D19–22) phases of a single

[3] Freezing down tissues from cynomolgus macaques did not impact results on the soluble markers measured at a later date.

menstrual cycle from each woman. Women were instructed to self-insert the Instead softcup™ into the vagina on the day of the study visit at the clinic. The cup was left *in situ* for a minimum of an hour up to a maximum of two hours prior to being removed from the vagina. On removal from the vagina, the Instead softcup™ with secretions was placed into a sterile pre-labeled 50ml falcon tube and immediately shipped on ice to the laboratory for storage at -80^{0}C until processing.

Blood (serum):

At the exact same visits and from exactly the same women, serum was also collected from each study participant. After venepuncture, 10mL of blood collected was centrifuged and serum collected. Serum was subsequently aliquoted into 1mL cryovials, which were then stored at -80^{0}C until used for the assay.

CELLULAR BIOLOGY AND TISSUE CULTURE:

Epithelial models:

1. HEC-1A cells

HEC-1A cells, an endometrial cell line derived from a human endometrial adenocarcinoma, were donated by Ms Julie Swales at the Imperial College London at passage six. We passaged and did experiments with these cells at passage 15. They were maintained in complete McCoy's medium (Sigma-Aldrich®, UK) supplemented with 10% FBS, L-glutamine and antibiotics (penicillin/streptomycin) in same concentrations used for shipping medium.

2. Caco-2 cells

Caco-2 cells, a colorectal cell line derived from a human colon adenocarcinoma, were donated by Dr Nathan West at an indeterminate passage. We passaged them three times before conducting the experiments presented in these analyses. They were maintained in complete Modified Dulbecco's Eagle's Medium (DMEM) (Sigma-Aldrich®, UK) supplemented with 10% FBS, L-glutamine and antibiotics (penicillin/streptomycin) in same concentrations used for shipping medium.

3. Endocervical primary epithelial cells:

Endocervical primary epithelial cells (EPECs) were prepared from either fresh or frozen hysterectomy specimens. Single cells were extracted, isolated, and purified using a combination of mechanical and biochemical digestion techniques: a block of fresh tissue of about 2*1*1.5cm^3 size was soaked overnight in Dispase II (Life Technologies, Gibco®, UK) at 4^0C prior to being soaked in trypsin-EDTA (Sigma-Aldrich®, UK) in the incubator at 37^0C 5% CO_2 for 20 minutes. For cells prepared from frozen tissue blocks, tissue blocks were first incubated in complete RPMI-1640 (Sigma-Aldrich®, UK) overnight at 37^0C 5% CO_2 prior to exposure to Dispase II in order to soak off dimethyl sulphoxide (DMSO – Sigma-Aldrich®, UK). We then used the pasteur pipette to tease out single cells from underlying stroma and tissues. Serial 3-sized nylon meshes (100, 70 and 30 μM) (pre-separation filters - Macs Miltenyi Biotec, UK) were subsequently used to isolate single epithelial cells from cellular discs and debris. We then seeded single epithelial cells in 12 well tissue culture plates with 800μL of complete keratinocyte serum free medium (K-SFM - Life Technologies, Gibco®, UK). We chose to use K-SFM in order to encourage pure epithelial cell growth while discouraging growth of fibroblasts. The same K-SFM had low calcium content (less than 60μM) in order to avoid premature cell differentiation of keratinocytes. The 12 well tissue culture plates were coated

with heat inactivated foetal bovine serum (FBS) (Life Technologies, Gibco®, UK) in order to encourage attachment of cells to the base of the wells. K-SFM was supplemented with human recombinant epidermal growth factor (rEGF), bovine pituitary extract (BPE), L-glutamine and antibiotics (penicillin/streptomycin) (Life Technologies, Gibco®, UK), 1µg/mL fungizone (Life Technologies, Gibco®, UK), and 10µg/mL gentamycin (Life Technologies, Gibco®, UK). A confluent monolayer took an estimated 21 days post plating to develop in 12 well tissue culture plates incubated at 37^0C 5% CO_2. TrypLE™ (Life Technologies, Gibco®, UK) was used to dislodge single cells from plasticware. After passaging EPECs twice in T-25 and T-75 tissue culture flasks, we subsequently seeded each well of the 24 well tissue culture plate or the Transwell® inserts with 50,000 cells at passage 3 in order to conduct experiments. For experiments in Transwell® inserts, apical and basal compartments were filled with 200 and 600µL of complete medium, respectively, and TEER was measured daily with a Voltohmmeter®. Constitutive baseline levels of MIP-3α levels were quantified in supernatants harvested when the TEER was maximal around Day 8 post plating.

4. Explant tissues

We prepared explant tissues (ET) from human and macaque tissue samples. From human tissues we prepared and studied the endocervix and ectocervix, while from macaque tissues we prepared and studied the endocervix only. For our experiments, ET from macaques were treated in the same manner as ET from humans. ET were prepared from fresh hysterectomy specimens as detailed above for primary epithelial cells. ET were prepared on the same day of womb resection by removing excess muscle tissue from epithelium and stroma and cutting the remaining tissue into 2-3mm*2-3mm blocks. Each tissue block was placed in a

single well of a round-bottomed 96 well plate with 200µL of complete media. This tissue was maintained in R-PMI 1640 medium (Sigma-Aldrich®, UK) supplemented with 10% FBS, L-glutamine and antibiotics (penicillin/streptomycin, gentamycin and fungizone) and incubated at 37^0C 5% CO_2. We harvested supernatants after 24 hours of plating for estimating constitutive levels of MIP-3α. For estimating stimulated levels of MIP-3α, we exposed explant tissues to stimulants immediately after preparing them and subsequently harvested supernatants 24 hours later. We afterwards estimated constitutive and stimulated MIP-3α levels with the sandwich enzyme-linked immunosorbent assay (Elisa) in human samples and the Luminex multiplex bead immunoassay in human and macaque samples.

Cryopreservation of tissues:

Following trypsinisation to prepare single cells, HEC-1A and Caco-2 cells were frozen down at 10^6 cells per mL in complete McCoy's medium and DMEM, respectively, supplemented with 5% DMSO. Single cell suspensions of EPECs were prepared with TrypLE™ and 10^6 cells per mL frozen down in 90% FBS and 10% DMSO. To freeze down blocks of tissue for subsequent ET and/or EPECs preparation, we cut hysterectomy samples into tissue blocks comprising epithelium and stromal tissue into maximal dimensions of 2cm long by 1cm wide, and 1cm in depth (epithelium to stroma). We then placed the tissue blocks into 1.8mL cryovials containing 1mL of sterile freezing mix (90% FBS and 10% DMSO). All epithelial tissue models were stored at -80^0C in a Mr Frosty for the first 24 to 48 hours before being transferred to liquid nitrogen for further storage until processing.

Thawing of tissues:

Vials of frozen tissues/cells from liquid nitrogen storage were transported to the laboratory in a vessel filled with dry ice. Once respective media had been pre-warmed to 37°C in the water bath, the cryovials containing tissues/cells were briefly placed in a 37°C waterbath, one vial at a time, and removed before the last triangular clump of ice had been thawed. Tissues/cells were then immediately transferred to respective vessels with pre-warmed media for incubation at 37^0C 5% CO_2 for 24 hours to wash off DMSO. Cell preparations were then passaged two or thee times over a 2-week period to achieve cell recovery while the tissue blocks were ready for explant tissue experiments after 24 hours of incubation.

Encouragement and enhancement of polarisation: Transwell® inserts:

Epithelial cells function in a polarised manner *in vivo* with unequal distribution of functions between the luminal and basolateral poles. Hence in this thesis epithelial cellular models were grown and studied with the aid of the Transwell® insert system (Clear Costar®, Corning®, UK) in certain instances. The Transwell® insert system is a system in which a plastic insert that comprises a membrane filter in the middle is inserted into each dome of the tissue culture plate in order to divide the dome into the apical and basal compartments. For epithelial cells, the use of permeable supports *in vitro* allows cells to be grown and studied in a polarised state under more natural conditions. With this system, cellular differentiation can also proceed to higher levels resulting in cells that morphologically and functionally better represent their *in vivo* counterparts. Further, these permeable supports permit cells to uptake and secrete molecules on both their basal and apical surfaces and thereby carry out metabolic activities in a more natural fashion. Hence Transwell® inserts provide independent access to both sides of a

monolayer, thus enhancing the ability to study transport, absorption, secretion, electrophysiological and other metabolic activities *in vitro*. Consequently, for our analyses, epithelial cellular models were grown on the microporous membrane of the apical compartment of the Transwell® insert system (24 well 0.4μm pore size 6.5mm polyester membrane diameter) to encourage epithelial polarisation while enhancing assessment of monolayer formation and its function.

Assessment of monolayer formation: transepithelial electrical resistance (TEER):

TEER is an electrophysiological measure of *in vitro* cellular permeability, which indirectly assesses formation of tight junctions. Using a Voltohmmeter® (EMD Millipore Millicell-ERS2, Merck Millipore, UK) electrical current was passed via the electrodes across the monolayers and TEER was calculated and expressed in Ohm's. Adequacy of confluence of the cellular monolayer was determined by an increase in TEER. A TEER reading above 300Ω was generally regarded as adequate in these experiments. However, for each cellular model we measured serial daily TEER until a maximal TEER had been reached for measuring constitutive levels of MIP-3α and conducting experiments on stimulated levels of MIP-3α.

CELL STAINING: SURFACE AND INTRACELLULAR MARKERS:

EPECs and HEC-1A cells grown in 24 well tissue culture plates at passage three and passage 15, respectively, were used to do flow cytometric analyses for phenotypic expression of Toll-like receptors (TLRs). After preparing single cell suspensions of each cell type, we seeded 10^6 cells per fluorescence-activated cell sorting (FACS) tube. We then stained cells with the Live/Dead stain

(LIVE/DEAD® Fixable Aqua Dead Cell Stain Kit (ThermoFisher Scintific, Molecular Probes™, UK)) before proceeding with whole cell staining, staining for both surface and intracellular TLRs. We permeabilised and fixed cells according to the manufacturer's protocol using the commercial Fixation/Permeabilisation solution kit (BD Cytofix Cytoperm™: BD Biosciences, UK). Specifically, we incubated cells with fluorescent antibodies for 45 minutes each before and after the permeabilisation and fixation step. We used mostly murine monoclonal antibodies (Table 2.1). We used antibodies at 1µL per 10^6 cells. After incubation with antibodies, cells were washed in Dulbecco's Phosphate-Buffered Saline (PBS) (ThermoFisher Scientific, Gibco®, UK) with 1% FBS and 0.1% sodium azide (Sigma-Aldrich®, UK) and analysed with a FACS flow cytometer software. The analysis was done in two panels in view of overlapping antibody stains.

Table 2.1: Antibodies used for TLR characterisation by flow cytometry

Antigen	Ig species and class	Clone	Fluorohrome conjugated	Manufacturer
TLR1	Goat polyclonal IgG	FAB1484A	APC	R&D Systems, Bio-Techne
TLR2	Mouse monoclonal IgG_{2B}	383936	PerCP	R&D Systems, Bio-Techne
TLR3	Mouse monoclonal IgG_1	40C1285.6	FITC	Abcam
TLR4	Mouse monoclonal IgG_{2a}	HTA125	PE-Cyanin 7	eBioScience
TLR5	Mouse monoclonal $IgG2_a$	19D759.2	PerCP	Novus Biologicals, Bio-Techne
TLR6	Mouse monoclonal IgG_1	TLR6.127 PE	PE	Biolegend®
MIP-3α	Mouse monoclonal IgG_1	67310	PE	R&D Systems, Bio-Techne
EpCAM	Mouse monoclonal IgG_1	EBA-1	FITC	BD Biosciences

IMMUNOSTIMULANTS:

TOLL-like receptor ligands

We tested the hypothesis that the exposure of epithelial cells to HIV-1 triggers MIP-3α secretion by epithelial cells in the FGT. We used a series of Toll-like receptor (TLR) ligands and recombinant interleukin 1 beta (IL-1β) as a positive control. Following initial dose titration experiments in HEC-1A cells immunostimulants were used at fixed concentrations throughout the study based on the levels of MIP-3α achieved following stimulation with TLR ligands in HEC-1A cells (*Table 2.2).*

Table 2.2: TLR ligands used to trigger MIP-3α secretion by epithelial models

TLR ligand	Full name of TLR ligand	Concentration	Manufacturer	Comments
TLR1/2	Pam_3CSK_4	20 µg/mL	Tocris, Bio-Techne	synthetic triacylated lipopeptide (LP) mimicking bacterial LP
TLR2	Zymosan	10 µg/mL	Sigma-Aldrich®	prepared from yeast cell wall of saccharomyces cerevisiae
TLR3	Poly I:C (Polyinosinic–polycytidylic acid sodium salt)	25 µg/mL	Sigma-Aldrich®	synthetic analog of double-stranded RNA (dsRNA), a molecular pattern associated with viral infection
TLR4	LPS (Lipopolysaccharides)	10 µg/mL	Sigma-Aldrich®	from *Escherichia coli* 0111:B4. LPS is a characteristic component of the cell wall of Gram-negative bacteria
TLR5	Flagellin	20 ng/mL	Sigma-Aldrich®	from Salmonella typhimurium
TLR6/2	FSL-1 (Pam2CGDPKHPKSF)	2 µg/mL	Invivogen	is a synthetic diacylated LP derived from Mycoplasma salivarium
IL-1β	IL-1β (recombinant interleukin beta)	10 ng/mL	R&D Systems, Bio-Techne	secreted pro-inflammatory cytokine that participates in the response to local injury and infection

Asssessment of cytotoxicity: Prestoblue® assay

We titrated the dose of immunostimulants using the Prestoblue® cell viability reagent (ThermoFisher scientific, Molecular Probes™, UK) to exclude cytotoxicity in HEC-1A cells. PrestoBlue® is a ready-to-use reagent for rapidly evaluating the viability and proliferation of live cells. It is a cell permeable resazurin-based solution that is modified by the reducing environment of the viable cell. It turns red in color in metabolically active cells. We plated 50,000 HEC-1A cells in 96 well tissue culture plates with 200µL of complete media, changing media every two to three days. Immunostimulants were applied on Day 5 and the cytotoxicity test done at 6 hours, 12 hours and 48 hours post stimulation. We added 20µL of PrestoBlue™ into each well and read the results after 20 minutes. Metabolic activity was subsequently assessed with an Elisa reader. Quantitation was based on a standard curve after optical density (OD) measurements at 570 nm on an Elisa reader. Metabolically active cells had higher absorbance values than cells that were not metabolically active.

IMMUNOASSAYS:

Sandwich MIP-3α Elisa:

The concentration of MIP-3α was measured in supernatants generated from epithelial cellular and tissue models using the sandwich Elisa. Supernatants were used undiluted in the assay as much as was possible. MIP-3α was measured using the human MIP-3α Duoset Elisa kit (R&D Systems, Bio-Techne, UK) according to the manufacturer's protocol. Briefly detection was enhanced using the streptavidin-horseradish peroxidase (HRP) enzyme system. The substrate was based on the hydrogen peroxide tetramethylbenzidine (H_2O_2 TMB) system. Data were collected

using the POLARstar Omega Elisa reader. Quantitation was based on a standard curve after OD measurements at 450nm on an Elisa reader. The lower limit of detection of MIP-3α with this assay was around 6,25 pg/mL.

Luminex multiplex bead assay:

- ***In-house 22-plex human Luminex panel:***

The Imperial College London laboratory had a pre-existing in-house Luminex panel that measured concentrations of 22 various cytokines. The concentrations of these 22 cytokines were measured in supernatants generated from epithelial cellular and tissue models. The cytokines measured fell in one of six functional groups: pro-inflammatory, adaptive, chemokine, growth, haematopoietic and antimicrobial peptide functions. Specifically, the cytokines included: interleukin 1 alpha (IL-1α), interleukin 1 beta (IL-1β), interleukin 6 (IL-6), interleukin 12 (IL-12), interleukin 16 (IL-16), tissue necrosis factor alpha (TNF-α), interleukin 2 (IL-2), interleukin 4 (IL-4), interleukin 15 (IL-15), interferon gamma (IFN-γ), interleukin 8 (IL-8), interferon gamma-induced protein 10 (IP-10), monokine induced by gamma-interferon (MIG), monocyte chemotactic protein 1 (MCP-1), macrophage inflammatory protein-1 beta (MIP-1β), stromal cell-derived factor 1 beta (SDF-1β), regulated on activation, normal T cell expressed and secreted (RANTES) granulocyte-macrophage colony-stimulating factor (GM-CSF), granulocyte-colony stimulating factor three (G-CSF), transforming growth factor beta (TGF-β), and interferon beta (IFN-β). Data were collected using a Bio- Plex^{TM} Suspension Array Reader (Bio-Rad Laboratories InC®). The lower limit of detection ranged between 1,7 and 266,6pg/mL for the cytokines measured. Specifically the cytokines with respective lower detection limits in pg/mL in this panel included: the lower limit of detection was 4.2pg/mL for IP-10, IL-1β, IL-16, GM-CSF, IL-4, IL-2, RANTES, IFN-γ, IFN-β, TNF-α, SDF-1β,

MIG, MIP-1β, IL-8, MCP-1, IL-6, G-CSF. The lower limit of detection was 2.4pg/mL for IL-1α, TGF-β, IL-12, and IL-15.

- ***Incorporating MIP-3α and IL-7 into the already existing 22-plex in-house assay:***

Until recently, MIP-3α was not measured routinely and hence it was not a constituent of commercially available Luminex kits. In order to conduct MIP-3α studies in this thesis we therefore had to incorporate it into the existing in-house panel. The original Luminex in-house panel comprised two sub-panels: the high-plex panel measuring four cytokines (IL-6, IL-8, MCP-1 and G-CSF) and the low-plex panel measuring the rest of the 18 cytokines. We subsequently added MIP-3α and interleukin 7 (IL-7) into the high-plex panel. This entailed, in a step-wise manner, coupling capture antibodies to the beads, testing for successful coupling, optimising standard concentrations, incorporating into the existing cocktails, and excluding cross-reactivity with the four other analytes that were already in the panel. The lower limit of detection was 4.2pg/mL and 0.8pg/mL for MIP-3α and IL-7, respectively *(Refer 2.A*). After optimising the high-plex panel by adjusting the concentrations for the standard curve and excluding cross-reactivity with other analytes, magnetic beads were used to do the assay *(Refer 2.B)*. These first two panels were subsequently used for analyses discussed in Chapter six of this thesis.

- ***A further in-house 8-plex human Luminex panel comprising more antimicrobial peptides and IL-10:***

The Imperial College London laboratory investigators subsequently developed an

A.

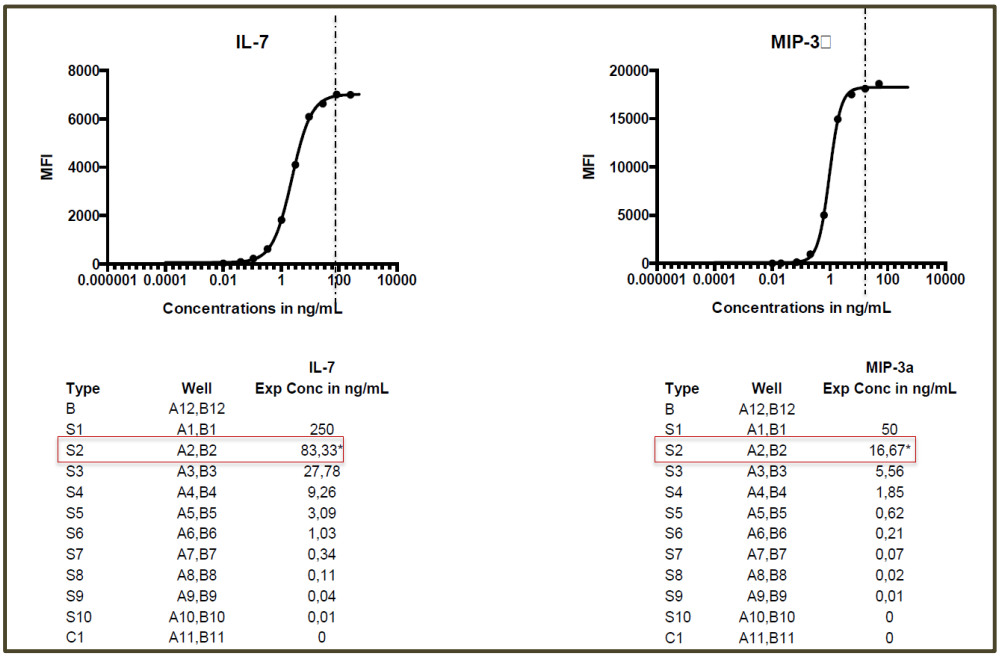

Type	Well	IL-7 Exp Conc in ng/mL
B	A12,B12	
S1	A1,B1	250
S2	A2,B2	83,33*
S3	A3,B3	27,78
S4	A4,B4	9,26
S5	A5,B5	3,09
S6	A6,B6	1,03
S7	A7,B7	0,34
S8	A8,B8	0,11
S9	A9,B9	0,04
S10	A10,B10	0,01
C1	A11,B11	0

Type	Well	MIP-3a Exp Conc in ng/mL
B	A12,B12	
S1	A1,B1	50
S2	A2,B2	16,67*
S3	A3,B3	5,56
S4	A4,B4	1,85
S5	A5,B5	0,62
S6	A6,B6	0,21
S7	A7,B7	0,07
S8	A8,B8	0,02
S9	A9,B9	0,01
S10	A10,B10	0
C1	A11,B11	0

B.

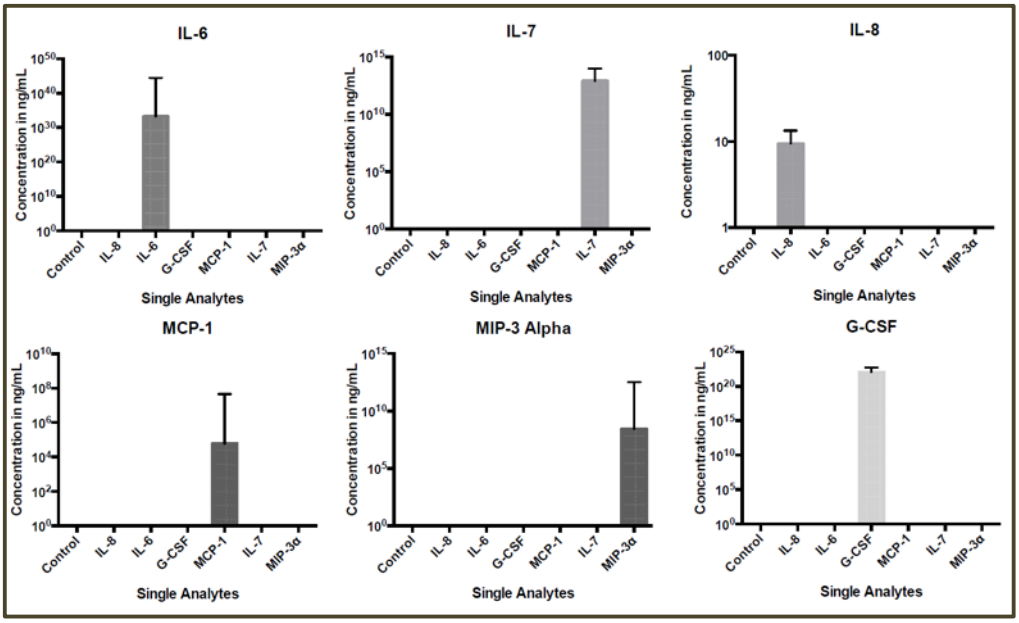

Figure 2: Bead coupling and Luminex optimisation of in-house panel: A.) standard concentrations titrated down until optimum concentration was established at the original S2 concentration. B.) cross reactivity of analytes in the high plex panel excluded.

additional 2 Luminex sub-panels to incorporate interleukin 10 (IL-10), an anti-inflammatory cytokine and seven other antimicrobial peptides: secretory leukocyte protease inhibitor (SLPI), Elafin, P-selectin, L-selectin, human beta defensin 2 (HBD2), human beta defensin 3 (HBD3), and human neutrophil peptides (HNP) 1-3. These latter two sub-panels were subsequently used for the analyses discussed in Chapter five of this thesis.

- ***Commercial macaque Luminex panel:***

Concentrations of 11 cytokines including MIP-3α were measured in supernatants generated from macaque EET using the commercial non-human primate Luminex multiplex bead assay. The cytokines measured fell in one of three functional groups: the pro-inflammatory, adaptive and chemokine groups. These cytokines were measured using the custom made MILLIPLEX MAP Non-Human Primate Cytokine/Chemokine - 11-Plex Premixed Immunology Multiplex Assay Kit (Merck-Millipore, France) according to the manufacturer's protocol. Data were collected using a Bio- Plex^{TM} Suspension Array Reader (Bio-Rad Laboratories InC®). The lower limit of detection ranged between 1.7 and 266.6pg/mL for the cytokines measured. Specifically the cytokines with respective lower detection limits in pg/mL in this panel included: IL-1α (14.3), IL-6 (1.4), IL-16 (64.3), TNF-β (39.0), IL-2 (5.5), IL-4 (61.9), IL-17A (1.7), IL-17E/IL-25 (266.6), IP-10 (5.9), MIP-3α (3.6), and RANTES (1.7).

Flow cytometry:

We conducted phenotypic studies of TLR expression on some epithelial cellular models. After conducting whole cell staining as described above, samples were analysed on the CyAn Advanced Digital Processing (ADP) High-Performance Flow

Cytometer (DakoCytomation), acquiring a minimum of 200 000 events. Gating was used to select epithelial cell populations based on typical patterns of forward scatter and side scatter. Raw data generated were subsequently analysed with FlowJo version 10.0.8.

MOLECULAR BIOLOGICAL TECHNIQUES:

In order to study the impact of viral exposure to epithelial models with regards to MIP-3α secretion, we acquired and/or prepared various viral preparations. Specifically we acquired one HIV-1 preparation and three Simian Immunodeficiency Virus (SIV) preparations while we prepared three HIV-1 preparations.

SIV preparations:

We used infectious whole SIVmac251/CSH and recombinant SIVmac251 gp130 (kindly donated by Professor Neil Berry at the National Institute for Biological Standards and Control (NIBSC), UK), and native SIVmac251 gp120 (generously donated by Professor Marjorie Robert-Guroff at the National Institutes of Health, National Cancer Institute, United States of America).

HIV-1 preparations:

We used readily available soluble recombinant HIV-1 CN54gp140 (kindly donated by Dr Katja Klein at the Imperial College London) while we made the following stocks: inactivated HIV-1 BaL, HIV-1 CN54gp120 viral-like particles (VLPs) and envelope deficient HIV-1 NL4-3.

Exclusion of endotoxin contamination: Polymyxin B test

We used Polymyxin B Sulphate (Calbiochem, Merck Millipore, UK) to exclude endotoxin contamination of recombinant CN54gp140. After dose titration we used it at 20µg/mL. We treated HEC-1A cells with Polymyxin B for 30 minutes prior to addition of various concentrations of gp140. Polymyxin B is a cationic antibiotic containing five positive charges associated with the free amino group on the diaminobutyric acid molecule. It has bactericidal action in Gram-negative bacteria. It has specifically been shown to bind to the negatively charged phosphate groups on lipopolysaccharides (LPS).

Growth of laboratory HIV-1 stocks:

1. ***R5 tropic whole BaL***

Virus was produced in anti-CD3 antibody [OKT3], phytohaemagglutinin (PHA), and interleukin-2 (IL-2) stimulated peripheral blood mononuclear cells (PBMCs). After cell lysis with Triton™ X-100 detergent (Sigma-Aldrich®, UK), supernatants were harvested and Aalto Elisa done to determine p24 antigen yields.

- ***Viral inactivation:***

Whole BaL was treated with 2,2*-dithiodipyridine (aldrithiol-2; AT-2) to render it non–infectious. After filtration of the viral solution above, 10µL of AT-2 stock solution was added to 1mL of virus solution. After overnight incubation at 4^0C virus particles were purified by ultracentrifugation, and estimation of p24 content conducted by Aalto p24 Elisa.

- ***TZM-bl luciferase based HIV-1 infectivity assay:***

The infectivity assay was done to confirm lack of infectivity of AT-2 treated virus.After titration to optimal viral concentration, TZM-bl cells were added to AT-2 inactivated virus per well of a 96 well tissue culture plate. After incubation at 37^0C for 24hours, supernatants were aspirated, cells lysed with the luciferase substrate, and light intensity of each well measured on the Luminimeter.

- ***Detection and characterization of viral replication: HIV-1 p24 antigen Elisa***

An Aalto HIV-1 p24 antigen Elisa kit (Aalto Bio Reagents, UK) was used to detect and quantify HIV p24 gag proteins in viral lysates and p24 quantitation was conducted according to the manufacturer's protocol. A chemiluminescent substrate for alkaline phosphatase with enhancer (CSPD with Sapphire) was used for detection. p24 was detected and quantified using the Luminimeter (SPECTROstar omega).

2. *X4 tropic envelope deleted NL4-3*

- ***DNA manipulation and transfection:***

X4 tropic NL4-3: env-deleted NL4-3 was formed from the PNL_LUC-R-ENV plasmid based on the HIV-1 proviral clone PNL4-3. Bacterial transformation with E. Coli using heat shock was used to amplify DNA. DNA was transfected into 293T cells using polyethylenimine (PEI). Supernatants with virus were harvested on day 3 post transfection. Viral p24 antigen was quantified using the ABL HIV-1 p24 antigen capture Elisa assay (ABLinc, UK), according to the manufacturers protocol. Quantitation was done based on a standard curve after OD measurements at 450 nm in an Elisa reader.

Production of non-infectious molecular clones:

3. *CN54gp120 VLPs*

- ***DNA manipulation and transfection***

gp120 virus-like particles (VLPs) were formed by assembly of the pREC-NFL vector with HIV-1 CN54gp120 envelope DNA. Bacterial transformation with E.coli using heat shock was used to amplify DNA. To isolate and purify DNA from bacterial culture, we used the Qiagen® miniprep kit. DNA digestion was done for gel identification. Nanodrop was used to quantify DNA in specimen and to assess for purification. The DNA was transfected into HEK-293T cells using polyethylenimine (PEI). Virus was concentrated using the ultrafiltration column. p24 was detected and quantified using the Luminimeter (SPECTROstar omega).

- ***Particle calculation with Nanosight technology***

The NanoSight Nanoparticle Analysis System was used to quantify VLPs. This system is a particle-by-particle methodology that measures the size of each particle from direct observations of diffusion and validates all data with video files of the particles moving under Brownian motion. It typically characterises nanoparticles from 10nm to 2000nm in solution.

DATA MANAGEMENT and STATISTICAL ANALYSES:

For *in vitro* cellular assays, cells were seeded in triplicate wells. Experiments were repeated at least three times before being included in the analyses for this thesis. For *ex vivo* explant tissue assays, explants were seeded at one explant per well but each condition was tested in triplicate. Data were generated from the Elisa and

Luminex immunoassays as discussed above and data managed and stored on Microsoft Excel (Version 2011 for Mac). For Elisa generated data, MIP-3α quantitation was done based on a 4PL regression curve fitted formula from the standard curve after OD measurements at 450 nm. For Luminex generated data, 5 PL regression curve fitted formula was used to calculate analyte concentrations from the standard curves on GraphPad Prism. Statistical analyses were performed using GraphPad Prism version 7 for Mac OS X (Prism, GraphPad Software, La Jolla, California, USA) and Microsoft Excel. Descriptive data were presented with schema prepared from Microsoft Excel and GraphPad Prism. Levels of MIP-3α and all other analyte levels were expressed in pg/mL. Results were reported in bar graphs with bars representing analyte levels in mean pg/mL and error bars representing standard deviation. Unpaired two sample *t*-tests were performed to compare unstimulated (medium only) to stimulated MIP-3α levels. Changes in mean concentrations of protein levels in CVF across the three visits per single menstrual cycle were evaluated using one-way analysis of variance (one-way ANOVA). One sample t-tests were used to assess statistical significance for down-/up-regulated analytes based on fold changes in analyte concentrations. For flow cytometry generated data, data was presented as histograms prepared on FlowJo version 10.0.8. Cell expression of TLRs was presented as a percentage of cells taking up the stain, comparing stained and unstained epithelial cells. P-values were taken as non-significant if $p>0.05$, and significant if $p \leq 0.05$ (*), $p \leq 0.01$ (**), $p \leq 0.001$ (***), and $p \leq 0.0001$ (****).

CHAPTER THREE

CONSTITUTIVE BASELINE EXPRESSION OF MIP-3α IN SIX BIOLOGICAL MATRICES

SUMMARY

Despite much progress made in elucidating the contribution of innate immunity in Human Immunodeficiency Virus (HIV) infection and transmission across mucosal surfaces, there still remain gaps to be addressed in understanding both the breadth and depth of innate immune responses and their contribution to pathogenesis, thereby informing the development of HIV prevention strategies. Until recently the role of epithelial surfaces as part of the mucosa in reducing /preventing HIV infection has been underestimated and yet epithelial surfaces are believed to contribute to the well-appreciated inefficiency of infection following exposure to virus. While biological determinants of the outcome of infection following exposure to sexually transmitted HIV include factors such as viral characteristics, host genetic architecture, and responses by the different limbs of the immune system at the portal of entry, the innate immune system is right at the forefront of exposure and is probably more potent in its response than previously recognised. Inherently, if we could understand this first step in pathogenesis, we could be better positioned and equipped to develop more robust and efficacious biomedical prevention strategies such as microbicides and vaccines to reduce the burden of HIV infection. We studied macrophage inflammatory protein-3 alpha (MIP-3α), a CC chemokine previously shown to be secreted primarily by the epithelium in various sites in the body. MIP-3α has been studied at length in humans but mostly in association with dermal and gastrointestinal tract conditions. Also, while it has somewhat previously been studied in the female genital tract (FGT), it has been studied mainly in the vaginal and endometrial sub-compartments but not in the

endocervical sub-compartment. Moreover, it has hardly ever been studied in the context of HIV infection. After the landmark study by Li *et al* highlighted the endocervix as the primary site of infection and the significant association of MIP-3α with early SIV infection events in the endocervical epithelium of macaques [96], we sought to study constitutive secretion patterns of the same in the human FGT, focusing mainly on the endocervical epithelial models. In view of the fact that the FGT functions in a compartmentalised fashion, and that the constitutive secretion pattern of MIP-3α had previously been shown to be in a very site-specific fashion, we included an endometrial cell line, endocervical primary epithelial cells (EPECs), endocervical explant tissues (EET), and cervicovaginal fluid (CVF) in our analysis. For comparison purposes and the sake of completeness, we also studied a colorectal cell line and serum. We evaluated secretory patterns of MIP-3α in polarised HEC-1A cells, an endometrial cell line, and EPECs grown on permeable supports. We subsequently validated results with levels secreted from the EET. We quantified levels of MIP-3α in tissue supernatants with either a sandwich Elisa or a Luminex multiplex bead array immunoassay. All FGT tissues studied including the CVF concentrate expressed MIP-3α constitutively. Constitutive levels of MIP-3α in these sub-compartmentss, however, varied, with highest levels seen in the endocervical models. The colorectal cell line also expressed constitutive MIP-3α while the blood compartment had below quantitation levels of MIP-3α. These results therefore showed that various sub-compartmentss the FGT are a rich source of MIP-3α, while also confirming epithelial surfaces as its dominant source in the FGT of humans.

INTRODUCTION

The epithelium is at the forefront of virus exposure yet the importance of studying and understanding how epithelium contributes to the appreciated inefficiency of HIV infection has been under-appreciated. The epithelium, over and above being a barrier, secretes and transports molecules, which modulate vulnerability and/or resistance to infection. Thus if we could understand the baseline innate epithelial status as it pertains to secretion of infection-modulating molecules, we would be better equipped to develop efficacious biomedical prevention strategies to reduce the burden of HIV infection in women.

Whereas previously the epithelium was thought to function solely as a barrier to passage of microorganisms, it has now become understood that it also has other immune functions that regulate infection across the genital epithelium [71, 98]. While the epithelium has been shown to secrete a range of cytokines and chemokines that link the innate to the adaptive immune systems on the one hand, it has also been shown to secrete a wide range of antimicrobial peptides such as defensins [99] and secretory leukocyte protease inhibitor (SLPI) [100] that have direct anti-HIV-1 activity. MIP-3α is one other such molecule [101].

MIP-3α is a chemokine that belongs to the CC chemokine group of molecules [81]. MIP-3α was first discovered through bioinformatics in 1997 [90]. From thence MIP-3α was studied in the FGT from the early 2000s. Data from *Sun et al* demonstrated for the first time that cells of the FGT secrete MIP-3α [102]. Their findings revealed

that an endometrial epithelial cell line (ECL), (HHUA1[4]), secreted MIP-3α both constitutively and on stimulation with the inflammatory mediators tumor necrosis factor alpha (TNF-α) and interleukin 1 beta (IL-1β). Subsequently, Cremel *et al* showed that the vagina ECL (SiHa[5]) and primary epithelial cells of the vagina equally secreted MIP-3α and that this secretion was both constitutive and up regulated by the inflammatory mediator IL-1β [93]. Data from Wira *et al* subsequently showed that primary epithelial cells of the endometrium secrete MIP-3α constitutively and on exposure to pathogen associated molecular patterns (PAMPs) poly I:C, a TLR 3 agonist [85]. However, none of these or other groups has studied secretion of MIP-3α by the human cervix, in the form of either the cervical epithelial lines or the cervical explant models. We therefore designed a study to primarily focus on the secretion of this molecule, MIP-3α, by the endocervical epithelial models.

This was particularly important and relevant against the backdrop of a study by Li *et al* highlighting the importance of the role that viral triggered secretion of MIP-3α by the epithelial cells has on initial events in Simian Immunodeficiency Virus (SIV) infection [96]. In this study, they noted that the accumulation of SIV RNA^+ $CD4^+$ T cells post exposure to virus in an SIV/Rhesus macaque model, was preceded by a subepithelial influx of plasmacytoid dendritic cells (pDCs) in the endocervix one day post inoculation, an effect that was not replicated in the vagina and transformation zone sub-compartments [96]. They subsequently determined that this accumulation of pDCs was associated with increased expression of MIP-3α.

[4] HHUA is an endometrial epithelial cell line shown to secrete MIP-3α on stimulation by TNF-α and IL-1β and not by LPS
[5] SiHa is a vaginal epithelial cell line shown to behave like primary vaginal cells with regards to epithelial cell differentiation and proliferative functions

Through a series of experiments they conducted, they concluded that exposure of endocervical epithelium to the viral inoculum triggers an “outside-in” signaling cascade which increases the expression of MIP-3α which in turn recruit pDCs, thereby commencing the sequence of events leading to productive infection. However, most studies focusing on the FGT have used endometrial cell lines to study HIV infection and transmission events, yet recent evidence suggest that the endocervix is the primary site of infection. Consequently this may not be entirely appropriate in view of the fact that several studies reveal that immune and endocrine functions and responses including secretion of molecules in the FGT occur in a compartmentalised fashion.

Givan *et al* studied leucocyte distribution and frequencies throughout the FGT starting from the fallopian tubes all the way down to the vagina, and his findings suggested a pattern of compartmentalisation of leucocyte distribution [56]. Data from Kumar *et al* showed that while SLPI was expressed throughout the FGT, it was however concentrated mainly in the endocervix versus endometrium, ectocervix, and vagina [96]. Likewise, Pudney *et al* showed that cellular immune responses concentrate in the transformation zone versus vagina, endocervix and ectocervix [58]. Endocervix was the primary compartment shown to develop productive infection after vaginal deposition of an SIV inoculum [96] and in an elegant study by Asin, it was shown that the ectocervix versus the endometrium is more readily infected with HIV and that it is more conducive to HIV replication [96]. The endometrium, on the other hand, is a site of extensive tissue remodelling during menstruation or parturition, which is characterised by finely-orchestrated processes to limit inflammation, involving a myriad of immune and endocrine factors. It is not unexpected therefore that the endocervix has the highest

concentration of these immune mediators as it represents the zone separating the richly colonised lower reproductive tract and the relatively sterile upper reproductive tract, being responsible for protection of the conceptus. In view of the fact that studies in this field have almost all used endometrial cell lines, we have hence designed a study that will primarily use endocervical cell lines and validate findings with EET.

We hypothesised that the endocervix, being immunologically distinct from other FGT sub-compartments and implicated in primary SIV infection, will have the highest concentration of MIP-3α in epithelial cell and tissue models versus endometrium and vagina, and that this concentration will be more pronounced in the explant tissues versus the cellular models.

MATERIALS and METHODS

We evaluated the constitutive expression of MIP-3α in *in vitro* epithelial cell models prepared from the different sub-compartments of the FGT, the endometrium and the endocervix; and the gastrointestinal tract (GIT). We used the *ex vivo* endocervical explant tissue model to validate results from the endocervical cellular model. We also measured constitutive MIP-3α levels in the cervicovaginal fluid and serum sub-compartments.

Epithelial cell lines:

- HEC-1A cells, an endometrial cell line derived from a human endometrial adenocarcinoma, were grown on the permeable membrane of the Transwell®

insert system (Corning®, UK) to encourage epithelial polarisation and assess monolayer formation (*Figure 3.1*). These cells were maintained in McCoy's medium (Sigma-Aldrich®, UK) supplemented with 10% foetal calf serum, L-glutamine, and antibiotics. Cells were seeded in the wells in the apical compartment only. Each well was seeded with 50,000 cells at passage 15, and apical and basal compartments were filled with 200 and 600µL of complete medium, respectively. Each test condition was tested in triplicate. We based the decision to work with a plating cell density of 50,000 cells

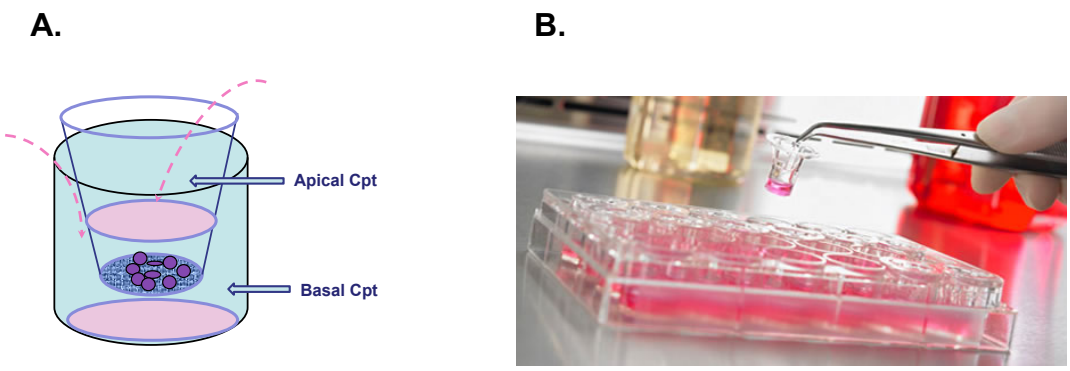

Figure 3.1 Schematic of the Transwell® insert system. (A.) shows cells (purple circles) plated on the permeable support in the apical chamber of the insert. Dotted lines denote media that was filled into both the apical and basal compartments at 200 and 600µL respectively. (B.) shows the plastic insert that separates apical from basal chambers of each dome of the 24 well tissue culture plate.

per well on the time it took to achieve 80 – 90% confluence on microscopy comparing 6 different plating densities (*Figure 3.2*). This decision was also based on the time it took to achieve lowest detectable levels of MIP-3α post plating on Elisa (*Figure 3.3*). Serial transepithelial electrical resistance (TEER) was measured daily with a Voltohmmeter® (EMD Millipore, Fisher Scientific,

UK) *Figure 3.4*) and constitutive baseline levels of MIP-3α levels were quantified in supernatants harvested when the TEER was maximal.

- Caco-2 cells, a colorectal cell line derived from a human colon adenocarcinoma, were grown in 24 well tissue culture plates. This cell line was grown in Dulbecco's modified eagle medium (DMEM - Sigma-

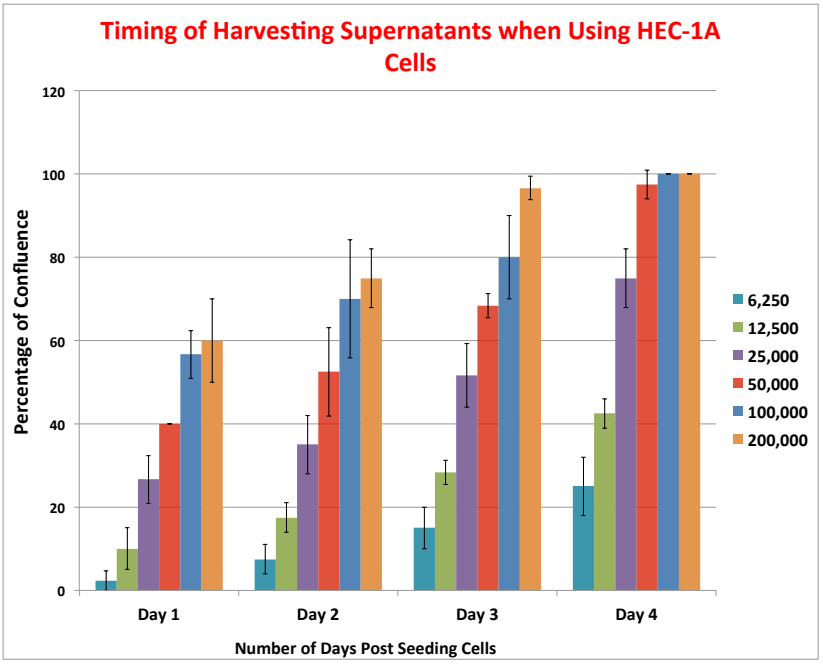

Figure 3.2 Bar graph showing percentage confluence achieved post cell plating as assessed on light microscopy (n=3). HEC-1A cells were plated in 24 well plates at different densities in 600µL of medium. Each test condition was tested in triplicate. Only cells plated at densities ≥50,000 reached confluence above 80% and this occurred on Day 4 post plating.

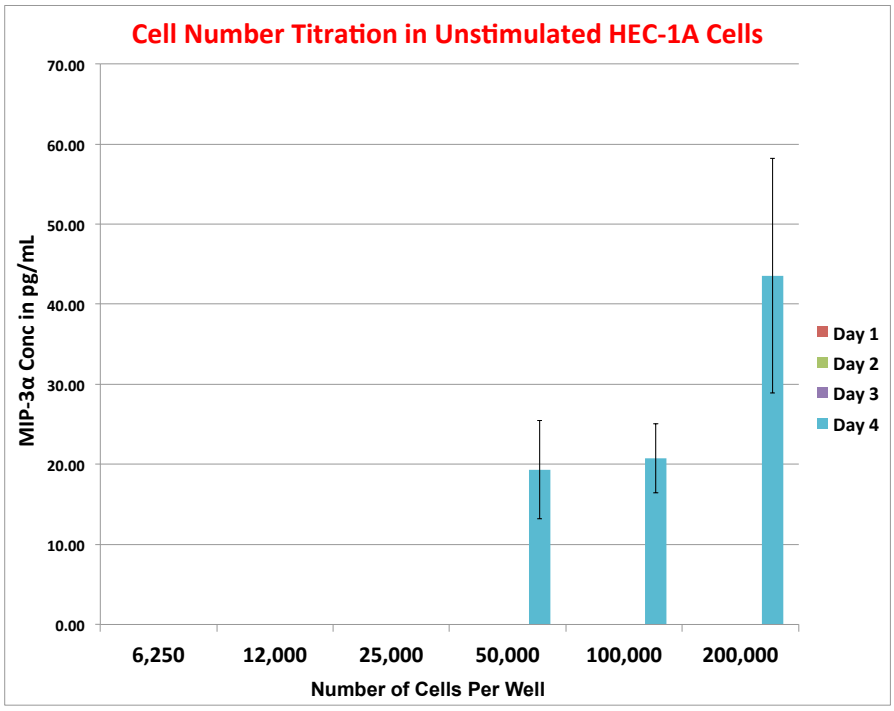

Figure 3.3 Bar graph showing threshold of MIP-3α detection as measured with a sandwich Elisa immunoassay (n=4). HEC-1A cells were plated in 24 well plates at various densities in 600µL of medium. Each test condition was tested in triplicate. MIP-3α levels were only detectable for the first time on Day 4 post plating and this was only with plating cell densities ≥50,000.

Figure 3.4 Schematic showing a Voltohmmeter for measuring transepithelial electrical resistance (TEER) in Transwell® Inserts. TEER is an electrophysiological measure of *in vitro* cellular permeability which indirectly assesses formation of tight junctions. TEER was measured on serial days starting from Day 1 post plating until the maximum was reached at which point it was estimated that cells had attained a near normal physiological functioning *in vivo*.

Aldrich®, UK) supplemented with 10% foetal calf serum, L-glutamine, and antibiotics. Each well was seeded with 50,000 cells filled with 600µL of complete medium. Each test condition was tested in triplicate. As part of optimisation, we harvested supernatants from three wells at a time on each day from Day 1 post plating and subsequently estimated MIP-3α levels on supernatants. After these experiments were completed we decided to define baseline as Day 4 post plating based on the time it took to detect lowest levels of MIP-3α (*Figure 3.5*). We also based this decision on the time it took to achieve 80 – 90% confluence post plating on microscopy and this was also on Day 4 post plating.

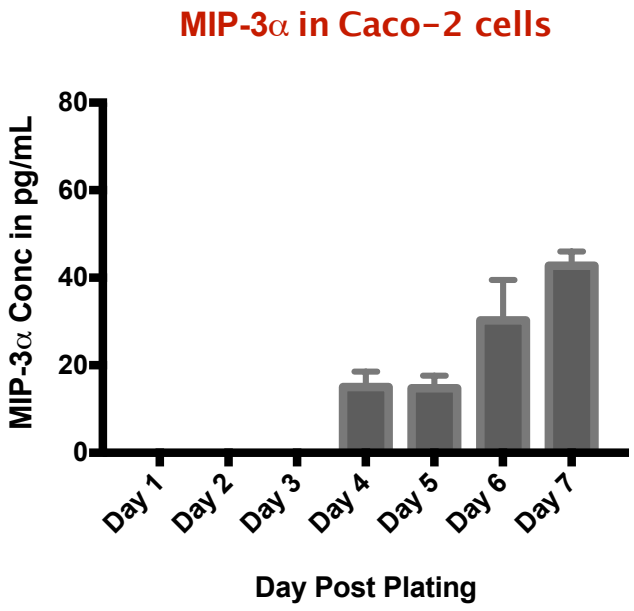

Figure 3.5 Bar graph showing threshold of MIP-3α detection as measured with a sandwich Elisa immunoassay (n=3). Caco-2 cells were plated in 24 well plates at 50,000 cells per well in 600µL of medium. Each test condition was tested in triplicate. MIP-3α levels were only detectable for the first time on Day 4 post plating.

Endocervical primary epithelial cells:

Endocervical primary epithelial cells (EPECs) were prepared from either fresh or frozen hysterectomy specimens. Single cells were extracted, isolated, and purified using a combination of mechanical and biochemical digestion techniques: a block of fresh tissue of about 2*1*1.5cm^3 size was soaked overnight in Dispase II (Life Technologies, Gibco®, UK) at 4^0C prior to being soaked in trypsin-EDTA (Sigma-Aldrich®, UK) in the incubator at 37^0C 5% CO_2 for 20 minutes. For cells prepared from frozen tissue blocks, tissue blocks were first incubated in complete RPMI-1640 (Sigma-Aldrich®, UK) overnight at 37^0C 5% CO_2 prior to exposure to Dispase II in order to soak off dimethyl sulphoxide (DMSO – Sigma-Aldrich®, UK). We then used the pasteur pipette to tease out single cells from underlying stroma and tissues. Serial 3-sized nylon meshes (100, 70 and 30 μM) were subsequently used to isolate single epithelial cells from cellular discs and debris. We then seeded single epithelial cells in 12 well tissue culture plates with 800μL of complete keratinocyte serum free medium (K-SFM - Life Technologies, Gibco®, UK). K-SFM was supplemented with human recombinant epidermal growth factor (rEGF), bovine pituitary extract (BPE), L-glutamine and antibiotics. A confluent monolayer took an estimated 21 days post plating to develop in 12 well tissue culture plates incubated at 37^0C 5% CO_2 (F*igure 3.6*). For experiments with EPECs, we subsequently seeded each well of the Transwell® insert with 50,000 cells at passage 3. Apical and basal compartments were filled with 200 and 600μL of complete medium respectively. TEER was measured daily with a Voltohmmeter® and constitutive baseline levels of MIP-3α levels were quantified in supernatants harvested when the TEER was maximal.

A. B.

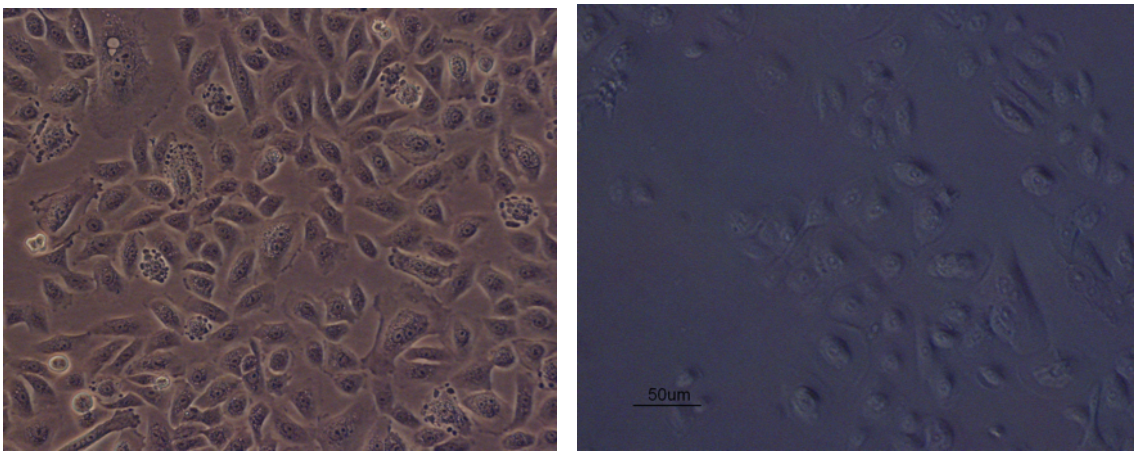

Figure 3.6. Endocervical primary epithelial cells (EPECS) on light microscopy in T25 flasks at passage 2 (A.) and at passage 3 (B.). Cells were suspended in K-SFM complete with antibiotics, rEGF, and BPE.

Cellular monolayer:

- ***Transwell inserts***

  The Transwell® insert system (*Figure 3.1*) was used to encourage epithelial polarisation and assess monolayer formation in HEC-1A cells and EPECs.

- ***Transepithelial electrical resistance (TEER):***

  Using a Voltohmmeter®, we passed electrical current (F*igure 3.6*) via the electrodes across the monolayers and TEER was calculated and expressed in Ohm's. A TEER reading above 300Ω was regarded as adequate in these experiments.

Endocervical explant tissues:

Endocervical explant tissues (EET) were prepared from tissue obtained from fresh hysterectomy specimens as detailed above for primary epithelial cells. EET were prepared on the same day of womb resection by removing excess muscle tissue from epithelium and stroma and cutting the remaining tissue into 2-3mm*2-3mm blocks (*Figure 3.7A and B.*). Each tissue block was placed in a single well of a round-bottomed 96 well plate with 200µL of complete media. This tissue was maintained in R-PMI 1640 medium (Sigma-Aldrich®, UK) supplemented with 10% foetal calf serum, L-glutamine and antibiotics and incubated at 37^0C 5% CO_2. We

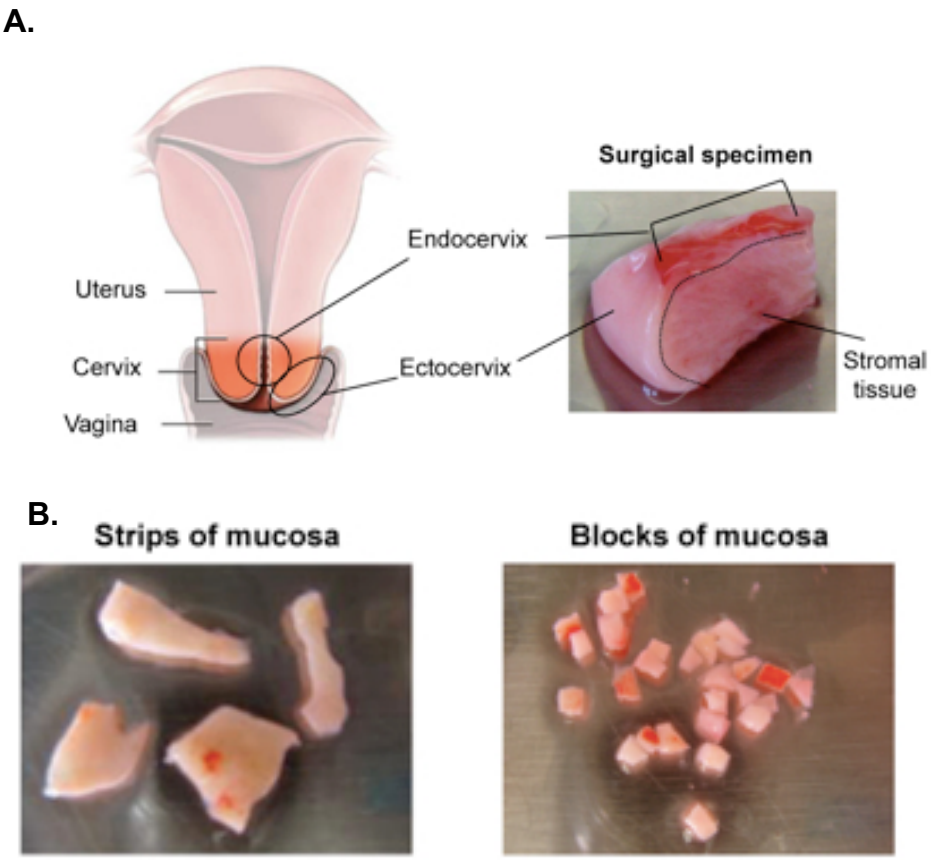

Figure 3.7. Endocervical explant tissues prepared from fresh hysterectomy specimens. Endocervix was dissected out of the womb (A.) and the blocks of explant tissues were subsequently prepared from the strips of endocervical tissue (B.). Source: [6].

harvested supernatants after 24 hours of plating. We subsequently estimated constitutive MIP-3α levels with a sandwich Elisa immunoassay.

Cervicovaginal secretions:

We collected CVF from the vaginal lumen with a menstrual cup, the Instead Cup™ (*Figure 3.8*), having been inserted and left in situ for 2 hours prior to being removed for storage. CVF was collected from women who were HIV uninfected. Consenting women were recruited from the vaccine clinic at St George's hospital, in London. Of note is that women were recruited if they had normal menstrual cycles and were outside of the menstrual window at the time of collecting the sample.

Blood:

Serum was also collected at the corresponding time points that CVF was collected

A.

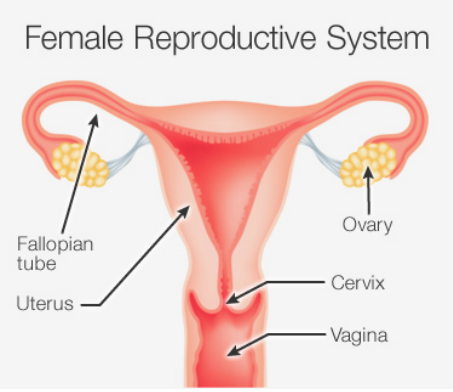

B.

Figure 3.8. Instead Cup™, a menstrual cup used to collect cervicovaginal fluid concentrate from the vagina in this study. Each woman was instructed to leave this cup (B.) in situ in the vagina (A.) for 2 hours post insertion.

and from the same participants. It was subsequently stored at -80^{0}C until the time that the MIP-3α estimation assay was performed.

Positive control:

For experiments estimating constitutive levels of MIP-3α, we used polyinosinic-polycytidylic acid (poly I:C), a Toll-like receptor (TLR) 3 agonist, as a positive control. We chose poly I:C because it is a synthetic analogue of double-stranded RNA (dsRNA), a molecular pattern associated with viral infection. It is recognised by TLR3 and it induces the activation of NF-ϰB and the production of cytokines. TLR3 is widely expressed in the endosomes on both poles of the epithelial cells of all FGT sub-compartments. Following dose titration experiments, poly I:C was used at a concentration of 25μg/mL (*Figure 3.9*). Cytotoxicity was excluded using Prestoblue®, (molecular probes™, Thermofisher scientific, UK) a cell viability indicator that turns red in color, becoming highly fluorescent in the presence of living actively proliferating cells (*Figure 3.10*). Absorbance was measured on an Elisa reader at an optical density (OD) of 570nm.

Media supplements:

Cellular and tissue models, with the exception of EPECs that were grown in K-SFM, were cultured in media supplemented with 10% heat inactivated foetal bovine serum (FBS) (Life Technologies, Gibco®, UK), 2 μM L-glutamine (Life Technologies, Gibco®, UK), and antibiotics (100 units/ml penicillin/streptomycin (Life Technologies, Gibco®, UK). Further, EET and EPECs were grown in 1μg/mL fungizone® (Life Technologies, Gibco®, UK), and 10μg/mL gentamycin (Life

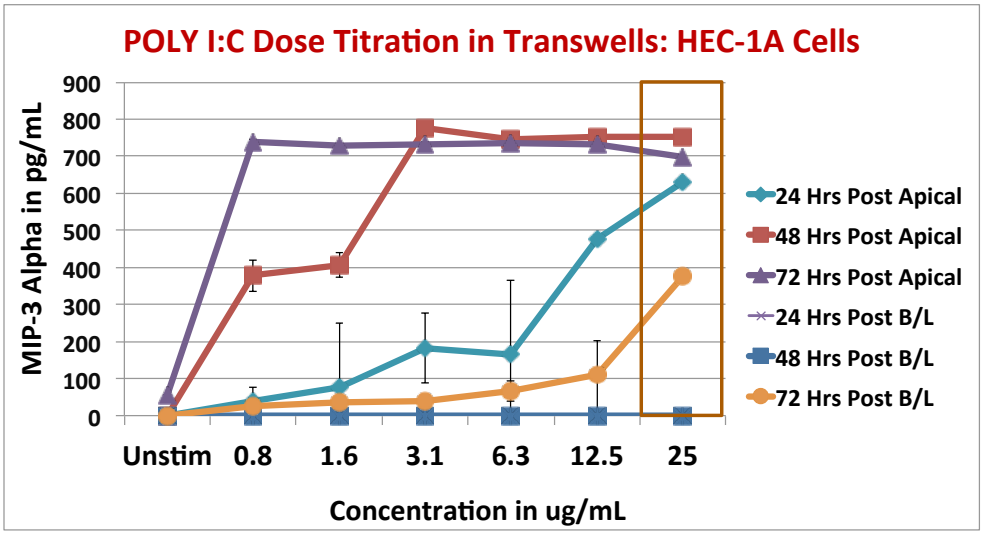

Figure 3.9. Dose titration of Poly I:C in HEC-1A cells seeded on the apical compartment of Transwell® inserts. HEC-1A cells were stimulated from apical and basal (B/L) compartments. Supernatants were harvested serially from Day 1 (24 Hrs) post plating to Day 3 (72 Hrs) post plating from the apical compartment. MIP-3α levels were quantified using the sandwich Elisa immunoassay. Conditions were tested in triplicate. Basal levels of MIP-3α approximated those of the apical compartment at a concentration of 25µg/mL of poly I:C in the first 24 hours post plating and we hence used this concentration for the rest of the experiments.

Technologies, Gibco®, UK).

Culture conditions:

Cellular and tissue models were cultured in respective media in the incubator at 37^0C in 5% CO_2. Supernatants were subsequently harvested and stored in round bottom 96 well tissue culture plates for future analysis with the respective protein quantitative immunoassay.

Storage:

Supernatants from EET and cellular models were stored in the freezer at -20^0C until future assay performance.

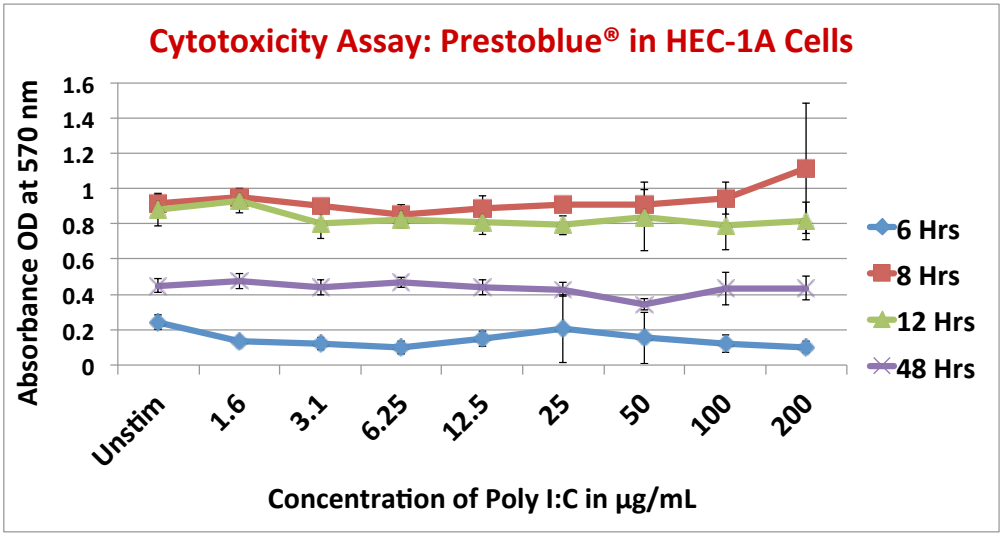

Figure 3.10. Cytotoxicity of Poly I:C in HEC-1A cells over first 48 hours post stimulation. HEC-1A cells were plated at 50,000 cells per well in 200µL of McCoy's medium in 96 well tissue culture plates. They were then stimulated with various concentrations of poly I:C on Day 5 post plating. The cytotoxicity assay was subsequently performed at four time points starting from six hours (6 Hrs) post plating to Day 2 (48 Hrs) post plating. Conditions were tested in triplicate. There was no evidence of cytotoxicity with all poly I:C concentrations tested over the first 48 hours post stimulation in HEC-1A cells.

Quantitative protein immunoassays:

The concentration of MIP-3α was measured in supernatants generated from cellular and tissue models using an Elisa sandwich assay. Conditions were tested in triplicate throughout the study. Supernatants were used undiluted in the assay as much as was possible. MIP-3α was measured using the human MIP-3α Duoset Elisa kit (R&D Systems, Bio-Techne, UK) according to the manufacturer's protocol. Briefly detection was enhanced using the streptavidin-horseradish peroxidase (HRP) enzyme system. The substrate was based on the hydrogen peroxide tetramethylbenzidine (H_2O_2 TMB) system. Data was collected using the POLARstar Omega ELISA reader. Quantitation was based on a standard curve after optical

density (OD) measurements at 450 nm on an Elisa reader. The lower limit of detection of MIP-3α with this assay was around 6,25 pg/mL.

The concentration of MIP-3α was also measured in CVF and serum using the Luminex multiplex bead assay. MIP-3α was measured as one of the cytokines in the in-house 6-plex high concentration panel (this will be discussed in greater detail in the next Chapters). Data was collected using a Bio- Plex™ Suspension Array Reader (Bio-Rad Laboratories InC®). The lower limit of detection of MIP-3α was 0.86pg/mL with this assay.

Statistical analyses:

Statistical analyses were performed using GraphPad Prism version 7 for Mac OS X (Prism, GraphPad Software, La Jolla, California, USA). For *in vitro* cellular assays, cells were seeded in triplicate wells. For *ex vivo* explant tissue assays, explants were seeded at one explant per well but each condition was tested in triplicate. For estimation of MIP-3α levels with Luminex in CVF and serum, each participant's samples were tested in triplicate. Statistical analyses were performed using GraphPad Prism version 7 for Mac OS X (Prism, GraphPad Software, La Jolla, California, USA). 5 PL regression curve fitted formula was used to calculate MIP-3α concentrations from the standard curves on GraphPad Prism for data generated from Luminex. For Elisa generated data, quantitation was done based on a 4PL regression curve fitted formula from the standard curve after optical OD CVF and serum measurements at 450 nm. Descriptive data were presented with schema prepared from Microsoft Excel (2011 version for Mac) and GraphPad Prism. Results were reported in bar graphs with bars representing the mean of

three tests and error bars representing standard deviation. Levels of MIP-3α were expressed in pg/mL.

RESULTS

In HEC-1A cells, an endometrial cell line, MIP-3α is expressed constitutively, and is apically polarized.

To study constitutive expression of MIP-3α we plated the apical compartment of Transwell® inserts with 50,000 HEC-1A cells per well in 200μL of complete McCoy's medium. We added 600μL of the same medium into the basal compartment. We then measured TEER serially from Day 1 post plating while also harvesting supernatants from both the apical and basal compartments on the same corresponding days. We measured MIP-3α levels on supernatants with a sandwich Elisa. Data showed that MIP-3α levels were detectable for the first time after maximal TEER had been reached on Day 4 post plating at which time they were detectable only in the apical compartment (*Figure 3.11*). TEER was highest around 500Ω on Day 4 post plating while MIP-3α levels were highest around Day 7 post plating at 60pg/mL. Detectable levels were consistently higher in the apical compartment than in the basal compartment. In fact, basal levels were not detectable until Day 8 post plating. The observation that TEER was maximal prior to detection of MIP-3α suggested the need for confluence and establishment of tight junctions for optimal functioning of the cell line. Hence we concluded that MIP-3α is a constitutively expressed chemokine by confluent HEC-1A cells. Additionally, it is secreted in an apically polarised fashion.

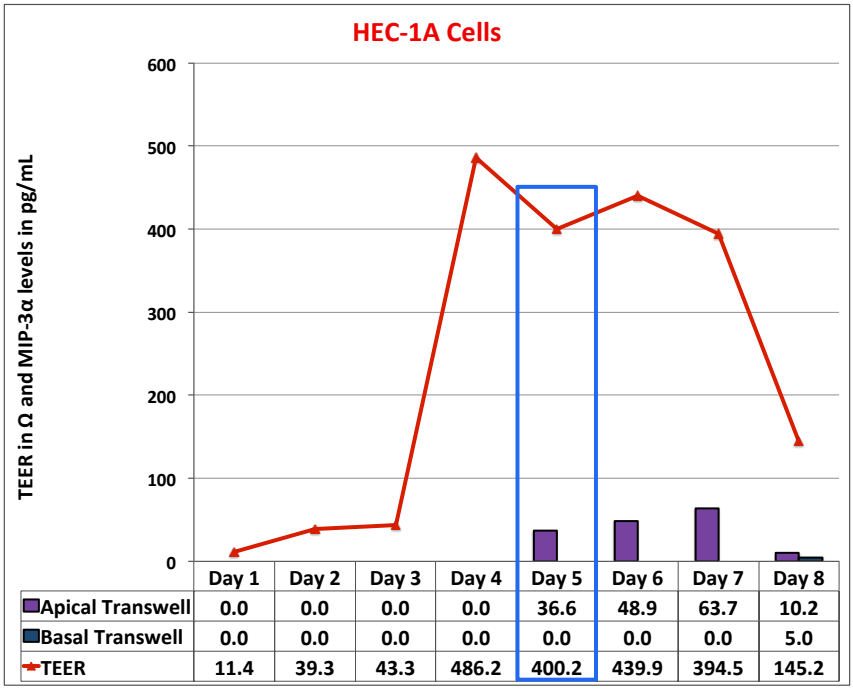

	Day 1	Day 2	Day 3	Day 4	Day 5	Day 6	Day 7	Day 8
Apical Transwell	0.0	0.0	0.0	0.0	36.6	48.9	63.7	10.2
Basal Transwell	0.0	0.0	0.0	0.0	0.0	0.0	0.0	5.0
TEER	11.4	39.3	43.3	486.2	400.2	439.9	394.5	145.2

Figure 3.11. Constitutive levels and polarisation of MIP-3α secretion in HEC-1A cells plated on permeable supports in the apical compartment of Transwell® inserts. TEER was measured serially from Day 1 post plating while supernatants were harvested from both compartments on corresponding days over a period of eight days. Conditions were tested in triplicate. MIP-3α levels were quantified with a sandwich Elisa. TEER was maximal on Day 4 post plating while highest MIP-3α levels were detected in the apical compartment on Day 7 post plating. MIP-3α levels were detectable for the first time on Day 5 post plating in the apical compartment. n-3

We again plated Transwell® inserts exactly as we had done in the above experiment but this time stimulated HEC-1A cells with poly I:C[6]. This we did in order to confirm the findings in unstimulated cells that MIP-3α secretion is apically polarised. We stimulated cells from both the apical and basal compartments using various poly I:C concentrations starting from 0.8µg/mL to 100µg/mL (*Figure 3.12*). We confirmed that MIP-3α secretion is apically polarised

[6] Polyinosinic:polycytidylic acid (poly I:C) is an immunostimulant. It is used in the form of its sodium salt to simulate viral infections. Poly I:C is known to interact with toll-like receptor (TLR) 3, which is expressed in the membrane of B-cells, macrophages and dendritic cells. Poly I:C is structurally similar to double-stranded RNA, which is present in some viruses and is a "natural" stimulant of TLR3. Thus, Poly I:C can be considered a synthetic analogue of double-stranded RNA.

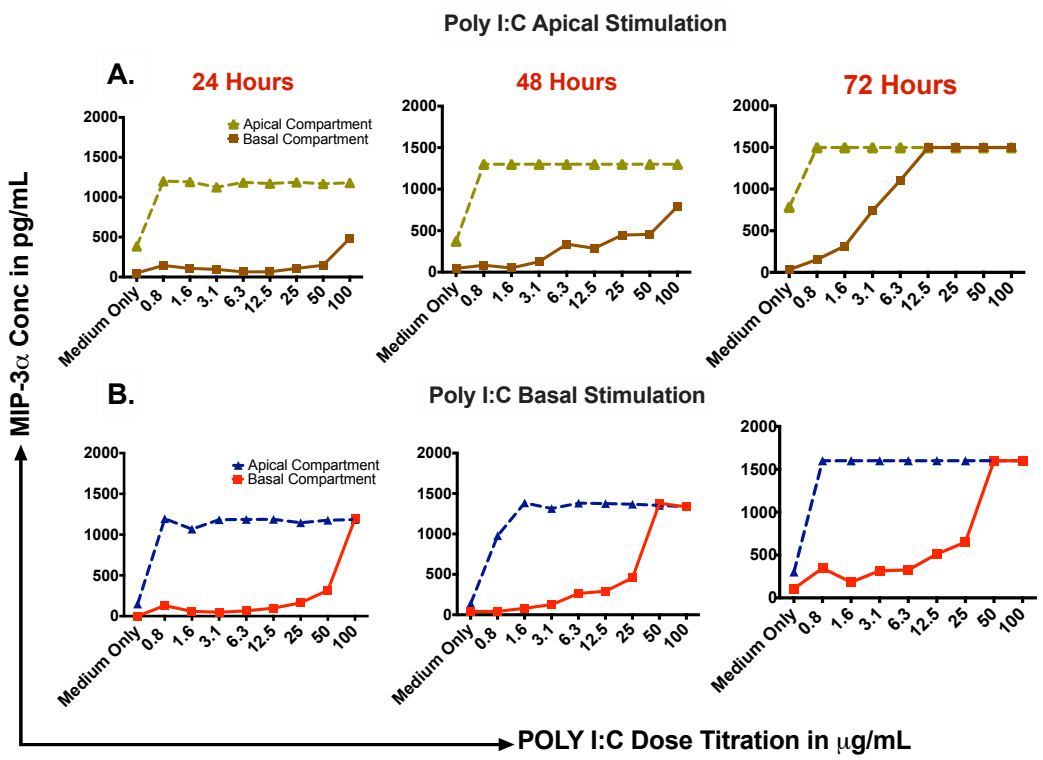

Figure 3.12. Polarisation of MIP-3α secretion in the first 72 hours following administration of serially titrated (A.) apical poly I:C and (B.) basal poly I:C in HEC-1A cells grown on Transwell® inserts. Cells were incubated at 37^0C, 5% CO_2 for 24 to 72 hours before harvesting supernatants for MIP-3α estimation on Elisa. Conditions were tested in triplicate. Stimulating cells from the apical and basal compartments with Poly I:C yielded similar results over various concentrations in the first 48 hours post stimulation - MIP-3α levels were consistently higher in the apical compartment versus the basal compartment with various Poly I:C concentrations. However, basal levels approximated apical levels at concentrations ≥ 25μg/mL at 72 hours post stimulation. n=3

in this model, irrespective of whether HEC-1A cells are stimulated or not. Again, levels were consistently highest in the apical compartment regardless of the pole stimulation and the concentration of the stimulant . This was particularly the case in the first 48 hours post stimulation. We concluded that constitutive expression of MIP-3α and its apical polarisation may be an important gradient responsible for homeostatically drawing CCR6 bearing cells such as pDCs to the peripheral tissues.

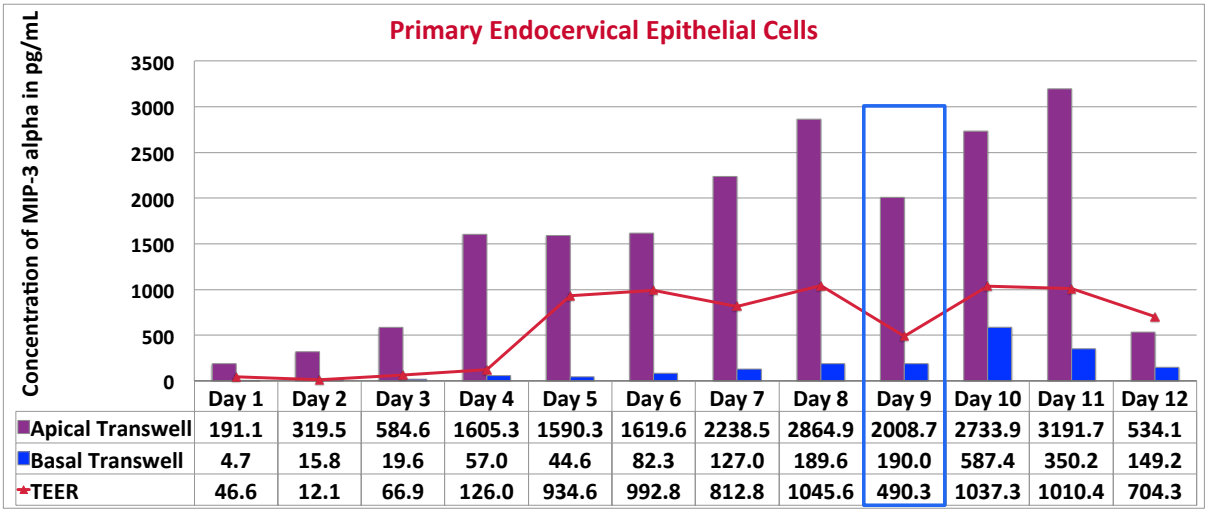

	Day 1	Day 2	Day 3	Day 4	Day 5	Day 6	Day 7	Day 8	Day 9	Day 10	Day 11	Day 12
Apical Transwell	191.1	319.5	584.6	1605.3	1590.3	1619.6	2238.5	2864.9	2008.7	2733.9	3191.7	534.1
Basal Transwell	4.7	15.8	19.6	57.0	44.6	82.3	127.0	189.6	190.0	587.4	350.2	149.2
TEER	46.6	12.1	66.9	126.0	934.6	992.8	812.8	1045.6	490.3	1037.3	1010.4	704.3

Figure 3.13. Constitutive levels and polarisation of MIP-3α secretion in EPECs plated on permeable supports in the apical compartment of Transwell® inserts over 12 days. TEER was measured serially from Day 1 post plating while supernatants were harvested from both compartments on corresponding days. Conditions were tested in triplicate. MIP-3α levels were quantified with a sandwich Elisa. TEER reached a plateau between Day 5 and Day 11 post plating. However, the highest TEER recorded was around 1000Ω on Day 8. Highest MIP-3α levels were detected in the apical compartment on Day 11 post plating. MIP-3α levels were detectable for the first time from Day 1 post plating in both compartments, however, apical compartment levels were constantly higher than the basal compartment levels. n=3

In endocervical primary epithelial cells, MIP-3α is expressed constitutively, and is apically polarized.

Having demonstrated constitutive expression of MIP-3α in the endometrial model, we proceeded to answer the question of whether the endocervical epithelial model would be any different from the endometrial epithelial model. We again plated the apical compartment of Transwell® inserts with 50,000 EPECs per well in 200µL of complete K-SFM medium. We added 600µL of the same medium into the basal compartment. We then measured TEER serially from Day 1 post plating while also harvesting supernatants from both the apical and basal compartments on the same corresponding days (*Figure 3.13*). We measured MIP-3α levels on supernatants with a sandwich Elisa. Results showed that MIP-3α levels were detectable from

Day 1 post plating, contrary to HEC-1A cells. Again, data demonstrated constitutive levels of MIP-3α, which however were at least 50-fold higher in EPECs than in HEC-1A cells (focusing only on maximal values for each model). Similarly to HEC-1A cells, MIP-3α was apically polarised in this endocervical model throughout the observation period and this was looking only at unstimulated levels. These findings confirm compartmentalisation of MIP-3α in the FGT - while both these sub-compartments produce MIP-3α, the levels are significantly different, being highest in the endocervical model.

In endocervical explant tissues, MIP-3α is expressed constitutively at high levels.

Having demonstrated constitutive MIP-3α secretion in EPECS, we went on to validate these results in an explant epithelial tissue model from the same sub-compartment. We did this because explant tissues are a bridge between *in vitro* and *in vivo* situations, being closer to an *in vivo* situation than single cells are. The explant tissue model comprises an epithelial layer embedded on the underlying stroma, which in turn encompasses all the other different cell types interspersed explant tissue model comprises an epithelial layer embedded on the underlying stroma, which in turn encompasses all the other different cell types interspersed within it. This architectural structure might be supportive and actually even significantly influence functioning of the epithelial cells in real life situations. We prepared explant tissue blocks from fresh hysterectomy specimens of six participants and plated them at one block per well in 200µL of complete RPMI-1640. We incubated tissues at 37^0C 5% CO2 for 24 hours prior to harvesting supernatants. We confirmed that endocervical tissues secrete high levels of MIP-

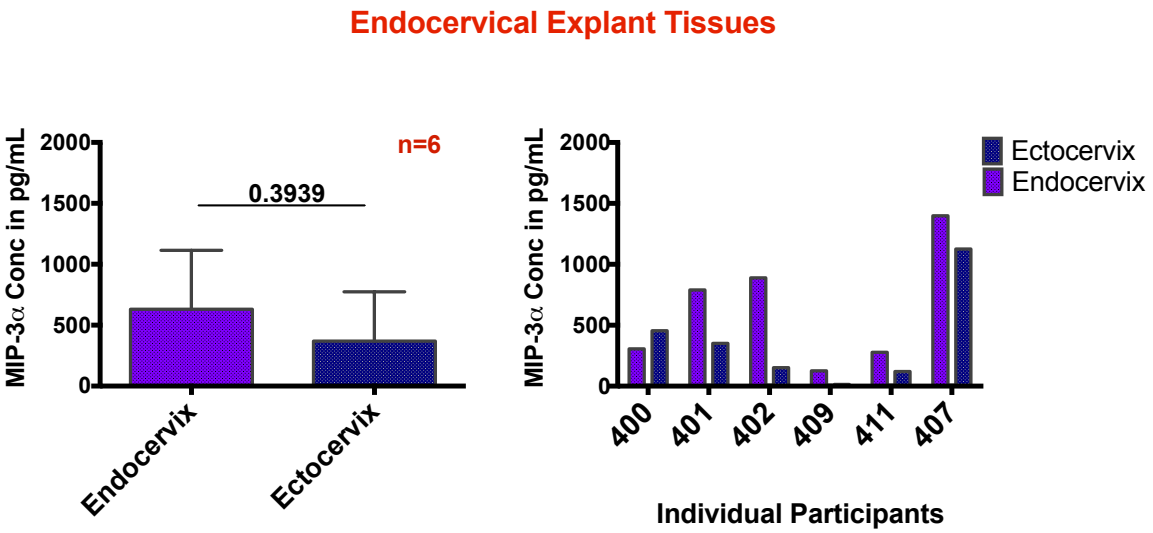

Figure 3.14. Constitutive levels of MIP-3α in EET. EET were prepared from fresh hysterectomy specimens of six participants on the same day of womb resection. One block of tissue was seeded per well of a 96 well tissue culture plate in 200µL of complete RPMI-1640. Supernatants were harvested 24 hours after incubation at 37^0C, 5% CO_2. Conditions were tested in triplicate. MIP-3α levels were quantified with a sandwich Elisa. MIP-3α levels were detectable in EET of all participants 24 hours post incubation. n=6. P-value<0.005 is statistically significant.

3α. Levels reached a mean of 600pg/mL in this endocervical model (*Figure 3.14*). These levels were higher than in the ectocervical model even though the difference did not reach statistical significance. Again these levels were 10-fold higher than in the endometrial cellular model, thereby confirming that the endocervix produces significantly higher levels of MIP-3α. It was interesting to note also that even though levels were high in both endocervical models (EET and EPECs), they were however higher in the cellular than in the explant tissue model prepared from the same participants – baseline constitutive levels in the EPECs (taken to be levels achieved a day after maximal TEER) were around 2000pg/mL while they were around 600pg/mL in the EET. The lower EET levels might be attenuated as a reflection of the paracrine effects of the cells in the surrounding stroma that are involved in controlling MIP-3α levels *in vivo.*

In cervicovaginal fluid, MIP-3α is expressed constitutively.

Having demonstrated MIP-3α constitutive expression in the *in vitro* and *ex vivo* tissue models from the upper FGT, we went on to study the lower FGT levels as represented by the concentrate of fluid from the vagina. We understood that levels seen studying *in vitro* and *ex vivo* tissue models might not reflect real life secretion levels and patterns of MIP-3α. For one, directly measured MIP-3α levels in supernatants of cellular and tissue models might exaggerate levels seen in real life. The fluid component of CVF is made of plasma transudate secreted through the vaginal wall and containing cervical mucus, endometrial and oviductal fluids, endocervical secretions, exfoliated cells, of plasma transudate secreted through the vaginal wall, water and many other different factors such as cholesterol, lipids,

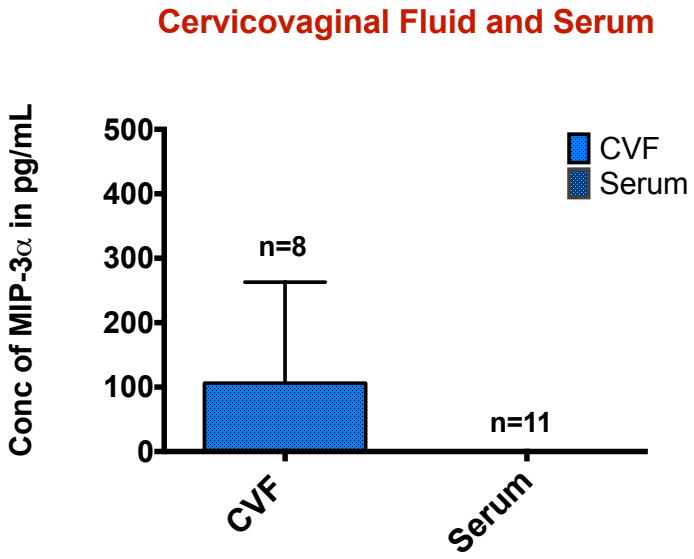

Figure 3.15. Constitutive levels of MIP-3α in CVF and serum. Using a menstrual cup, CVF concentrate was collected from HIV uninfected women – consenting women were instructed to self-insert and to then remove the cup after two hours of leaving it *in situ* at the clinic. At the same visit and at the same time, corresponding serum samples were collected from the same women. MIP-3α levels were subsequently quantified with a Luminex multiplex bead assay. MIP-3α levels were tested in triplicate from each woman. MIP-3α levels were detectable at high levels in the CVF of these women, however, no MIP-3α was detectable in their serum.

mucin, carbohydrates, amino acids, proteins and inorganic ions – all which may dilute levels and perhaps even function of our protein of interest. We then proceeded to collect a CVF concentrate from 11 HIV uninfected women attending the HIV vaccine institute at St George's hospital, in London. At the same visit and from the same participants, we also collected serum and estimated MIP-3α levels in both compartments using the Luminex multiplex bead assay. Data showed that there were high constitutive levels of MIP-3α in the CVF concentrate of eight of 11 women included in this analysis. Average levels of MIP-3α in the CVF of these women were 100pg/mL (*Figure 3.15*). However, we could not include the other three women in this analysis as the CVF of these other women appeared overtly abnormal; containing pus, blood and thick clumps of mucus, findings which

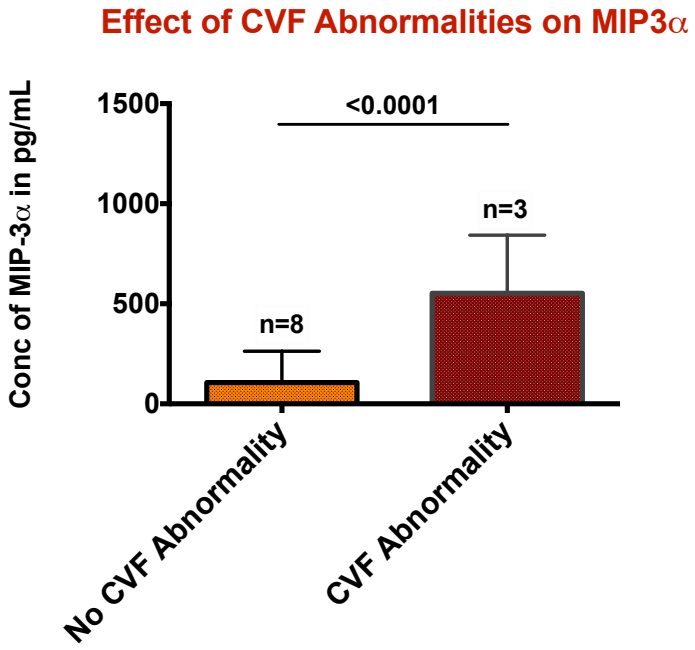

Figure 3.16. Constitutive levels of MIP-3α in CVF, comparing normal CVF and abnormal CVF. Using a menstrual cup, CVF concentrate was collected from HIV uninfected women – consenting women were instructed to self-insert and to then remove the cup after two hours of leaving it *in situ* at the clinic. On inspection, CVF from three women looked abnormal – it had pus, blood and thick mucoid clumps. MIP-3α levels from the CVF of these women were significantly higher than MIP-3α levels from the other eight women with normal looking CVF. P-value <0.005 is statistically significantly.

suggest an u nderlying inflammatory state. CVF results from these women were subsequently analysed separately (*Figure 3.16)*. Levels of MIP-3α in these women were significantly higher at 500pg/mL than in the CVF of women without these abnormalities at a mean level of 100pg/mL. These findings suggest therefore that while MIP-3α levels were already constitutively high in the CVF of women, they were however significantly higher where there were CVF abnormalities suggesting the presence of underlying inflammation. These findings therefore suggest inflammation as a significant driver of MIP-3α levels in the FGT.

In serum, MIP-3α is not expressed constitutively.

Until recently, the blood compartment in humans has been studied almost solely in order to try and understand HIV infection events, and even infer initial infection events at the level of the FGT. However, there has been a recent call and move towards collecting and analysing more FGT specimens in order to study and understand correlates of protection at the level of viral entry. Accordingly we proceeded to study these two compartments alongside each other in order to assess if there might be any correlations in the levels and secretion patterns of MIP-3α. We proceeded to estimate constitutive levels of MIP-3α in serum in order to compare levels with the FGT levels. As already mentioned above, serum was collected at the same visit and from the same women from whom we also collected CVF. In 11 women included in this analysis, there was no detectable MIP-3α in this compartment with this assay in all of the women included in this analysis (*Figure 3.15*). These findings therefore confirm the epithelial source of MIP-3α on the one hand, while they make a case for studying FGT infection events separately from

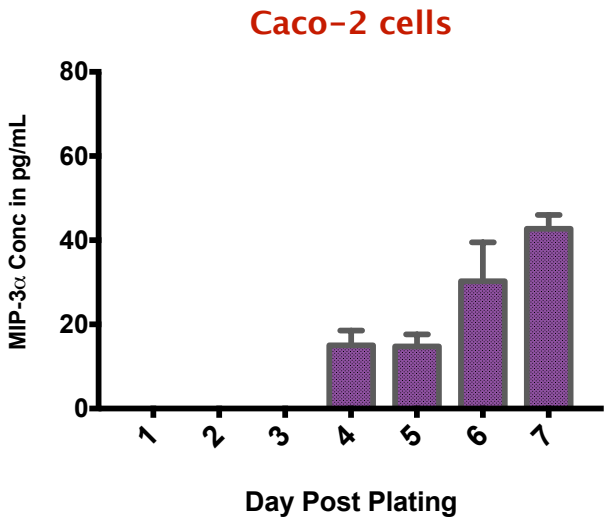

Figure 3.15. Constitutive levels of MIP-3α in Caco-2 cells over the first seven days post plating. Caco-2 cells were seeded at 50,000 cells per well of a 24 well tissue culture plate in 600µL of complete DMEM. Supernatants were harvested serially, daily starting from Day 1 post plating to Day 7 post plating. We estimated MIP-3α levels in supernatants using the sandwich Elisa immunoassay. MIP-3α was constitutively detected in this epithelial model from Day 4 post plating albeit at very low levels.

blood on the other hand.

In Caco-2 cells, a colorectal cell line, MIP-3α is expressed constitutively, albeit at low levels.

Having demonstrated constitutive MIP-3α secretion in different sub-compartmentss of the FGT and having confirmed its epithelial source in this compartment, we proceeded to study another epithelial site outside of the FGT for comparison purposes. We chose the colorectal site for its similar epithelial architecture to the other tissues studied, columnar epithelium, while also considering the involvement of the gastrointestinal tract (GIT) by HIV infection. We plated 24 well tissue culture plates with 50,000 Caco-2 cells per well in 600µL of complete DMEM. After

incubating them at 37^0C, 5%CO_2 for 24 hours, we serially harvested supernatants from Day 1 post plating and estimated MIP-3α levels with a sandwich Elisa immunoassay. Again data showed that Caco-2 cells secrete MIP-3α constitutively, and this they did in a very similar pattern to HEC-1A cells, an endometrial cell line. Each of these two models had the threshold for detection of MIP-3α levels at Day 4 post plating in 24 well plates plating with 50,000 cells per well. Moreover, the average levels MIP-3α on this day were similar around 20pg/mL for Caco-2 cells and for HEC-1A cells (data showed earlier under methods section). These findings confirm epithelial source of MIP-3α in the two cell lines from two different sites.

DISCUSSION

We studied the pattern of MIP-3α secretion in three FGT sub-compartments, focusing on constitutive secretion in various matrices, including a cell line, primary epithelial cells, tissue explants and secretions. Numerous studies have reported constitutive MIP-3α secretion in the FGT, but used epithelial cell lines and primary cell models, concentrating only on the fallopian tubes, endometrium, and vagina in the non HIV context [93, 95, 101]. However, after findings from the landmark study in 2009 by Li *et al* suggested a significant role of MIP-3α in early SIV transmission events in the endocervix [96] it was important to assess the role of MIP-3α in the human endocervix in the context of HIV infection. This study has therefore extended this body of knowledge by studying humans, focusing primarily on primary cells from the endocervix. Moreover, it has focused also on explant tissues, which no other study has done previously.

FGT tissue matrices studied i.e. HEC-1A cells, EPECs, EET and CVF

secrete/express MIP-3α constitutively albeit at varying concentrations. In contrast, MIP-3α levels were below level of quantitation in serum using this assay platform. These findings therefore confirm previous findings that epithelial cells are a dominant source of MIP-3α [103] and extend them by demonstrating that levels are highest in the endocervical models studied. Levels were highest with the EPECs followed by EET – the attenuated levels with the EET model could be more reflective of an *in vivo* situation where the presence of the stroma and the other cells within it could have a paracrine role to play in controlling its levels. The difference in levels between EET and EPECs highlights the significance of studying various models to answer different but related questions. While the EPECs reveal the highest levels of MIP-3α that can be achieved by a pure preparation of epithelial cells, they however, do not reveal the effect that the surrounding tissues might have on the levels of MIP-3α. The differences in levels of MIP-3α seen in different sub-compartments further confirm the notion of compartmentalisation in the FGT. It has been shown that expression of soluble proteins and antimicrobial proteins is compartmentalised along the female reproductive tract [104, 105]. Boomsma *et al* showed different levels of cytokines comparing levels in secretions from the endometrium and those from the endocervix collected simultaneously from the same women. Likewise, Wira *et al* demonstrated varying levels of soluble proteins in supernatants of primary cells from the cervix, fallopian tubes and uterus [106]. Moreover, FGT sub-compartments are differentially responsive to hormones, thus culminating in a differential modulation of local immunoendocrine responses [107, 108]. Given high constitutive levels of expression of MIP-3α by human epithelial cells, and particularly by the endocervix, which is now becoming known as the primary target site of SIV/HIV infection [58, 109, 110], the role of MIP-3α in modulating initial events in HIV transmission in this site remains to be defined.

It is perhaps not surprising that the pattern of constitutive MIP-3α secretion would be high in the endocervix. The endocervix is a distinct organ that forms a bridge separating the richly colonized lower reproductive tract (vagina and ectocervix) and the relatively sterile upper tract (endometrium and fallopian tubes). Histologically the vaginal and ectocervical epithelia are morphologically similar while the endocervical epithelium is uniquely different comprising a single layer of columnar cells with glandular-like folds interspersed within it. On the other hand, the endometrium, whilst also lined by single columnar epithelium, is a site of extensive tissue remodelling characterised by finely orchestrated processes to limit inflammation. The endocervix is distinctly an area of high endocrine and paracrine functions, as previously evidenced by high antimicrobial protein expression and secretion of antibodies [111, 112]. The endocervix is a major reservoir of T lymphocytes in the female genital tract and is also the primary site of antibody production [55, 58]. Endocervix is the most common site of infection for Human Papilloma Virus, Chlamydia Trachomatis, and Neisseria Gonorrhoea. The endocervix, therefore, is likely to be an important site involved in the robust innate and adaptive immune responses that participate in the delicate function of protection of the upper FGT from pathogens.

Proteins in the secretions from the endocervix are said to overlap to a great extent with those in the CVF as these secretions are a subfraction of CVF, but there are still great differences in the composition of the secretions collected from these two sub-compartmentss [112]. CVF is an extracellular fluid with an important role in the innate immunity; it has been shown that an estimated 10% of the proteins it contains have an immunological function [112]. Many studies have used CVF as samples for the analysis of proteins and found correlations between different

expression profiles and specific pathologies [113]. Accordingly we proceeded to estimate levels of MIP-3α in the CVF sub-compartment. The purpose for this was that it would allow us to get an indirect estimation of the levels of MIP-3α in *in vivo* cervical secretions. Levels of MIP-3α were relatively high in the CVF sub-compartment and thereby confirming that the human endocervix has a high constitutive expression of MIP-3α. This is particularly important against the backdrop of preferential sites of infection by different organisms – information that would be crucial in designing targeted strategies that aim to focus on the primary site of infection in order to prevent infection or manipulate the specific immune responses to that organism. However, it has been shown that CVF constituents are secreted differentially throughout the tract and one can never appreciate the precise contribution of each sub-compartments in expressing a particular protein.

While basal levels of MIP-3α were high in the CVF of HIV uninfected women at the mean of 100pg/mL, they were however even higher in the CVF of participants with CVF abnormalities suggesting underlying inflammation. CVF of these women had pus, blood, and thick mucoid clumps. Women in this study were seen and specimens collected outside of their menstrual period and hence these changes could not be attributable to menstrual periods (timing of specimen collection will be discussed in greater detail in the next chapter). These abnormalities were in keeping with a diagnosis of cervicitis, an inflammatory condition that is the commonest cause of a bloody and/or mucopurulent vaginal discharge outside menses. Cervicitis in the FGT is commonly due to Neisseria Gonorrhoea, Chlamydia Trachomatis and/or Trichomonas Vaginalis [114]. We unfortunately could not confirm these diagnoses by microbiological testing for technical reasons. Following the discovery of MIP-3α through bioinformatics in 1997, inflamed tonsils

were shown by Dieu *et al* to have the highest levels of MIP-3α, thereby suggesting a close association between MIP-3α and inflammation for the first time in 1998 [86]. Subsequent to that, several studies have confirmed that MIP-3α levels are highest in the presence of inflammation [91, 115, 116]. In fact, MIP-3α is described as a molecule that attracts leucocyte populations to mucosal sites and particularly, inflamed mucosal sites [103, 117]. The findings in this study that MIP-3α levels were five-fold higher where there was a suggestion of underlying inflammation confirm that MIP-3α levels are highest in the presence of inflammation and that inflammation is a dominant driver of its levels.

Epithelial cells have a structural polarised orientation with an apical surface to the lumen and a basolateral surface to the basement membrane and underlying cells that is crucial to their functioning in the mucosal lumen. Polarised epithelial cell culture systems are hence largely preferred in studying and extrapolating *in vivo* situations as they maintain distinct apical and basolateral surfaces in order to better simulate *in vivo* relationships between the host and relevant infectious organisms. They exhibit many of the phenotypic and functional characteristics of columnar epithelium, which is characteristic of the endometrium and endocervix. Because we hypothesised that subepithelial (i.e. basal) rather than apical MIP-3α is involved in the ”outside-in” signalling mechanism of HIV infection, we accordingly studied HEC-1A cells and EPECs in a polarised culture system. Employing this system revealed that constitutive MIP-3α levels were higher in the apical compartment than in the basal compartment with all cellular models studied in a polarised culture system. This for one would explain the high levels of MIP-3α in the CVF samples collected from the vaginal lumen where it might be expressing its other function of being an antimicrobial. MIP-3α, over and above being a

chemokine, possesses anti-HIV activity [101] and general antimicrobial activity against at least six other bacteria and fungal species at varying concentrations [118]. It could be that the disparity in the concentrations of MIP-3α between the apical and basal compartment are reflective of its various functions. Particularly, MIP-3α, while functioning as an antimicrobial in high concentrations in the lumen, might on the other hand be functioning mainly as a chemokine in low concentrations in the basal compartment. Uniquely, MIP-3α is the sole ligand for chemokine receptor 6 (CCR6) [84, 119], which is expressed on pDCs, and some subsets of T and B lymphocytes. Our data would therefore suggest that in humans most of MIP-3α secreted constitutively is passed into the lumen and hence outside of the body while the minimal levels that are secreted subepithelially are required to maintain the homeostasis of CCR6-bearing cells in the lamina propria of the endocervix.

When MIP-3α was first discovered in 1997, it was identified in foetal lung, liver and pancreas. Further investigations revealed a high MIP-3α expression in appendix, tonsil, liver, and placenta on the one hand, while finding weak expression in thymus, lymph nodes, and small intestine [120]. Izadpanah *et al* subsequently confirmed the secretion of MIP-3α by various intestinal epithelial cell lines including Caco-2 cells [121]. Their results confirmed constitutive secretion of low levels of MIP-3α and its basal polarisation on polarised culture systems. Having studied MIP-3α secretion in HEC-1A cells, we proceeded to studying MIP-3α levels in non polarised Caco-2 cells, in which it became evident that this cell line secretes constitutive levels of MIP-3α at baseline albeit at low levels. While the levels in this model were as low as in the HEC-1A cellular model, polarisation was different judging by the results from the study by Izadpanah. This would therefore

confirm findings by Schutyser *et al* who suggested that MIP-3 secretion patterns vary in epithelial cells from different body sites, hence emphasising the significance of studying MIP-3α extensively for the site one is interested in [89].

CONCLUSION

Findings of this thesis chapter make it very clear that there is widespread constitutive secretion of MIP-3α in the FGT, where it is secreted at high levels. The pattern of secretion however occurs in a very compartmentalised manner with the highest levels occurring in the endocervix, which highlights the importance of focusing on studying the pattern of secretion in the sub-compartment of interest. Epithelial cells are a dominant source of MIP-3α and inflammation appears to be the dominant driver of its secretion.

CHAPTER FOUR STIMULATED LEVELS OF MIP-3α, STIMULATING WITH ENVELOPE AND NON ENVELOPE HIV-1 PREPARATIONS

SUMMARY

Being at the forefront of virus exposure, how the genital epithelium contributes to the appreciated inefficiency of Human Immunodeficiency Virus (HIV) infection has been underestimated. Over and above being a barrier the epithelium secretes and transports molecules, which modulate vulnerability and/or resistance to infection. Its distinctive role includes the detection of the presence of harmful stimuli through pattern recognition receptors (PRRS) such as Toll-like receptors (TLRs) and to then relay this information to the adaptive immune system through secretion and up-regulation of various cytokines and chemokines. If we could understand the earliest innate epithelial responses following exposure to virus, we could be better equipped to develop efficacious biomedical prevention strategies to reduce the burden of HIV infection in women. This chapter focuses on the epithelial-HIV interface, testing the hypothesis that macrophage inflammatory protein-3 alpha (MIP-3α) secretion is up-regulated in the endocervical sub-compartment of humans following HIV-1 exposure, when the viral envelope proteins interact with the apical epithelial surface. We studied MIP-3α patterns of secretion by female genital tract (FGT) epithelial tissue models, comparing levels of MIP-3α following stimulation with various HIV-1 preparations in order to tease out whether or not the viral envelope is involved in triggering MIP-3α secretion. Specifically, we prepared and studied HIV-1 envelope proteins: soluble recombinant trimeric CN54gp140 glycoprotein and CN54gp120 virus-like particles (VLPs); and also prepared and studied R5 tropic whole virus, inactivated HIV-1 BaL, and envelope-deleted virus, HIV-1 NL4-3. Alongside stimulating with these viral preparations, we stimulated the

same epithelial models with TLR ligands one through to six as a positive control. The epithelial models we studied included the HEC-1A endometrial cell line, endocervical primary epithelial cells (EPECs), endocervical explant tissues (EET), and the Caco-2 colorectal cell line. We grew cells and tissues on tissue culture plates, except for HEC-1A cells which we also grew in Transwell® inserts. We analysed MIP-3α levels in supernatants by a sandwich quantitative Elisa immunoassay. We also did flow cytometric studies to phenotype TLR expression on HEC-1A cells and EPECs. All the epithelial models studied secreted MIP-3α constitutively, however, none of them secreted further amounts of MIP-3α after stimulation with any of the HIV-1 preparations, thereby confirming that HIV-1, in any form, does not trigger MIP-3α secretion by epithelial cells in humans. Using various viral concentrations, 10^4 to 10^6 viral particles per well, did not have any impact on triggering increased MIP-3α secretion. Neither did stimulating from either pole of the membrane have any impact on triggering further MIP-3α secretion in HEC-1A cells grown in Transwell® inserts. Contrary to the lack of response seen following exposure to HIV-1, epithelial models differentially responded to various TLR ligands, except EET in which there was complete non-response to TLR ligands: all TLR ligands except TLR4 and TLR6 triggered significant MIP-3α secretion in HEC-1A cells, while all TLR ligands except TLR2 and TLR4 triggered significant MIP-3α levels in EPECs, and only TLR1 and TLR6 triggered significant MIP-3α levels in Caco-2 cells. These results therefore confirm that the pattern of MIP-3α secretion by epithelial cells is both site-specific and inducing agent-specific. However, TLR expression did not match the response to TLR ligands in respective epithelial models with regards to MIP-3α secretion in HEC-1A cells and EPECs. Notably, the expression of TLR4 was significantly higher in both HEC-1A cells and

EPECs and yet the TLR4 ligand did not trigger MIP-3α secretion in either of these cell types.

INTRODUCTION

In humans the probability of HIV infection is low at 1:200 – 1:2000 heterosexual exposures [122] and thereby suggesting that the epithelium is efficient as a barrier to HIV. Whereas previously the epithelium was thought to function solely as a physical barrier to the passage of microorganisms, it has now become understood that it also has a range of immune functions that regulate infection across the genital epithelium [71, 107].

The sensing of microbial exposure by the innate immune system involves various PRRs that recognize conserved pathogen-associated molecular patterns (PAMPs). Recent studies identified several classes of PRRs including TLRs, nucleotide oligomerisation domain (NOD)-like receptors (NLRs), retinoic acid inducible gene I (RIG-I)-like receptors (RLRs) and cytosolic DNA sensors such as members of the AIM2 family [123]. To date, at least 10 TLRs have been identified in mammals, with 10 subtypes of TLRs recognized in humans and 12 subtypes recognized in mice. TLRs 1 to 9 are common to both.

Epithelial cells express TLRs 1 through to 10, albeit in a very site-specific manner. For instance, airway epithelial cells express TLR1 to TLR10 [124], while intestinal epithelial cells express TLR1 to TLR4, TLR6 and TLR9 [125] and gastric epithelial cells express TLR2, TLR4 and TLR5 [126]. In the FGT primary human endometrial epithelial cell cultures and the uterine epithelial cell line (ECL) ECC-1 express

TLR1–9 genes [127]. Epithelial cells derived from normal human vagina, ectocervix, and endocervix on the other hand express TLR1, TLR2, TLR3, TLR5, and TLR6 [128].

TLR1/2 and TLR2/6 can discriminate triacyl- and diacyl-lipopeptide, respectively. The TLR4-mediated response to lipopolysaccharide (LPS) is well known for its critical role in innate immune control of Gram-negative bacterial infection. LPS is recognised by TLR4 in association with a co-receptor CD14 and the extracellular accessory TLR4-associated soluble factor, MD-2 [129]. TLR5 recognises a protein, flagellin, which is a specific component of the bacterial flagellum [130]. With the exception of neutrophils and pDCs, TLR3 is widely expressed in innate immune cells where it is activated by the double stranded RNA analogue poly I:C, where it contributes to the production of type I interferons and cytokines in macrophages [131]. TLR7 and TLR8 are two closely related receptors that are recognised for their antiviral and antitumor activity in the endosome; any long single-stranded RNA (ssRNA) is capable of activating them [132]. TLR9 responds to viral and bacterial DNA and is highly expressed in pDCs, innate cells renowned for their ability rapidly to produce large amounts of type I interferon [133].

In alignment with exposure to harmful stimuli triggering secretion of chemokines and cytokines by epithelial cells, various studies have previously demonstrated secretion of MIP-3α in response to inflammatory cytokines, TLR ligands, seminal plasma and Simian Immunodeficiency Virus (SIV). Results from Sun *et al* demonstrated that the endometrial ECL, (HHUA[7]), secreted MIP-3α on stimulation

[7] HHUA is an endometrial ECL shown to secrete MIP-3α on stimulation by TNF-α and IL-1β and not by LPS

with inflammatory mediators TNF-α and IL-1β [134]. Data from Cremel *et al* showed that the vagina ECL (SiHa[8]) and primary cells of the vagina equally secreted MIP-3α and this secretion was up-regulated by inflammatory mediator IL-1β [93]. Wira *et al* subsequently showed that primary epithelial cells of the endometrium also secreted MIP-3α on exposure to poly I:C, a TLR3 agonist [85]. In the context of heterosexual transmission, its expression was shown to also be significantly stimulated by seminal plasma in the SiHa cell line, regardless of whether the seminal plasma donor was HIV infected or uninfected [135].

SIV has previously been studied and shown to interact directly with epithelial cells in the FGT. Li *et al* noted that the accumulation of SIV RNA+ $CD4^+$ T endocervical cells post exposure to virus in a SIV/Rhesus macaque model was preceded by the sub-epithelial influx of plasmacytoid dendritic cells (pDCs) one day post inoculation [96]. They subsequently showed that the accumulation of these pDCs was associated with the accumulation of MIP-3α in the first one to three days post inoculation. Through a series of experiments they concluded that exposure of endocervical epithelium to the viral inoculum increases the expression of MIP-3α which in turn recruit pDCs in the first few days immediately post viral exposure, thereby commencing the sequence of events leading to productive infection. However, secretion of MIP-3α by the endocervix in humans during the first few days post HIV exposure has not previously been investigated.

In human models, Nazli *et al* demonstrated that novel interactions between HIV-1 and epithelial cells, prior to established productive infection and replication, could

[8] SiHa is a vaginal ECL shown to behave like primary vaginal cells with regards to epithelial cell differentiation and proliferative functions

potentially play an important role in initiating HIV infection and immune activation [136]. The findings of their study demonstrated that exposure of endometrial epithelial cells to HIV-1 whole virus or surface glycoprotein gp120 induced a remarkable up-regulation of a number of different chemokines and inflammatory cytokines within 24 hours of exposure, including IL-1, IL-6, IL-8 and tumor necrosis factor alpha (TNF-α). Their data further showed that TNF-α in turn led to the disruption in barrier function that was associated with viral and bacterial translocation across the epithelial monolayers. Again this group in another publication studying endometrial primary epithelial cells provided a mechanism for up-regulation of cytokines in the first 24 hours post HIV exposure and they reported that HIV-1 gp120 signals through TLR2 and TLR4 in the presence of heparin sulphate in order to trigger proinflammatory cytokine production via activation of the NF-kB pathway [137]. Thus these two studies provide evidence for direct interaction of HIV with the epithelium in early HIV infection events. Similarly, we sought to establish whether these findings could be replicated in the human endocervix focusing on MIP-3α, a chemokine already shown to have a significant role in early SIV infection events in the macaque FGT.

MATERIALS and METHODS

Epithelial models:

We used exactly the same epithelial models that we used in the preceding chapter on constitutive levels of MIP-3α to study the impact of stimulating epithelial models with various stimulants. Briefly, we evaluated the stimulated expression of MIP-3α in *in vitro* epithelial cell models prepared from the different sub-compartments of the FGT, the endometrium and the endocervix; and the gastrointestinal tract (GIT).

We then used the *ex vivo* endocervical explant tissue model to validate results from the endocervical cellular model. Specifically, epithelial models included cell lines, the HEC-1A endometrial and Caco-2 colorectal cell lines; endocervical primary epithelial cells (EPECs), and endocervical explant tissue (EET).

Tissue culture:

We prepared and incubated these epithelial models exactly as we had done in the same preceding chapter. We seeded cells in 24 well tissue culture plates (Corning® Costar®, UK), and EET in 96 round well tissue culture plates (Corning® Costar®, UK). Additionally, we seeded HEC-1A cells on permeable supports in Transwell® inserts (Corning® Costar®, UK).

Viral preparations:

Various HIV-1 preparations were used to answer the question of whether or not the viral envelope is the requirement for triggering of MIP-3α secretion in epithelial models. Particularly, studies were performed using envelope proteins representative of gp120 and gp140 trimers, inactive whole virus, and envelope-deleted virus. Below are details of the methods of preparing these:

(i) *Soluble recombinant HIV-1 gp140 trimeric protein*: Dr Katja Klein at the Imperial College London donated this protein. Briefly it was a clade C envelope clone p97CN54 that was obtained originally from a Chinese patient. gp120 plus ED of gp41, designated as CN54gp140, was produced in CHO cells as a recombinant product. Purity of the product was confirmed by mass spectrometric analysis. Polymyxin B Sulphate (Merck Millipore, UK) test was used to exclude endotoxin contamination of this protein prior to experiments

in this project. The range of concentrations used for this protein in our experiments was 6,25ng/mL to 200ng/mL.

(ii) *HIV-1 gp120 virus-like particles (VLPs):* VLPs were formed from the assembly of the pREC-NFL vector with HIV-1 CN54gp120 envelope DNA. The particular VLPs we used were rendered non-infectious by deletion of the 5' LTR region. The pREC-NFL-HIV-1 CN54gp120 plasmid (a shuttle vector containing the near full-length (NFL) HIV DNA was transfected into HEK-293T cells using polyethylenimine (PEI) (Sigma-Aldrich®, UK). Bacterial transformation with E.coli was used to amplify DNA. PEI was used at a ratio of 3:1 to DNA. HEK-293 T cells were grown in FreeStyle™ 293 Expression medium (ThermoFisher Scientific, Gibco®, UK) and supernatants were harvested on day 3 post transfection. Virus was concentrated using the Amicon Ultra-15 Centrifugal Filter Units (Merck Millipore, UK). We subsequently used VLPs at a concentration of 10^4 to 10^6 particles per well. p24 antigen concentration was quantified on p24 Elisa and viral particles were also counted on the Nanosight nanoparticle analysis system as described below.

- *HIV-1 p24 antigen Elisa*, a direct sandwich Elisa, was subsequently used to detect and quantify HIV p24 gag proteins in viral lysates. An Aalto HIV-1 p24 antigen Elisa kit (Aalto Bio Reagents, UK) was used and p24 quantitation was conducted according to the manufacturer's protocol. Supernatants were diluted 1:20 to 1:1000. Virus was inactivated in 1% Empigen. A chemiluminescent substrate for alkaline phosphatase with

enhancer (CSPD with Sapphire) was used for detection. p24 was detected and quantified using the Luminimeter (SPECTROstar omega).

- *Particle count with NanoSight Nanoparticle Analysis System:* this technology visualises, measures and characterises virtually all nanoparticles in terms of size, concentration, zeta potential and aggregation was used to measure and quantify the concentration of viral particles per mL in lysates diluted 1:50 (*Figure 4.1*). This system is a particle-by-particle methodology that measures the size of each particle from direct observations of diffusion and validates all data with video files of the particles moving under Brownian motion. It typically characterises nanoparticles from 10nm to 2000nm in solution.

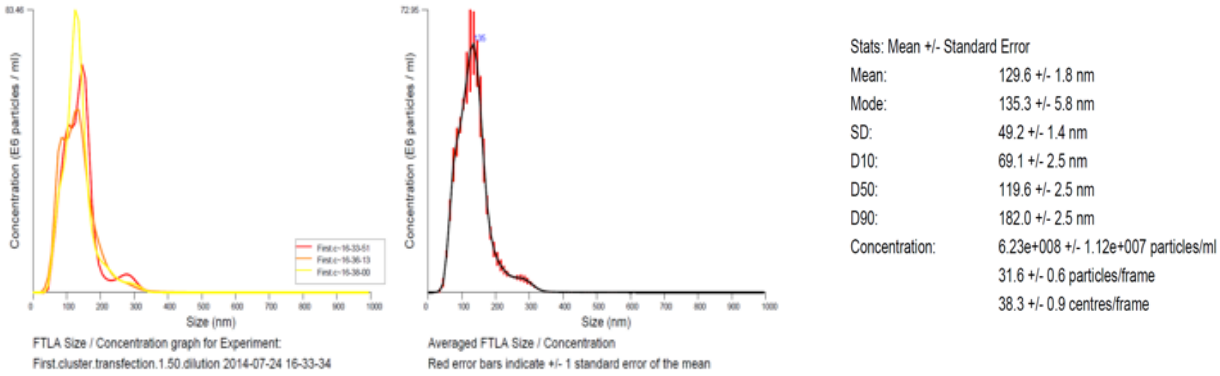

Figure 4.1: Nanosight nanoparticle estimation of the size of CN54gp120 virus-like particles (VLPs)

(iii) *R5 tropic whole virus, HIV-1 strain BaL: this viral preparation was used inactivated as per the protocol described below. BaL* was produced in anti-CD3 antibody [OKT3], phytohemagglutinin (PHA), and interleukin-2 (IL-2) stimulated peripheral blood mononuclear cells (PBMCs). After cell lysis with Triton™ X-100 detergent (Sigma-Aldrich®, UK), supernatants were harvested and Aalto HIV-1 p24 antigen Elisa as described above was done to determine p24 yields.

- *Inactivation of BaL using AT-2 Treatment*: BaL particles were treated with 2,2*-dithiodipyridine (aldrithiol-2; AT-2) (Sigma-Aldrich®, UK) to render them non–infectious. AT-2 treated virus is comparable to untreated virus except that its viral cycle terminates before initiation of reverse transcription. Further, in contrast to virions inactivated by conventional methods such as heat or formalin treatment, it retains viral and host cell-derived proteins on virion surfaces, thereby preserving envelope conformational and functional integrity. After filtration of the viral solution above, 10µL of AT-2 stock solution was added to 1mL of virus solution. After overnight incubation at 4^0C virus particles were purified by ultracentrifugation, and estimation of p24 content conducted by Aalto HIV-1 p24 antigen Elisa assay.

- *TZM-bl luciferase based HIV-1 infectivity assay*: this assay was done to confirm lack of infectivity of AT-2 treated virus. After titration to optimal viral concentration of 20000RLU, 100ul of TZM-bl cells in complete Dulbecco's Modified Eagle's Medium (DMEM) (Sigma-Aldrich®, UK) were added to 100µL of AT-2 inactivated virus per well of a 96 well

tissue culture plate. After incubation at 37^0C for 24hours, supernatants were aspirated, cells lysed with luciferase substrate, and light intensity of each well was measured on Luminimeter (SPECTROstar omega).

(iv) *HIV-1 envelope deleted virus, X4 tropic NL4-3:* env-deleted NL4-3 was formed from the PNL_LUC-R-ENV plasmid based on the HIV-1 proviral clone PNL4-3. Plasmids were grown with ampicillin selection. Bacterial transformation with E. Coli using heat shock was used to amplify DNA. DNA was transfected into 293T cells using polyethylenimine (PEI). PEI was used at a ratio of 3:1 to DNA. 293 T cells were grown in Dulbecco's Modified Eagle's Medium (DMEM) and supernatants with virus were harvested on day 3 post transfection. Viral p24 antigen was quantified using the ABL HIV-1 p24 antigen capture Elisa assay (ABLinc., UK), according to the manufacturer's protocol, with supernatants diluted 1:100 to 1:100,000. Detection was enhanced using the peroxidase substrate. Quantitation was done based on a standard curve after optical density (OD) measurements at 450 nm in an Elisa reader.

Virus particle calculation from the p24 Elisa results:

Concentrations of various viral preparations as calculated from the p24 antigen Elisa:

BaL = 120,2 ng/mL
VLPs = 548,4 ng/mL
NL4-3 = 350,3 ng/mL

Relationships from the literature:

1) 1 physical particle of virus has 2000 p24 molecules

2) 1 physical particle of virus has 15 spikes (which are trimers) of gp120, which is equivalent to 45 molecules
3) 1 physical particle of virus has 15 spikes (which are trimers) of gp140, which is equivalent to 45 molecules
4) 1 physical particle of virus has $0,8*10^{-7}$ ng of p24

Calculations:

Stock concentrations in physical particles per mL calculated from Elisa p24 concentrations:

Based on: 1 physical particle of virus has $0,8*10^{-7}$ ng of p24

- BaL: $1*120,2ng/mL / 0,8*10^{-7} = 1,5 * 10^{9}$ pp/mL
- VLPs: $1*548,4$ ng/mL / $0,8*10^{-7} = 6,86 * 10^{9}$ pp/mL
- NL4-3: $1*350,335$ ng/mL / $0,8*10^{-7} = 4,39 * 10^{9}$ pp/mL

Immunostimulants:

Following initial dose titration experiments in HEC-1A cells immunostimulants were used at fixed concentrations based on the levels of MIP-3α achieved following stimulation. We used constant concentrations throughout all tissue models. IL-1β was used as positive control for activation at 10 ng/ml (R&D Systems, Bio-Techne, Abingdon, UK), Pam_3CSK_4 (TLR1/2) at 20 µg/ml (Tocris, Bio-Techne, Abingdon, UK), Zymosan (TLR2) at 10 µg/ml (Sigma-Aldrich®, UK), Poly I:C Polyinosinic–polycytidylic acid sodium salt (TLR3) at 25 µg/ml (Sigma-Aldrich®, UK), LPS (Lipopolysaccharides from *Escherichia coli* 0111:B40) (TLR4) at 10 µg/ml (Sigma-Aldrich, UK), Flagellin (Flagellin from Salmonella typhimurium) (TLR5) at 20 ng/mL (Sigma-Aldrich®, UK), and FSL-1 (Pam2CGDPKHPKSF) (TLR2/6) at 2 µg/ml

(Invivogen, UK).

Phenotyping TLRs on Flow Cytometry:

EPECs and HEC-1A cells grown in 24 well tissue culture plates at passage three and passage 15, respectively, were used to do flow cytometric analyses for phenotypic expression of TLRs. EPECs were harvested on Day 8 post plating while HEC-1A cells were harvested on Day 5 post plating. Briefly, single cells were obtained by incubating the monolayer of EPECs with TrypLE™ (ThermoFisher Scientific, UK) at 37^0C 5% CO_2 for 5 minutes to generate a single cell suspension. On the other hand, 1% trypsin-EDTA (Sigma-Aldrich®, UK) was used to prepare single cells from HEC-1A cells. We conducted whole cell staining for each cell type, staining for both surface and intracellular TLRs, and hence the cells were fixed and permeabilised using the commercial Fixation/Permeabilisation solution kit (BD Cytofix Cytoperm™: BD Biosciences, UK). Specifically, we incubated cells with fluorescent antibodies before and after the permeabilisation step. We used antibodies at 1µL per 1*10^6 cells. We used mostly murine monoclonal antibodies, which were conjugated with various fluorochromes: antibodies to epithelial cells included an epithelial antibody that binds an epithelial surface antigen and epithelial glycoprotein-2, fluorescein isothiocyanate (FITC) - conjugated anti-human EpCAM (clone EBA-1, BD Biosciences, UK); peridinin-chlorophyll protein complex (PerCP)-conjugated anti-human TLR2 (clone 383936, R&D Systems, Bio-Techne, UK); FITC-conjugated anti-human TLR3 (clone 40C1285.6, Abcam, UK); phycoerythrin (PE)-Cyanin 7-conjugated anti-human TLR4 (clone HTA125, eBioScience, UK); PerCP-conjugated anti-human TLR5 (clone 19D759.2, Novus Biologicals, Bio-Techne, UK); PE-conjugated anti-human TLR6 (clone TLR6.127 PE, Biolegend®, UK); and PE-conjugated anti-human MIP-3α (clone 67310, R&D

Systems, Bio-Techne, UK). We also used goat polyclonal allophycocyanin (APC)-conjugated anti-human TLR1 (clone FAB1484A, R&D Systems, Bio-Techne, UK). Live dead staining was performed with the LIVE/DEAD® Fixable Aqua Dead Cell Stain Kit (ThermoFisher Scintific, Molecular Probes™, UK) according to the manufacturer's instructions. Samples were subsequently analysed on the CyAn Advanced Digital Processing (ADP) High-Performance Flow Cytometer (DakoCytomation), acquiring 200 000 events. Raw data generated was subsequently analysed with FlowJo version 10.0.8.

Quantitative protein immunoassay:

The concentration of MIP-3α was measured in supernatants generated from cellular and tissue models using an Elisa sandwich assay. Conditions were tested in triplicate throughout the study. Supernatants were used undiluted in the assay as much as was possible. MIP-3α was measured using the human MIP-3α Duoset Elisa kit (R&D Systems, Bio-Techne, UK) according to the manufacturer's protocol. Briefly detection was enhanced using the streptavidin-horseradish peroxidase (HRP) enzyme system. The substrate was based on the hydrogen peroxide tetramethylbenzidine (H_2O_2 TMB) system. Data were collected using the POLARstar Omega ELISA reader. Quantitation was based on a standard curve after OD measurements at 450 nm on an Elisa reader. The lower limit of detection of MIP-3α with this assay was around 6,25 pg/mL.

Statistical analyses:

For *in vitro* cellular assays, cells were seeded in triplicate wells. For *ex vivo* explant tissue assays, explants were seeded at one explant per well but each condition

was tested in triplicate. *In vitro* assays were repeated for a minimum of three experiments before being included in the study results. For Elisa generated data, quantitation was done based on a 4PL regression curve fitted formula from the standard curve after OD measurements at 450 nm. Statistical analyses were performed using GraphPad Prism version 7 for Mac OS X (Prism, GraphPad Software, La Jolla, California, USA). Descriptive data were presented with schema prepared from Microsoft Excel (2011 version for Mac) and GraphPad Prism. Unpaired two sample *t*-tests were performed to compare unstimulated (medium only) to stimulated MIP-3α levels. P-values were taken as non-significant if $p>0.05$, and significant if $p \leq 0.05$ (*), $p \leq 0.01$ (**), $p \leq 0.001$ (***), and $p \leq 0.0001$ (****). For flow cytometry generated data, data was presented as histograms prepared on FlowJo version 10.0.8. Cell expression of TLRs was presented as a percentage of cells taking up the stain, comparing stained and unstained epithelial cells. Results were reported in bar graphs with bars representing the mean of three tests and error bars representing standard deviation. Levels of MIP-3α were expressed in pg/mL throughout the study.

RESULTS

TLR4 is the highest expressed TLR in endocervical primary epithelial cells and HEC-1A cells

Previous studies using different techniques, polymerase chain reaction (PCR) and immunohistochemistry, found inconsistent results with regards to TLRs expressed by the endocervical epithelium. Particularly, there was no consistency regarding the expression of TLR4. Moreover, no one has studied this sub-compartment answering this question of TLR expression on EPECs using the flow cytometric immunoassay. We hence started our assessment of epithelial responses to microbial stimulation by first phenotyping TLR expression on EPECs. We prepared EPECs from three hysterectomy specimens collected from women in the reproductive age group. We stained EPECs on Day 8 post plating and HEC-1A cells on Day 5 post plating when the cells had reached respective maximal TEER.

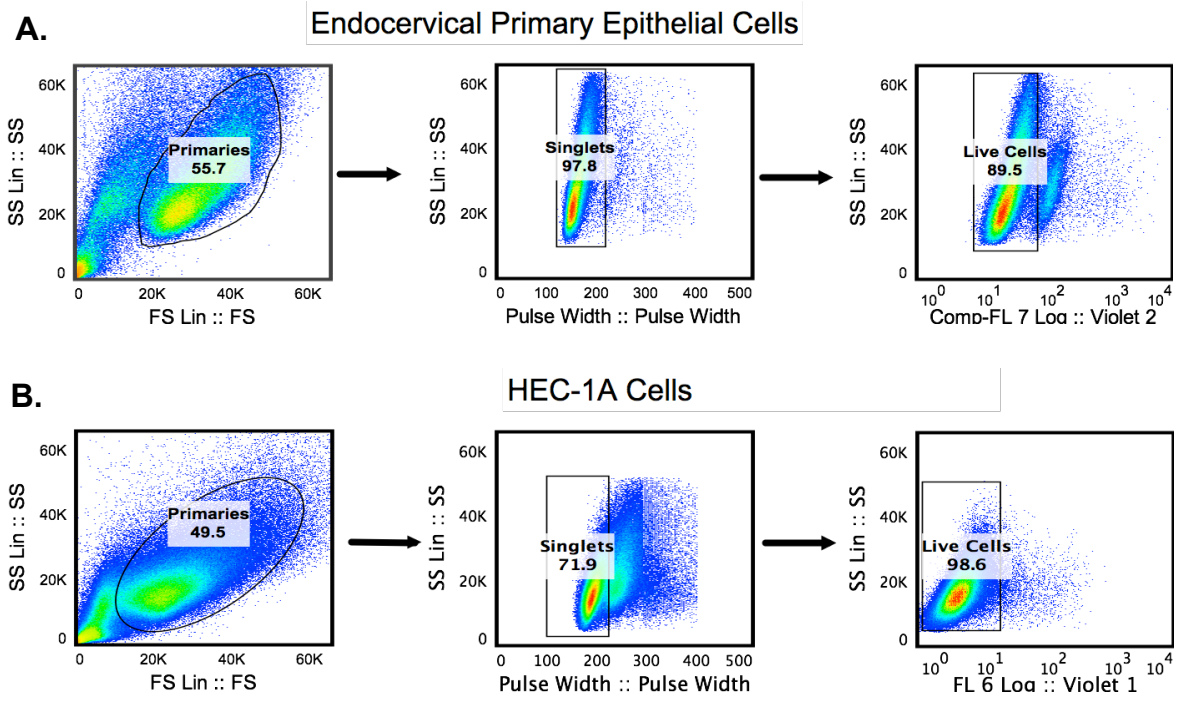

Figure 4.2: Gating strategy for epithelial cells on flow cytometry. A. EPECs and B. HEC-1A cells. We gated on live cells for the analysis on TLR expression by epithelial cells.

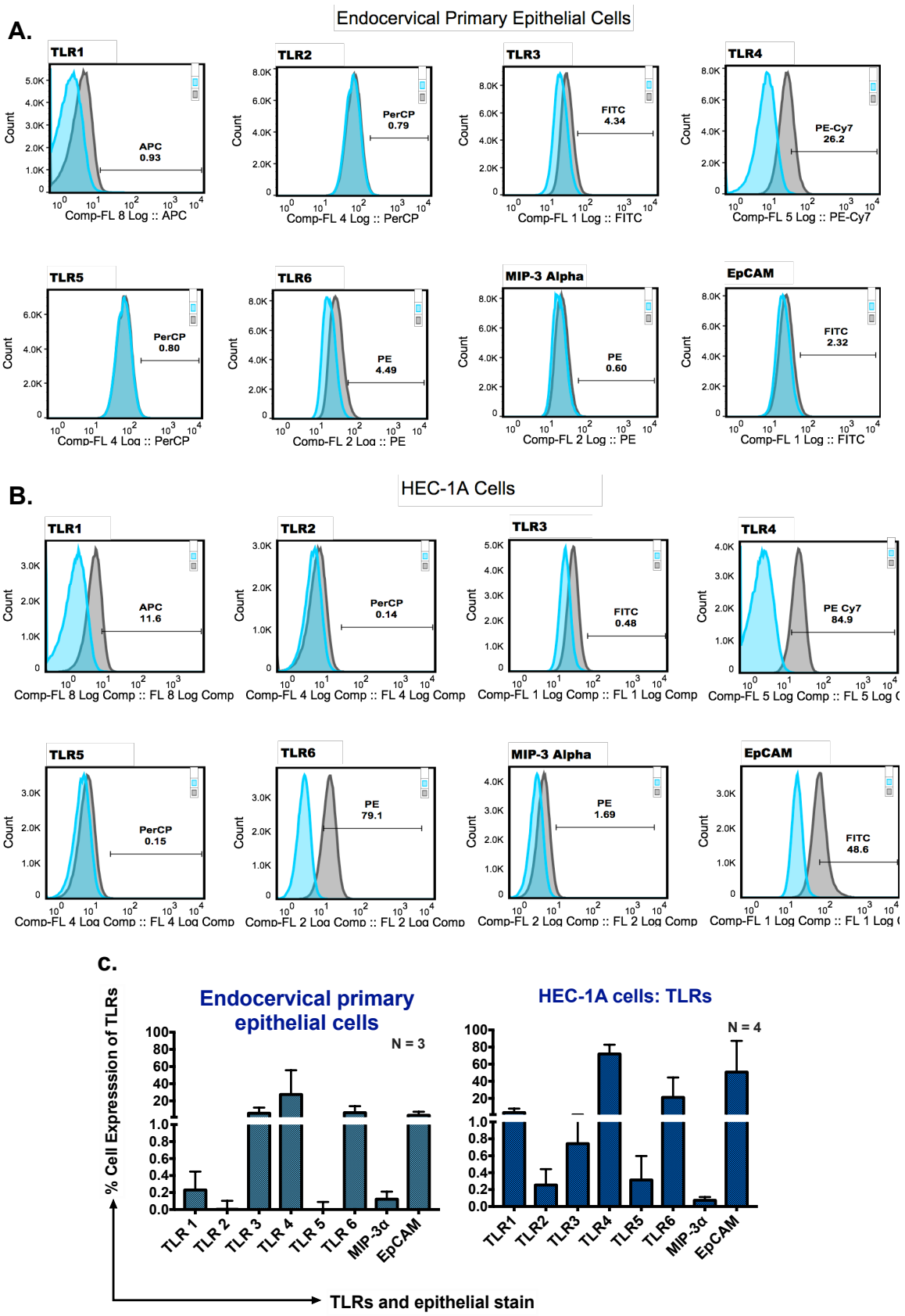

Figure 4.3: Flow cytometric analyses of cellular expression of TLRs on EPECs and HEC-1A cells. A. and B. are histogram graphical presentations of TLRs expressed on these two cell types with blue curves denoting unstained cells and gray curves denoting antibody stained cells. Shown in the curves are the percentages of epithelial cells expressing intracellular and surface TLRs, comparing stained and unstained cells. C. is a bar graphical presentation of the same data. TLR4 is the highest expressed TLR in both models. TLRs 1, 3, and 6 are also highly expressed in both models while TLRs 2 and 5 are poorly expressed.

We did whole cell staining for each of the first six TLRs, regardless of whether TLRs are understood to be normally expressed on the surface or intracellularly in the literature. There was a high proportion of live cells amongst both cell types, above 80% of gated epithelial cells (*Figure 4.2*). There were more cells staining positively for EpCAM , an epithelial cell stain, among HEC-1A cells versus EPECs. This was not surprising as HEC-1A cells, a cell line, are likely to be a homogenous population of epithelial cells as opposed to EPECs, which were prepared fresh from hysterectomy samples. There was generally a similar distribution of TLRs between these two epithelial models studied, however, HEC-1A cells had higher TLR expression than EPECs. Both the EPECs and HEC-1A cells demonstrated highest cell expression for TLR4 and TLR6 with expression being highest in HEC-1A cells than in EPECs at around 20% and 70%, respectively. TLR 2 and TLR5 were barely detectable in EPECs even though they were also low in HEC-1A cells. Both TLR1 and TLR3 were expressed in both sub-compartments. These findings that epithelial cells in the FGT differentially express TLRs confirm that the FGT has the capacity to respond to a variety of microbials.

Kinetics of MIP-3α in HEC-1A cells: MIP-3α is detectable within 4 hours of stimulation with poly I:C, a TLR3 ligand

Having demonstrated that HEC-1A cells express all the first six TLRs including TLR3, we proceeded to study the kinetics of MIP-3α in this cell line. We plated HEC-1A cells in 24 well tissue culture plates at 50,000 cells per well in 600µL of complete McCoy's medium. We subsequently stimulated them with poly I:C, a TLR3 ligand, 24 hours after seeding and incubating them at 37^0C 5% CO_2. We stimulated with a wide range of poly I:C concentrations starting from a

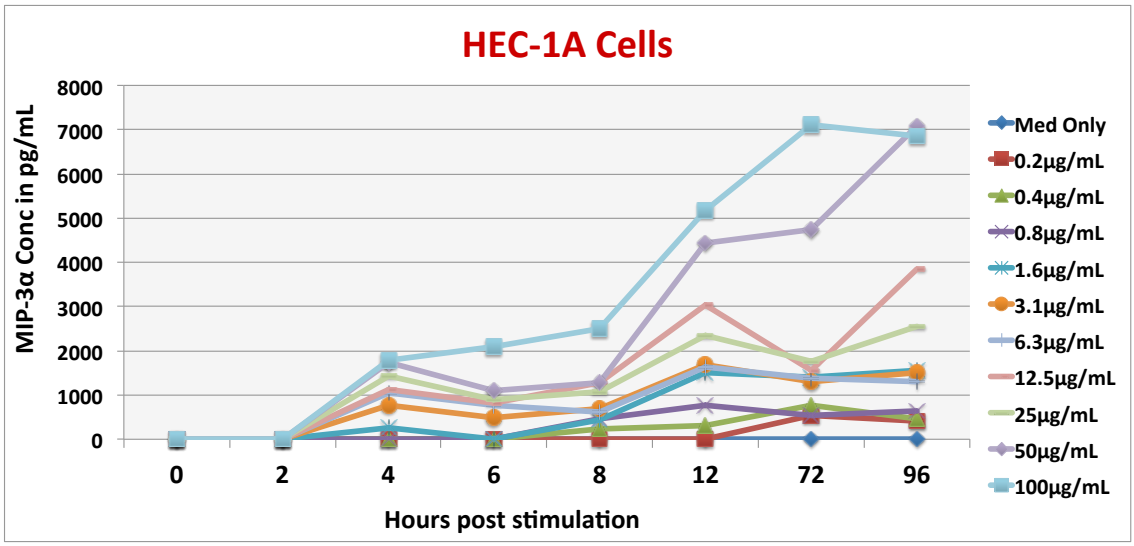

Figure 4.4: Kinetics of MIP-3α over 96 hours in HEC-1A cells, an endometrial cell line. We grew HEC-1A cells in 24 well tissue culture plates in 600µL of medium. We plated and incubated cells for 24 hours before stimulating them with various concentrations of poly I:C, a TLR3 ligand. Conditions were tested in triplicate and levels of MIP-3α were quantified in supernatants with a sandwich Elisa. MIP-3α levels were not detectable in unstimulated cells over this period. However, MIP-3α was detectable from as early as 4 hours post stimulation, stimulating with as little as 1.6µg/mL of poly I:C.

concentration of 0.2µg/mL through to 100µg/mL. We subsequently harvested supernatants from baseline (0 hours) prior to stimulation and then from two hours post stimulation, initially harvesting at two-hour intervals through to 96 hours post stimulation (*Figure 4.4*). We quantified MIP-3α levels in supernatants with a sandwich Elisa. MIP-3α levels were detectable within four hours of stimulation, stimulating with poly I:C, and this was with a poly I:C concentration of as little as 1.6µg/mL. Levels reached a maximum of about 2000pg/mL stimulating with 200µg/mL of poly I:C. MIP-3α was not detected throughout this period in unstimulated cells. Having previously demonstrated constitutive secretion of MIP-3α by the HEC-1A cell line, these findings that poly I:C triggers MIP-3α secretion confirm that MIP-3α is a chemokine that is secreted both constitutively and on induction in this sub-compartment. Further they confirm that MIP-3α secretion can be triggered as early as within 24 hours post stimulation on microbial exposure.

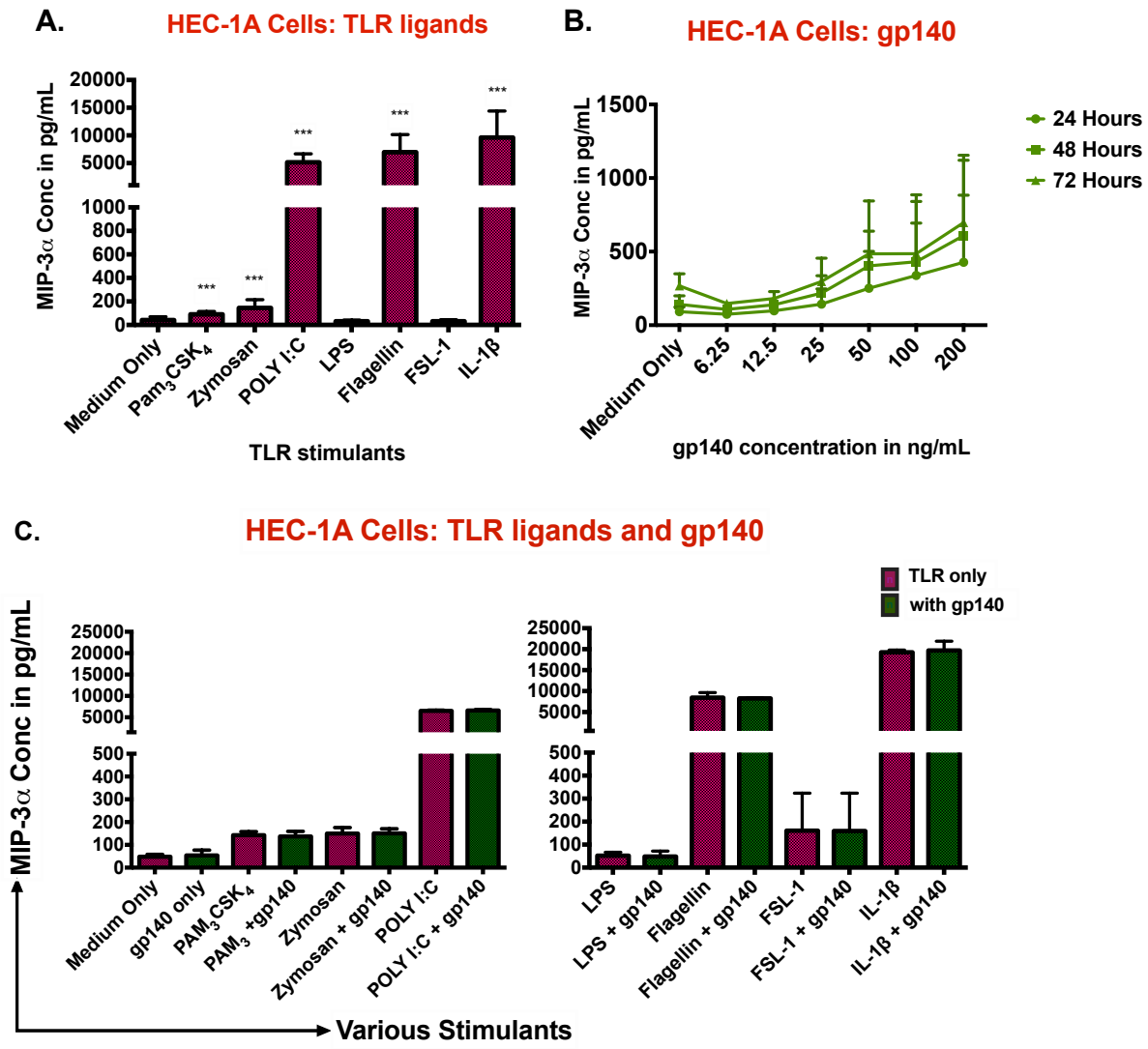

Figure 4.5: Stimulated levels of MIP-3α in HEC-1A cells stimulating with TLR ligands 1 through 6 and HIV-1 soluble CN54gp140 trimeric protein, an envelope glycoprotein, n=3. We used IL-1β as a positive control. We plated 50,000 HEC-1A cells in 24 well tissue culture plates in 600µL of medium. We incubated cells for five days before stimulating them with various TLR ligands and gp140 concentrations. Conditions were tested in triplicate and levels of MIP-3α were quantified in supernatants with a sandwich Elisa. MIP-3α secretion was significantly elevated following exposure to TLR ligands 1, 2, 3 and 5 (A.). However, it was not significantly elevated following exposure to gp140, regardless of concentration used and duration of exposure to gp140 (B.). Co-stimulating HEC-1A cells with gp140 and various TLR ligands did not trigger further elevation of MIP-3α levels above those triggered by TLR ligands alone (C.). *t* tests were performed to compare unstimulated to stimulated MIP-3α levels. P-values were taken as non-significant if $p>0.05$, and significant if $p \leq 0.05$ (*), $p \leq 0.01$ (**), $p \leq 0.001$ (***), and $p \leq 0.0001$ (****).

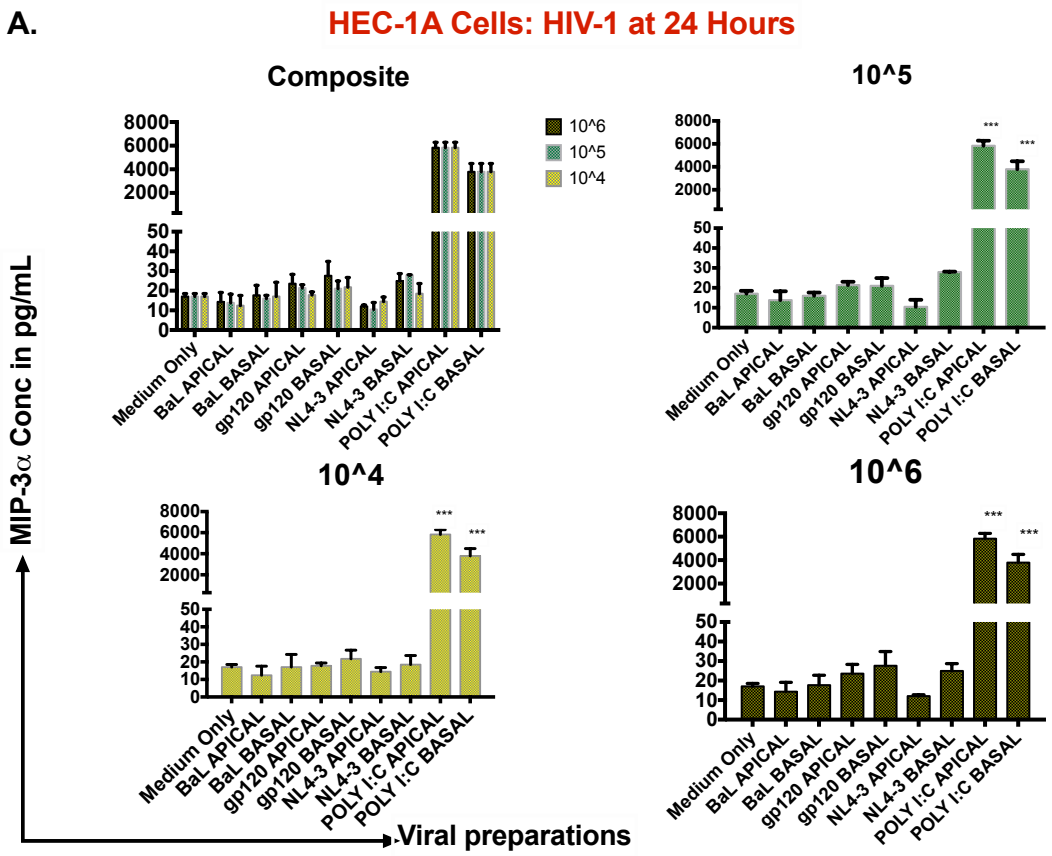
A.
HEC-1A Cells: HIV-1 at 24 Hours
Composite
10^5
10^4
10^6
10^6
10^5
10^4
MIP-3α Conc in pg/mL
Viral preparations
Medium Only
BaL APICAL
BaL BASAL
gp120 APICAL
gp120 BASAL
NL4-3 APICAL
NL4-3 BASAL
POLY I:C APICAL
POLY I:C BASAL

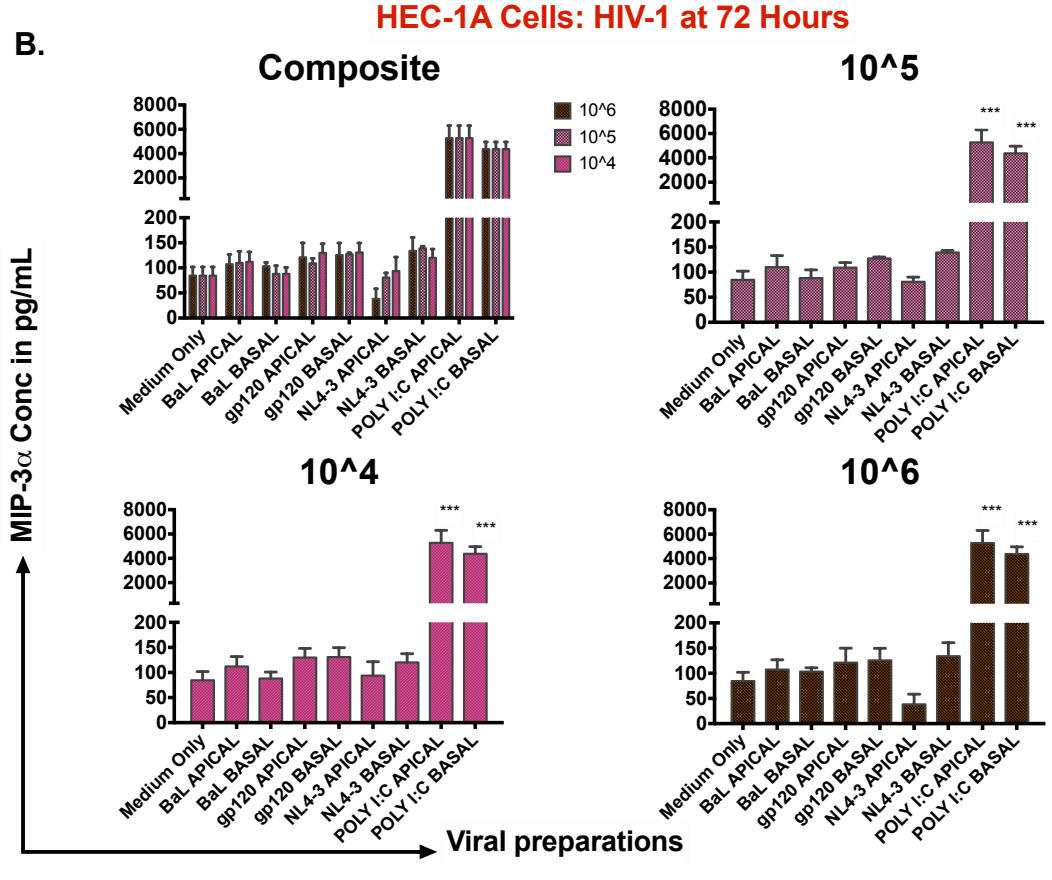
B.
HEC-1A Cells: HIV-1 at 72 Hours
Composite
10^5
10^4
10^6
10^6
10^5
10^4
MIP-3α Conc in pg/mL
Viral preparations
Medium Only
BaL APICAL
BaL BASAL
gp120 APICAL
gp120 BASAL
NL4-3 APICAL
NL4-3 BASAL
POLY I:C APICAL
POLY I:C BASAL

Figure 4.6: Stimulated levels of MIP-3α in HEC-1A cells stimulating with various envelope and non-envelope HIV-1 preparations, n=3. Specifically we stimulated with HIV-1 CN54gp120 virus-like particles (VLPs), R5 tropic whole virus, inactivated HIV-1 BaL, and HIV-1 NL4-3 deleted in Env. We used poly I:C as a positive control. We plated 50,000 HEC-1A cells on permeable supports of Transwell® inserts. We added 200μL and 600μL of medium into the apical and basal compartments, respectively. We incubated cells for five days before stimulating them with various viral preparations. We stimulated with various concentrations of virus, from 10^4 to 10^6 viral units per well and we stimulated from both poles of the inserts i.e. apical and basal. We subsequently harvested supernatants at two time points, 24 hours (A.) and 72 hours (B.) post stimulation, and quantified levels of MIP-3α in the apical compartment of the Transwell® inserts. Conditions were tested in triplicate and levels of MIP-3α were quantified in supernatants with a sandwich Elisa. HIV-1 did not trigger significant secretion of MIP-3α in HEC-1A cells. Epithelial pole of stimulation and concentration of viral particles used to stimulate HEC-1A cells did not impact the levels of secreted MIP-3α. *t* tests were performed to compare unstimulated to stimulated MIP-3α levels. P-values were taken as non-significant if $p>0.05$, and significant if $p \leq 0.05$ (*), $p \leq 0.01$ (**), $p \leq 0.001$ (***), and $p \leq 0.0001$ (****).

HIV-1 preparations do not trigger MIP-3α secretion in HEC-1A cells, however, TLR1, TLR2, TLR3, and TLR5 ligands trigger significant MIP-3α secretion in HEC-1A cells

Having confirmed TLR expression and that the secretion of MIP-3α is stimulated in the FGT, we sought to assess the extent to which TLR ligands trigger MIP-3α secretion. We also wanted to determine whether or not HIV-1 triggers MIP-3α secretion, and if it does, what the pattern of this secretion is. In order to answer these questions, we used HEC-1A cells in the exact same set up we had used them to undertake constitutive MIP-3α studies in the preceding chapter. We initially plated 50,000 HEC-1A cells in 24 well tissue culture plates in 600μL of complete McCoy's medium. We incubated them for five days before stimulating them with TLR ligands 1 through 6, and various gp140 concentrations. Specifically we stimulated with HIV-1 soluble CN54gp140 trimeric protein, an envelope glycoprotein, stimulating with a range of concentrations from 6ng/mL to 200ng/mL. We stimulated with TLR ligands for 24 hours before harvesting supernatants,

whereas we stimulated with gp140 for 24 to 72 hours, harvesting supernatants at the respective 24-hour intervals. Levels of MIP-3α were subsequently quantified in supernatants with a sandwich Elisa. MIP-3α secretion was significantly elevated following exposure to TLR ligands 1, 2, 3 and 5 (*Figure 4.5A.*) even though the pattern of up-regulation did not correlate with TLRs expressed on HEC-1A cells from our findings. TLRs 4 and 6 were the highest expressed TLRs on HEC-1A cells yet the highest levels of MIP-3α were seen with TLR3 and TLR5 ligands. However, MIP-3α levels were not significantly elevated following exposure to gp140, regardless of the concentration used and the duration of exposure to gp140 (*Figure 4.5B.*). TLR ligands are used widely as adjuvants in the literature. Co-stimulating HEC-1A cells with gp140 and various TLR ligands in this analysis did not trigger further elevation of MIP-3α levels above those triggered by TLR ligands alone (*Figure 4.5C.*), thus suggesting that the action of gp140 on HEC-1A cells is not potentiated by TLR ligands.

In view of the highly immunogenic HIV-1 gp140 trimer not triggering further MIP-3α secretion in HEC-1A cells, we proceeded to answer the question of the impact of the rest of viral preparations including whole virus on MIP-3α secretion by HEC-1A cells. We wanted to establish whether this was a pattern unique to gp140 or whether it would be replicated with another envelope preparation and whole virus preparation. We particularly wanted to determine whether in the context of MIP-3α secretion the stimulatory action of HIV-1 is dependent on (i) the presence of viral envelope or not, (ii) dose of virus or not, (iii) duration of epithelial exposure to virus or not, and (iv) epithelial pole of exposure or not. We seeded 50,000 HEC-1A cells on permeable supports of Transwell® inserts. We added 200µL and 600µL of complete McCoy's medium into the apical and basal compartments, respectively.

We incubated cells for five days before stimulating them with various envelope and non-envelope viral preparations. Specifically we stimulated with HIV-1 CN54gp120 virus-like particles (VLPs), R5 tropic whole virus, inactivated HIV-1 BaL, and HIV-1 NL4-3 deleted in Env. We used poly I:C as a positive control. We stimulated with various concentrations of virus, from 10^4 to 10^6 viral units per well and we stimulated from both poles of the inserts, alternating apical and basal compartments (*Figure 4.6*). We subsequently harvested supernatants at two time points, 24 hours (*Figure 4.6A*.) and 72 hours (*Figure 4.6B.)* post stimulation, and quantified levels of MIP-3α in supernatants from the apical compartment of the Transwell® inserts. Conditions were tested in triplicate and levels of MIP-3α were quantified in supernatants with a sandwich Elisa. HIV-1 did not trigger significant secretion of MIP-3α in HEC-1A cells. Using whole virus or envelope alone did not make any difference to levels of MIP-3α secreted. The epithelial pole of stimulation and concentration of viral particles used to stimulate HEC-1A cells also did not impact the levels of secreted MIP-3α: MIP-3α levels were not different stimulating from the apical or the basal compartments. Neither did duration of exposure trigger significant further secretion of MIP-3α: MIP-3α levels were not different stimulating for 24 or 72 hours. These findings thus confirm that HIV-1 does not trigger MIP-3α secretion in the human endometrial cell line.

HIV-1 preparations do not trigger MIP-3α secretion in Caco-2 cells, however, TLR1 and TLR6 ligands trigger significant MIP-3α secretion in Caco-2 cells

Following discovery of MIP-3α, its secretion pattern was shown to be inconsistent being inducing agent-specific and secretion site-dependent. Hence we wanted to establish whether the epithelial non-response to HIV-1 seen in the context of

Caco-2 Cells

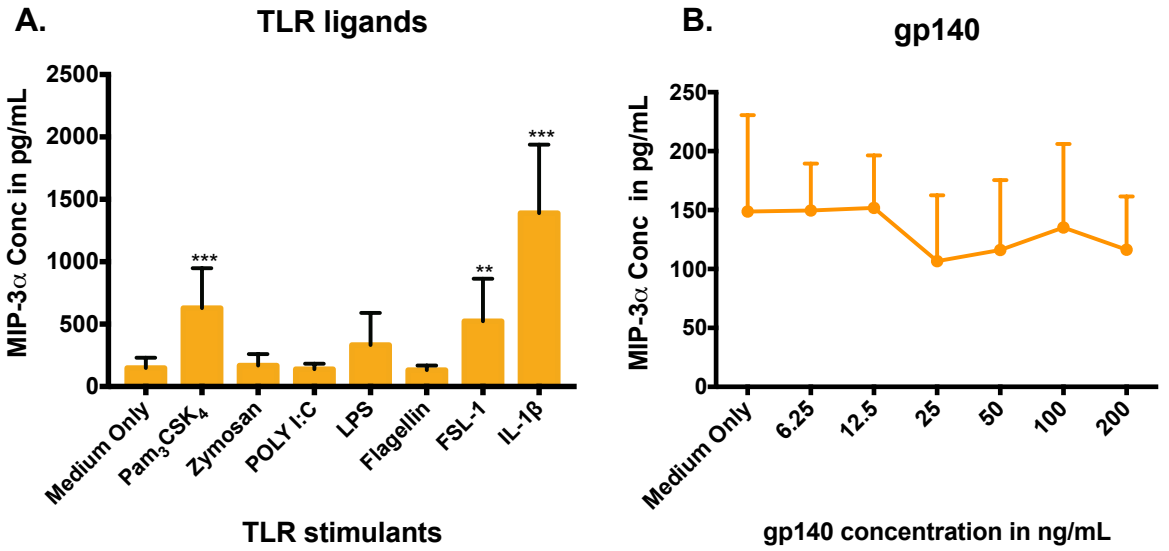
A.
TLR ligands
MIP-3α Conc in pg/mL
2500
2000
1500
1000
500
0
***
***
**
Medium Only
Pam3CSK4
Zymosan
POLY I:C
LPS
Flagellin
FSL-1
IL-1β
TLR stimulants
B.
gp140
MIP-3α Conc in pg/mL
250
200
150
100
50
0
Medium Only
6.25
12.5
25
50
100
200
gp140 concentration in ng/mL

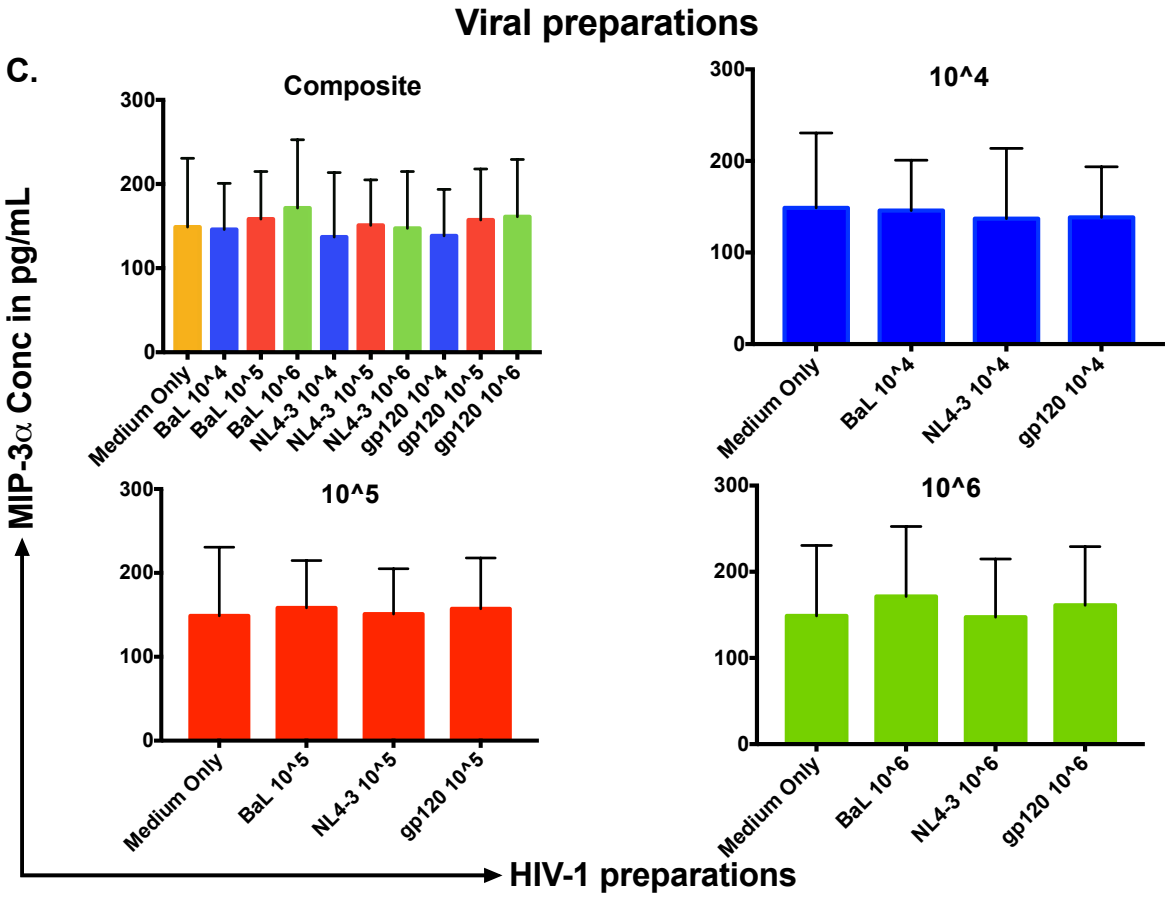
Viral preparations
C.
MIP-3α Conc in pg/mL
Composite
300
200
100
0
Medium Only
BaL 10^4
BaL 10^5
BaL 10^6
NL4-3 10^4
NL4-3 10^5
NL4-3 10^6
gp120 10^4
gp120 10^5
gp120 10^6
10^4
Medium Only
BaL 10^4
NL4-3 10^4
gp120 10^4
10^5
Medium Only
BaL 10^5
NL4-3 10^5
gp120 10^5
10^6
Medium Only
BaL 10^6
NL4-3 10^6
gp120 10^6
HIV-1 preparations

Figure 4.7: Stimulated levels of MIP-3α in Caco-2 cells stimulating with TLR ligands 1 through 6 and various envelope and non-envelope HIV-1 preparations, n=3. Specifically we stimulated with HIV-1 soluble CN54gp140 trimeric protein, an envelope glycoprotein, HIV-1 CN54gp120 virus-like particles (VLPs), R5 tropic whole virus, inactivated HIV-1 BaL, and HIV-1 NL4-3 deleted in Env. We used IL-1β as a positive control. We seeded 50,000 HEC-1A cells in 24 well tissue culture plates in 600μL of medium. We incubated cells for five days before stimulating them with various TLR ligands, and various viral preparations at various concentrations. Conditions were tested in triplicate and levels of MIP-3α were quantified in supernatants with a sandwich Elisa. MIP-3α secretion was significantly elevated following exposure to TLR ligands 1 and 6 (A.). The soluble trimer of HIV-1 CN54gp140, tested at various concentrations, did not trigger MIP-3α secretion in Caco-2 cells (B.). Neither did the other preparations of HIV-1 at various concentrations trigger MIP-3α secretion in Caco-2 cells (C.). *t* tests were performed to compare unstimulated to stimulated MIP-3α levels. P-values were taken as non-significant if $p>0.05$, and significant if $p \leq 0.05$ (*), $p \leq 0.01$ (**), $p \leq 0.001$ (***), and $p \leq 0.0001$ (****).

MIP-3α with the endometrial cell line would be replicated in another body site outside of the FGT. We thus proceeded to study MIP-3α secretion patterns in an epithelial colorectal cell line derived from an adenocarcinoma, the Caco-2 cell line. Once again, we seeded 50,000 Caco-2 cells in 24 well tissue culture plates in 600μL of complete DMEM. We incubated them for five days before stimulating them with TLR ligands 1 through 6, and various HIV-1 preparations we used in the experiments with HEC-1A cells above. Specifically we stimulated with HIV-1 soluble CN54gp140 trimeric protein, an envelope glycoprotein, stimulating with a range of concentrations from 6ng/mL to 200ng/mL. We also stimulated with concentrations ranging from 10^4 to 10^6 viral particles per well with HIV-1 CN54gp120 virus-like particles (VLPs), R5 tropic whole virus, inactivated HIV-1 BaL, and HIV-1 NL4-3 deleted in Env. We stimulated with all stimulants for 24 hours before harvesting supernatants for the sandwich Elisa. MIP-3α secretion was significantly elevated following exposure to TLR ligands 1 and 6 (*Figure 4.7A.*), a result which was significantly different from that seen in HEC-1A cells. In HEC-1A cells, MIP-3α secretion was significantly elevated following exposure to TLRs 1, 2,

3 and 5. Notably though, similarly to HEC-1A cells, there was still no elevation in MIP-3α levels stimulating with all the HIV-1 preparations, regardless of dose of virus or presence of envelope. These results that TLR ligands differentially trigger MIP-3α secretion in two different body sites while it is not triggered by exposure to HIV-1 in both these sites confirm that HIV-1 does not trigger epithelial cells to secrete further amounts of MIP-3α.

HIV-1 preparations do not trigger MIP-3α secretion in endocervical primary epithelial cells, however, TLR1, TLR3, TLR5 and TLR6 ligands trigger significant MIP-3α secretion in the same cells

We confirmed lack of MIP-3α secretion on exposure to HIV-1 by two ECL taken from two different body sites. However, our study had primarily aimed to focus on the endocervical sub-compartment, and hence we proceeded to study stimulated MIP-3α secretion patterns in endocervical epithelial models stimulating with the same stimulants as we had used in the two epithelial models above. Once again, we seeded 50,000 EPECs in 24 well tissue culture plates in 600μL of complete K-SFM. We incubated them for eight days before stimulating them with TLR ligands 1 through 6, and various HIV-1 preparations we used in the experiments with HEC-1A and Caco-2 cells above. Specifically we stimulated with HIV-1 soluble CN54gp140 trimeric protein, an envelope glycoprotein, stimulating with a range of concentrations from 6ng/mL to 200ng/mL. We also stimulated with concentrations ranging from 10^4 to 10^6 viral particles per well with HIV-1 CN54gp120 virus-like particles (VLPs), R5 tropic whole virus, inactivated HIV-1 BaL, and HIV-1 NL4-3 deleted in Env. We stimulated with all stimulants for 24 hours before harvesting supernatants for the sandwich Elisa. MIP-3α secretion was significantly elevated following exposure to TLR ligands 1, 3, 5 and 6 (*Figure 4.8A.*), a result which was

Endocervical primary epithelial cells

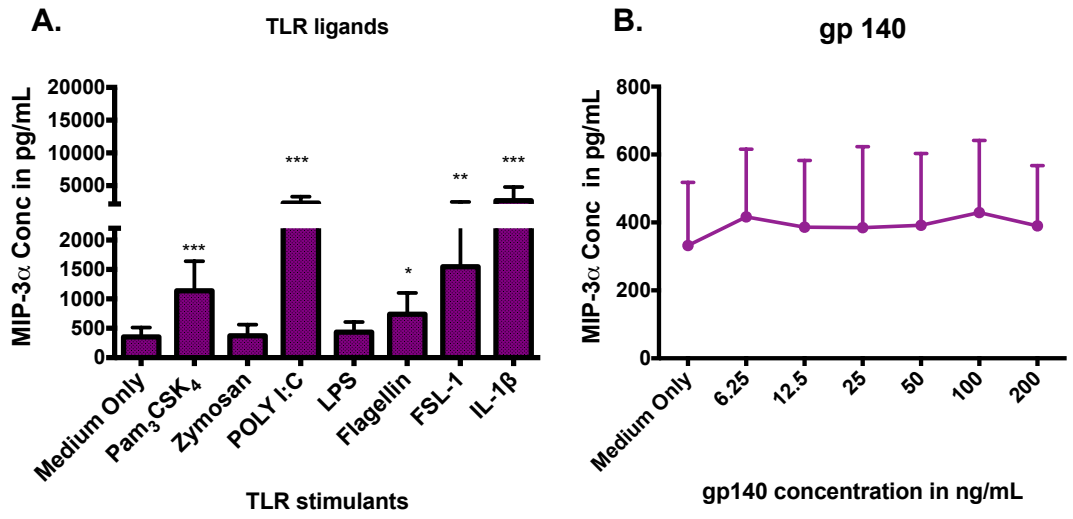

Viral preparations

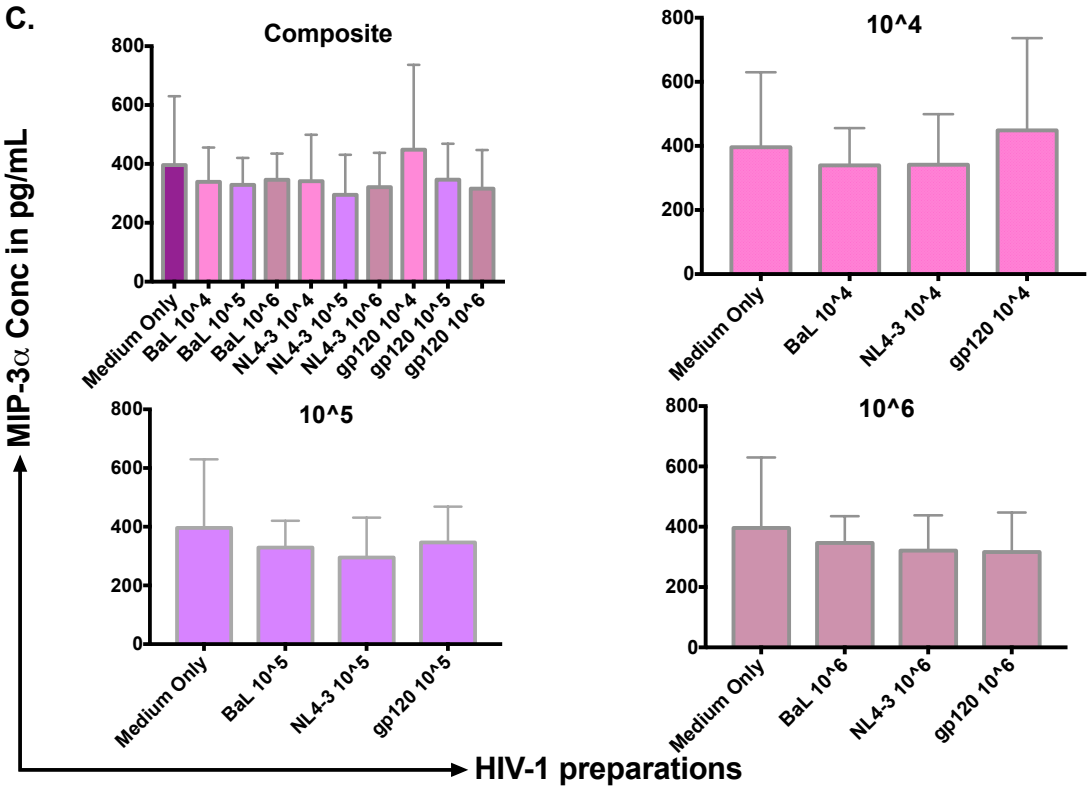

Figure 4.8: Stimulated levels of MIP-3α in EPECs stimulating with TLR ligands 1 through 6 and various envelope and non-envelope HIV-1 preparations, n=3. Specifically we stimulated with HIV-1 soluble CN54gp140 trimeric protein, an envelope glycoprotein, HIV-1 CN54gp120 virus-like particles (VLPs), R5 tropic whole virus, inactivated HIV-1 BaL, and HIV-1 NL4-3 deleted in Env. We used IL-1β as a positive control. We seeded 50,000 EPECs in 24 well tissue culture plates in 600μL of medium. We incubated cells for eight days before stimulating them with various TLR ligands, and various viral preparations at various concentrations. Conditions were tested in triplicate and levels of MIP-3α were quantified in supernatants with a sandwich Elisa. MIP-3α secretion was significantly elevated following exposure to TLR ligands 1, 3, 5 and 6 (A.). The soluble trimer of HIV-1 CN54gp140, tested at various concentrations, did not trigger MIP-3α secretion in EPECs (B.). Neither did the other preparations of HIV-1 trigger MIP-3α (C.). *t* tests were performed to compare unstimulated to stimulated MIP-3α levels. P-values were taken as non-significant if $p>0.05$, and significant if $p \leq 0.05$ (*), $p \leq 0.01$ (**), $p \leq 0.001$ (***), and $p \leq 0.0001$ (****).

however somewhat different from that seen in HEC-1A and Caco-2 cells. In HEC-1A cells, MIP-3α secretion was elevated following exposure to TLRs 1, 2, 3 and 5 while in Caco-2 cells it was elevated in response to TLR ligands 1 and 6. All three cell types responded significantly to stimulation by TLR1 ligand while none of them responded to the TLR4 ligand stimulation. Notably again, similarly to both HEC-1A and Caco-2 cells, there was still no elevation in MIP-3α levels stimulating with all the HIV-1 preparations. Further, except for TLRs 4 and 5, the pattern of up-regulation following exposure to TLR ligands somewhat matched TLRs expressed on EPECs. TLRs 1, 3, 4, and 6 were the highest expressed TLRs while TLR ligands 1, 3, 5 and 6 triggered highest MIP-3α levels in EPECs. Again, these results, that TLR ligands trigger MIP-3α secretion in three different body sites, albeit in a different pattern, while HIV-1 preparations do not trigger further secretion of MIP-3α in all these sites, further strengthen the evidence that HIV-1 does not trigger epithelial cells to secrete MIP-3α.

Neither HIV-1 preparations nor TLR ligands trigger MIP-3α secretion in the endocervical explant tissues.

Having demonstrated the lack of response to HIV-1 in EPECs, we went on to validate these results in another endocervical epithelial model, the endocervical explant tissue model. Explant tissues are a form of *ex vivo* culture models designed as a bridge between cell cultures and *in vivo* models. They are prepared from a sample of tissue taken from part of the organ of interest through biopsy or resection, which is then dissected free of underlying musculature. Thus the remaining tissue comprises both mucosal and submucosal components. Their greatest strength is that they do not disrupt the natural organisation of the tissues, and they preserve the interactions between the epithelial cells and the underlying stromal cells. For these experiments, we recruited women in the reproductive age group scheduled for a hysterectomy for their own health. We subsequently prepared explant tissues from their endocervices, which we prepared and used fresh i.e. within 2 to 4 hours of resection from the body. We plated one explant per well of a 96 well tissue culture plate in 200µL of complete RPMI-1640 medium. We stimulated them with TLR ligands 1 through 6, and various HIV-1 preparations as we had used in the experiments with HEC-1A, Caco-2 cells and EPECs above. Specifically we stimulated with HIV-1 soluble CN54gp140 trimeric protein, an envelope glycoprotein, stimulating with a range of concentrations from 6ng/mL to 200ng/mL. We also stimulated with concentrations ranging from 10^4 to 10^6 viral particles per well with HIV-1 CN54gp120 virus-like particles (VLPs), R5 tropic whole virus, inactivated HIV-1 BaL, and HIV-1 NL4-3 deleted in Env. We stimulated with all stimulants for 24 hours before harvesting supernatants for the sandwich

Endocervical explant tissues

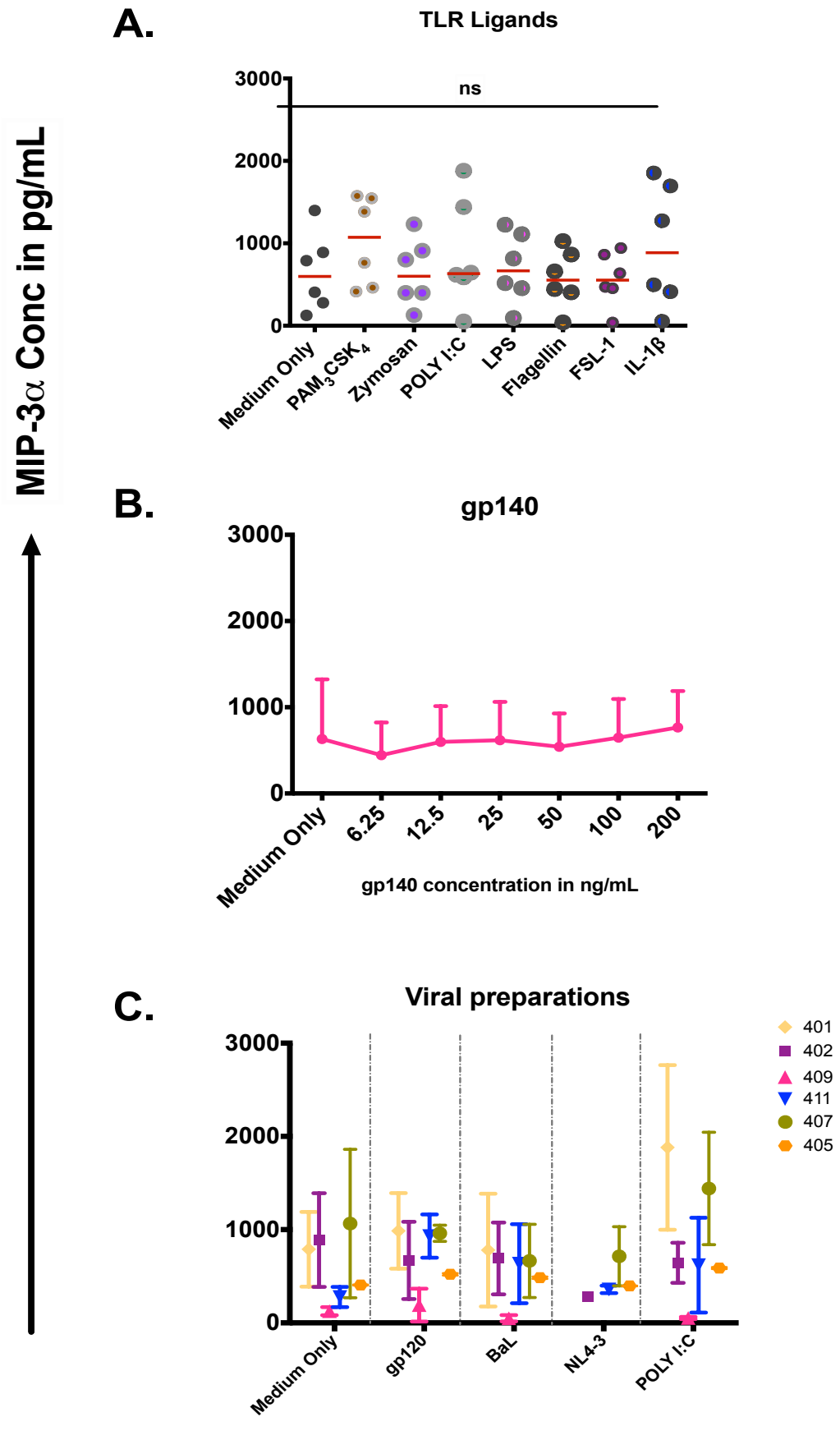

Figure 4.9: Stimulated levels of MIP-3α in EET stimulating with TLR ligands 1 through 6 and various envelope and non-envelope HIV-1 preparations, n=6. Specifically we stimulated with HIV-1 soluble CN54gp140 trimeric protein, an envelope glycoprotein, HIV-1 CN54gp120 virus-like particles (VLPs), R5 tropic whole virus, inactivated HIV-1 BaL, and HIV-1 NL4-3 deleted in Env. We used IL-1β as a positive control. We plated one explant tissue block per well in a 96 well tissue culture plate in 200μL of medium. We prepared and stimulated explant tissues immediately post womb resection. We stimulated them with various TLR ligands, and various viral preparations at various concentrations. Conditions were tested in triplicate and levels of MIP-3α were quantified in supernatants with a sandwich Elisa. Supernatants were harvested 24 hours post stimulation. MIP-3α secretion was constitutively high in EET. TLR ligands did not trigger MIP-3α secretion in EET (A.). Neither did the soluble trimer of HIV-1 CN54gp140, tested at various concentrations (B.) or other preparations of HIV-1 trigger MIP-3α (C.). *t* tests were performed to compare unstimulated to stimulated MIP-3α levels. P-values were taken as non-significant if $p>0.05$, and significant if $p \leq 0.05$ (*), $p \leq 0.01$ (**), $p \leq 0.001$ (***), and $p \leq 0.0001$ (****).

Elisa. We tested each condition in triplicate. EET secreted high constitutive levels of MIP-3α, however, secretion was not significantly elevated following exposure to either TLR ligands or HIV-1 preparations (*Figure 4.9*). Notably, TLR ligands that had differentially triggered MIP-3α secretion in EPECs, another endocervical model, did not trigger significant MIP-3α secretion in EET. Neither did the soluble trimer of HIV-1 CN54gp140, tested at various concentrations. Again, these results that HIV-1 preparations do not trigger further secretion of MIP-3α exposure to HIV-1 in all these sites further strengthen the evidence that HIV-1 does not trigger epithelial cells to secrete MIP-3α.

DISCUSSION

We studied the pattern of stimulated MIP-3α secretion focusing on various epithelial matrices, including two cell lines, primary epithelial cells, and explant tissues. Numerous studies have studied epithelial secretion of MIP-3α in the FGT, but did not focus on the endocervix. Instead they focused on ECL and primary cell models, concentrating only on the fallopian tubes, endometrium and vagina, and these studies were not undertaken in the HIV context [93, 95, 101]. Further, numerous studies have reported stimulated MIP-3α secretion in the FGT, but they only used chemical compounds and proinflammatory mediators such as phorbol myristate acetate (PMA), ionomycin, tumour necrosis factor alpha (TNF-α), and lipopolysaccharide (LPS) to trigger its secretion [138]. However, after findings from the landmark study in 2009 by Li *et al* suggested a significant role of MIP-3α in early SIV transmission events in the endocervix of macaques [96], it was important to assess the role of MIP-3α in the human endocervix in the context of HIV infection. This study has therefore extended this body of knowledge by studying the impact of HIV-1 exposure on MIP-3α secretion patterns by explant tissues and primary cells from the endocervix of humans.

Chemokines are categorised according to whether their secretion is induced or stimulated; MIP-3α is a chemokine that is secreted both constitutively and on stimulation [88]. However, its secretion is known to be specific for both epithelial cell site and inducing agent [96]. Hence, after demonstrating constitutive secretion patterns, we studied MIP-3α secretion following stimulation with TLR ligands 1 through 6, soluble envelope trimeric HIV-1 CN54gp140 protein, HIV-1 envelope CN54gp120 VLPs, inactivated R5 tropic HIV-1 BaL whole virus, and envelope

deleted HIV-1 NL4-3. We did this in two body sites, the FGT and the GIT.

According to our findings studying the impact of both envelope and non-envelope HIV-1 preparations on epithelial models, there is no evidence that HIV-1 triggers MIP-3α secretion in the epithelium of the FGT and the GIT. Despite demonstrable constitutive MIP-3α secretion by all epithelial models studied in the preceding chapter, HIV-1 preparations did not trigger further MIP-3α secretion in the HEC-1A endometrial cell line, Caco-2 colorectal cell line, EPECs and EET. Using a range of concentrations of HIV-1 preparations did not alter the outcome. Neither did exposing epithelial models to HIV-1 for different lengths of time. In HEC-1A cells grown on permeable supports, the pole of stimulation also did not have an impact on the outcome. These results confirm findings from the study by Berlier *et al* who studied the impact of seminal plasma (SP) exposure on the secretion of MIP-3α in the SiHa vaginal ECL [135]. SP was collected from HIV infected and HIV infected male participants. Their data showed that MIP-3α secretion was significantly triggered by exposure to SP, however, there was no significant difference between the elevated levels of MIP-3α following exposure to the two varying participant populations. Their data hence suggested that it was not HIV directly that triggered MIP-3α secretion in this vaginal model but rather that it was another constituent in SP. Seminal factors already known to facilitate viral infection include pH alteration, amyloid fibrils derived from seminal phosphatases, complement fragments and bioactive peptides responsible for inducing mucosal inflammatory reactions [139].

HIV-1 envelope preparations are considered the principal target for preventative vaccines and hence we studied envelope preparations that are highly immunogenic, trimeric gp140 and gp120 VLPs. Heterodimers of the

transmembrane glycoprotein (gp41) and a surface glycoprotein (gp120) are used to generate trimeric envelope glycoproteins (Env) similar to those that are displayed on HIV virions. The glycoproteins gp41 and gp120 are synthesised initially as a single gp160 polypeptide that is subsequently cleaved to generate the noncovalently associated gp120/gp41 complex. gp140 forms a soluble trimer that is actually considered to be a better representation of the functional trimeric Env spike of HIV-1 than gp120. The development of soluble versions of trimeric Env, such as gp140, that display biochemical and structural properties similar to those observed on infectious viruses, is of considerable interest in the context of designing vaccines against HIV/AIDS. gp140 has been shown in different preclinical studies to be highly immunogenic [140], which may offer improvements over monomeric gp120. gp140 is considered to be particularly more superior to the corresponding gp120 as an immunogen with regards to inducing more potent and cross-reactive neutralising responses. In the context of mucosal studies, gp140 has been studied as a form of mucosal immunisation where it has been shown to induce local antibody responses [141-143]. There is however no report in the literature of gp140 studied in the context of triggering innate epithelial responses reported here. Nevertheless, as immunogenic as gp140 is reported to be, it failed to induce secretion of MIP-3α levels that are above unstimulated levels in our study. Similarly, the highly immunogenic preparation of gp120 i.e. VLPs did not trigger secretion of high MIP-3α levels. VLPs are highly immunogenic as they are formed from the assembly of envelope and/or capsid proteins from many viruses.

These findings that our HIV-1 envelope preparations did not trigger MIP-3α production confirm that HIV-1 envelope does not trigger MIP-3α production in epithelial cells. These findings are, however, contradictory to those of Nazli *et al*,

who indicated in two publications that HIV-1 gp120, is sufficient to induce a direct cytokine response in endometrial primary epithelial cells (EMPECs) [136, 137]. Nazli *et al* exposed EMPECs to recombinant gp120, UV-inactivated HIV-1 and env-deleted HIV-1 and measured levels of TNF-α, IL-6, IL-1α, IL-8 and MCP-1 in supernatants. Significantly enhanced production was observed for all cytokines and chemokines; in particular, TNF-α and IL-8 were up-regulated in response to HIV-1. Notably whole infectious HIV-1 and UV-inactivated HIV-1 enhanced the levels of cytokine production by EMPECs, comparable with levels induced by recombinant gp120 protein exposure. They thus concluded that HIV-1 gp120 alone was sufficient for facilitating this effect. Consequently, their study provided proof of concept that viral envelope preparations can induce secretion of chemokines in epithelial cells. Their findings therefore suggest that if MIP-3α secretion in epithelial cells could be triggered by gp120, then we would have observed this effect in our study.

Whole R5 tropic BaL inactivated with aldrithiol-2 (AT-2) also did not trigger MIP-3α in any epithelial models in our study. AT-2 is a reagent shown to covalently modify the essential zinc fingers in the nucleocapsid protein of HIV-1 thereby arresting the viral life cycle before initiation of reverse transcription [144]. Sankapal *et al* studied pure ectocervical and colonic primary epithelial cells, looking at the impact of HIV-1 exposure on mRNA expression of CXCL10 and CXCL11 chemokines [145]. Their study demonstrated that CXCL10 and CXCL11 mRNA expression was significantly higher in the ectocervical epithelia exposed to HIV compared with those exposed to control supernatant, and that induction of such chemokines required infectious HIV as opposed to gp120 and inactivated BaL. They also inactivated their virus preparation with AT-2. Their study therefore provided proof of concept that HIV can

and does trigger expression of chemokines, except that the requirement for this biological interaction is whole infectious virus. However this is contradictory to findings by Fontenot *et al* who showed that epithelial cells are capable of secreting the cytokine TSLP on exposure to HIV, regardless of whether it is infectious or not [146]. Significantly high levels of TSLP expression on PCR and Elisa were observed in ECL from the cervix cultured with both X4 and R5 strains of HIV-1 that were infectious as well as inactivated by treatment with AT-2. Their results demonstrated that exposure to diverse HIV-1 strains, both infectious and noninfectious, can result in efficient induction of chemokine expression in a variety of epithelial cells. Another limitation with the study by Sankapal *et al* was that their study concentrated on transcriptional levels rather than protein levels of chemokine expression. However, these two studies did not study MIP-3α secretion. Nevertheless, based on their findings, it would seem therefore that it is difficult to predict what the stimulated secretion pattern of any chemokine is likely to be following viral exposure.

We phenotyped TLR expression in two epithelial models, HEC-1A cells and EPECs, and results indicated that these epithelial models do express a variety of TLRs as assessed on flow cytometry. Specifically, these cell types showed a similar pattern of TLR expression with TLRs 1, 3, 4, and 6 being the highest expressed TLRs in both of them. This was not the first time that TLR expression was studied in the FGT but various other groups employing different techniques have studied TLR expression, finding inconsistent results [127, 128, 147, 148]. Specifically, the only two studies that studied TLR expression in the endocervix employed PCR and immunohistochemical techniques showing contradictory results with regards to TLR4 expression. There was a high and unique pattern of

TLR4 expression on immunohistochemistry [147] while there was complete lack of TLR4 expression using the PCR technique [128]. Hence our results of high TLR4 expression confirmed the findings by Fazeli *et al*. Interestingly though, none of the epithelial models we studied responded to the TLR4 ligand by secreting significant levels of MIP-3α. We used LPS (Lipopolysaccharides from *Escherichia coli)* as the TLR4 ligand in our studies. The lack of a response to the TLR4 ligand despite high expression of TLR4 in our study could be because the secretion of MIP-3α is not signalled via the TLR4 signalling pathway or it could be because of the reported lack of CD14 and MD-2. We did not study the expression of MD-2 and CD14 but mucosal epithelial cells are reported to express TLR4 but not CD14, a co-receptor required for LPS recognition [149]. Further EPECs lack MD-2 according to finding by Fichorova and colleagues [128] yet the literature reports that TLR4 and MD-2 are indispensable for LPS responses [150]. On the other hand, the study by Nazli *et al,* the only study to study the mechanism behind innate epithelial responses following gp120 exposure, showed that TRLs 2 and 4 mediated the association between gp120 and epithelial responses in endometrial epithelial cells [137]. Hence the lack of response to the TLR4 ligand in our study was most likely because MIP-3α does not signal through the TLR4 pathway,

The epithelial cellular models responded differentially to TLR ligands to secrete significant levels of MIP-3α while EET did not significantly respond to TLR ligands. Specifically Caco-2 cells significantly responded to TLR ligands 1 and 6, while HEC-1A cells significantly responded to TLR ligands 1, 2, 3 and 5, and EPECs significantly responded to TLR ligands 1, 3, 5 and 6. In summary, all epithelial cellular models responded significantly to PAM_3CSK_4 (TLR1/2 ligand), while HEC-1A cells and EPECs responded significantly to poly I:C (TLR3 ligand) and flagellin

(TLR5 ligand) with regards to MIP-3α secretion. Additionally, Caco-2 cells and EPECs responded significantly to FSL-1 (TLR2/6 ligand) while HEC-1A cells also responded significantly to Zymosan (TLR2 ligand). These findings of MIP-3α being secreted in response to a wide variety of TLR ligands confirm that these routes can induce MIP-3α secretion. Further, they suggest that MIP-3α induction is not restricted to a single agent but rather that it is in response to a variety of microbes. Lastly, these findings suggest that MIP-3α secretion likely signals via multiple signaling pathways. TLR3 recognises viral double stranded RNA, while TLR5 recognises the protein flagellin. TLR2 in association with TLR1 recognise bacterial triacylated lipopeptides whileTLR2 in association with TLR6 recognise bacterial diacylated lipopeptides. The recognition of PAMPs by TLRs initiates a signalling cascade that results in the activation of transcription factors such as NF-κB and interferon regulatory factors leading to the production of pro-inflammatory cytokines and type 1 interferons. Five cytoplasmic adaptors, MyD88, Mal, Trif, TRAM and SARM, are utilized by the TLRs to activate these signaling pathways [151]. Each TLR recognises a different PAMP in a complex pattern of dimerisation to allow them to signal. Most TLRs form homodimers to allow them to signal. Specifically TLRs 3, 4, 5 and 9 function as homodimers while TLRs 1 and 6 heterodimerise with TLR2 to recognize PAMPs. On the other hand, TLR7 and TLR8 recognize single-stranded RNA even though Wang *et al* has recently shown that TLR7, 8 and 9 can interact with each other [152]. We used TLR ligand stimulation as a positive control in these experiments, and hence the demonstrable response to various microbial preparations in the form of TLR ligands alongside non-response to HIV-1 preparations confirm that HIV-1 does not trigger MIP-3α secretion in epithelial models. The non-response to TLR ligands in the EET could be because of the attenuated response due to paracrine and/or autocrine effects of the surrounding

cells in the stroma.

CONCLUSION

Having confirmed constitutive secretion of MIP-3α in the FGT in the previous chapter, the findings of this thesis chapter extend those results by demonstrating that MIP-3α secretion is stimulated in the epithelial models, and particularly those of the endocervix. Findings of response to stimulation with various microbial preparations were replicated in all epithelial cellular models and thereby confirming that MIP-3α secretion can be and is induced via various signaling pathways. However, there was no evidence that HIV-1 triggers further MIP-3α secretion in all the epithelial models including models from the human endocervix. Neither was there evidence that HIV-1 triggers MIP-3α secretion in the endometrial and colorectal cell lines. These results therefore suggest that MIP-3α is unlikely to play a significant role in mucosal early HIV infection events in the first 24 hours post HIV-1 exposure in humans.

CHAPTER FIVE MIP-3α IN THE CONTEXT OF OTHER SOLUBLE MARKERS AND ANTIMICROBIAL PEPTIDES IN THE HUMAN FEMALE GENITAL TRACT

SUMMARY

More than three decades into the Human Immunodeficiency Virus (HIV) pandemic, women globally bear the brunt of this epidemic yet there is hardly any strategy that women can use to protect themselves against HIV acquisition. Of all the biomedical preventive strategies tested to date, only one can be primarily used and controlled by women and this is only available in some countries. Of the potential strategies women could use, clinical trial results have been conflicting and perplexing. Biological reasons underlying these conflicting results remain unknown. Scientists believe that the greatest opportunities for successful interventions to prevent sexual HIV transmission are in the initial stages of infection at the portal of entry where there are the greatest host advantages and viral vulnerabilities. While a preventive vaccine holds better hope for this group, progress in its development is hindered by limited understanding of the mucosal defences at the portal of entry i.e. reproductive/genital tract in the context of heterosexual transmission. This is largely due to limited access to female genital tract (FGT) specimens, unavailability/inadequacy of research methods to sample and process these tissue specimens, and poorly standardised assay platforms for genital mucosal work. The endocervix, compared to vagina and endometrium, is less studied, as it is a narrow passage that is poorly accessible to most sampling methods in the FGT. The endocervix, however, according to recent evidence, is the primary target of infection in Simian Immunodeficiency Virus (SIV)/HIV infection. Situated between the microbial laden vagina and the relatively sterile endometrium, the endocervix is

distinctly lined by columnar epithelium that is coated by cervical mucus. Cervical mucus consists of various soluble proteins (SPs) and antimicrobial peptides (AMPs) secreted by various immune and epithelial cells that are part of the mucosal layer. While the FGT mucosal layer on the one hand secretes cytokines and chemokines such as MIP-3α that regulate resistance and/or susceptibility to infection, on the other hand it secretes AMPs that possess antiviral activity; hence the resulting infection is a result of the balance between the two. We therefore sought to study MIP-3α response patterns in the first 24 hours post microbial exposure alongside other SPs and AMPs that have been implicated in HIV infection. Particularly, we investigated constitutive and stimulated secretion patterns of thirty-three innate markers in the human FGT, with a particular focus on the endocervical sub-compartment. We studied mostly secretion from endocervical explant tissues (EET), but also studied ectocervical explant tissues (ECET) and the HEC-1A endometrial cell line. We stimulated the EET with various envelope and non-envelope HIV-1 preparations including s*oluble CN54gp140 trimeric protein*, CN54*gp120 virus-like particles (VLPs)*, *R5 tropic whole virus, HIV-1 strain BaL,* and *NL4-3, deleted in Env.* We also stimulated with Toll-like receptor ligands (TLRs) 1 through to 6. We quantified analyte levels in supernatants collected 24 hours after stimulation with the Luminex multiplex bead immunoassay. All the 33 analytes were secreted constitutively in the EET, albeit at varying levels. MIP-3α levels were amongst the levels of SPs and AMPs that are in the highest concentrations in the EET. Levels of AMPs were generally higher than those of SPs. HIV-1 preparations did not induce further significant production of any SPs and AMPs including MIP-3α in the EET. On the other hand, TLR ligands differentially induced significant fold changes in 10 analytes including IL-1α, IL-1β, IL-6, IL-8, RANTES, MIP-1β, SDF-1β, IFN-β, SLPI, and L-selectin in the EET. Most

AMPs in our panel have direct anti-HIV-1 activity. Hence the strong presence of high concentrations of AMPs with antagonistic HIV effect in our study might explain the lack of response of the EET to various HIV-1 preparations.

INTRODUCTION

The mucosal surfaces are the first structure that HIV-1 encounters in the body and therefore their physical and functional characteristics are important determinants of the outcome of exposure to HIV-1. Mucosal surfaces constitute the commonest portal of entry and transmission route for HIV. Of the currently estimated 33 million infections, more than 90% would have gained entry into the body through gastrointestinal and genital tracts, with the FGT alone comprising almost 40% [63]. The FGT is divided into various anatomical sub-compartments i.e. the endometrial, endocervical, transformation zone, ectocervical, and the vaginal, the relative contribution to infection of which is distinct at each site. Consequently defensive mechanisms to infection vary between these sites.

The cervix is a bridge between the endometrium and the vagina that is constitutionally and immunologically distinct from these sub-compartments. The endocervix, making about a third of the uterus, is lined by columnar epithelium interspersed with numerous glands. This “glandular” or columnar epithelium is composed of a single layer of mucin secreting cells. Longitudinal folds and invaginations make up the so-called endocervical glands (they are not true glands, but are actually a single layer of columnar epithelium-lined crypts, which extend to a depth of 5-7 mm). Endocervical epithelial cells have attributes that limit microbial access and establishment of infection, and these include tight intercellular

junctions, production of mucus, and secretion of innate immune mediators. With respect to the first attribute, the intercellular junctions maintain the integrity and organisation of epithelia and thus providing a physical barrier against microbe invasion [153]. With regards to the second attribute, mucus secreted by endocervical epithelial cells is also critical in establishing a protective barrier against microbes that are present at mucosal sites. Mucus not only forms a physical protective barrier against external environmental challenges but also houses an array of antimicrobial molecules [65]. Hence the endocervix has been shown to be an area of high endocrine and paracrine functions, as evidenced by secretion of antibodies and high antimicrobial protein expression [111]. Some of the AMPs detected in cervical mucus include the following: human defensins which are small cationic AMPs and include the α-defensins, the so-called human neutrophil peptides 1 to 3 (HNP1-3) that are released from the neutrophils, and the β-defensins, the so-called human β-defensins 1 to 4 (HBD-1-4) secreted by epithelial cells [72]. Secretory leukocyte protease inhibitor (SLPI) is an antimicrobial polypeptide already known to be in a high concentration in the cervical mucus plug [73]. Lysozyme and lactoferrin are known antimicrobial components of epithelial secretions, which include cervical mucus [74]. AMPs thus form an extra protective layer of the endocervix and exert their effect by disrupting microbial membranes and metabolic processes of microbes.

Most of our recent understanding of the process of HIV mucosal transmission comes from animal models and *in vitro* studies. The SIV/*Rhesus macaque* model of HIV transmission has led to an increased understanding of the interactions between virus and host during the sexual transmission of HIV as discussed above. In a series of transmission studies and publications Miller *et al* showed that vagina

and cervix were both primary sites of HIV transmission in the SIV/Rhesus macaque model [66, 154, 155]. However, there is now evidence that the primary site of infection post exposure to HIV inoculum in animals is the cervix, and particularly the endocervix and transformation zone [110]. Li *et al* showed evidence that the single epithelial layer of endocervix and transformation zone (junction between endocervix and ectocervix) has a high target cell density and turnover, which may be the site of SIV infection [96]. The vagina has also been shown by the same group to be another important site of infection, albeit only second to the cervix. However, Asin *et al* have shown that in human beings, post HIV challenge in explant studies of the ectocervix and endometrium, transcription factors concentrated in the former [109]. Furthermore, Pudney *et al* showed that the cervix, especially the transformation zone, is the major inductive and effector site for cell-mediated immunity in the lower FGT [58]. They showed that the endocervix had a high concentration of intraepithelial lymphocytes and concluded that this provided evidence that the cervix is a primary infection site for HIV-1 [58], while the primary target cell to be infected across the cervical mucosa is the memory $CD4^+$ T cells [156].

In a landmark study by Li *et al*, they noted that the accumulation of SIV RNA+ CD4+ T cells post exposure to virus in an SIV/*Rhesus macaque* model, was preceded by a subepithelial influx of plasmacytoid dendritic cells (pDCs) in the endocervix one day post inoculation (d.p.i.), an effect that was not replicated in the vagina and transformation zone sub-compartments [96]. They subsequently showed that this accumulation of pDCs was associated with increased expression of MIP-3α, a molecule which had earlier been shown to be a strong chemoattractant for pDCs [103]. Through a series of experiments they concluded

that the exposure and binding of SIV to epithelial cells in the FGT induced an "outside-in" signalling cascade i.e. exposure of endocervical epithelium to the viral inoculum increases the expression of MIP-3α, which in turn recruits pDCs, thereby commencing the sequence of events leading to productive infection. This study thus highlighted the endocervix as the primary site of infection while also highlighting the role of a chemokine, MIP-3α, secreted by the epithelium in the initial SIV infection events in macaque FGT.

While the mucosal epithelium secretes MIP-3α and other SPs, which are implicated in promoting susceptibility to infection, it on the other hand secretes AMPs, that possess anti-HIV-1 activity, hence the resulting infection is a result of the balance between the two. Some AMPs have been shown to have direct anti-HIV-1 activity and they include some human defensins, lysozyme, lactoferrin, SLPI, and elafin/trappin-2 [100, 157-161]. Human β-defensins 2 and 3 (HBD-2 and HBD-3) have been shown to inhibit HIV-1 replication through modulation of the CXCR4 co-receptor as well by interacting directly with the virions (defensins share structural homology as well as the receptor CCR6+ with MIP-3α) [162]. Lysozyme and lactoferrin have been shown to inhibit infection by HIV-1 *in vitro* by preventing the adsorption and penetration of the virus [163]. SLPI has been shown to be reduced in vaginal fluid of HIV-infected persons [164], and elafin/ trappin-2 has recently been identified as a new anti-HIV factor which directly interacts with the virus for its inhibition [158]. However, these AMPs show differential up-regulation in the different sub-compartments of the FGT and hence studying AMPs necessitates the study of different sub-compartments, using different tissue models, and various viral requirements in order to understand factors that influence resistance and/or susceptibility to infection in that particular site. Ultimately this would be crucial in

designing targeted strategies that aim to focus on the primary site of infection in order to prevent infection or manipulate the specific immune responses to that organism.

With the understanding that MIP-3α, as we have studied it, is unlikely to be a sole player in the early HIV mucosal transmission events and with the findings of the preceding chapter that the human endocervical models do not respond to stimulation with various HIV-1 preparations, we sought to study MIP-3α alongside 32 other innate markers and AMPs. We wanted to identify other innate markers that might be part of the initial response to HIV-1 exposure in humans in the first 24 hours post HIV-1 exposure instead of MIP-3α. Further we wanted to ascertain whether the lack of responsiveness of the endocervix to HIV-1 preparations was unique to MIP-3α or whether it was a widespread phenomenon generalisable to other innate markers in the endocervix in response to HIV-1? We extended our study to focus not only on the epithelium, but also on the rest of the mucosal layer using explant tissues. Explant tissues are prepared from a sample of an organ of interest removed from the body through biopsy or resection, which is then dissected free of underlying musculature. The remaining tissue, which comprises mucosal and submucosal components, forms an explant model. Inherently, they comprise epithelium suspended on the rest of the mucosa and stroma. Cells in the lamina propria have been shown to have paracrine effects that contribute to the functioning of the cells of the epithelium. This was particularly important in view of the findings in the preceding chapter showing different responses between primary epithelial cell preparations and explant tissues.

MATERIALS and METHODS

Epithelial models:

We used the exact same epithelial models that we used in the preceding two chapters on constitutive and stimulated levels of MIP-3α to study the impact of microbial exposure on various epithelial models. Briefly, we evaluated the constitutive and stimulated expression of MIP-3α and 32 other innate markers and AMPs in *the ex vivo* explant tissue epithelial model prepared from the endocervix (EET). We also evaluated constitutive expression of MIP-3α and 32 other innate markers and AMPs in the ectocervical explant tissues (ECET) and the HEC-1A endometrial cell line. EET and ECET were prepared from tissues obtained from fresh hysterectomy specimens, within 2 to 4 hours of womb resection. Consenting HIV uninfected women at low risk for HIV infection, and scheduled for a hysterectomy for a non-cancerous lesion were recruited into this study from the Women's Centre at the John Radcliffe hospital in Oxford.

Tissue culture:

We prepared and incubated the epithelial models exactly as we had done in the preceding two chapters. Each tissue block of the EET and ECET was placed in a single well of a round-bottomed 96 well tissue culture plate with 200µL of complete media. These tissues were maintained in RPMI-1640 medium (Sigma-Aldrich®, UK) supplemented with 10% foetal calf serum, L-glutamine and antibiotics and incubated at 37^0C 5% CO_2. For HEC-1A cells, we seeded 50,000 cells in 24 well tissue culture plates (Corning® Costar®, UK). Additionally for some experiments, we seeded 50,000 HEC-1A cells on permeable supports in the apical compartment of Transwell® inserts (Corning® Costar®, UK), with 200 and 600µL of complete

McCoy's medium in apical and basal compartments, respectively. We incubated HEC-1A cells for five days, changing medium regularly every two to three days, in order to achieve confluence and maximal transepithelial electrical resistance (TEER) before harvesting supernatants for estimating analyte levels.

Viral preparations:

Various HIV-1 preparations were used to stimulate epithelial models in order to answer the question of the pattern of secretion of 33 innate markers in the first 24 hours after stimulation. Notably, we prepared and used exactly the same viral preparations as we used in the preceding chapter on MIP-3α. Specifically, we prepared and studied HIV-1 envelope proteins: soluble recombinant trimeric CN54gp140 glycoprotein and CN54gp120 viral-like particles (VLPs); and also prepared and studied R5 tropic whole virus, inactivated HIV-1 BaL, and envelope-deleted virus, HIV-1 NL4-3. Whereas we used gp140 at a concentration of 100ng/mL, we used other viral preparations at 10^5 particles per well, stimulating explant tissues for 24 hours at a time.

Immunostimulants:

Following initial dose titration experiments in HEC-1A cells immunostimulants were used at fixed concentrations based on the levels of MIP-3α achieved following stimulation. We used constant concentrations throughout all tissue models. IL-1β was used as positive control for activation at 10 ng/ml (R&D Systems, Bio-Techne, Abingdon, UK), Pam_3CSK_4 (TLR1/2) at 20 μg/ml (Tocris, Bio-Techne, Abingdon, UK), Zymosan (TLR2) at 10 μg/ml (Sigma-Aldrich®, UK), Poly I:C Polyinosinic–polycytidylic acid sodium salt (TLR3) at 25 μg/ml (Sigma-Aldrich®, UK), LPS (Lipopolysaccharides from *Escherichia coli* 0111:B40) (TLR4) at 10 μg/ml (Sigma-

Aldrich, UK), Flagellin (Flagellin from Salmonella typhimurium) (TLR5) at 20 ng/mL (Sigma-Aldrich®, UK), and FSL-1 (Pam2CGDPKHPKSF) (TLR2/6) at 2 µg/ml (Invivogen, UK). We stimulated all models for 24 hours before harvesting supernatants to estimate analyte levels.

Quantitative protein immunoassay: measurements of soluble markers and antimicrobial peptides:

The concentrations of 25 SPs and 8 AMPs including MIP-3α were measured in tissue supernatants using the Luminex multiplex bead assay. The SPs measured fell in one of six functional groups: pro-inflammatory, anti-inflammatory, adaptive, chemokine, haematopoietic and growth factors (*Figure 5.1*). Specifically, they included: interleukin 1 alpha (IL-1α), interleukin 1 beta (IL-1β), interleukin 6 (IL-6), interleukin 12 (IL-12), interleukin 16 (IL-16), tissue necrosis factor alpha (TNF-α), interleukin 2 (IL-2), interleukin 4 (IL-4), interleukin 15 (IL-15), interleukin 17 (IL-17), interferon gamma (IFN-γ), interleukin 8 (IL-8), interferon gamma-induced protein 10 (IP-10), monocyte chemotactic protein 1 (MCP-1), monokine induced by gamma-interferon (MIG), macrophage inflammatory protein three alpha (MIP-3α), macrophage inflammatory protein-1 beta (MIP-1β), normal T cell expressed and secreted (RANTES), stromal cell-derived factor 1 beta (SDF-1β), interleukin 10 (IL-10), interleukin 7 (IL-7), granulocyte-colony stimulating factor three (G-CSF), granulocyte-macrophage colony-stimulating factor (GM-CSF), and transforming growth factor beta (TGF-β). The eight AMPs included: interferon beta (IFN-β), secretory leukocyte protease inhibitor (SLPI), Elafin, P-selectin, L-selectin, human beta defensin 2 (HBD2), human beta defensin 3 (HBD3), and human neutrophil peptides (HNP) 1-3. We measured SPs and AMPs with a custom made 33-plex Luminex in-house panel comprising four panels: the high-plex cytokine panel, the

low-plex cytokine panel, the high-plex AMP panel and the low-plex AMP panel. The distinction was made based on the maximum detection levels in supernatants. After optimising all panels by adjusting the concentrations for the standard curve and excluding cross-reactivity with other analytes, magnetic beads were used to do the assay. For all experiments, conditions were tested in triplicate. However, for the subsequent Luminex assay, all supernatants from the same test condition were pooled before being dispensed into duplicate wells of the Luminex assay plate. Supernatants were used undiluted for the two high-plex panels while they were diluted 1:10 and 1:50 for the low-plex AMPs and cytokine panels, respectively. Data were collected using a Bio- Plex™ Suspension Array Reader (Bio-Rad Laboratories InC®). The lower limit of detection ranged between 1,7 and 266,6pg/mL for the cytokines measured. Specifically for the SPs the respective lower detection limits in pg/mL in this panel were 4.2pg/mL for IP-10, IL-1β, IL-16, GM-CSF, IL-4, IL-2, RANTES, IFN-γ, IFN-β, TNF-α, SDF-1β, MIG, MIP-1β, IL-7, IL-8, MCP-1, IL-6, G-CSF. The lower limit of detection was 0.8pg/mL for MIP-3α and 2.4pg/mL for IL-1α, TGF-β, IL-12, and IL-15. For the AMPs the respective lower detection limits in pg/mL were 0.001pg/mL for HBD 4, 0.5pg/mL for L-selectin and HBD 3, 1pg/mL for IFN-β, 10pg/mL for Elafin, 50pg/mL for SLPI, 100pg/mL for P-selectin and 2000pg/mL for HNP 1-3. Concentrations of SPs and AMPs that were below the lower limit of detection of the assay were reported as the mid-point between the lowest concentrations measured for each cytokine and zero.

Statistical analyses:

For *ex vivo* explant tissue assays, explants were seeded at one explant per well but each condition was tested in triplicate. For *in vitro* cellular assays, cells were

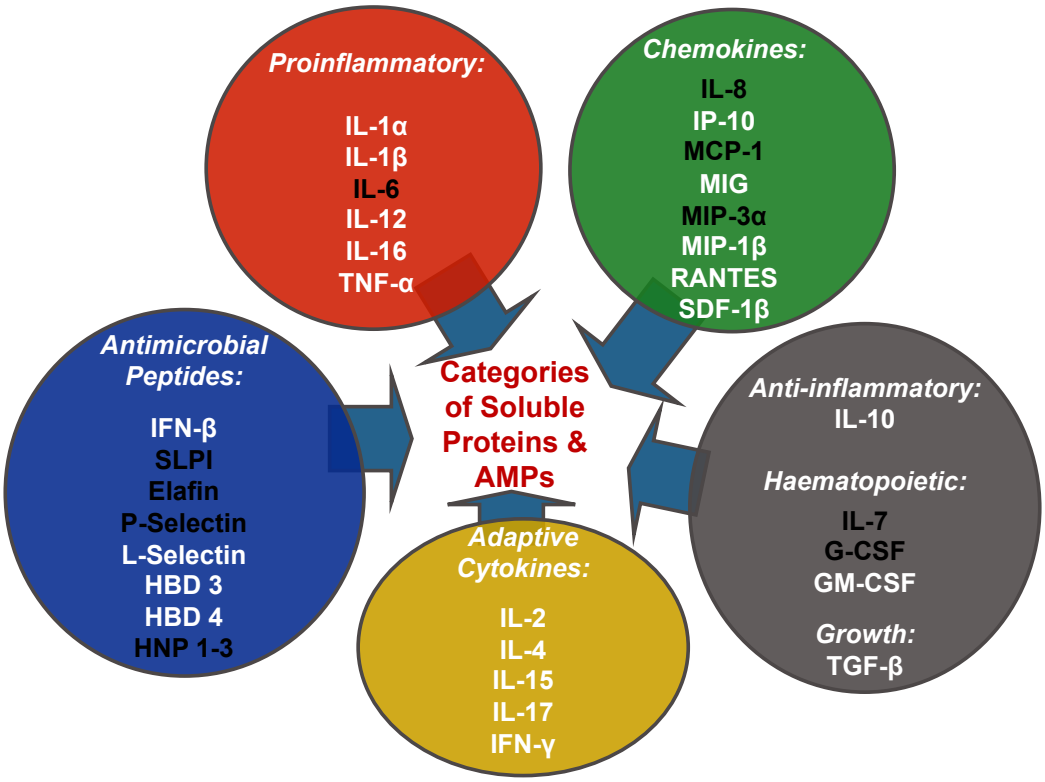

Figure 5.1: Categories of soluble proteins and antimicrobial peptides included in our custom-made in-house 33-plex Luminex assay. The 10 analytes highlighted in blue text are those included in the respective high-plex panels while the rest are included in the low-plex panels for for both SPs and AMPs. Colour codes of the circles correspond to the colour codes in the graphical presentation of data in the rest of the thesis chapter.

seeded in triplicate wells. *In vitro* assays were repeated for a minimum of three experiments before being included in the study results. Cytokine levels were measured with the Luminex multiplex bead immunoassay. Statistical analyses were performed using GraphPad Prism version 7 for Mac OS X (Prism, GraphPad Software, La Jolla, California, USA). The 5 PL regression curve fitted formula was used to calculate cytokine concentrations from the standard curves on GraphPad Prism. Descriptive data were presented with schema prepared from Microsoft Excel (version 2011 for Mac) and GraphPad Prism. Results were reported in bar graphs and stacked columns with bars representing cumulative levels of SPs and

AMPs stimulating with each stimulant. Box and whisker plots showing the impact of each stimulant on each cytokine were presented. The horizontal line within the bar represents median while the outer horizontal lines represent the 25^{th} and 75^{th} centiles. We calculated fold changes by dividing stimulated with unstimulated analyte levels. One sample t-tests were used to assess statistical significance for down-/up-regulated analytes based on fold changes in analyte concentrations. In this analysis, we defined significantly up-/down-regulated cytokines as those that were at least 1.5 fold higher/lower than the unstimulated value plus a p-value of <0.05. Levels of MIP-3α were expressed in pg/mL throughout the study.

RESULTS

Descriptive characteristics:

In view of the evidence that HIV-1 does not trigger further secretion of MIP-3α in the endocervix of humans in the preceding chapter, we undertook to study constitutive and stimulated patterns of secretion of 32 other SPs and AMPs in the human cervix by exposing it to various microbial preparations including HIV-1 preparations and TLR ligands. We did this in order to compare the secretion pattern of MIP-3α to that of other SPs and AMPs secreted by the human endocervix. In order to conduct this analysis, we analysed supernatants of endocervical and ectocervical explant tissues prepared from the wombs of six women attending the Women's centre at the John Radcliffe hospital in Oxford. These women were recruited because they were scheduled for a hysterectomy for their own health. Notably, the hysterectomy was indicated for a non-cancerous lesion and they were excluded from participating if they had any cervical lesion including local infection (*Table 5.1*). Their mean age was 44 years.

Table 5.1 Attributes of participants enrolled and included in this analysis

Patient Identifier	Age	Parity	Diagnosis	Medical Treatment
PID401	44	P0+4	Pelvic pain and congenital uterine abnormality	Thyrozidine
PID402	51	P4	Menorrhagia	Haematinics
PID405	42	P5	Menorrhagia	None
PID407	39	P2	Menorrhagia	Combined oral contraceptives
PID409	47	P2	Menorrhagia and fibroids	Fibrinolytics
PID411	41	P5	Menorrhagia	Combined oral contraceptives

The constitutive levels of MIP-3α in the human EET are amongst the levels of SPs and AMPs with highest concentrations in the endocervix.

Having studied MIP-3α in solitude in the preceding chapters, we went on to evaluate its constitutive secretion alongside other SPs and AMPs that have been shown to be secreted in the FGT. Specifically, we wanted to contrast and compare its constitutive secretion pattern to that of other SPs and AMPs in the FGT. Previous studies have characterised constitutive SPs in the different sub-compartments of the FGT and showed that IL-8, MCP-1 and IL-6 are in the highest concentrations in the FGT, however, these studies did not include MIP-3α in the same panel. Hence, we have extended this body of knowledge profiling FGT SPs by including MIP-3α. In order to achieve this we prepared explant tissues from the endocervices of six women undergoing a hysterectomy, within 2 to 4 hours of resection from the body. We plated 96 well tissue culture plates with one explant

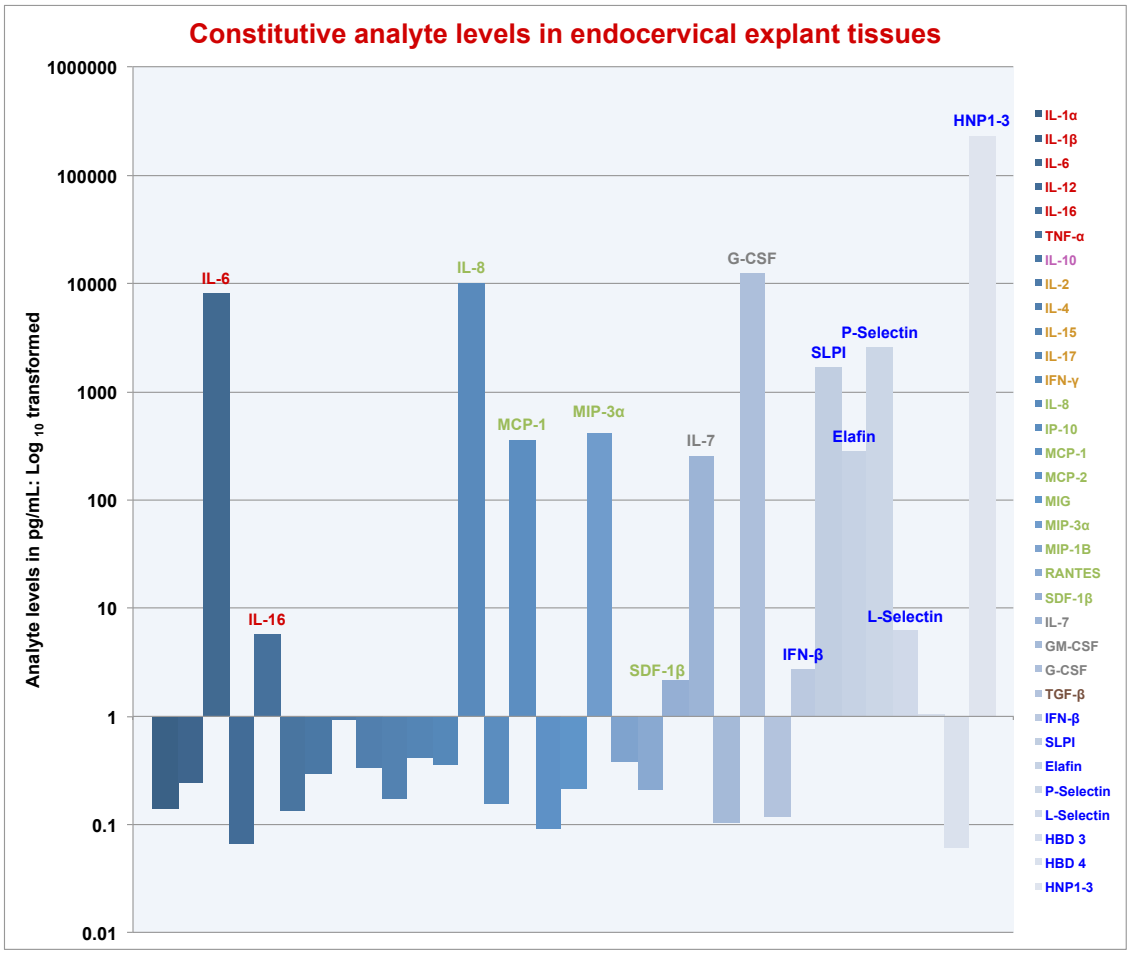

Figure 5.2: Mean constitutive expression of 33 analytes (25 soluble proteins and 8 antimicrobial peptides) measured in supernatants of endocervical explant tissues, n=6. Explant tissues were prepared fresh from hysterectomy samples, within 2 hours of womb resection. EET were immediately incubated in tissue culture plates in 200uL of medium. Supernatants were harvested 24 hours later and analyte levels quantified with the Luminex multiplex bead assay. Analyte names are colour coded according to analyte functional grouping: red=pro-inflammatory, purple=anti-inflammatory, yellow=adaptive, green=chemokine, gray=haematopoietic, brown=growth and blue=antimicrobial peptide. 14 analytes had expression levels above 1pg/mL.and six of these were in the antimicrobial peptide category. MIP-3α levels were amongst the SPs and AMPs in the highest concentrations in the EET.

Table 5.2: Descriptive analysis: 25 soluble proteins and 8 antimicrobial peptides in EET and ECET

Analyte functional categories	Analytes (SPs and AMPs)	Endocervix				Ectocervix				P value
		Median (Range) pg/mL	Mean pg/mL	SD	SE	Median (Range) pg/mL	Mean pg/mL	SD	SE	
Anti-inflammatory	IL-1α	0.1 (0.1-0.4)	0.1	0.1	0.1	0.2 (0.1-0.2)	0.2	0.0	0.0	0.1797
	IL-1β	0.2 (0.1-0.6)	0.2	0.2	0.1	0.1 (0.1-1.0)	0.3	0.4	0.2	0.6991
	IL-6	8240.0 (2917.0-15005.0)	8160.0	5102.0	2083.0	15721.0 (399.8-27517.0)	14606.0	10110.0	4127.0	0.2403
	IL-12	0.1 (0.1-0.1)	0.1	0.0	0.0	0.1 (0.1-0.1)	0.1	0.0	0.0	0.8182
	IL-16	4.8 (3.7-11.1)	5.8	2.8	1.1	8.4 (5.7-13.7)	8.9	2.7	1.1	0.0649
	TNF-α	0. (0.1-0.2)	0.1	0.0	0.0	0.1 (0.1-0.1)	0.1	0.0	0.0	0.6991
Pro-inflammatory	IL-10	0.3 (0.3-0.3)	0.3	0.0	0.0	0.3 (0.3-0.3)	0.3	0.0	0.0	0.8182
Adaptive	IL-2	0.1 (0.0-5.2)	0.9	2.1	0.9	0.0 (0-0.1)	0.0	0.0	0.0	0.5887
	IL-4	0.3 (0.3-0.4)	0.3	0.0	0.0	0.3 (0.3-0.4)	0.3	0.0	0.0	0.619
	IL-15	0.2 (0.0-0.3)	0.2	0.1	0.1	0.1 (0.0-0.3)	0.1	0.1	0.1	0.3312
	IL-17	0.4 (0.4-0.4)	0.4	0.0	0.0	0.4 (0.4-0.4)	0.4	0.0	0.0	0.6991
	IFN-γ	0.4 (0.3-0.4)	0.4	0.0	0.0	0.4 (0.3-0.4)	0.4	0.0	0.0	0.2879
Chemokine	IL-8	10722.0 (3832.0-15010.0)	10154.0	3637.0	1485.0	4993.0 (99.9-13627.0)	5770.0	4901.0	2001.0	0.0931
	IP-10	0.2 (0.1-0.2)	0.2	0.0	0.0	0.2 (0.1-1.3)	0.4	0.5	0.2	0.4848
	MCP-1	350.3 (265.7-476.1)	360.7	92.7	37.9	199.3 (84.5-559.7)	289.9	211.6	86.4	0.3939
	MCP-2	0.1 (0.1-0.1)	0.1	0.0	0.0	0.1 (0.1-0.1)	0.1	0.0	0.0	0.5887
	MIG	0.2(0.2-0.2)	0.2	0.0	0.0	0.2 (0.2-0.2)	0.2	0.0	0.0	0.9004
	MIP-3α	393.6 (365.6-489.3)	412.0	49.8	20.3	376.0 (360.5-394.4)	377.8	13.9	5.7	0.3095
	MIP-1β	0.4 (0.1-0.6)	0.4	0.2	0.1	0.5 (0.2-1.8)	0.6	0.6	0.2	0.4848
	RANTES	0.2 (0.1-0.4)	0.2	0.2	0.1	0.2 (0.0-0.7)	0.3	0.2	0.1	>0.9999
	SDF-1β	2.4 (1.0-2.9)	2.1	0.8	0.3	2.5 (1.3-5.3)	2.8	1.5	0.6	0.4848
Hematopoietic	IL-7	258.6 (245.9-262.4)	255.8	6.8	2.8	246.9 (239.5-256.5)	246.8	6.5	2.7	0.0563
	GM-CSF	0.1 (0.1-0.2)	0.1	0.0	0.0	0.1 (0.1-0.2)	0.1	0.0	0.0	0.9372
	G-CSF	12994.0 (8318.0-16433.0)	12426.0	3317.0	1354.0	6610.0 (382.0-21653.0)	8812.0	7784.0	3178.0	0.2403
Growth	TGF-β	0.12 (0.1-0.1)	0.1	0.0	0.0	0.1195 (0.1-0.2)	0.1	0.0	0.0	0.8182
Antimicrobial peptides	IFN-β	2.0 (1.8-5.9)	2.7	1.6	0.7	1.815 (1.7-2.4)	1.9	0.3	0.1	0.1667
	SLPI	1568.0 (1245.0-2275.0)	1669.0	403.0	164.5	1093.0 (258.6-1344.0)	985.3	375.9	153.5	*0.0087
	Elafin	242.0 (152.8-529.0)	281.7	136.0	55.5	1228.0 (445.8-12361.0)	3117.0	4588.0	1873.0	*0.0043
	P-Selectin	2475.0 (2317.0-3326.0)	2594.0	370.7	151.3	2140.0 (1686.0-2353.0)	2108.0	260.6	106.4	*0.0087
	L-Selectin	6.4 (3.0-8.9)	6.2	1.9	0.8	7.697 (0.4341-12.5)	7.5	4.2	1.7	0.4848
	HBD3	1.0 (0.6-1.5)	1.0	0.4	0.2	1.4 (0.7723-5.2)	1.9	1.6	0.7	0.2403
	HBD4	0.1 (0.0-0.1)	0.1	0.0	0.0	0.1 (0.0-0.1)	0.1	0.0	0.0	>0.9999
	HNP1-3	139040.0 (40646.0-514091.0)	232716.0	216208.0	88267.0	31934.0 (12630.0-82366.0)	36888.0	24273.0	9909.0	*0.0087

Asterisks denote statistical significance in differences between endocervical and ectocervical levels, p-value<0.05

per well in 200µL of complete RPMI-1640 medium. We incubated them for 24 hours at 37^0C in 5% CO_2 prior to harvesting supernatants. We quantified constitutive levels of 25 SPs and eight AMPs in the supernatants of EET with the Luminex multiplex bead assay. All SPs and AMPs in our panel were above the lower limit of detection with our assay and thus indicating that the EET secretes all the analytes of interest constitutively. We confirmed what we had already shown using the Elisa sandwich assay in the preceding chapter that MIP-3α constitutive levels are high in the EET at a mean of 400pg/mL (*Figure 5.2, Table 5.2*). This MIP-3α level is second only to IL-8 (10,154pg/mL) when compared to other chemokine levels. Otherwise it is second to AMPs HNP1-3 (232,716pg/mL), P-Selectin (2,594pg/mL), SLPI (1,669pg/mL), and other cytokines G-CSF (12,426pg/mL) and IL-6 (8,160pg/mL). Further, six of the eight AMPs in our panel had concentrations above 1pg/mL making them an analyte class frequently high in the EET. This finding that AMPs are in the highest concentration in the EET is significant as some of these AMPs have been shown to have direct anti-HIV-1 activity and this finding might thus explain the unresponsiveness of the human endocervix to HIV-1 preparations.

Compartmentalisation: HNP 1-3, SLPI and P-Selectin are significantly higher in the endocervix than in the ectocervix, while Elafin is significantly higher in the ectocervix than in the endocervix.

We studied constitutive MIP-3α secretion patterns in various matrices in the preceding chapter and our data showed that the secretion patterns and levels of MIP-3α vary between different sub-compartments thus confirming that there is

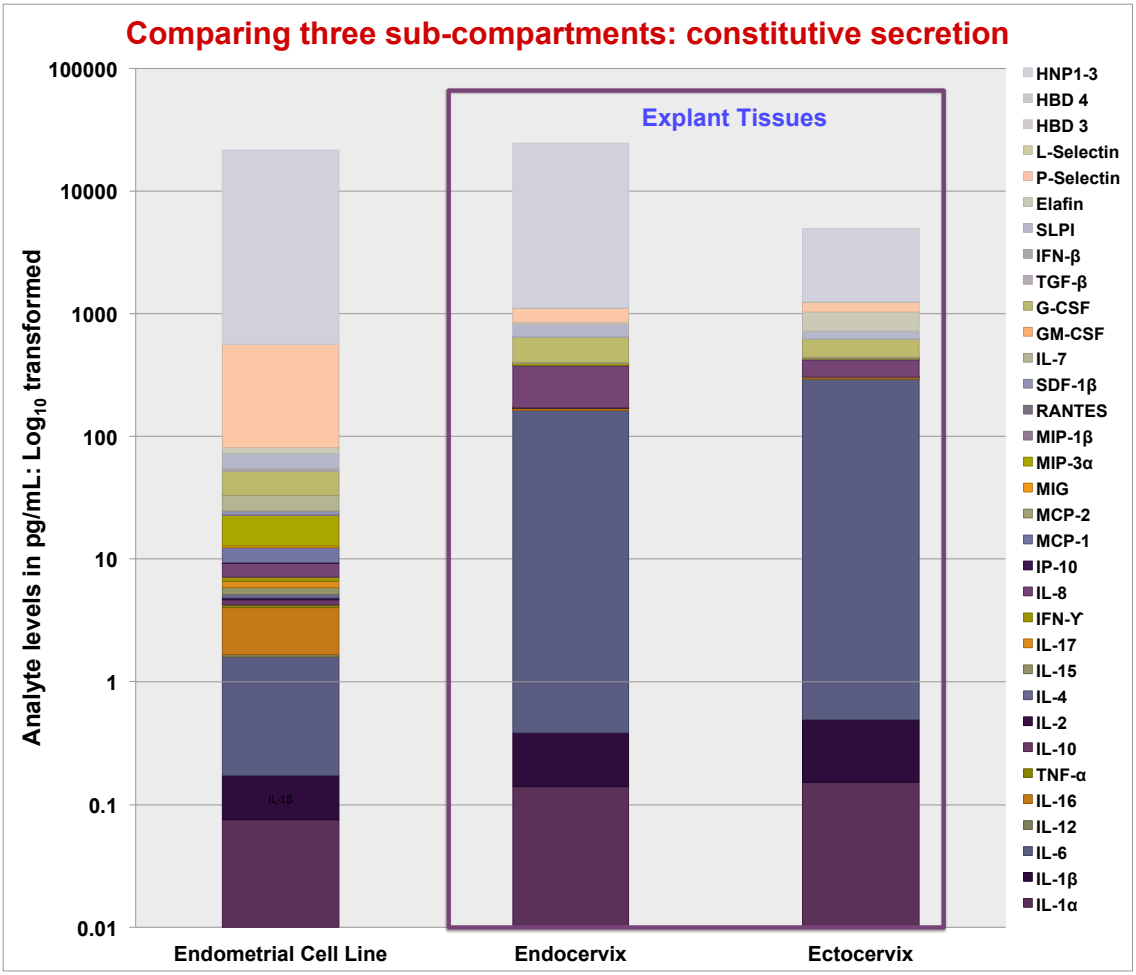

Figure 5.3: Mean constitutive expression of 33 analytes (25 soluble proteins and 8 antimicrobial peptides) measured in supernatants of endocervical explant tissues (n=6), ectocervical explant tissue (n=6) and HEC-1A endometrial cell line (n=1). Explant tissues were prepared fresh from hysterectomy samples, within 2 hours of womb resection. EET and ECET were immediately incubated in tissue culture plates in 200uL of medium. Supernatants were harvested 24 hours later and analyte levels quantified with the Luminex multiplex bead assay. We plated 50,000 HEC-1A cells in 24 well tissue culture plates in 600µL of medium. We incubated cells for five days before harvesting supernatants to estimate various constitutive analyte levels. Conditions were tested in triplicate. The endocervix had higher cumulative analyte concentrations than the ectocervix. The endometrial cell line, compared to EET and ECET, had a distinct pattern of constitutive expression of SPs and AMPs

compartmentalisation of MIP-3α secretion in the FGT. Further, we studied TLR expression and stimulated pattern of secretion of MIP-3α in different sub-compartments and showed once again that TLR expression and responses to TLR ligand stimulation in various sub-compartments differed between these sub-compartments. We hence extended these studies by evaluating the extent to which there is compartmentalisation in the FGT in the context of various other SPs and AMPs. We compared constitutive levels of 25 SPs and 8 AMPs in three epithelial models representing the three sub-compartments of the FGT: the endocervix, the ectocervix and the endometrium. We prepared explant tissues from the endocervices and ectocervices of six women undergoing a hysterectomy, within 2 to 4 hours of resection from the body. We plated 96 well tissue culture plates with one explant per well in 200µL of complete RPMI-1640 medium. We incubated them for 24 hours at 37^0C in 5% CO_2 prior to harvesting supernatants. We used HEC-1A cells in the exact same set up we had used them to undertake constitutive MIP-3α studies in the preceding chapter. We plated 50,000 HEC-1A cells in 24 well tissue culture plates in 600µL of complete McCoy's medium. We incubated them for five days at 37^0C in 5% CO_2, changing media every two to three days. On Day 5 we changed media, and incubated them for one more day prior to harvesting supernatants for estimating levels of SPs and AMPs. We quantified constitutive levels of 25 SPs and eight AMPs in the supernatants of EET, ECET, and HEC-1A cells with the Luminex multiplex bead assay. All SPs and AMPs in our panel were above the lower limit of detection with our assay and thus suggesting that all these models secrete all the analytes of interest constitutively. The pattern of secretion of all SPs and AMPs was similar between the ectocervix and endocervix (*Figure 5.3*), however, cumulative analyte concentrations were higher in the endocervix than in the ectocervix and thus suggesting that the endocervix secretes higher levels of

some analytes in the panel. We conducted Mann Whitney statistical tests comparing analyte levels in the EET and the ECET: not all analyte levels were similar between the two sub-compartments (*Table 5.2*): HNP 1-3 (232,716pg/mL, p-value=0.0087), SLPI (1,669, p-value=0.0087) and P-Selectin (2,594pg/mL, p-value=0.0087) levels were significantly higher in the endocervix than in the ectocervix, 36,880pg/mL, 985pg/mL, 2,108pg/mL, respectively. On the other hand, Elafin was significantly higher in the ectocervix (93,117pg,mL, p-value=0.0043) than in the endocervix (281,7pg/mL). We compared the pattern of secretion of all these 33 analytes between these models and the HEC-1A cells, and the data showed that the pattern is distinct in HEC-1A cells compared to EET and ECET even though we did not run any statistical test to test the effect size of the differences. We only analysed the levels from HEC-1A cells from a single experiment in this study even though the test conditions were in triplicate. These results therefore confirm what we already established earlier, that the various sub-compartments in the FGT are immunologically distinct which explains the differential predilection of various microbes for unique sub-compartments throughout the FGT.

The human endocervix secretes a wide range of SPs and AMPs constitutively, however, stimulating with either HIV-1 or TLR ligands does not dramatically alter the pattern of secretion and the proportions of secreted SPs and AMPs.

According to the results from the preceding chapter, the EET does not secrete further MIP-3α in response to stimulation with either TLR ligands or HIV-1 preparations. Having demonstrated constitutive secretion of all SPs and AMPs in

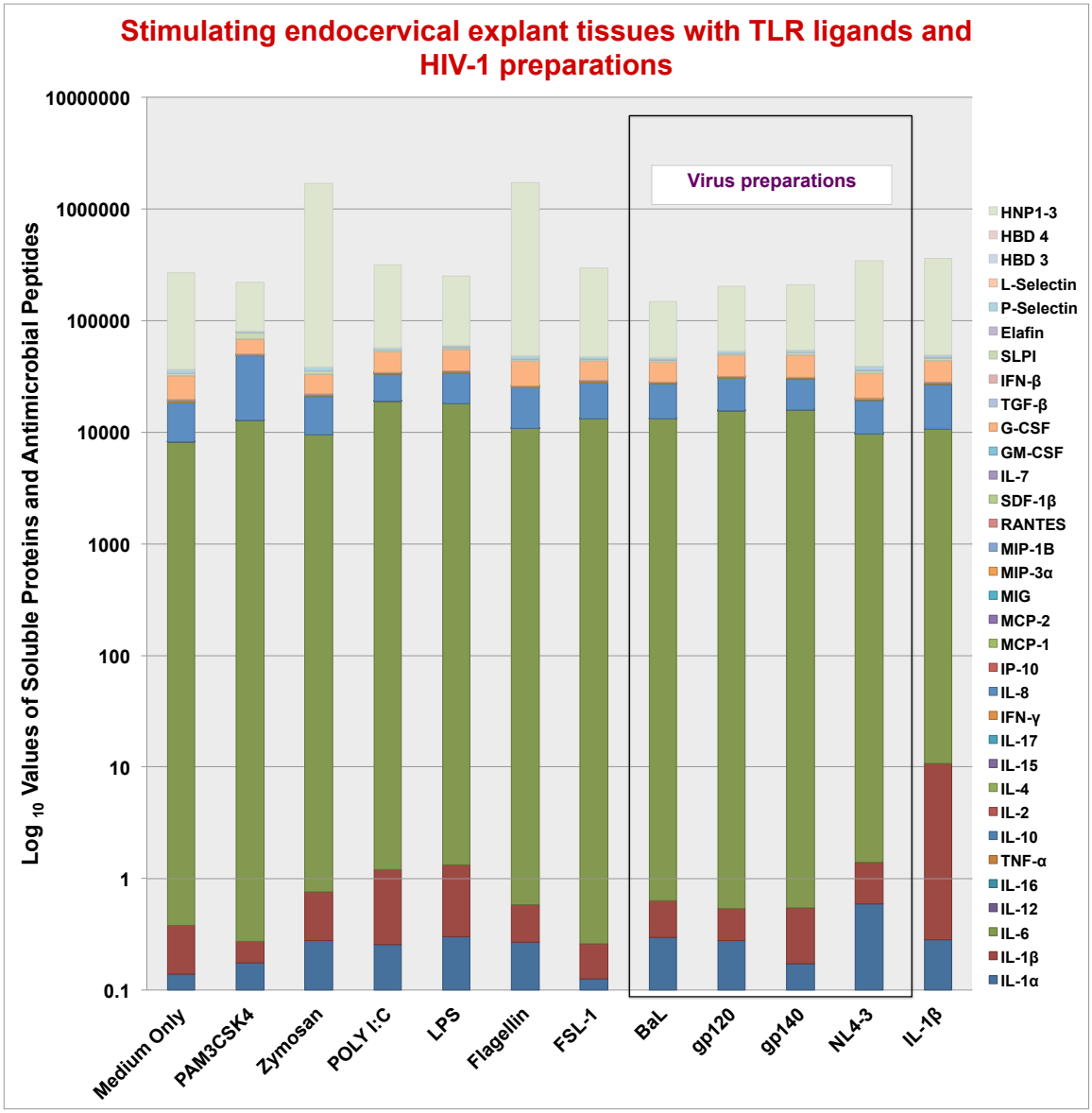

Figure 5.4: Stimulated levels of 25 SPs and 8 AMPs in EET stimulating with TLR ligands 1 through 6 and various envelope and non-envelope HIV-1 preparations, n=6. Specifically we stimulated with HIV-1 soluble CN54gp140 trimeric protein, an envelope glycoprotein, HIV-1 CN54gp120 virus-like particles (VLPs), R5 tropic whole virus, inactivated HIV-1 BaL, and HIV-1 NL4-3 deleted in Env. We used IL-1β as a positive control. We plated one explant tissue block per well in a 96 well tissue culture plate in 200µL of medium. We prepared and stimulated explant tissues immediately post womb resection. Conditions were tested in triplicate and levels of MIP-3α were quantified in supernatants with the Luminex assay. Supernatants were harvested 24 hours post stimulation. All SPs and AMPs were constitutively secreted in the EET. Except for IL-1β that was high following stimulation with recombinant IL-1β, there were no overt differences in the pattern of responses of various SPs and AMPs following stimulation with TLR ligands and HIV-1 preparations.

our panel, we went on to assess whether similarly to MIP-3α, other SPs and AMPs would not be secreted further on stimulation with TLR ligands and HIV-1 preparations, or whether contrary to it, their secretion would be triggered by TLR ligands and HIV-1 preparations in the EET. We again plated one explant per well of a 96 well tissue culture plate in 200μL of complete RPMI-1640 medium. We stimulated them with TLR ligands 1 through 6, and various HIV-1 preparations as we had used in the preceding chapter. Specifically we stimulated with HIV-1 soluble CN54gp140 trimeric protein, an envelope glycoprotein, stimulating with 100ng/mL. We also stimulated with 10^5 viral particles per well with HIV-1 CN54gp120 virus-like particles (VLPs), R5 tropic whole virus, inactivated HIV-1 BaL, and HIV-1 NL4-3 deleted in Env. With regards to TLR ligands, we stimulated EET with the exact same concentrations we had used in the preceding chapter. EET were prepared from tissues obtained from fresh hysterectomy specimens, within 2 to 4 hours of womb resection. HIV uninfected women in the reproductive age group, and scheduled for a hysterectomy for a non-cancerous lesion were recruited into this study. We plated 96 well tissue culture plates with one explant per well in 200μL of complete RPMI-1640 medium. Test conditions were tested in triplicate. We stimulated with all stimulants for 24 hours before harvesting supernatants for quantification of analytes with the Luminex immunoassay. We focused only on the EET epithelial model for this analysis. Neither TLR ligands nor HIV-1 preparations dramatically altered the pattern of secretion of SPs and AMPs in a distinct pattern, comparing unstimulated (medium only) to stimulated tissues, stimulating with various TLR ligands and HIV-1 preparations (*Figure 5.4*). This would therefore suggest that even if there are changes in levels of SPs and AMPs following stimulation with either TLR ligands or HIV-1 preparations, these changes are subtle.

A.

Viral preparations

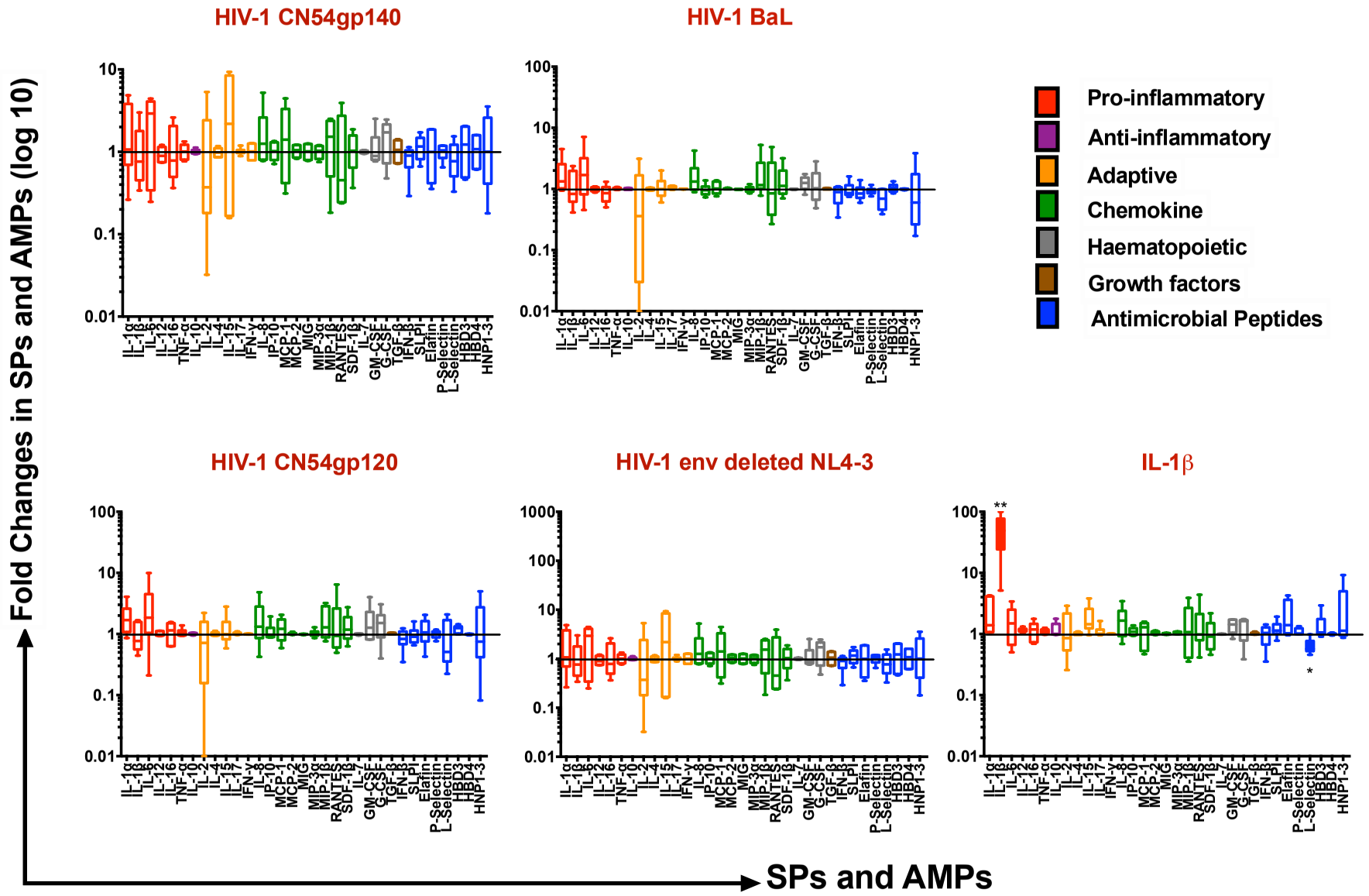

B.

TLR ligands

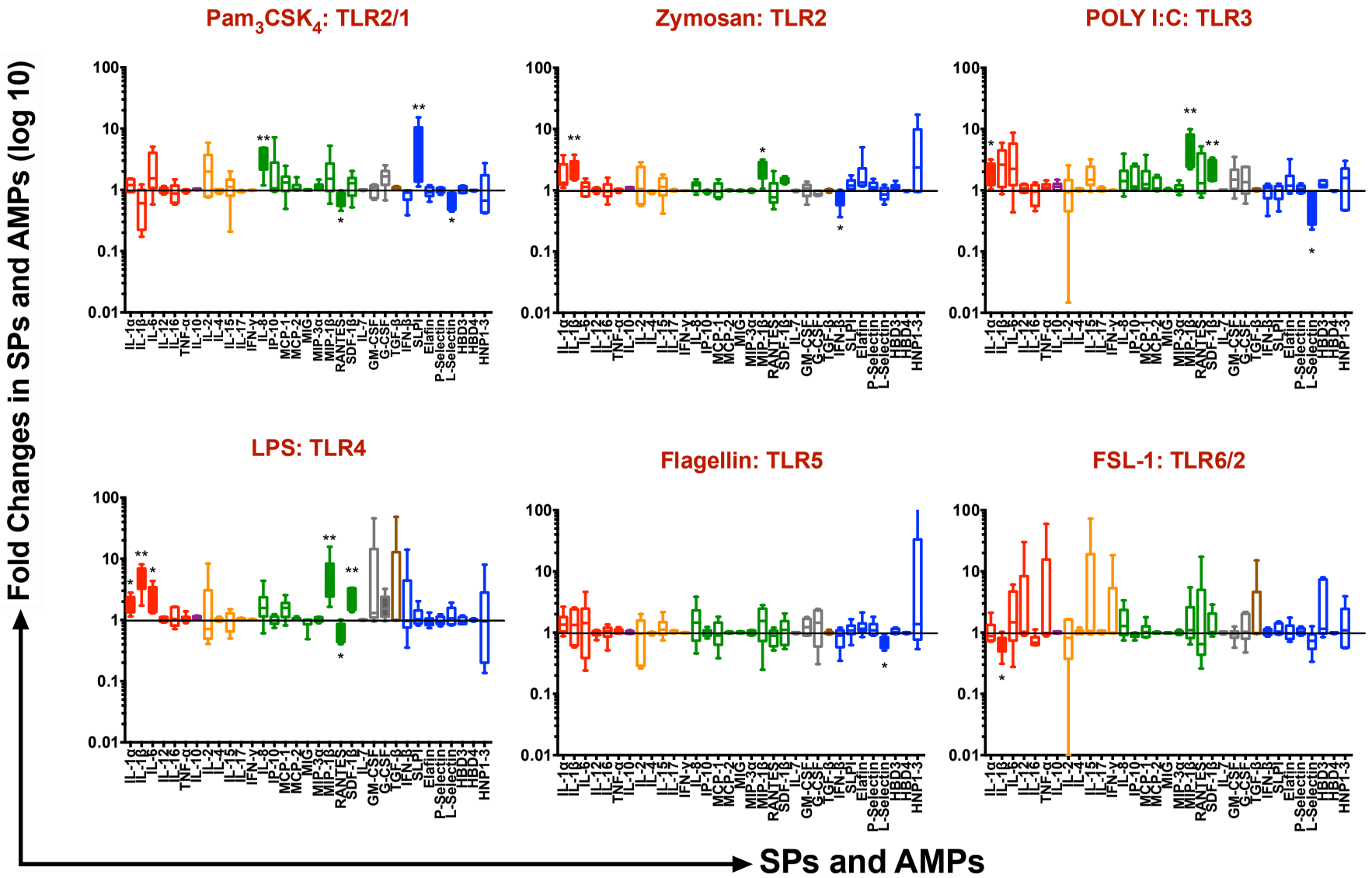

Figure 5.5 Box and whisker curves showing the impact of each stimulant on the level of each analyte, (n=6). The horizontal line within the box represents the median while the whiskers represent minimum and maximum values. Stimulants included envelope and non-envelope HIV-1 preparations (A.) while TLR ligands included ligands 1 through to 6 (B.). IL-1β was used as a positive control. Specifically we stimulated with HIV-1 soluble CN54gp140 trimeric protein, an envelope glycoprotein, HIV-1 CN54gp120 virus-like particles (VLPs), R5 tropic whole virus, inactivated HIV-1 BaL, and HIV-1 NL4-3 deleted in Env. Analytes included 25 SPs and 8 AMPs. Analyte levels were measured with the Luminex multiplex bead immunoassay. Box and whiskers, representing each analyte, are colour coded according to analyte functional grouping: red=pro-inflammatory, purple=anti-inflammatory, yellow=adaptive, green=chemokine, gray=hematopoietic, brown=growth and blue=antimicrobial peptide. Analyte fold changes were calculated by dividing the stimulated values by the unstimulated values. Significantly up- and/or down-regulated cytokines are defined by a fold change of at least 1.5 and are denoted by solid bars. One sample t test was employed to test the statistical significance of the fold change from one. Statistically significant fold changes are denoted with an asterisk. P-values were taken as non-significant if $p>0.05$, and significant if $p \leq 0.05$ (*), $p \leq 0.01$ (**), $p \leq 0.001$ (***), and $p \leq 0.0001$ (****). HIV-1 preparations did not trigger any significant fold changes in all analytes while TLR ligands differentially down-/up-regulated various analytes.

Table 5.3 Summary of significantly up- and down-regulated SPs and AMPs in the human EET following stimulation with various stimulants: TLR ligands and virus preparations

Immunostimulants	Up-regulated SPs and AMPs	Down-regulated SPs and AMPs
Pam_3CSK_4 (TLR1/2)	**↑ IL-8, SLPI**	**↓ RANTES and L-Selectin**
Zymosan (TLR2)	**↑ IL-1β, MIP-1β**	**↓ IFN-β**
Poly I:C (TLR3)	**↑ IL-1α, MIP-1β, SDF-1β**	**↓ L-Selectin**
LPS (TLR4)	**↑ IL-1α, IL-1β, IL-6, MIP-1β, SDF-1β**	**↓ RANTES**
Flagellin (TLR5)		**↓ L-Selectin**
FSL-1 (TLR2/6)		**↓ IL-1β**
IL-1β	**↑ IL-1β**	**↓ L-Selectin**
HIV-1 CN54gp140		
HIV-1 CN54gp120		
HIV-1 BaL		
HIV-1 envelope deleted NL4-3		

Contrary to MIP-3α which is not secreted in response to stimulation with TLR ligands and HIV-1 preparations in the human EET, 10 SPs and AMPs are either up-regulated or down-regulated significantly in response to stimulation with TLR ligands but not HIV-1 preparations

While some AMPs have been shown to have direct antiviral activity, an important aspect of the activity of cytokines and chemokines in viral infection is the induction and orchestration of the antiviral response. A wide range of mechanisms are involved including alteration of the expression of MHC molecules, adhesion and co-stimulatory molecules, and direct activation or deactivation of immune cells. These latter changes may thus lead to either down- or up-regulation of SPs aimed at virus clearance. We thus studied a wide range of SPs and AMPs secreted by EET in response to stimulation with various viral preparations and TLR ligands. In particular, we studied the pattern of either up-regulation or down-regulation of each analyte by assessing fold changes of each analyte in response to TLR ligand and viral stimulation. Studying a wide range of cytokines was particularly important as we had learned in the human EET that the EET did not secrete further MIP-3α in response to these immunostimulants. We again prepared EET on receiving hysterectomy specimens and added various stimulants to a maximum volume of 200μL of RPMI-1640 media per well prior to overnight incubation at 37^0C 5% CO_2. We harvested supernatants 24 hours post stimulation and incubation, and quantified analyte levels using the multiplex bead array assay. We then proceeded to study cytokines that were either up- or down-regulated following exposure to various viral and TLR ligand stimulants. We defined a significant fold change as a change of at least 1.5, dividing stimulated levels by those of unstimulated levels for respective SPs and AMPs in this analysis. Moreover, statistical significance was defined as a p-value of <0.05. All

SPs and AMPs were neither down- nor up-regulated on exposure to all HIV-1 preparations in this analysis (*Figure 5.5A, Table 5.3*). Conversely, there was differential up- or down-regulation of SPs and AMPs in response to various TLR ligands. L-selectin was frequently down-regulated while MIP-1β and SDF-1β were frequently up-regulated. Specifically, L-Selectin, RANTES and IFN-β were significantly down-regulated on exposure to Pam_3CSK_4, Zymosan, Poly I:C, LPS, Flagellin and IL-1β while IL-1β was down-regulated on exposure to FSL-1. LPS significantly up-regulated a high number of pro-inflammatory cytokines and chemokines (IL-1α, IL-1β, IL-6, MIP-1β, and SDF-1β). Zymosan, LPS, and Poly I:C up-regulated MIP-1β. These findings that the EET is differentially responsive to TLR ligands while not responsive to any of the HIV-1 preparations confirms that the EET is potentially responsive to approaching microbes, however, that its response varies and may be unique to each approaching organism. The endocervix is known to respond to viral infections; it is infected by Human Papilloma Virus for instance. Therefore the lack of response to HIV-1 preparations in the context of 33 analytes in this analysis suggests that the endocervix does not respond to HIV-1 in humans, and that this unresponsiveness is specific for HIV-1.

DISCUSSION

This thesis chapter reviewed the pattern of secretion of 33 SPs and AMPs in the FGT. SPs and AMPs were quantified in the supernatants of EET prepared from six HIV uninfected women at low risk for HIV infection. Women recruited and whose wombs were subsequently sampled were scheduled to undergo a hysterectomy for their own health. The chapter focused initially on the constitutive

pattern of secretion of all these SPs and AMPs. Eight pro-inflammatory cytokines, one anti-inflammatory cytokine, five adaptive cytokines, nine chemokines, three hematopoietic cytokines, one growth factor and eight antimicrobial peptides constituted the panel. Efforts have been underway for a considerable period of time to define soluble and cellular biomarkers that are prevalent in the FGT and to determine their normal ranges collecting samples with various devices. Further, efforts have been underway to determine those that are associated with the risk of HIV infection and also those that could be used in microbicide trials to assess subclinical mucosal inflammation in the FGT and hence increase product safety. This has particularly been important after some microbicides were found to be associated with exacerbated inflammation in the FGT and thus paradoxically enhancing HIV infection risk [165]. Microbicides are topical formulations which when applied intravaginally provide protection against HIV infection and other sexually transmitted pathogens through direct microbicidal action and/or enhancement of natural defence mechanisms in the cervicovaginal environment. Hence our study contributed to this ongoing work in the field.

Numerous studies have reported results on the constitutive pattern of secretion of a panel of SPs and AMPs in the FGT; however, they did not include MIP-3α in their panels [166, 167]. Further, in some studies that used *in vitro* models, they used epithelial cell lines and primary cell models, focusing mainly on the fallopian tubes, endometrium, and vagina in the non-HIV context [168]. Those that did focus on HIV infection collected and quantified cytokines and innate immune mediators in cervicovaginal fluid samples [169]. A few other studies that looked at the endocervix studied endocervical swabs and sponges as opposed to the explant tissue model [170, 171]. However, after findings from the landmark study

in 2009 by Li *et al* suggested a significant role for MIP-3α in early SIV transmission events in the endocervix [96], it became necessary to assess the role of MIP-3α alongside these other SPs and AMPs in the human endocervix in the context of HIV infection. This study has therefore extended this body of knowledge by studying tissue explants from the endocervix, quantifying a wide range of SPs and AMPs simultaneously in the context of HIV infection. Moreover, most FGT studies have typically studied IL-1α, IL-1β, IL-1-receptor antagonist, IL-6, IL-8, TNF-α and SLPI [169], but we have expanded this panel and included numerous other analytes. Specifically, we have added MIP-3α to our panel which no other group has done.

All analytes were above the lower limit of detection in all cases, hence indicating that constitutive levels of SPs and AMPs are detectable at high concentrations in the EET. Our data, focusing on a panel of 33 analytes, confirmed what we had shown previously, namely that the EET secretes MIP-3α at high concentrations. Moreover, in a panel comprising 32 other analytes, our data showed that the constitutive level of MIP-3α in the EET is amongst the SPs and AMPs that occur in the highest concentrations in the FGT. The levels of HNP 1-3 were the highest concentration of any analyte, followed by G-CSF, IL-8, IL-6, P-selectin, SLPI, MIP-3α, MCP-1, IL-7, Elafin, L-selectin, IL-16, IFN-β, and SDF-1β. Fichorova *et al* studied 14 analytes in the supernatants of the End1/E6/E7 endocervical immortalised cell line and showed that IL-8 was present in the highest concentration, followed by IL-6, IL-7, TGF-β, RANTES, and SLPI [168]. Conversely, Lieberman *et al* estimated levels of 10 cytokines in endocervical mucus collected with a cervical sponge and showed that IL-8 was present in the highest concentration, followed by IL-6, IL-1β, IL-12, IL-10, IL-2, IL-13, IL4, IL-5,

and IFN-γ [171]. Lastly Dezzutti *et al* estimated levels of SPs and AMPs in endocervical swab specimens and established that IL-8 was detected in the highest concentration, followed by SLPI, HNP1-3, IL-6, IL-1β, and IL-12 [170]. Evidently, even though sample collection methods varied and analytes included in the panels had minimal overlap, levels of IL-8, IL-6, IL-7 and HNP1-3 were high across all studies, thus indicating that levels of these analytes are consistently high in the endocervix of humans. While our findings concur with these other studies, they contribute further to this body of knowledge by showing that MIP-3α is amongst the SPs and AMPs in the highest concentrations in the endocervix. MIP-3α is understood to be a chemokine that is prevalent in mucosal and inflamed sites [103], hence it is therefore not surprising that it is found in high concentrations in the FGT. The FGT, due to changes imposed by constant menstrual cycle demands, is purported to be a mucosal site of constant inflammation [172]. Moreover, immune activation, resulting in increased or decreased expression of soluble immune proteins, is a frequent occurrence in the FGT. It can be caused by infection, both sexual and reproductive tract infections, irritation as could be seen with insertion of intravaginal products, or epithelial trauma as could be seen secondary even to non-coercive sexual intercourse.

The endocervix, a bridge separating the richly colonised lower reproductive tract and the relatively sterile upper tract, has been shown to be an area of high endocrine and paracrine functions, characterised by high antimicrobial protein expression and secretion of antibodies [111]. A single layer of columnar epithelial cells arranged into crypts lines the endocervical canal. These crypts form functional glands, which secrete cervical mucus. The daily mucus production varies from 600 mg during mid-cycle to 20-60mg during other periods of the

menstrual cycle [173]. This mucus bathing the endocervical columnar epithelium is a viscous hydrocolloid of associated and entangled mucins and other secreted proteins, which acts as both a physical barrier and a trap for microbes. In a study by Miller *et al*, following deposition into the cervicovaginal canal, SIV virions were effectively trapped into the cervical mucus, thus being prevented from accessing the underlying epithelium and establishing productive infection [66]. Boomsma *et al* compared constitutive levels of 16 analytes between the endocervical and endometrial secretions, and showed that seven of the 11 that were significantly different in concentrations were higher in the endocervical than in the endometrial secretions [174]. Dezzutti *et al* compared levels of analytes in flocked swabs collected from the endocervix and swabs from the vagina and showed that seven of the eight analytes were significantly higher in the endocervical than in the vaginal secretions [170]. The endocervix has for a long time been understood to be a rich source of polymeric immunoglobulin A (IgA) which is found in abundance in cervical mucus as opposed to the lower FGT (vagina and ectocervix) [175]. Similarly, our results confirmed high secretion of SPs and AMPs in the EET. We compared constitutive analyte levels between the endocervix and the ectocervix and showed that the analyte levels of three innate markers, SLPI, P-selectin and HNP1-3, were significantly higher in the former than in the latter: only Elafin was higher in the ectocervix. It is, however, not surprising that the endocervix would have this potent immune defence characterised by high levels of SPs and AMPs as it is a site primarily responsible for protecting the conceptus during pregnancy from outside harm. It could be that the immune defence system in the endocervix exploits this attribute in its fight against HIV infection.

Some AMPs, including some in our panel, such as SLPI, α-defensins, β-

defensins, type I interferons (IFN-α and IFN-β), lysozyme, lactoferrin, Elafin/ trappin-2 and some classes of cystatins have all been shown to have direct anti-HIV-1 activity *in vitro* [176, 177]. Of the 14 analytes with mean concentrations above 1pg/mL, half were AMPs, thus indicating that AMPs frequently occur in higher concentrations than SPs in the EET. AMPs, a class of peptides with antimicrobial and immune modulating properties, reside at the forefront of host barrier defences where they are broadly effective against bacteria, fungi, viruses, and protozoa. They are hence known as endogenous antibiotics. Co-incidentally, even though MIP-3α has been classified as a chemokine for the purposes of this analysis, it is however a kinocidin [178]. Kinocidins are a select group of microbicidal cytokines and chemokines that also possess antimicrobial activity. MIP-3α has previously been demonstrated to have antimicrobial activity against a wide range of organisms including *Escherichia coli, Pseudomonas aeruginosa, Moraxella catarrhalis, Streptococcus pyogenes, Enterococcus faecium, Staphylococcus aureus*, and *Candida albicans* [179]. Recently, it has also been shown to have anti-HIV-1 activity [85]. IL-8, another chemokine occurring at high concentrations in the EET, as discussed above, is another kinocidin effective against *Candida albicans* [180]. Evidently, the EET is fraught with AMPs with documented anti-HIV-1 activity. Further, over and above microbicidal action, some AMPs may also possess anti-inflammatory activities. *In vitro* studies using human monocytes found that LPS- and lipoteichoic acid (LTA)-induced activation of NF-κB was inhibited by SLPI [181]. Inflammation has been shown to be in a pathway to productive SIV infection in the SIV/Rhesus macaque model [96]. Suppressing inflammation with glycerol monolureate (GML), a broad spectrum anti-inflammatory, dampened inflammation and reduced HIV infection in a study by Li *et al* [96]. Hence the presence of high concentrations of AMPs may be beneficial

in more ways than one i.e. by demonstrating direct anti-HIV-1 activity while also demonstrating anti-inflammatory activity. The high concentrations of AMPs could be the reason that our results did not show any increase in SPs and AMPs in the EET on exposure to HIV-1. Notwithstanding that organisms such as Human Papilloma Virus, Chlamydia Trachomatis and Neisseria Gonorrhoea infect the endocervix, it is possible that HIV-1 is not able to exploit and bypass the endocervical defences in humans to establish infection.

To date, the issue of the primary site of infection of HIV-1 has not been without controversy. Although it is believed that HIV-1 can primarily infect different sub-compartments of the FGT i.e. the endometrial, endocervical, transformation zone, ectocervical and vaginal, the relative contribution of each site to the establishment of the initial infection is not known and there is no agreement as to what the primary site of infection actually is. In this analysis there was no evidence that HIV-1 triggered further secretion of any of the 33 analytes in the panel in the EET, showing that this part of the FGT does not respond to the presence of this virus. Initial studies suggested that the vagina was the primary site of HIV/SIV infection. In a series of transmission studies and publications Miller *et al* showed that vagina was the primary site of SIV transmission in the SIV/Rhesus macaque model [154, 155]. In their study, the lack of the cervix and uterus did not affect establishment of SIV infection, a finding strongly suggesting that target cells for SIV were present in the vaginal mucosa. In humans, a woman born without a cervix and uterine body, although a very short vagina was present, was found to have established HIV infection following heterosexual intercourse, thus providing further evidence for vaginal HIV transmission [182]. Again in humans, HIV incidence was

not lowered in women wearing a diaphragm for HIV prevention in Africa, thus providing further evidence for vaginal transmission of HIV [183]. The diaphragm is a physical barrier that is worn over the cervix for the purpose of prevention of pregnancy. Covering the cervix, it prevents sperm and infectious pathogens from ascending into the upper genital tract. Evidence that the primary site of infection post exposure to HIV inoculum in animals is the cervix, and particularly the endocervix and transformation zone is fairly recent (Haase, 2011). In this study we found high levels of MIP-3α, an inflammatory chemokine, in the endocervix. This could explain the high rates of infection in the populations with high pre-existing inflammation.

CONCLUSION

MIP-3α levels are amongst the levels of SPs and AMPs that are in the highest concentrations in the EET. The high concentration of MIP-3α in the EET might be reflective of the high levels of immune activation that characterise the FGT. The FGT is constantly exposed to inflammatory conditions secondary to irritation from infections, intravaginal insertions and vaginal intercourse. The EET demonstrated high constitutive secretion of a wide variety of SPs and AMPs in our panel, but mostly AMPs and other cytokines with antimicrobial function including MIP-3α. Most AMPs in our panel have direct anti-HIV-1 activity. Hence the strong presence of high concentrations of AMPs with antagonistic HIV effect in our study might explain the lack of response of the EET to various HIV-1 preparations.

CHAPTER SIX INTERPLAY BETWEEN ENDOCRINE AND IMMUNE SYSTEMS: IMPACT OF CHANGES IN MENSTRUAL CYCLE PHASES ON LEVELS OF MIP-3α AND OTHER SOLUBLE MARKERS

SUMMARY

The female genital tract (FGT) mucosa has long been appreciated to be an immunohormonal system influenced by menstrual cycle phases and exogenous hormone administration, yet the extent of impact of these changes on Human Immunodeficiency Virus (HIV) infection has not been fully studied. Human and non-human primate (NHP) studies suggest that there is an increased vulnerability to HIV and Simian Immunodeficiency Virus (SIV) infection, respectively, during the post-ovulatory phase when levels of progesterone predominate. If we could understand the baseline innate mucosal status as it pertains to secretion of infection-modulating molecules and the endocrine regulation of these molecules over the different phases of the menstrual cycle, we could be better equipped to develop efficacious biomedical prevention strategies to reduce the risk of HIV infection in women. This chapter aimed to investigate the influence of fluctuations of endogenous hormones on the stability of innate immune markers associated with increased vulnerability/resistance to HIV infection in the FGT. We recruited 31 HIV uninfected women in the reproductive age group from an HIV vaccine institute at St George's Hospital in London. Using a menstrual cup, we collected a concentrate of cervicovaginal fluid (CVF) longitudinally at three time-points from each woman during the phases of a single menstrual cycle: oestrogenic (D5–8), mid-ovulatory (D14–16), and progestogenic (D19–22). We also collected corresponding serum samples at the same time-points that CVF was collected.

Concentrations of MIP-3α αnd 23 other cytokines with pro-inflammatory, adaptive, chemoattractant, growth and haematopoietic functions were measured using the Luminex multiplex bead assay. We described profiles of main protein categories for each time-point and evaluated changes in mean concentrations of protein levels using one-way analysis of variance (ANOVA). Our results showed that chemokines and pro-inflammatory cytokines were the most prevalent proteins in the FGT irrespective of menstrual phase. Haematopoietics and adaptive proteins, however, fluctuated according to menstrual phase: the oestrogenic phase was characterised by higher levels of haematopoietics while the mid-ovulatory phase was characterised by higher levels of adaptive cytokines.

There were no significant differences in mean MIP-3α levels in CVF over the three different phases of a single menstrual cycle on ANOVA, ($F_{1.23, 8.63}=6.96$, MS=19177, p=0.3076, thereby suggesting that fluctuations in endogenous hormones do not drive MIP-3α levels in the FGT. However, the levels of IL-1β, G-CSF, and TGF-β were significantly higher in the oestrogenic than in the mid-ovulatory and progestogenic phases (p=0,0246, p=0,0477, and p=0,0406 respectively), while levels of IFN-β (p=0.0201) were significantly higher in the mid-ovulatory versus the proliferative and secretory phases. Of 24 cytokines measured, MIG, MIP-1β and TNF-α were not quantifiable in the absence of underlying CVF abnormalities and hence their presence/detectability suggested some underlying CVF abnormality. In women without underlying CVF abnormalities IL-1α, IL-8, and IP-10 were in the highest concentrations while in women with CVF changes suggesting underlying inflammation IL-1α, IL-6, IL-16, MCP-1, MIP- 3α, RANTES, SDF-1 β, and IL-7 were also significantly up-regulated. Lastly the levels and profile of CVF cytokines were distinct from the

levels and profile of serum cytokines, highlighting the inappropriateness of using blood samples as a surrogate marker for FGT events.

INTRODUCTION

Increased vulnerability to HIV in women is multifactorial ranging from behavioural to biological causes. Significant biological factors at the level of the mucosa include structural and biochemical changes due to fluctuation in hormone levels as with menstrual changes and exogenous hormone administration [47, 48].

Yeaman *et al* studied HIV receptor expression on uterine epithelial cells and demonstrated varying expression of CD4, CXCR4, CCR5 and galactoceramide receptors during the various phases of the menstrual cycle [184]. Their data showed that expression of these receptors varied with the expression of CD4 and CCR5 receptors, being highest in the proliferative phase versus the other menstrual phases. It is also believed that endogenous hormones modulate susceptibility to SIV and HIV-1 by altering the availability of target cells in the vaginal epithelium and stroma. Lu *et al* conducted a study in rhesus macaques and showed that the frequency of immunoglobulin (Ig) and antibody secreting cells was significantly higher in tissues collected in the peri-ovulatory period than in tissues collected in other phases of the cycle [185]. Their data also demonstrated that the levels of IgA and IgG in genital secretions significantly fluctuated throughout the menstrual cycle in a pattern similar to that of humans [186]. The highest levels of Ig occurred during menses, while the lowest levels occurred around the time of ovulation. Again in a study by White *et al*, cytotoxic T lymphocytes in the FGT exhibited high cytotoxic activity during the proliferative

phase and almost complete loss of this activity during the luteal phase [187]. Over and above the demonstrable impact of hormonal fluctuations on target cells, it is also appreciated that secretion of some of the antiviral proteins and cytokines in CVF are regulated by hormone status. For example the concentrations of human β-defensin 2 (HBD2) and secretory leucocyte protease inhibitor (SLPI), shown to have anti-HIV-1 activity [188, 189], were high in cervical mucus without microbicide use during ovulation [190] while they were lower in CVF during ovulation following application of the microbicide PRO 2000 [191].

Besides immune changes seen with normal endogenous hormone level variations, there is evidence that some altered hormonal states characterised by higher than normal endogenous hormone levels also influence HIV infection dynamics in the FGT. Hwang *et al* showed that in young girls maturity of cervical epithelium around puberty, implying presence or absence of cervical ectopy, was associated with higher levels of pro-inflammatory cytokines [45], which may increase the susceptibility of the adolescent FGT to HIV infection. Cervical ectopy is a phenomenon whereby, due to high levels of oestrogen, the inner part of the endocervix is pushed out and becomes exposed to the environment of the vagina cavity, thereby leading to transformation of the epithelium from columnar to squamous. This regulation may result in alteration of both barrier and innate immunity attributes of the epithelium and the consequent HIV infection risk. Similarly, pregnancy itself, a highly hormonal state characterised by high progesterone levels, is an opportune time when women have been shown to transmit HIV more than non-pregnant women. In addition, some data suggest that pregnant women are more likely to acquire HIV than their non-pregnant counterparts [192]

While endogenous hormonal changes alter HIV dynamics in the FGT on the one hand, exogenous hormonal administration has also been shown to have an impact on HIV risk on the other hand. Depot medroxyprogesterone acetate (DMPA), a progesterone-only contraceptive drug that is injected intramuscularly every 3 months, is one such hormonal preparation. DMPA is an aqueous suspension for depot injection of the acetylated pregnane 17α-hydroxyprogesterone and exerts its mechanism of action and biological effects by binding to both progesterone and glucocorticoid receptors. Depo-Provera is the brand name for this 150 mg aqueous injection. Its previously demonstrable biological effects at the genital tract level include reduction in epithelial thickness with associated reduction in the number of epithelial cell layers, cellular transformational changes, changes in vaginal microbiota with impairment in hydrogen peroxide (H_2O_2) producing lactobacilli colonisation [193]. All these changes have been shown to be associated with increased risk of sexually transmitted infections (STIs) including HIV; alteration of immune responses including recruitment of T cells, macrophages and other target cells; enhanced receptor expression on CD4+ cells; suppression of antibody responses, suppression of T cell activity; and alteration of cytokine expression [194]. In 1996, data reported from NHP studies indicated a 7-fold increased risk of SIV transmission due to epithelial thinning in the presence of DMPA [195]. To date, in SIV-rhesus transmission studies, macaques are pretreated with progesterone to enhance epithelial thinning and consequent infection. This effect is, however, not as pronounced as in humans. In 2007 Morrison *et al* published results of a *post hoc* analysis in humans in which they found that there was an association between hormonal contraceptive use, and particularly DMPA, and HIV risk. Stratification of the younger age group into women aged 18–20 and 21–24 years

was undertaken and this showed that among participants between 18–20 years of age, there was a strong increase in HIV risk for DMPA (AHR 9.29, 95% CI 2.72–31.69) [196]. Documentation of the association between DMPA and high risk of HIV infection has since been replicated in numerous human studies published in a meta-analysis by Polis *et al* [197].

In sharp contrast to progesterone, oestrogen and its derivatives have been shown to exert a strong protective effect against HIV and SIV infection. Oestrogen induces thickening of the vaginal stratified epithelium in both humans and female macaques [198-200]. However, the oestrogen-induced expansion of the epithelial layer is less pronounced in humans compared with female macaques [199, 200]. Smith *et al* demonstrated that oestrogen applied systemically in the form of subcutaneous implants protected against intravaginal challenge of ovariectomised female rhesus macaques with highly pathogenic SIVmac251 [198]. They reported that whereas the average thickness of the epithelial layer was about 10μm in untreated ovariectomised female macaques, it expanded to about 240μm in the oestrogen treated animals. In postmenopausal women, a hormonal state characterised by low oestrogen, low oestrogen was shown to be associated with thinning of the vaginal epithelium and atrophy [201]. Clinical evidence shows that atrophic vaginitis is successfully treated with local or systemic oestrogen therapy, resulting in thickening of the vaginal wall. A thick epithelium might be beneficial in that it might block access of the virus to target cells in the epithelial and sub epithelial layers. Further, oestrogen treatment has been shown to decrease cervicovaginal pH in the human FGT and that of female macaques, thereby making it hostile to the virus [199, 202].

This chapter therefore aims to investigate the influence of changes in levels of endogenous hormones with the menstrual cycle on the stability of MIP-3α levels and those of other innate immune markers associated with increased vulnerability/resistance to HIV infection in the FGT. Specifically, we hypothesise that MIP-3α levels will be highest in the secretory phase where they would probably contribute to the high risk of HIV infection. This chapter also aims to compare and contrast levels and profiles of innate markers in CVF versus those in serum.

MATERIALS and METHODS

Study design, setting, population, cohort and size:

The project discussed in this chapter was designed as a prospective cohort observational study with biological samples collected longitudinally over three time-points from each participant. Access to serum and genital tract secretions was made possible through a cohort in St George's hospital, a hospital affiliated with the Imperial College in London. The entire study, from participant recruitment to sample collection and sample analyses in the laboratory, was conducted in the United Kingdom. Women were recruited as part of the CASHIR study. CASHIR is an acronym for characterisation of the activity and stability of anti HIV-1 agents in the presence of female genital secretions and establishing methods to measure immune responses. It was primarily designed with an aim to standardise methods to measure immune responses to newly designed HIV vaccines and to develop tests that can accurately and reliably measure immune responses to vaccines. 31 women were subsequently recruited and followed up longitudinally

over one calendar month. The CASHIR study team under the leadership of Dr Clifford Jones screened, recruited, and collected samples for this study.

Eligibility criteria:

HIV uninfected women of reproductive age (18-45 years) at low risk for HIV infection were recruited from an HIV vaccine institute. Women were recruited only if they provided informed consent. Consenting women were eligible to participate only if they had regular monthly menstrual periods with an average menstrual cycle of 28 days. Women could not participate if they were actively menstruating, had an intrauterine contraceptive device in situ and had had unprotected (condoms) sexual intercourse in the preceding 24 hours before specimen collection.

Ethical consent:

Informed consent was sought and obtained at screening from all study participants prior to recruitment. Ethical, and Research and Development

Figure 6.1. Pictorial of the Instead softcup™, the menstrual cup used to collect a concentrate of cervocivaginal secretions from the vagina. Women were instructed to self-insert the cup at the clinic during the study visit. The cup remained in the vagina for up to two hours before it could be removed.

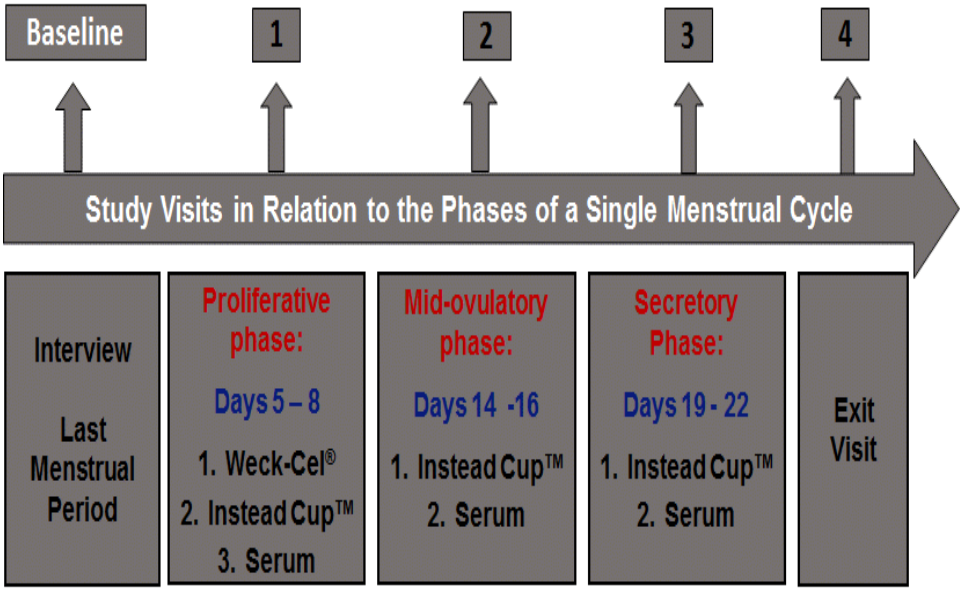

Figure 6.2. Pictorial of the schedule of study visits for collecting biological specimens (CVF and serum) from women. Every woman was seen five times during the study period with specimens collected at visits one through three as indicated in the schematic. The three study visit windows corresponded to the different phases of the menstrual cycle: proliferative, mid-ovulatory, and secretory.

committees in the London NHS Trusts approved the study. Specifically the study was approved through the St George's NHS Trust.

Collection of samples:

CVF was collected using the Instead softcup™ *(Figure 6.1)* a vaginal cup used originally as a menstrual cup. A concentrate of CVF was collected longitudinally at three time points corresponding to the estrogenic (D5–8), mid-ovulatory (D14–16), and progestogenic (D19–22) phases of a single menstrual cycle from each woman (*Figure 6.2*). We instructed women to self-insert the Instead softcup™ into the vagina on the day of the study visit at the clinic. The cup was left in situ for a

minimum of an hour up to a maximum of two hours prior to being removed from the vagina. At the same corresponding visits and from the exact same women, serum was also collected from each study participant.

Sample handling, storage and processing of CVF:

On removal from the vagina, the Instead softcup™ with secretions was placed into a sterile pre-labeled 50ml falcon tube. Falcon tubes containing Instead softcup™ samples were then immediately transferred to ice at the clinic where they remained until they reached the laboratory. They could, however, not remain in the clinic for more than an hour. Falcon tubes were stored frozen at -80^{0}C until batch processing and analysis. On the evening prior to further processing, falcon tubes containing the Instead softcup™ samples were transferred to the 2-8°C fridge and allowed to thaw overnight. They were then centrifuged at 13000 *rpm* for 15 minutes. The Instead softcups™ within the falcon tubes were then removed with sterile forceps while the vaginal mucus that had collected at the bottom of the tube remained. Using a positive-displacement pipette, 100µL of vaginal mucus was aspirated from the falcon tube to a pre-labelled 2mL microfuge tube. Then we added 100µL of extraction buffer to the vaginal mucus. We made as many aliquots as was possible with the amount of mucus available. We then stored all processed Instead softcup™ samples at 2-8°C for further processing the next day. The following day, after removal of sample from the fridge, we added an additional 200LµL of extraction buffer into each tube and centrifuged the tube again at 13000rpm for 5 minutes at 4^{0}C. We then carefully collected the clarified supernatant (300-400µL) and layered it on the spin-X filter. Clarified solution at the bottom of the tube was collected for performing the assay.

Extraction buffer:

Extraction buffer was prepared by reconstituting 1 vial of protease inhibitor cocktail set I (Calbiochem®, Merck Millipore, UK) in 1ml of sterile distilled H_20 per vial (100X solution) mixed with 20μl of 10% sodium azide solution plus 1.5g of sodium chloride (0.25M final concentration) (Sigma-Aldrich®, UK) made up to a final volume of 100mL with 1XDPBS (Life technologies, Gibco®, UK) solution.

Sample handling, storage and processing of serum:

After venepuncture, 10mL of blood collected was centrifuged and serum collected. Serum was subsequently aliquoted into 1mL cryovials which were then stored at -80^0C until used for the assay. On the morning of the assay, serum was thawed and heat inactivated within an hour. We heat inactivated it by incubating at 56 °C for 30 minutes.

Cytokine Measurements:

The concentrations of 24 cytokines including MIP-3α were measured in CVF and serum using the Luminex multiplex bead assay. The cytokines included: interferon gamma-induced protein 10 (IP-10), interleukin 1 beta (IL-1β), interleukin 16 (IL-16), granulocyte-macrophage colony-stimulating factor (GM-CSF), interleukin 4 (IL-4), interleukin 2 (IL-2), regulated on activation, normal T cell expressed and secreted (RANTES), interferon gamma (IFN-γ), interferon beta (IFN-β), tissue necrosis factor alpha (TNF-α), stromal cell-derived factor 1 beta (SDF-1β), monokine induced by gamma-interferon (MIG), macrophage inflammatory protein-1 beta (MIP-1β), interleukin 7 (IL-7), interleukin 8 (IL-8), monocyte chemotactic

protein 1 (MCP-1), interleukin 6 (IL-6), granulocyte-colony stimulating factor three (G-CSF), macrophage inflammatory protein three alpha (MIP-3α), interleukin 1 alpha (IL-1α), transforming growth factor beta (TGF-β), interleukin 12 (IL-12), and interleukin 15 (IL-15). The cytokines measured fell in one of six functional groups: pro-inflammatory, adaptive, chemokine, growth, haematopoietic and antimicrobial peptide functions (*Figure 6.3*). We measured cytokines with a custom made 24-plex Luminex in-house panel comprising two sub panels: the high-plex and the low-plex panels (described in the previous chapter). After optimising both panels by adjusting the concentrations for the standard curve and excluding cross-reactivity with other analytes, magnetic beads were used to do the assay. Serum and CVF were each pooled before being dispensed into triplicate wells of the Luminex assay plate. CVF was used diluted 1:4 while serum was used undiluted in the assay. Data were collected using a Bio- Plex^{TM} Suspension Array Reader (Bio-Rad Laboratories InC®). The lower limit of detection ranged between 1,7 and 266,6pg/mL for the cytokines measured. Specifically the cytokines with respective lower detection limits in pg/mL in this panel included: the lower limit of detection was 4.2pg/mL for IP-10, IL-1β, IL-16, GM-CSF, IL-4, IL-2, RANTES, IFN-γ, IFN-β, TNF-α, SDF-1β, MIG, MIP-1β, IL-7, IL-8, MCP-1, IL-6, G-CSF. The lower limit of detection was 0.8pg/mL for MIP-3α and 2.4pg/mL for IL-1α, TGF-β, IL-12, and IL-15. Cytokine concentrations that were below the lower limit of detection of the assay were reported as the mid-point between the lowest concentrations measured for each cytokine and zero.

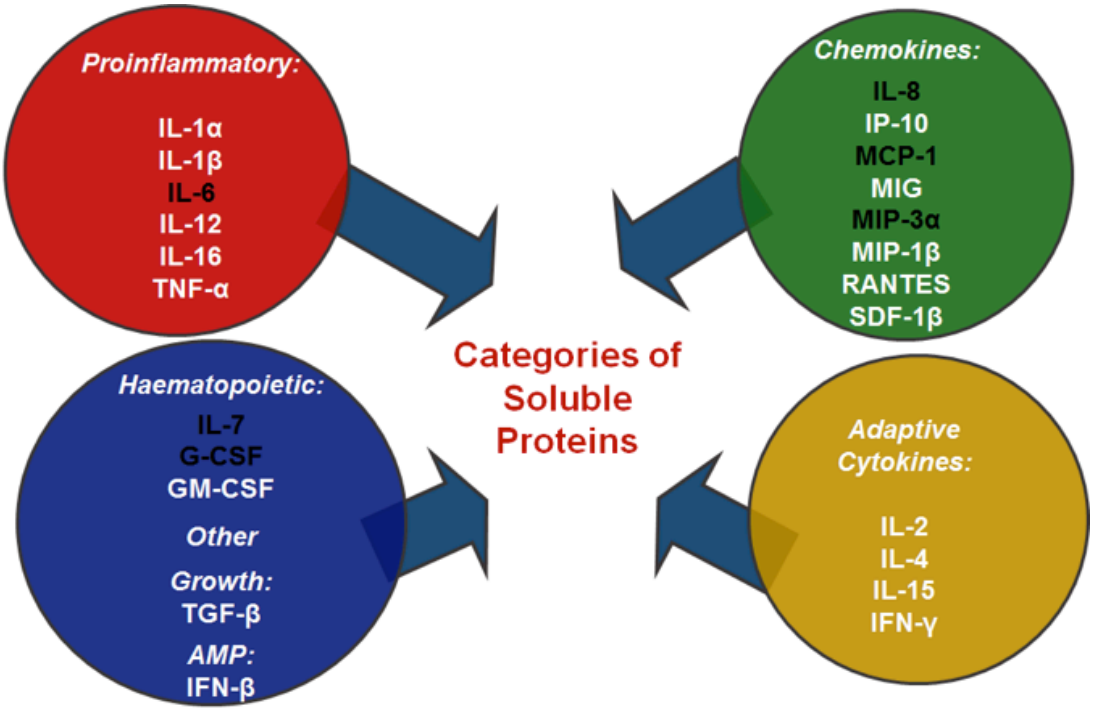

Figure 6.3: Categories of soluble proteins included in our 24-plex Luminex in-house panel. The six analytes highlighted in blue are those included in the high-plex panel while the rest are included in the low-plex panel. Colour codes of the circles correspond to the colour codes in the graphical presentation of data in the rest of the text.

Statistical analyses:

Statistical analyses were performed using GraphPad Prism version 7 for Mac OS X (Prism, GraphPad Software, La Jolla, California, USA) 5 PL regression curve fitted formula was used to calculate cytokine concentrations from the standard curves on GraphPad Prism. Descriptive data were presented with schema prepared from Excel and GraphPad Prism. Results were reported in bar graphs with bars representing analyte levels in mean pg/mL and error bars representing standard deviation. For CVF and serum Luminex analyses, profiles of expression of main protein categories were described for each time-point based on median levels and range. Changes in mean concentrations of protein levels across the

three visits per single menstrual cycle, also expressed in pg/mL, were evaluated using one-way analysis of variance (one-way ANOVA) For *ex vivo* explant tissue assays, explants were seeded at one explant per well but each condition was tested in triplicate. When an overall statistically significant difference was measured ($p<0.05$), a Tukey posttest was performed to adjust the p-values for multiple comparisons. The p-values and the respective comparisons for which they were calculated are indicated in the figures. Chi-square tests were used to assess significant differences in protein levels of women with CVF abnormalities versus those with no abnormalities. Differences in median values were used to construct pie curves and the heatmap.

RESULTS

Descriptive data analysis

31 women were eligible to participate in this study. However, only 11 women were eligible for inclusion in this analysis. These 11 women each had samples collected longitudinally at three successive study visits corresponding to the proliferative, mid-ovulatory and secretory phases of a single menstrual cycle; both CVF and serum were collected. We collected CVF with the Instead softcup™, a vaginal cup originally used as a menstrual cup. We inspected and quantified the amount of CVF collected from each cup. Volume of CVF collected with the Instead softcup™ from these women during each of the three visits ranged between 100 and 650µL (*Figure 6.4*). CVF amounts tended to be higher in the mid-ovulatory and secretory phases than in the proliferative phase, however,

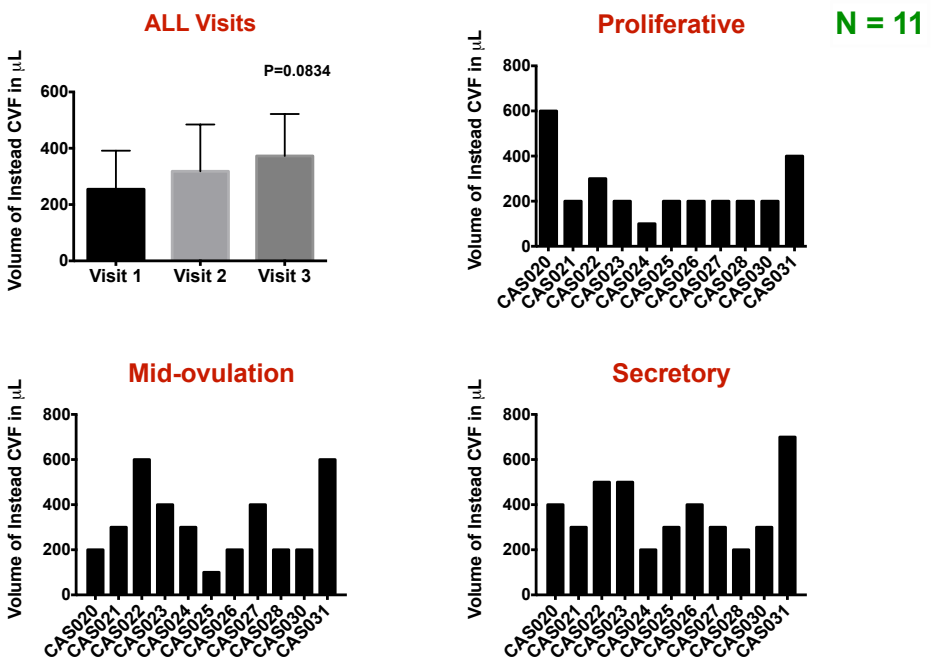

Figure 6.4 Bar curves showing the volume of CVF collected with the Instead softcup™ from the vagina cavity of 11 women during each of the three study visits corresponding to the proliferative, mid-ovulation and secretory phases of the menstrual cycle. The differences in the volume of CVF collected during the three menstrual phases did not reach statistical significance.

these differences did not reach statistical significance on ANOVA analyses (F1.47, 14.74)=6.96, MS=38485, p=0.0834. On inspection of CVF, three participants, CAS024, CAS027, and CAS028, had gross abnormalities in their CVF properties ranging from bloody, purulent, and thick mucoid clumps (*Table 6.1*). We proceeded to quantify 24 cytokines in CVF with the Luminex multiplex bead assay; IL-12, IL-15, and MCP-2 were not detectable in the CVF, regardless of the study visit (*Table 6.2*). The three participants with abnormal looking CVF: CAS024, CAS027, and CAS028 persistently had cytokine values that were out of range for various cytokines (*Figure 6.5*). They actually qualified as severe outliers. A severe outlier was defined as a value that was at least three times higher than the 75th centile of the interquartile range (*Table 6.3*). These three participants were hence subsequently analysed separately from the rest of the other 8 participants.

Table 6.1 Gross appearance of CVF was abnormal in three participants

Participant ID	Proliferative	Mid-ovulation	Secretory
CAS024	**bloody brown**		**mucoid thick clumps**
CAS027		**mucoid thick clumps**	
CAS028	**bloody mucoid**	**purulent**	

Chemokines and pro-inflammatory cytokines are dominant in the FGT throughout the different phases of the menstrual cycle: IL-8, IP-10, and IL-1α

Epithelial and stromal cells of the FGT, which secrete various cytokines, possess endocrine as well as immune and microbial receptors, and are hence hormonally regulated. To characterise baseline mucosal secretion patterns of infection

Table 6.2: Descriptive analysis of various cytokines in CVF over the three menstrual cycle phases: median and range

Analyte	Proliferative		Mid-ovulation		Secretory		
	No of binned values (% of out of range values)	Median (Range) in pg/mL	No of binned values (% of out of range values)	Median (Range) in pg/mL	No of binned values (% of out of range values)	Median (Range) in pg/mL	*TOTAL*
Pro-inflammatory Cytokines							
IL-1α	11 (0%)	489.3 (37.6 - 5443.0)	11 (0%)	249.4 (6.2 - 1379.0)	11 (0%)	434.3 (3.8 - 1176.0)	**33 (0%)**
IL-1β	11 (0%)	154.5 (11.6 - 1598.0)	11 (0%)	76.5 (2.9 - 1169.0)	10 (9%)	61.2 (3.5 - 1195.0)	**32 (3%)**
IL-6	9 (18%)	72.5 (14.4 - 493.2)	9 (18%)	41.9 (2.4 - 459.3)	9 (18%)	44.4 (13.2 - 314.2)	**27 (18%)**
***IL-12**	0 (100%)		0 (100%)		0 (100%)		**0 (100%)**
IL-16	7 (36%)	74.6 (6.7 - 17737.0)	5 (55%)	37.9 (36.6 - 158.1)	5 (55%)	37.9 (22.4 - 4545.0)	**17 (48%)**
***TNF-α**	1 (91%)	22.8 (22.8 - 22.8)	0 (100%)		0 (100%)		**1 (97%)**
Adaptive Cytokines							
IL-2	10 (9%)	64.7 (6.7 - 176.2)	11 (0%)	111.9 (55.4 - 187.3)	10 (9%)	84.8 (6.9 - 147.4)	**31 (6%)**
IL-4	5 (55%)	8.6 (1.4 - 85.0)	2 (82%)	16.6 (15.7 - 17.4)	1 (91%)	12.7 (12.7 - 12.7)	**8 (76%)**
***IL-15**	0 (100%)		0 (100%)		0 (100%)		**0 (100%)**
IFN-γ	11 (0%)	117 (12.5 - 127.6)	11 (0%)	116.5 (112.5 - 126.4)	11 (0%)	116.5 (114.4 - 127.6)	**33 (0%)**
Chemokines							
IL-8	11 (0%)	566.4 (138.6 - 7616.0)	11 (0%)	614.5 (22.3 - 7766.0)	11 (0%)	612.8 (12.4 - 12989)	**33 (0%)**
IP-10	11 (0%)	314.8 (74.1 - 2274.0)	10 (9%)	225.9 (21.6 - 838.7)	10 (9%)	318.1 (16.4 - 748.5)	**31 (6%)**
MCP-1	11 (0%)	7.4 (0.6 - 49.7)	8 (27%)	3.7 (0.6 - 68.7)	7 (36%)	1.3 (0.3 - 174.7)	**26 (21%)**
***MCP-2**	0 (100%)		0 (100%)		0 (100%)		**0 (100%)**
MIG	2 (82%)	409.7 (243.1 - 576.3)	2 (82%)	471 (215.7 - 726.3)	1 (91%)	368 (368.0 - 368.0)	**5 (85%)**
MIP-3α	7 (36%)	326.8 (24.5 - 834.7)	6 (45%)	456.6 (9.5 - 714.7)	6 (45%)	257.9 (57.7 - 785.3)	**19 (42%)**
MIP-1β	4 (64%)	206.3 (31.4 - 56.8)	2 (82%)	97.9 (45.8 - 149.9)	2 (82%)	131.8 (22.2 - 241.4)	**8 (76%)**
RANTES	7 (36%)	4.7 (1.3 - 56.8)	5 (55%)	2.8 (0.5 - 37.8)	5 (55%)	4.2 (1.4 - 16.9)	**17 (48%)**
SDF-1	7 (36%)	8.1 (1.5 - 383.6)	7 (36%)	8.6 (1.7 - 43.2)	7 (36%)	7.6 (1.3 - 192.9)	**21 (36%)**
Haematopoietics							
IL-7	8 (27%)	16.6 (2.4 - 25.5)	8 (27%)	16.5 (3.0 - 19.2)	9 (18%)	16.0 (0.6 - 23.7)	**25 (24%)**
G-CSF	11 (0%)	162.4 (24.5 - 416.4)	10 (9%)	136.6 (4.3 - 2322.0)	10 (9%)	136.2 (2.2 - 3875.0)	**31 (6%)**
GM-CSF	11 (0%)	7.0 (1.4 - 21.6)	11 (0%)	6.6 (1.6 - 19.9)	11 (0%)	7.1 (1.1 - 20.0)	**33 (0%)**
Growth Factor							
TGF-β	11 (0%)	117.9 (18.6 - 3529.0)	11 (0%)	24.8 (13.7 - 1538.0)	11 (0%)	21.3 (13.5 - 896.5)	**33 (0%)**
Antimicrobial Peptide							
IFN-β	7 (36%)	17.48 (2.8 - 29.2)	7 (36%)	17.8 (15.6 - 21.9)	7 (36%)	17.3 (2.5 - 22.1)	**21 (36%)**
Total	**173 (35%)**		**158 (40%)**		**154 (42%)**		**485 (39%)**

Red bars represent analytes that were not detectable in CVF on Luminex in this analysis

Table 6.3 Cytokine values that were defined as outliers in pg/mL

Cytokines	Proliferative				Mid-ovulation				Secretory			
	Interquartile Range	Mild Outlier 1.5*IQR	Severe Outlier 3*IQR	75th Centile	Interquartile Range	Mild Outlier 1.5*IQR	Severe Outlier 3*IQR	75th Centile	Interquartile Range	Mild Outlier 1.5*IQR	Severe Outlier 3*IQR	75th Centile
Proinflammatory Cytokines												
IL-1α	687.08	1030.62	2061.24	5443.0	594.3	891.45	1782.9	1379.0	610.4	915.6	1831.2	1176.0
IL-1β	142.7	214.05	428.1	1598.0	146.8	220.2	440.4	1169.0	426.82	640.23	1280.46	1195.0
IL-6	243.19	364.785	729.57	493.2	155.35	233.025	466.05	459.3	94.3	141.45	282.9	314.2
IL-12												
IL-16	528.738	793.107	1586.214	17737.0	63.05	94.575	189.15	158.1	2267.5	3401.25	6802.5	4545.0
TNF-α				22.8								
Adaptive Cytokines												
IL-2	75.11	112.665	225.33	176.2	60.7	91.05	182.1	187.3	98.32	147.48	294.96	147.4
IL-4	65.038	97.557	195.114	85.0	1.7	2.55	5.1	17.4				12.7
IL-15												
IFN-α	8.1	12.15	24.3	127.6	7.9	11.85	23.7	126.4	6.5	9.75	19.5	127.6
Chemokines												
IL-8	1922.9	2884.35	5768.7	7616.0	2797.1	4195.65	8391.3	7766.0	5765.2	8647.8	17295.6	12989.0
IP-10	339.9	509.85	1019.7	2274.0	319.8	479.7	959.4	838.7	313.5	470.25	940.5	748.5
MCP-1	35.277	52.9155	105.831	49.7	50.05	75.075	150.15	68.7	46.3	69.45	138.9	174.7
MCP-2												
MIG	333.2	499.8	999.6	576.3	510.6	765.9	1531.8	726.3				368.0
MIP-3α	582.17	873.255	1746.51	834.7	585.4	878.1	1756.2	714.7	486.7	730.05	1460.1	785.3
MIP-1β	307.29	460.935	921.87	347.3	104.1	156.15	312.3	149.9	219.2	328.8	657.6	241.4
RANTES	40.053	60.0795	120.159	56.8	19.5	29.25	58.5	37.8	10.9	16.35	32.7	16.9
SDF-1	312.005	468.0075	936.015	383.6	8.8	13.2	26.4	43.2	15.6	23.4	46.8	192.9
Haematopoietics												
IL-7	6.48	9.72	19.44	25.5	3.65	5.475	10.95	19.2	8.8	13.2	26.4	23.7
G-CSF	195.42	293.13	586.26	416.4	280.85	421.275	842.55	2322.0	724.05	1086.075	2172.15	3875.0
GM-CSF	9.132	13.698	27.396	21.6	6.4	9.6	19.2	19.9	6.1	9.15	18.3	20.0
Growth Factor												
TGF-β	140.03	210.045	420.09	3529.0	164.3	246.45	492.9	1538.0	125.8	188.7	377.4	896.5
Antimicrobial Peptide												
IFN-β	6.58	9.87	19.74	29.2	3.8	5.7	11.4	21.9	2.3	3.45	6.9	22.1

Blue text represents analyte values that were defined as severe outliers. A severe outlier was defined as a value that was at least three times higher than the 75th centile of the interquartile range.

	IL-1α	Mild Outlier 1.5*IQR	Severe Outlier 3*IQR
20	763.9	1030.6	2061.2
21	626.3	1030.6	2061.2
22	499.5	1030.6	2061.2
23	76.8	1030.6	2061.2
24	287.3	1030.6	2061.2
25	54.4	1030.6	2061.2
26	372.2	1030.6	2061.2
27	927.1	1030.6	2061.2
28	5443.4	1030.6	2061.2
30	489.3	1030.6	2061.2
31	37.6	1030.6	2061.2

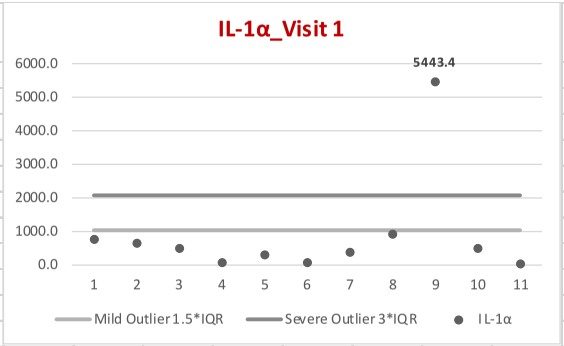

	IL-1β	Mild Outlier 1.5*IQR	Severe Outlier 3*IQR
20	58.3	214.1	428.1
21	164.7	214.1	428.1
22	154.5	214.1	428.1
23	121.8	214.1	428.1
24	216.2	214.1	428.1
25	11.6	214.1	428.1
26	127.1	214.1	428.1
27	1597.7	214.1	428.1
28	141.5	214.1	428.1
30	264.5	214.1	428.1
31	292.3	214.1	428.1

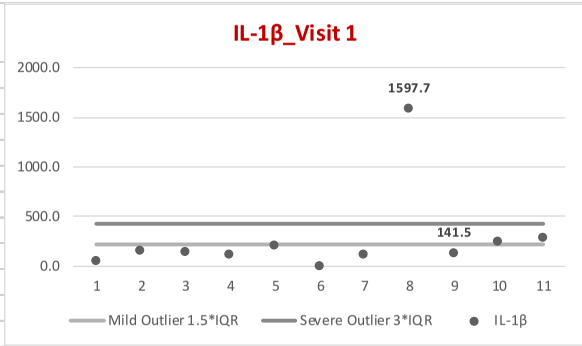

	IL-1α	Mild Outlier 1.5*IQR	Severe Outlier 3*IQR
20	6.2	891.5	1782.9
21	249.4	891.5	1782.9
22	142.0	891.5	1782.9
23	214.9	891.5	1782.9
24	469.9	891.5	1782.9
25	1378.7	891.5	1782.9
26	83.2	891.5	1782.9
27	729.8	891.5	1782.9
28	1186.6	891.5	1782.9
30	385.9	891.5	1782.9
31	135.5	891.5	1782.9

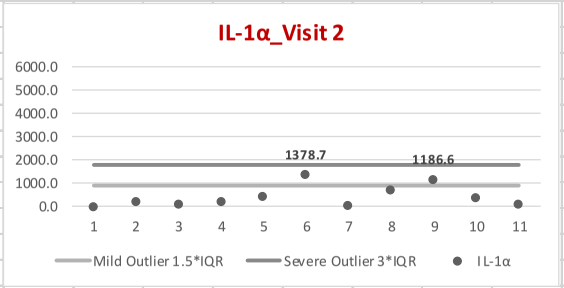

	IL-1β	Mild Outlier 1.5*IQR	Severe Outlier 3*IQR
20	5.8	220.2	440.4
21	64.6	220.2	440.4
22	8.8	220.2	440.4
23	127.3	220.2	440.4
24	152.6	220.2	440.4
25	83.6	220.2	440.4
26	2.9	220.2	440.4
27	791.9	220.2	440.4
28	1168.9	220.2	440.4
30	76.5	220.2	440.4
31	3.5	220.2	440.4

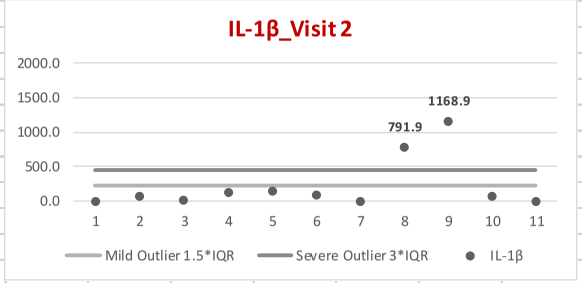

	IL-1α	Mild Outlier 1.5*IQR	Severe Outlier 3*IQR
20	1175.5	915.6	1831.2
21	185.4	915.6	1831.2
22	3.8	915.6	1831.2
23	311.8	915.6	1831.2
24	434.3	915.6	1831.2
25	642.1	915.6	1831.2
26	48.4	915.6	1831.2
27	795.8	915.6	1831.2
28	646.8	915.6	1831.2
30	882.2	915.6	1831.2
31	293.8	915.6	1831.2

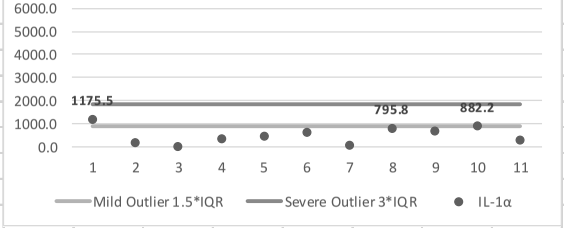

	IL-1β	Mild Outlier 1.5*IQR	Severe Outlier 3*IQR
20	3.5	640.2	1280.5
21	31.6	640.2	1280.5
22	5.9	640.2	1280.5
23	54.6	640.2	1280.5
24	353.8	640.2	1280.5
25	116.9	640.2	1280.5
26		640.2	1280.5
27	746.4	640.2	1280.5
28	1194.6	640.2	1280.5
30	51.8	640.2	1280.5
31	67.7	640.2	1280.5

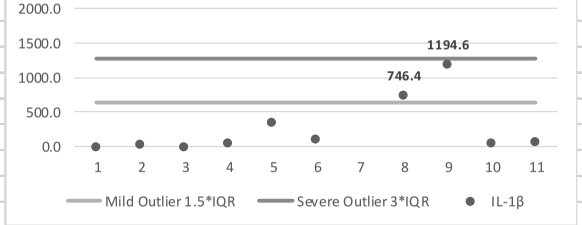

	IL-6	Mild Outlier 1.5*IQR	Severe Outlier 3*IQR
20		364.8	729.6
21		364.8	729.6
22	72.5	364.8	729.6
23	158.6	364.8	729.6
24	419.2	364.8	729.6
25	52.8	364.8	729.6
26	14.4	364.8	729.6
27	163.6	364.8	729.6
28	493.2	364.8	729.6
30	43.6	364.8	729.6
31	57.2	364.8	729.6

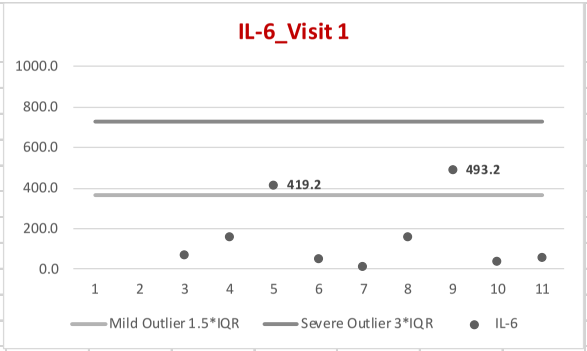

	IL-16	Mild Outlier 1.5*IQR	Severe Outlier 3*IQR
20	45.9	793.1	1586.2
21	6.7	793.1	1586.2
22	74.6	793.1	1586.2
23	6.7	793.1	1586.2
24	17736.9	793.1	1586.2
25		793.1	1586.2
26		793.1	1586.2
27	144.2	793.1	1586.2
28	535.4	793.1	1586.2
30		793.1	1586.2
31		793.1	1586.2

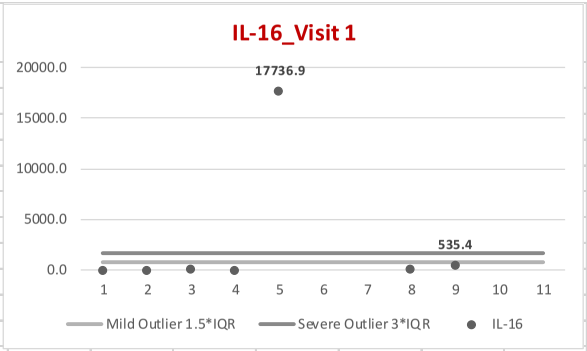

	IL-6	Mild Outlier 1.5*IQR	Severe Outlier 3*IQR
20		233.0	466.1
21	59.9	233.0	466.1
22		233.0	466.1
23	132.7	233.0	466.1
24	41.9	233.0	466.1
25	33.8	233.0	466.1
26	16.2	233.0	466.1
27	459.3	233.0	466.1
28	211.7	233.0	466.1
30	17.5	233.0	466.1
31	2.4	233.0	466.1

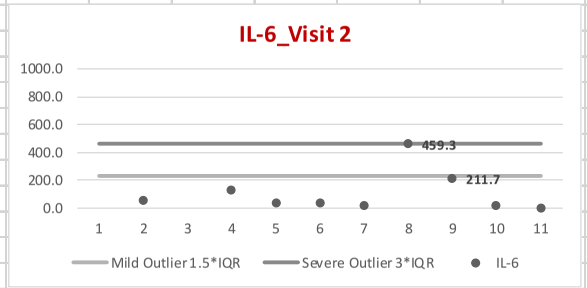

	IL-16	Mild Outlier 1.5*IQR	Severe Outlier 3*IQR
20	37.9	94.6	189.2
21	42.4	94.6	189.2
22	37.9	94.6	189.2
23	36.6	94.6	189.2
24		94.6	189.2
25		94.6	189.2
26		94.6	189.2
27		94.6	189.2
28	158.1	94.6	189.2
30		94.6	189.2
31		94.6	189.2

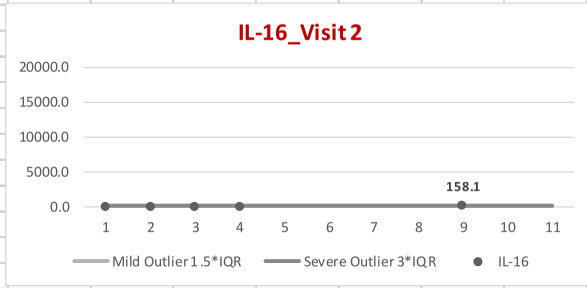

	IL-6	Mild Outlier 1.5*IQR	Severe Outlier 3*IQR
20		141.5	282.9
21	44.4	141.5	282.9
22		141.5	282.9
23	71.6	141.5	282.9
24	158.1	141.5	282.9
25	29.4	141.5	282.9
26	13.2	141.5	282.9
27	45.5	141.5	282.9
28	314.2	141.5	282.9
30	19.6	141.5	282.9
31	21.6	141.5	282.9

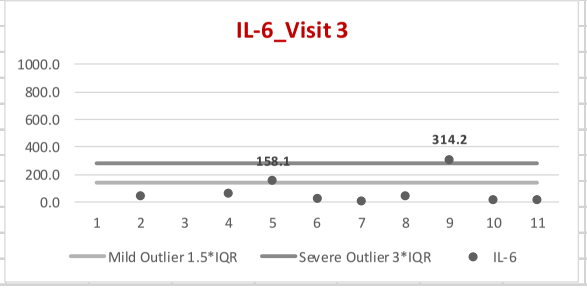

	IL-16	Mild Outlier 1.5*IQR	Severe Outlier 3*IQR
20	36.6	3401.3	6802.5
21	37.9	3401.3	6802.5
22	49.3	3401.3	6802.5
23	22.4	3401.3	6802.5
24		3401.3	6802.5
25		3401.3	6802.5
26		3401.3	6802.5
27		3401.3	6802.5
28	4544.7	3401.3	6802.5
30		3401.3	6802.5
31		3401.3	6802.5

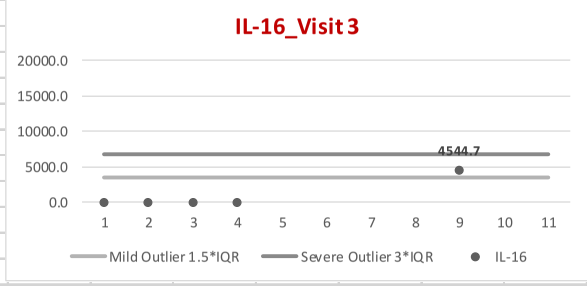

	IL-8	Mild Outlier 1.5*IQR	Severe Outlier 3*IQR
20	13770.4	54733.77	109467.54
21	5855.36	54733.77	109467.54
22	7055.92	54733.77	109467.54
23	23030.08	54733.77	109467.54
24	104129.04	54733.77	109467.54
25	49895.92	54733.77	109467.54
26	13702.72	54733.77	109467.54
27	#VALUE!	54733.77	109467.54
28	#VALUE!	54733.77	109467.54
30	#VALUE!	54733.77	109467.54
31	31139.36	54733.77	109467.54

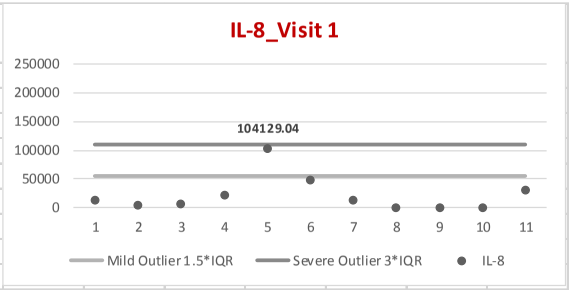

	IL-8	Mild Outlier 1.5*IQR	Severe Outlier 3*IQR
20	8846.72	107623.08	215246.16
21	70773.68	107623.08	215246.16
22	5251.04	107623.08	215246.16
23	86821.6	107623.08	215246.16
24	128629.04	107623.08	215246.16
25	22837.6	107623.08	215246.16
26	3645.36	107623.08	215246.16
27	#VALUE!	107623.08	215246.16
28	#VALUE!	107623.08	215246.16
30	20894.48	107623.08	215246.16
31	40804.64	107623.08	215246.16

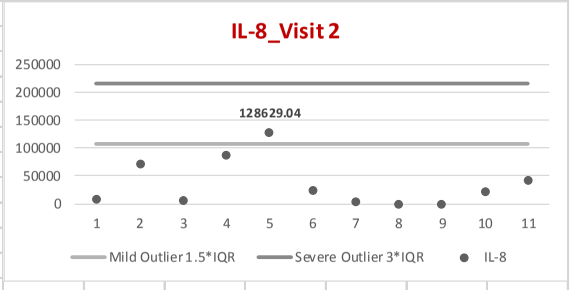

	IL-8	Mild Outlier 1.5*IQR	Severe Outlier 3*IQR
20	23223.2	67897.8	135795.6
21	61599.04	67897.8	135795.6
22	5310.96	67897.8	135795.6
23	49952.32	67897.8	135795.6
24	120847.6	67897.8	135795.6
25	15710.08	67897.8	135795.6
26	2892.48	67897.8	135795.6
27	#VALUE!	67897.8	135795.6
28	#VALUE!	67897.8	135795.6
30	24194.72	67897.8	135795.6
31	32002.24	67897.8	135795.6

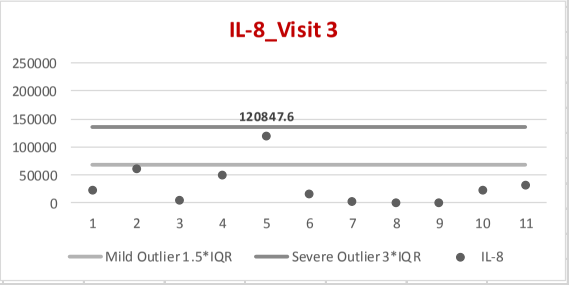

	IP-10	Mild Outlier 1.5*IQR	Severe Outlier 3*IQR
20	1863.43	5819.58	11639.16
21	1647.7	5819.58	11639.16
22	5743.15	5819.58	11639.16
23	1918.96	5819.58	11639.16
24	18524.4	5819.58	11639.16
25	3709.04	5819.58	11639.16
26	1159.44	5819.58	11639.16
27	6040.63	5819.58	11639.16
28	4488.57	5819.58	11639.16
30	2242.4	5819.58	11639.16
31	2421.32	5819.58	11639.16

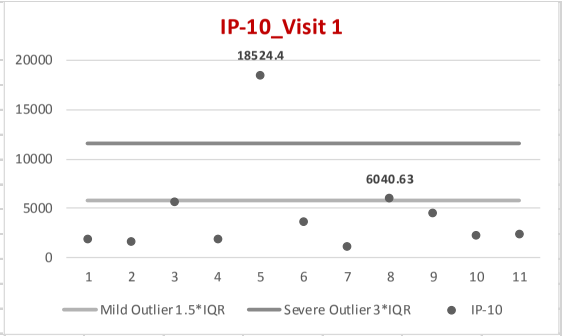

	IP-10	Mild Outlier 1.5*IQR	Severe Outlier 3*IQR
20	1559.18	6295.065	12590.13
21	1262.01	6295.065	12590.13
22	2593.36	6295.065	12590.13
23	1009.24	6295.065	12590.13
24	1688.16	6295.065	12590.13
25	5458.72	6295.065	12590.13
26	1465.92	6295.065	12590.13
27	5711.88	6295.065	12590.13
28	6672.05	6295.065	12590.13
30	1530.18	6295.065	12590.13
31	369.91	6295.065	12590.13

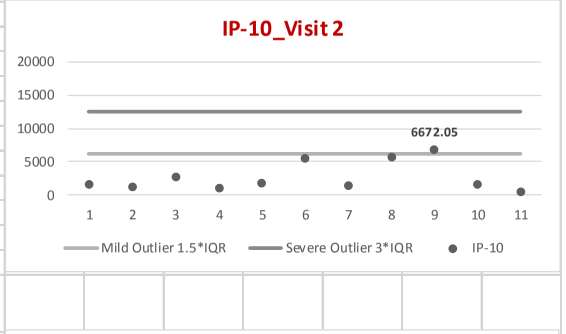

	IP-10	Mild Outlier 1.5*IQR	Severe Outlier 3*IQR
20	3179.05	3067.23	6134.46
21	1344.18	3067.23	6134.46
22	1810.47	3067.23	6134.46
23	408.86	3067.23	6134.46
24	2030.56	3067.23	6134.46
25	1785.28	3067.23	6134.46
26	1027.6	3067.23	6134.46
27	5175.16	3067.23	6134.46
28	5896.26	3067.23	6134.46
30	2881.03	3067.23	6134.46
31	1134.23	3067.23	6134.46

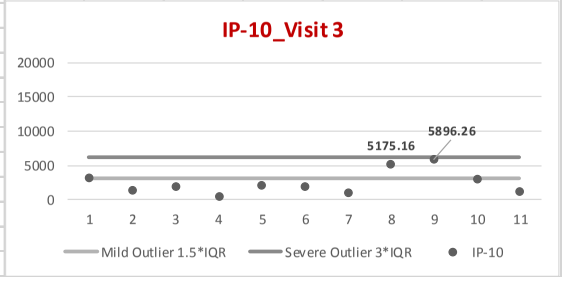

	MIG	Mild Outlier 1.5*IQR	Severe Outlier 3*IQR
20	348.9	1964.28	3928.56
21	312.7	1964.28	3928.56
22	1658.42	1964.28	3928.56
23	383.93	1964.28	3928.56
24	978.32	1964.28	3928.56
25	507.36	1964.28	3928.56
26	468.32	1964.28	3928.56
27	3308.3	1964.28	3928.56
28	2046.62	1964.28	3928.56
30	297.34	1964.28	3928.56
31	414.29	1964.28	3928.56

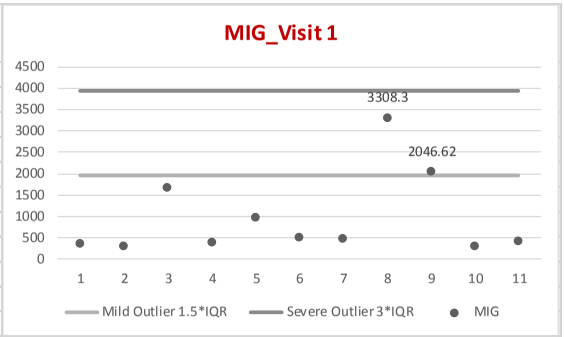

	MIG	Mild Outlier 1.5*IQR	Severe Outlier 3*IQR
20	243.78	1463.295	2926.59
21	194.14	1463.295	2926.59
22	297.85	1463.295	2926.59
23	235.75	1463.295	2926.59
24	297.36	1463.295	2926.59
25	1211.28	1463.295	2926.59
26	468.32	1463.295	2926.59
27	3054.84	1463.295	2926.59
28	1984.19	1463.295	2926.59
30	289.5	1463.295	2926.59
31	149.56	1463.295	2926.59

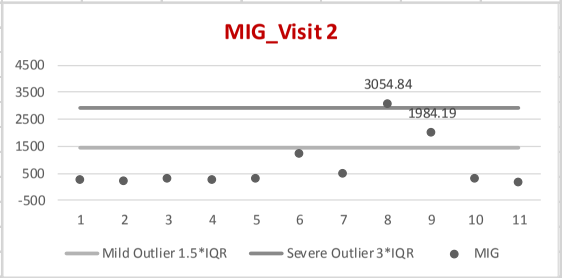

	MIG	Mild Outlier 1.5*IQR	Severe Outlier 3*IQR
20	431.31	613.62	1227.24
21	185.48	613.62	1227.24
22	348.9	613.62	1227.24
23	167.75	613.62	1227.24
24	327.92	613.62	1227.24
25	594.56	613.62	1227.24
26	128.96	613.62	1227.24
27	1593.31	613.62	1227.24
28	2419.38	613.62	1227.24
30	320.41	613.62	1227.24
31	232.22	613.62	1227.24

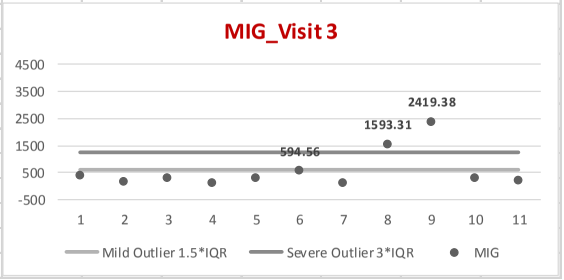

	MIP-1β	Mild Outlier 1.5*IQR	Severe Outlier 3*IQR
20	29.81	697.905	1395.81
21	262.62	697.905	1395.81
22	31.94	697.905	1395.81
23	28.03	697.905	1395.81
24	2808.32	697.905	1395.81
25	91.84	697.905	1395.81
26	23.04	697.905	1395.81
27	493.3	697.905	1395.81
28	2809.72	697.905	1395.81
30	25.2	697.905	1395.81
31	86.44	697.905	1395.81

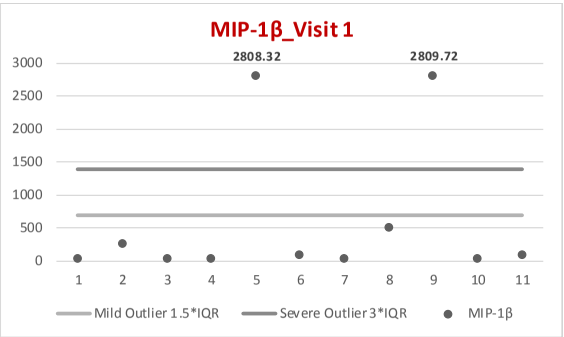

	MIP-1β	Mild Outlier 1.5*IQR	Severe Outlier 3*IQR
20	22.5	140.175	280.35
21	25.2	140.175	280.35
22	22.28	140.175	280.35
23	27.93	140.175	280.35
24	115.84	140.175	280.35
25	30.48	140.175	280.35
26	20.64	140.175	280.35
27	262.01	140.175	280.35
28	1144.02	140.175	280.35
30	22.39	140.175	280.35
31	49.23	140.175	280.35

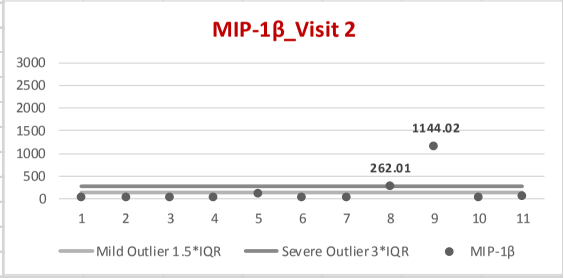

	MIP-1β	Mild Outlier 1.5*IQR	Severe Outlier 3*IQR
20	34.24	18.825	37.65
21	27.53	18.825	37.65
22	22.71	18.825	37.65
23	27.63	18.825	37.65
24	36.72	18.825	37.65
25	27.76	18.825	37.65
26	19.36	18.825	37.65
27	217.66	18.825	37.65
28	1903.55	18.825	37.65
30	24.17	18.825	37.65
31	34.03	18.825	37.65

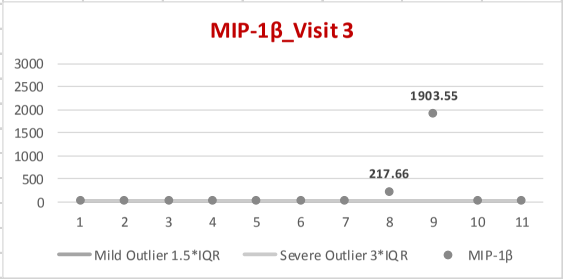

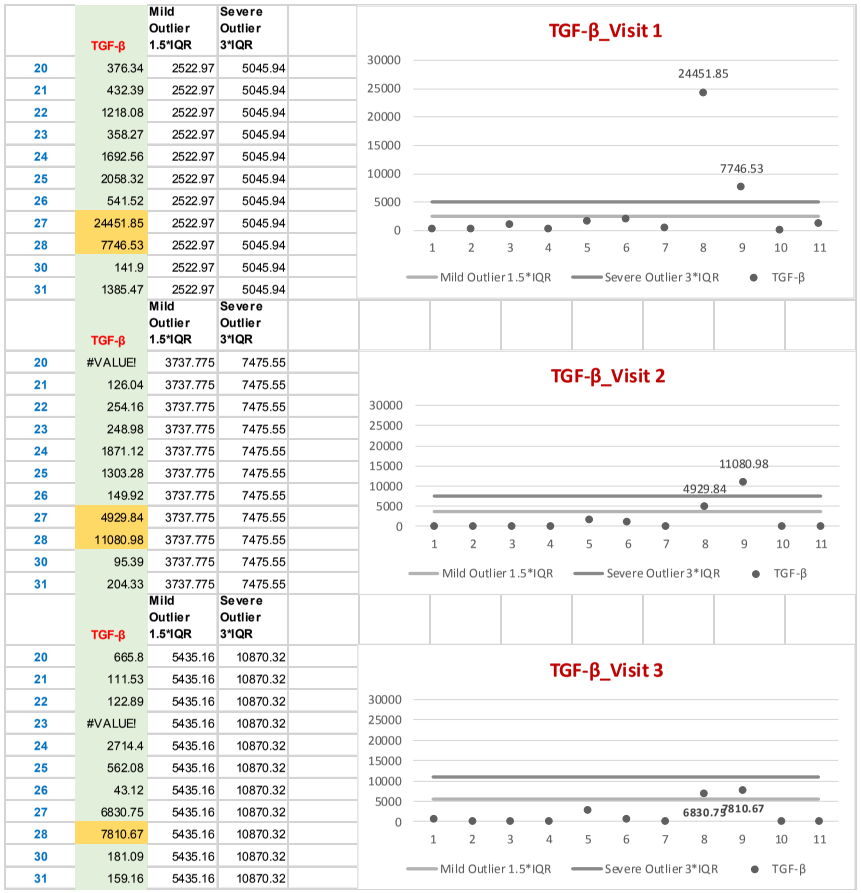

	TGF-β	Mild Outlier 1.5*IQR	Severe Outlier 3*IQR
20	376.34	2522.97	5045.94
21	432.39	2522.97	5045.94
22	1218.08	2522.97	5045.94
23	358.27	2522.97	5045.94
24	1692.56	2522.97	5045.94
25	2058.32	2522.97	5045.94
26	541.52	2522.97	5045.94
27	24451.85	2522.97	5045.94
28	7746.53	2522.97	5045.94
30	141.9	2522.97	5045.94
31	1385.47	2522.97	5045.94

	TGF-β	Mild Outlier 1.5*IQR	Severe Outlier 3*IQR
20	#VALUE!	3737.775	7475.55
21	126.04	3737.775	7475.55
22	254.16	3737.775	7475.55
23	248.98	3737.775	7475.55
24	1871.12	3737.775	7475.55
25	1303.28	3737.775	7475.55
26	149.92	3737.775	7475.55
27	4929.84	3737.775	7475.55
28	11080.98	3737.775	7475.55
30	95.39	3737.775	7475.55
31	204.33	3737.775	7475.55

	TGF-β	Mild Outlier 1.5*IQR	Severe Outlier 3*IQR
20	665.8	5435.16	10870.32
21	111.53	5435.16	10870.32
22	122.89	5435.16	10870.32
23	#VALUE!	5435.16	10870.32
24	2714.4	5435.16	10870.32
25	562.08	5435.16	10870.32
26	43.12	5435.16	10870.32
27	6830.75	5435.16	10870.32
28	7810.67	5435.16	10870.32
30	181.09	5435.16	10870.32
31	159.16	5435.16	10870.32

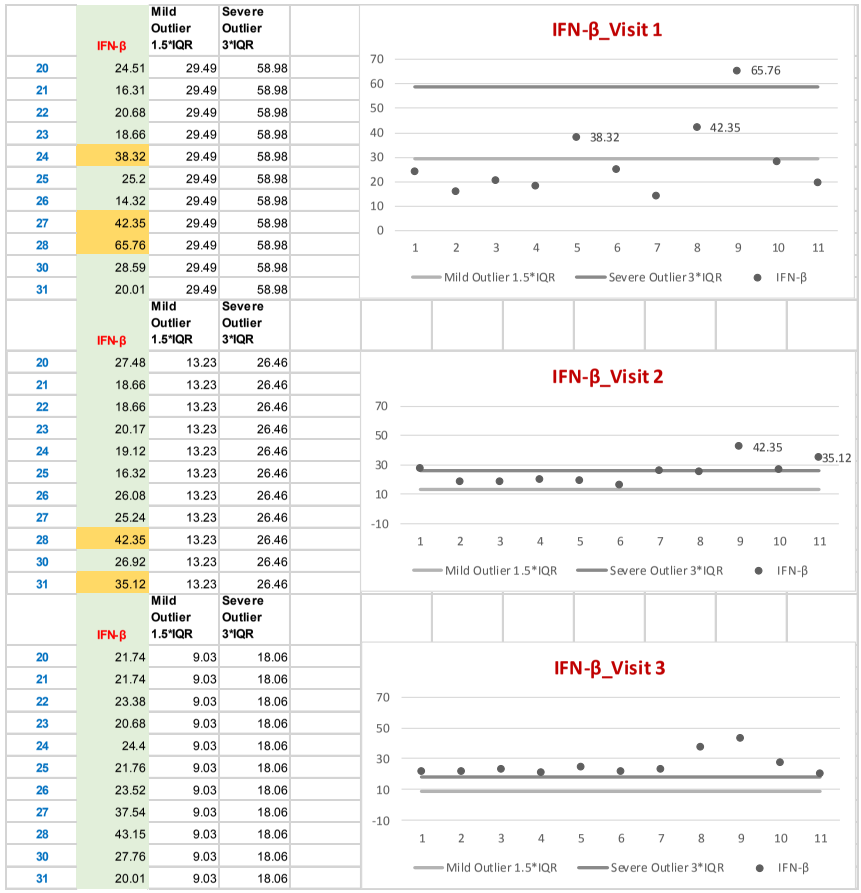

	IFN-β	Mild Outlier 1.5*IQR	Severe Outlier 3*IQR
20	24.51	29.49	58.98
21	16.31	29.49	58.98
22	20.68	29.49	58.98
23	18.66	29.49	58.98
24	38.32	29.49	58.98
25	25.2	29.49	58.98
26	14.32	29.49	58.98
27	42.35	29.49	58.98
28	65.76	29.49	58.98
30	28.59	29.49	58.98
31	20.01	29.49	58.98

	IFN-β	Mild Outlier 1.5*IQR	Severe Outlier 3*IQR
20	27.48	13.23	26.46
21	18.66	13.23	26.46
22	18.66	13.23	26.46
23	20.17	13.23	26.46
24	19.12	13.23	26.46
25	16.32	13.23	26.46
26	26.08	13.23	26.46
27	25.24	13.23	26.46
28	42.35	13.23	26.46
30	26.92	13.23	26.46
31	35.12	13.23	26.46

	IFN-β	Mild Outlier 1.5*IQR	Severe Outlier 3*IQR
20	21.74	9.03	18.06
21	21.74	9.03	18.06
22	23.38	9.03	18.06
23	20.68	9.03	18.06
24	24.4	9.03	18.06
25	21.76	9.03	18.06
26	23.52	9.03	18.06
27	37.54	9.03	18.06
28	43.15	9.03	18.06
30	27.76	9.03	18.06
31	20.01	9.03	18.06

Figure 6.5 Outlier curves for various analyte values in pg/mL. Three participants had persistent outlier values in CVF: CAS024, CAS027, and CAS028. Texts in blue denote participant identifier numbers. Yellow highlighted boxes denote outlier values.

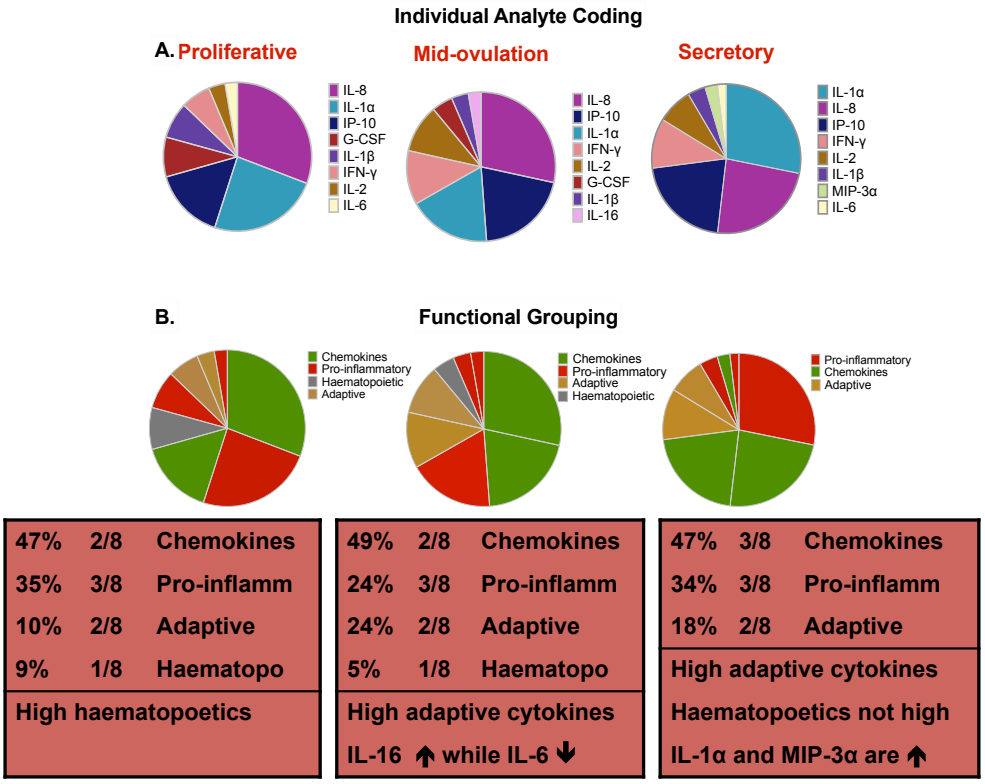

Figure 6.6 Pie curves of the profile of highest eight cytokines per visit colour coded according to (A.) individual analyte, and (B.) functional grouping across the three study visits corresponding menstrual cycle phases, (n=8). The cytokine with highest concentration is at 12 o'clock moving clockwise. Analyte levels, expressed in pg/mL, were quantified on Luminex. IL-8, IP-10, and IL-1α were consistently high (A.). Frequency and median concentrations of chemoattractant and pro-inflammatory cytokines remained the highest throughout the menstrual cycle in this cohort (B.). Haematopoietics tended to be high in the proliferative phase whereas adaptive cytokines were highest in the mid-ovulatory and secretory phase. MIP-3α only appeared in the top 8 analytes in the secretory phase.

modulating soluble proteins and describe how they are influenced by fluctuations in the endogenous hormone levels during single menstrual cycle, we measured 24 different cytokines in the CVF of women collected over the three menstrual cycle phases. With Luminex, we quantified cytokines with chemokine, pro-inflammatory, adaptive, haematopoietic, antimicrobial peptide and growth functions. Looking at only the highest eight cytokines in CVF at each visit, IL-8, IP-10, IL-1α, and IFN-γ, occurred in highest concentrations throughout the three visits with median levels exceeding 100pg/mL for each of these cytokines (*Figure 6.6A.*). Otherwise the

levels of IL-1β, IL-6, IL-16, IL-2, IL-4, MIP-3α, MIP-1β, G-CSF, TGF-β, and IFN-β were also differentially high with levels ranging between 10 and 100pg/mL at baseline over the three visits. Of note, however, was that the profiles of the top eight cytokines were similar between the three visits; they did not vary drastically during the three menstrual phases. Looking at the functional categories, chemokine and pro-inflammatory cytokines were persistently high throughout the menstrual cycle (*Figure 6.6B.*) while haematopoietics were higher in the proliferative than in the mid-ovulatory and secretory phase. Adaptive cytokines, on the other hand increased gradually from the proliferative through to the mid-ovulatory and secretory phases. These findings that chemokines and pro-inflammatory cytokines occur in the highest concentrations in the FGT point to the fact that the FGT is a dynamic environment characterised by constant changes in leucocyte populations in order to meet the changing demands placed on the FGT.

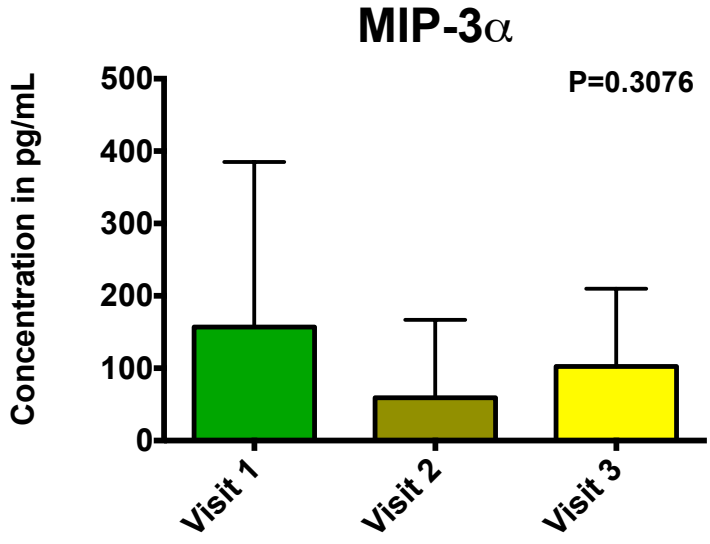

Figure 6.7 Constitutive levels of MIP 3α in CVF collected longitudinally at three time points in a single menstrual cycle, n=8: Visit 1 = proliferative phase, Visit 2 = mid-ovulatory phase, and Visit 3 = secretory phase. MIP 3α levels, expressed in pg/mL, were quantified on Luminex. One-way ANOVA analysis was conducted to compare mean concentrations across visits. Variations in MIP-3α over the three visits did not reach statistical significance. P-values were taken as non-significant if $p>0.05$, and significant if $p \leq 0.05$ (*), $p \leq 0.01$ (**), $p \leq 0.001$ (***), and $p \leq 0.0001$ (****).

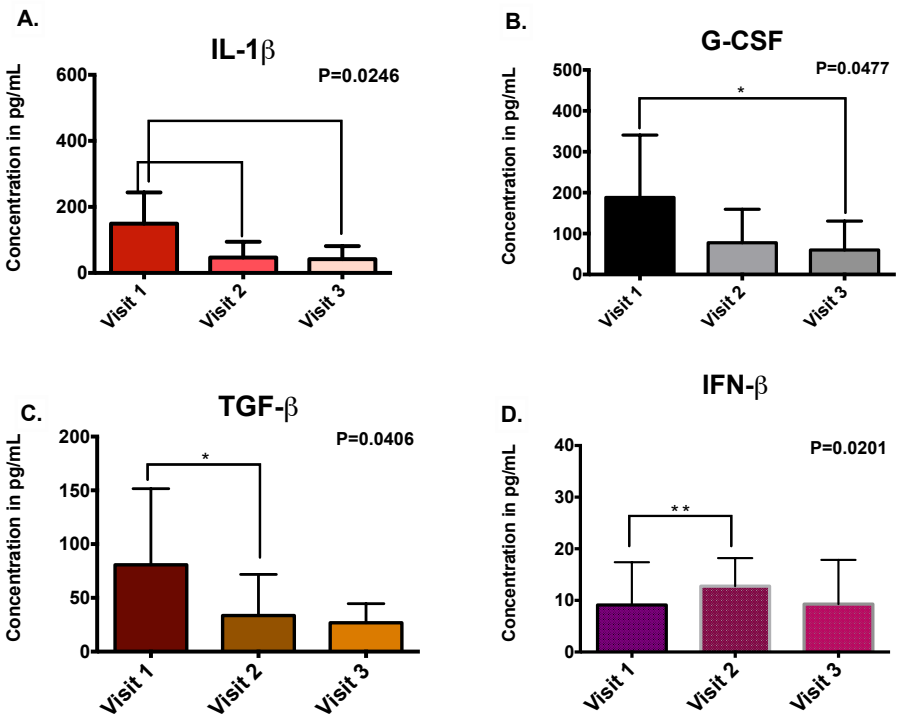

.

Figure 6.8 Constitutive levels of IL-1β, G-CSF, TGF-β and IFN-β in CVF collected longitudinally at three time points in a single menstrual cycle, n=8: Visit 1 = proliferative phase, Visit 2 = mid-ovulatory phase, and Visit 3 = secretory phase. Analyte levels, expressed in pg/mL, were quantified on Luminex. One-way ANOVA analysis was conducted to compare mean concentrations across visits. Variations in mean levels of IL-1β, G-CSF, TGF-β and IFN-β reached statistical significance with a trend towards proliferative levels being highest for the first three analytes while being highest at mid-ovulation for IFN-β. P-values were taken as non-significant if $p>0.05$, and significant if $p \leq 0.05$ (*), $p \leq 0.01$ (**), $p \leq 0.001$ (***), and $p \leq 0.0001$ (****).

Hormonal fluctuations during the menstrual cycle phases do not cause significant fluctuations in MIP-3α levels in CVF, however, they do cause significant fluctuations in the CVF levels of other soluble proteins in women at low risk for HIV infection.

With recent evidence suggesting a significant role of MIP-3α in the early SIV infection events and with the reported heightened vulnerability to HIV and SIV in the secretory phase, we hypothesised that MIP-3α levels will be highest in the secretory phase of the menstrual cycle. We evaluated levels of MIP-3α in CVF collected longitudinally at three time points from each woman over a single

Table 6.4: ANOVA table for individual cytokines that were detectable in CVF on Luminex analysis

Cytokines	ANOVA table	Sum of Squares	DF	Mean Square	F	P value
IL-1α	Treatment (between columns	57932	2	28966	0.1995	0.7899
	Individual (between rows)	1100299	7	157186		
	Total	3190534	23			
IL-1β	Treatment (between columns	58976	2	29488	6.958	*0.0246
	Individual (between rows)	29957	7	4280		
	Total	148268	23			
IL-6	Treatment (between columns	2709	2	1355	2.311	0.1502
	Individual (between rows)	26659	7	3808		
	Total	37575	23			
IL-16	Treatment (between columns	409.3	2	204.7	1.43	0.2715
	Individual (between rows)	5600	7	800		
	Total	8012	23			
IL-2	Treatment (between columns	4399	2	2200	1.241	0.3177
	Individual (between rows)	23126	7	3304		
	Total	52347	23			
IFN-γ	Treatment (between columns	9.171	2	4.585	0.4224	0.5564
	Individual (between rows)	153.1	7	21.87		
	Total	314.2	23			
IL-8	Treatment (between columns	3953167	2	1976583	0.5831	0.4997
	Individual (between rows)	17483605	7	2497658		
	Total	68896963	23			
IP-10	Treatment (between columns	13823	2	6912	0.3319	0.7222
	Individual (between rows)	331585	7	47369		
	Total	636996	23			
MCP-1	Treatment (between columns	320.9	2	160.5	1.852	0.2088
	Individual (between rows)	462.4	7	66.06		
	Total	1996	23			
MIP-3α	Treatment (between columns	38354	2	19177	1.249	0.3076
	Individual (between rows)	310952	7	44422		
	Total	564327	23			
RANTES	Treatment (between columns	2.309	2	1.154	0.7766	0.4761
	Individual (between rows)	12.19	7	1.741		
	Total	35.31	23			
SDF-1	Treatment (between columns	4.924	2	2.462	0.4261	0.5367
	Individual (between rows)	290	7	41.43		
	Total	375.8	23			
IL-7	Treatment (between columns	1.62	2	0.8101	0.5514	0.5517
	Individual (between rows)	1372	7	196		
	Total	1394	23			
G-CSF	Treatment (between columns	77459	2	38730	4.543	*0.0477
	Individual (between rows)	125683	7	17955		
	Total	322484	23			
GM-CSF	Treatment (between columns	20.34	2	10.17	0.2233	0.6517
	Individual (between rows)	316.2	7	45.17		
	Total	974.3	23			
TGF-β	Treatment (between columns	13831	2	6916	5.483	*0.0406
	Individual (between rows)	29894	7	4271		
	Total	61382	23			
IFN-β	Treatment (between columns	67.82	2	33.91	8.354	*0.0201
	Individual (between rows)	1144	7	163.4		
	Total	1268	23			

Asterisk represents statistical significance as defined by p-values<0.05

menstrual cycle. Mean baseline MIP-3α levels somewhat fluctuated over the menstrual cycle, but variations did not reach statistical significance on one-way ANOVA analysis (F(1.23, 8.62)=1.25, MS=19177, p=0.3076) *(Figure 6.7, Table 6.4, Table 6.5).* Alongside MIP-3α, we measured 23 other cytokines over the three menstrual cycle phases. Levels of most of these cytokines did not vary significantly over the different phases of the menstrual cycle except for constitutive levels of IL-1β (F(1.21, 8.49)=6.96, MS=29488, p=0.0246), G-CSF (F(1.46, 10.21)=4.54, MS=38730, p=0.0477), TGF-β (F(1.29, 8.54)=5.48, MS=6916, p=0.0406) and IFN-β (F(1.09, 7.59)=8.35, MS=33.91, p=0.0201), which varied significantly over the three menstrual cycle phases (*Figure 6.8, Table 6.4, Table 6.5*). Mean cytokine baseline levels for IL-1β, G-CSF, and TGF-β were significantly higher in the proliferative phase than in the mid-ovulatory and secretory phases while baseline levels for IFN-β were highest at mid-ovulation. These data confirm that there is endogenous hormonal influence on the levels of cytokines detected in CVF as evidenced by significant variations in levels of IL-1β, G-CSF, TGF-β

Table 6.5 Descriptive analysis table for MIP-3α and cytokines with levels that varied significantly across the various menstrual cycle phases

						95% CI for Mean			
Cytokine		**N**	**Mean**	**SD**	**SE**	**Lower Bound**	**Upper Bound**	**Minimum**	**Maximum**
MIP-3α	Visit 1	8	156.9	228	80.63	-33.74	347.6	12.23	636.6
	Visit 2	8	59.21	107.6	38.03	-30.72	149.1	4.8	297.4
	Visit 3	8	102.4	107.5	38.02	12.54	192.3	28.9	292.1
IL-1β	Visit 1	8	149.4	94.44	33.39	70.41	228.3	11.64	292.3
	Visit 2	8	46.63	47.75	16.88	6.705	86.54	2.9	127.3
	Visit 3	8	41.94	39.46	13.95	8.946	74.93	3.5	116.9
G-CSF	Visit 1	8	188.2	152.7	53.97	60.6	315.8	24.53	416.4
	Visit 2	8	77.68	81.8	28.92	9.293	146.1	2.2	228.3
	Visit 3	8	59.75	70.79	25.03	0.5712	118.9	1.1	160
TGF-β	Visit 1	8	80.77	70.77	25.02	21.6	139.9	18.59	219.4
	Visit 2	8	33.53	38.32	13.55	1.493	65.56	13.7	127.8
	Visit 3	8	26.83	17.8	6.292	11.95	41.7	13.5	58.7
IFN-β	Visit 1	8	9.112	8.288	2.93	2.183	16.04	1.399	18.19
	Visit 2	8	12.76	5.428	1.919	8.224	17.3	7.8	19.9
	Visit 3	8	9.288	8.565	3.028	2.127	16.45	1.3	18.7

Visit 1 = proliferative phase, Visit 2 = mid-ovulatory phase, and Visit 3 = secretory phase

and IFN-β with menstrual cycle phases, however that, MIP-3α is not hormonally regulated.

CVF abnormalities alter the profile of cytokines and significantly increase levels of MIP-3α and those of other cytokines.

Having excluded endogenous hormonal influence on baseline cytokine levels, we sought to determine the impact of underlying CVF abnormalities suggesting inflammation on the levels of cytokines including MIP-3α. Three of 11 women included in this analysis had abnormal gross CVF appearance *(Table 6.1).*

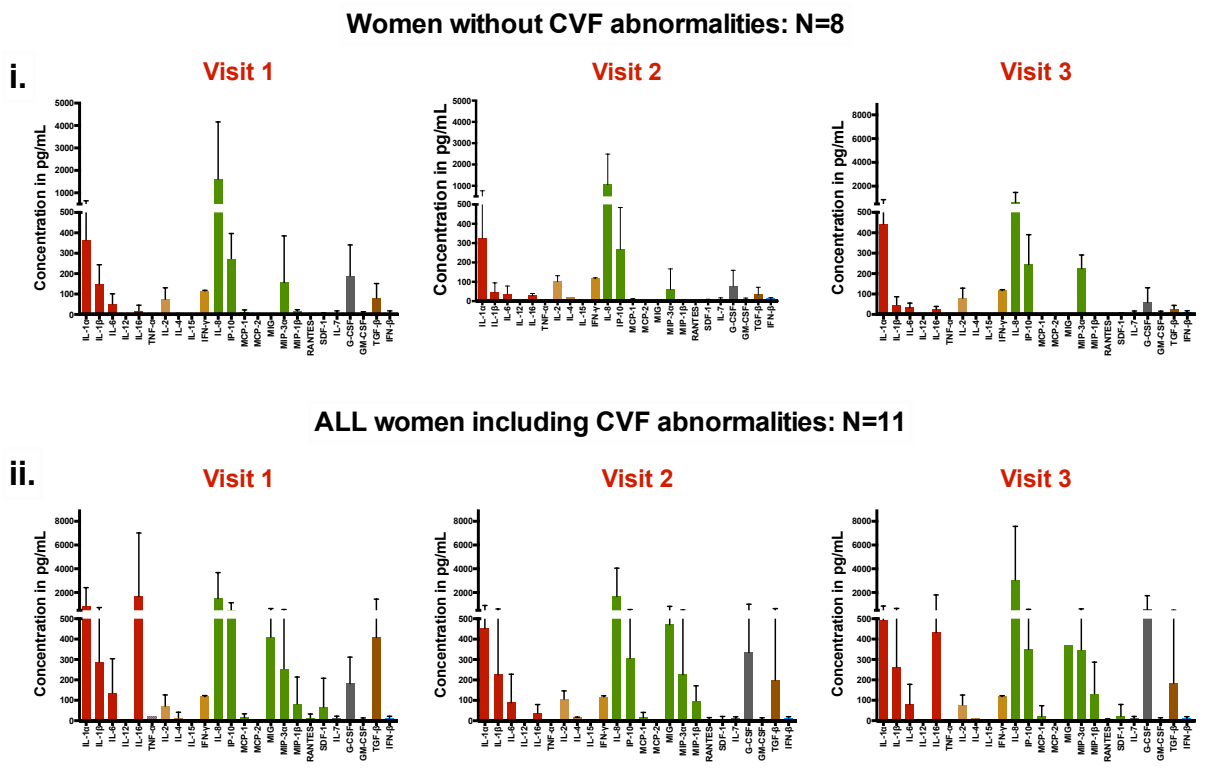

Figure 6.9 Levels of MIP-3α and 23 other soluble proteins colour coded according to protein functional grouping and measured over a single menstrual cycle in (i.) women without gross CVF abnormalities and (ii.) all women in the cohort including those with gross CVF abnormalities. There were no overt differences in profiles of these proteins across the cycle in the absence of CVF abnormalities. However, presence of CVF abnormalities altered the profile and concentrations of proteins. Bars represent mean concentrations while error bars represent standard deviation. All analyte concentrations are expressed in pg/mL and were measured with Luminex.

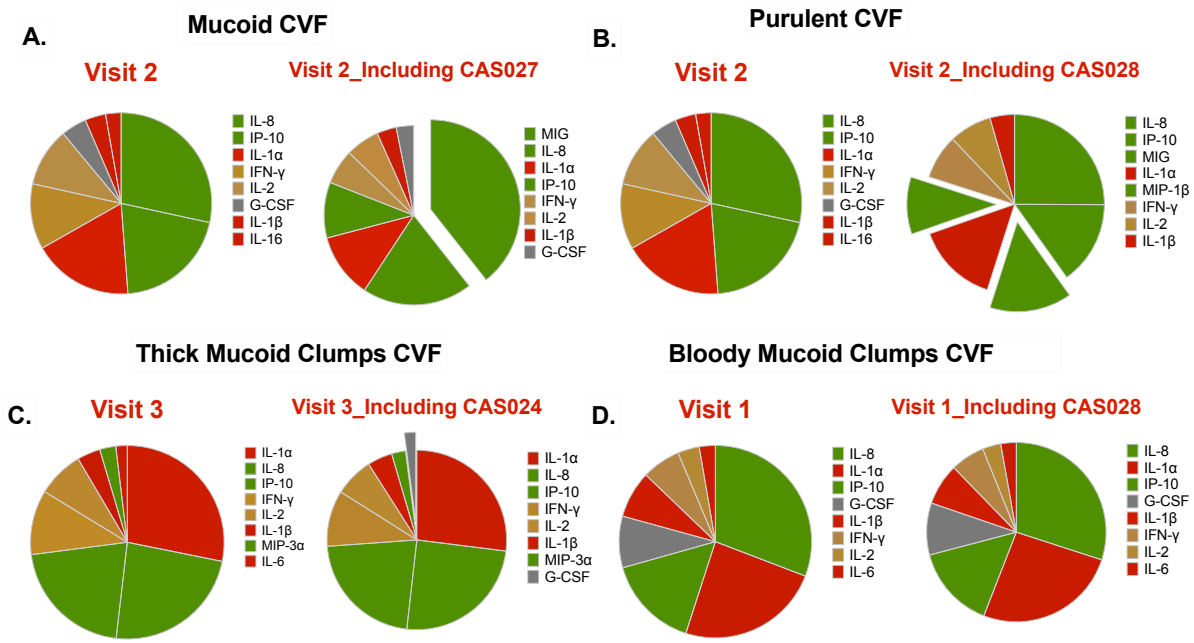

Figure 6.10 Pie curves of top eight cytokines depicting the effect of including women with known gross CVF abnormality by visit category. Exploded slices denote differences between the curve on the left comprising data from CVF of normal women (n=8) and the curve on the right including the single woman with abnormal CVF per visit (n=9). The cytokine with highest concentration is at 12 o'clock moving clockwise. Women with CVF abnormalities have a distinct profile of cytokines in CVF versus women with no abnormality. MIG and MIP-1β, which were otherwise not featuring in the top eight cytokines, were detectable in large amounts in the presence of (A.) mucoid and (B.) purulent abnormalities.

Including women with these abnormalities in the analysis altered the profile and baseline levels of most cytokines. Most cytokines in the chemokine and pro-inflammatory categories tended to be up-regulated (*Figure 6.9*). In the eight women without CVF abnormalities, IL-12, IL-15, MCP-2, MIG, MIP-1β and TNF-α were not detectable with this assay. However in an all-inclusive analysis with 11 women, MIG, MIP-1β and TNF-α were also detectable suggesting that the presence of these cytokines implied underlying pathology. MIG and MIP-1β levels in these three women were high enough as to be among eight cytokines with the highest concentrations in CVF (*Figure 6.10)*. Specifically levels of MIG and MIP-1β in CVF went from being undetectable in the eight women without abnormalities to

average values of 350 and 470pg/mL in the three women with CVF abnormalities, respectively. Concentrations of chemokines remained the highest cytokine concentrations in CVF even in the three women with CVF abnormalities throughout the phases of the menstrual cycle (*Figure 6.11*). MIP-3α levels were notably higher in women with CVF abnormalities than in women without CVF abnormalities, and this was the trend throughout the phases of the menstrual cycle (*Figure 6.12*). At this point, MIP-3α levels were amongst the levels of cytokines in the highest eight concentrations across all visits. In fact, MIP-3α levels were five-fold higher in women with CVF abnormalities than in women without CVF changes and this fold change reached statistical significance with a p-value of 0.0191 (*Table 6.6*). Fold increases in cytokine levels for other cytokines ranged from two to 100, and these fold changes reached statistical significance (*Table 6.5*). However, CVF levels of adaptive cytokines, IL-2 and IFN-γ were not influenced by presence of abnormalities. GM-CSF, was also not influenced by CVF abnormalities. These data imply that genital pathology, rather than hormonal fluctuations, is the main driver of increased MIP-3α secretion as well as that of most other cytokines in the FGT this analysis.

Levels of RANTES and IL-2 in CVF correlate significantly with those in serum; however, the direction of the correlation is not constant.

Until recently, the blood compartment has been studied extensively as a surrogate marker towards understanding infection events in peripheral sites including the FGT. Lately, there has however been a move towards collecting biological specimens from the peripheral sites and to study the primary site of infection directly, which in the context of heterosexual HIV transmission is the FGT. We

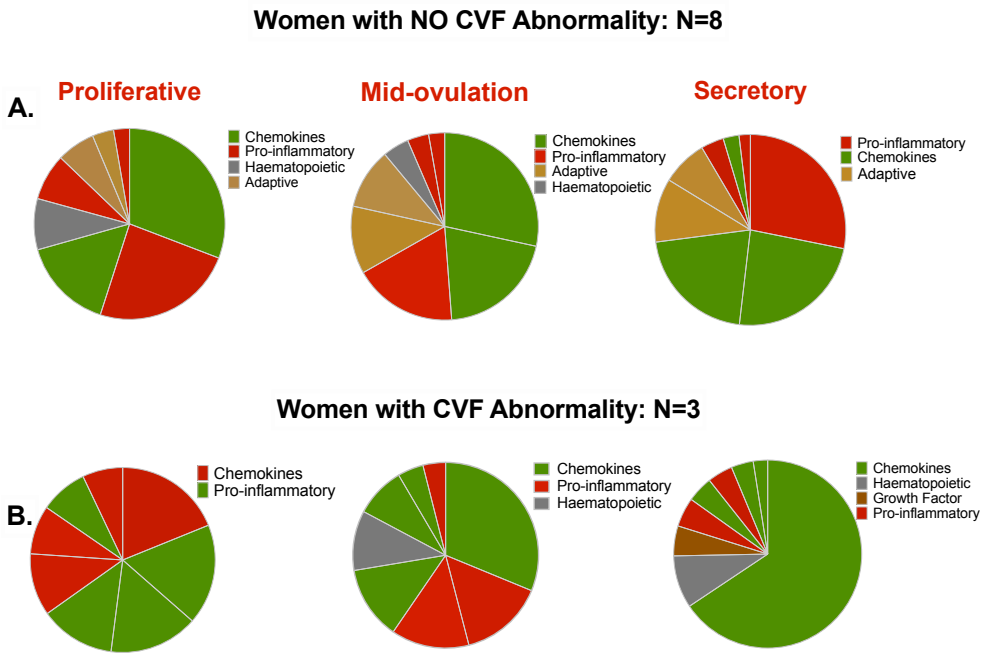

Figure 6.11 Pie curves of eight cytokines with highest concentrations in CVF comparing women with CVF abnormalities and women without CVF abnormalities by functional category of cytokines. In the three women with CVF abnormalities, chemokines formed 62%, 57%, and 76% of cytokines in the proliferative, mid-ovulatory and secretory phases, respectively, while pro-inflammatory cytokines formed 38%, 32%, and 9% of cytokines in the same phases respectively (B.).

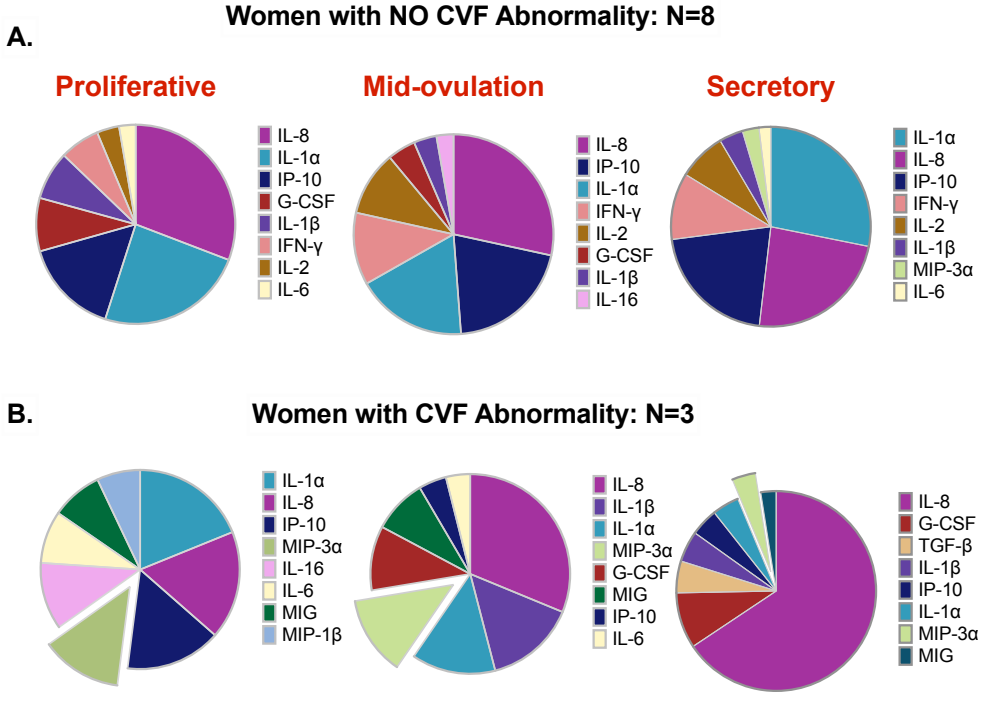

Figure 6.12 Pie curves of eight cytokines with highest concentrations in CVF comparing women with CVF abnormalities and women without CVF abnormalities by individual levels of cytokines. In the three women with CVF abnormalities (B.), contrary to women without CVF abnormalities (A.), MIP-3α levels were high in all three phases of the menstrual cycle featuring in the eight cytokines with highest concentrations in CVF. Exploded pie slices denote MIP-3α.

Table 6.6 Fold changes in cytokines that are up-regulated in the presence of CVF abnormalities

Functional Category	Cytokine	CVF category	N	Mean	SE	Fold change	P value
Pro-inflammatory	**IL-1α**						
		No abnormality	24	377.5	76.0	3.2	<0.0001
		Abnormality	9	1213.0	536.5		
	IL-6						
		No abnormality	24	37.1	8.3	6.9	<0.0001
		Abnormality	9	256.3	57.5		
	IL-16						
		No abnormality	24	23.6	3.8	109.2	<0.0001
		Abnormality	9	2575.0	1958.0		
Adaptive	**IL-2**						
		No abnormality	24	81.9	9.7	1.0	0.3609
		Abnormality	9	84.9	20.1		
	IFN-γ						
		No abnormality	24	116.5	0.8	1.1	0.1455
		Abnormality	9	122.7	0.7		
Chemokines	**IL-8**						
		No abnormality	24	1095.0	353.3	4.3	0.0002
		Abnormality	9	4703.0	1532.0		
	IP-10						
		No abnormality	24	241.3	34.0	3.0	<0.0001
		Abnormality	9	733.5	209.9		
	MCP-1						
		No abnormality	24	4.7	1.9	10.6	<0.0001
		Abnormality	9	50.4	17.6		
	MIP-3α						
		No abnormality	24	106.2	32.0	5.2	0.0191
		Abnormality	9	552.5	96.8		
	RANTES						
		No abnormality	24	1.1	0.3	19.4	<0.0001
		Abnormality	9	22.3	6.6		
	SDF-1						
		No abnormality	24	4.2	0.8	26.1	<0.0001
		Abnormality	9	108.8	50.2		
Haematopoietic	**IL-7**						
		No abnormality	24	9.0	1.6	2.2	0.0242
		Abnormality	9	19.6	1.2		
	GM-CSF						
		No abnormality	24	8.4	1.3	0.8	0.2294
		Abnormality	9	6.8	1.4		

This analysis included only cytokines that were not driven by hormonal fluctuations in the menstrual cycle, and thus, it excluded cytokines in Table 6.5. Exploded pie slices denote MIP-3α. P-values were taken as non-significant if $p>0.05$, and significant if $p \leq 0.05$.

hence studied the blood compartment alongside the FGT compartment in order to determine differences and similarities between the two compartments with regards to baseline secretion patterns of a few cytokines in our panel of interest. We also wanted to determine the impact of endogenous hormonal fluctuations over the menstrual cycle on cytokine levels in blood. We collected serum at every time point that we collected CVF and hence we collected serum longitudinally over three successive visits of the menstrual cycle. The visits once again co-incided with the proliferative, mid-ovulatory and secretory phases of the menstrual cycle. We then quantified 24 cytokines with pro-inflammatory, chemokine, adaptive, growth, haematopoietic, and antimicrobial peptide functions with the Luminex multiplex bead assay. Of the 24 cytokines measured, 12 were below the level of quantitation in serum with this assay: IL-1α, IL-1β, IL-6, IL-12, TNF-α, IFN-γ, IL-8, MIP-3α, SDF-1β, IL-7, GM-CSF, and IFN-β (*Figure 6.13A.*). Five other cytokines IL-4, IL-12, IL-15, MIG and MCP-2 were not detectable in CVF of eight women included in this analysis, and we could hence only assess correlations in cytokines that were detectable in both serum and CVF: IL-16, IL-2, IP-10, MCP-1, RANTES, TGF-β, and G-CSF (*Figure 6.13B.*). Of these seven cytokines, two showed statistically significant correlations between the two compartments RANTES (r=-0.6156, p=0.0001), which correlated negatively, and IL-2 (r=0.6503, p=0.0257), which correlated positively (*Figure 6.13C.*). Our findings, that most cytokines that are detected in CVF are not detected in serum, confirm that it is not appropriate to study the one compartment to extrapolate about the other compartment in HIV pathophysiological studies. This is further confirmed by the unpredictability of correlation patterns in cytokine levels quantified between the two compartments; only three cytokines correlated significantly between the two compartments in this

A.

Cytokines	Serum	CVF
IL-1α	ND	
IL-1β	ND	
IL-6	ND	
IL-12	ND	ND
TNF-α	ND	ND
IL-4		ND
IL-15		ND
IFN-γ	ND	
IL-8	ND	
MCP-2		ND
MIG		ND
MIP-3α	ND	
MIP-1β		ND
SDF-1β	ND	
IL-7	ND	
GM-CSF	ND	
IFN-β	ND	

B.

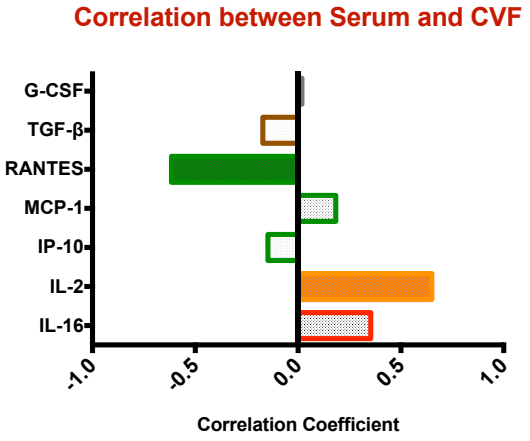

C.

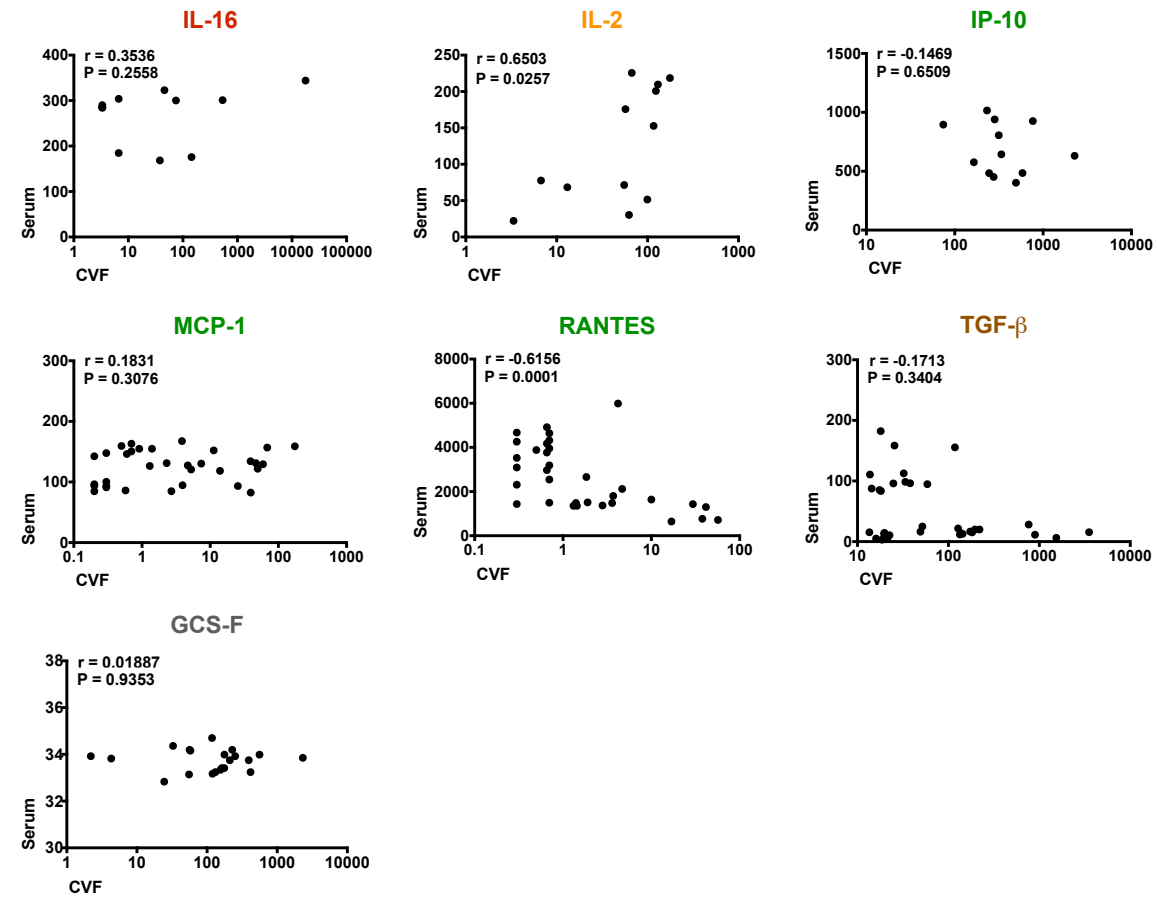

Figure 6.13 Correlation of cytokine levels in serum and in CVF, colour coded according to functional group (n=8). A. 12 cytokines measured were not detectable (ND) in serum with this assay. B. Levels of RANTES and IL-2 correlated significantly between the two compartments as indicated in the correlation coefficient graph. Solid bars denote significantly elevated cytokines as defined by p-value of $p<0.05$. C. Correlation scatter graphs of the seven cytokines detectable in both serum and CVF.

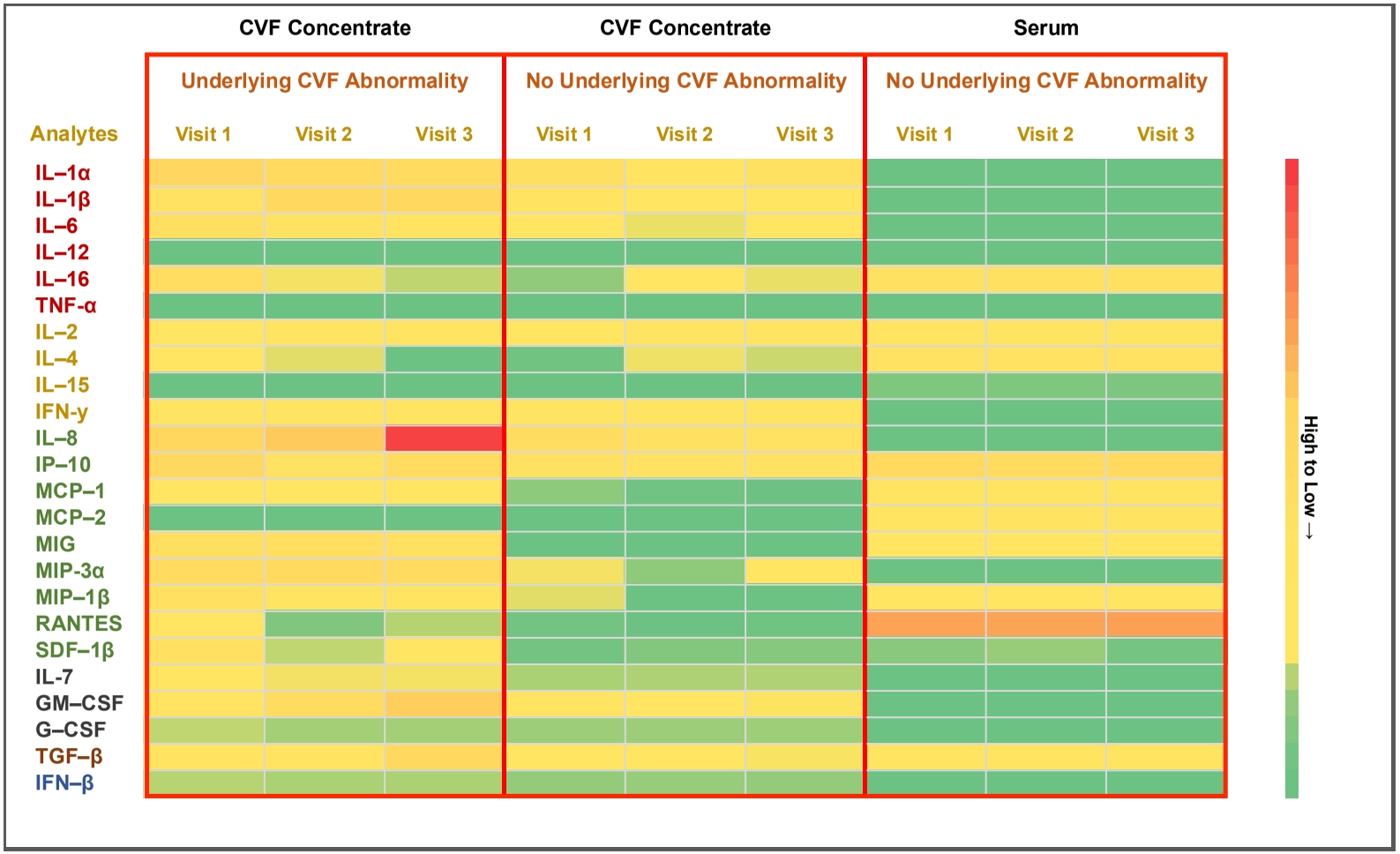

Figure 6.14 Heatmap representing all the cytokines by functional category measured in serum and CVF of women with or without grossly abnormal CVF appearance. Visit 1 = proliferative phase, Visit 2 = mid-ovulatory phase, and Visit 3 = secretory phase. The profiles of cytokines differed between the two highlighted compartments, serum and CVF. Most cytokines were either not detected or very low in serum. On the other hand cytokines were up-regulated in CVF where there were underlying abnormalities. RANTES was highest in serum whereas it was only up-regulated in CVF in the presence of CVF abnormalities. All cytokine concentrations are expressed in pg/mL and were measured with the Luminex multiplex bead assay.

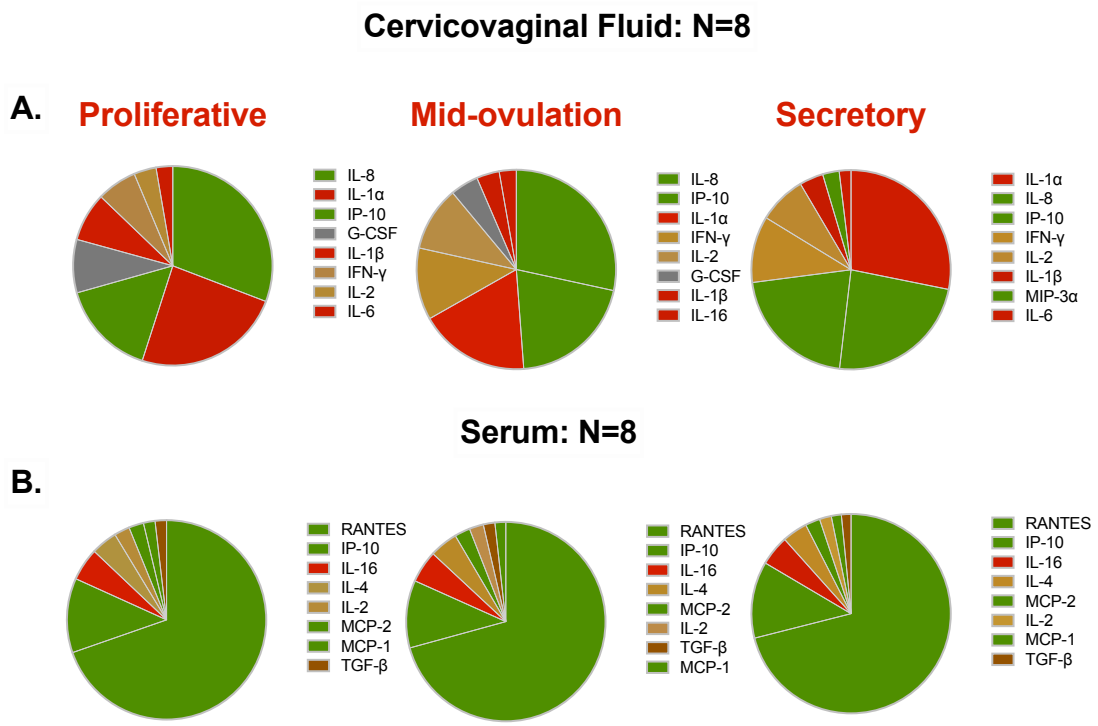

Figure 6.15 Pie curves of eight cytokines with highest concentrations comparing CVF with serum by functional category of cytokines. There were stark differences in the profile of cytokines between the two compartments. Levels of chemokines were very high in serum, contrary to levels of pro-inflammatory cytokines which were low at around 5% throughout the menstrual cycle. In serum there was no change in the profile of the cytokines in the highest concentrations throughout the menstrual cycle. RANTES had the highest concentration in all three phases of the menstrual cycle.

analysis. Even for the three cytokines that correlated, the correlations were in different directions.

Hormonal fluctuations during the menstrual cycle phases do not cause significant fluctuations in the levels of soluble proteins in serum.

The FGT, unlike the blood compartment, may be greatly influenced by the interplay between the endocrine and immune systems, and hence our findings that CVF levels of cytokines are differentially driven by hormonal fluctuations prompted us to study the blood compartment in order to compare and contrast the extent to which hormones influence cytokines in blood. The profile of cytokines in the blood compartment, serum, was different from the profile of cytokines the CVF

Table 6.6: ANOVA table for individual cytokines measured in serum

Cytokines	ANOVA table	Sum of Squares	DF	Mean Square	F	P value
IL-16	Treatment (between columns)	728.3	2	364.1	3.184	0.171
	Individual (between rows)	37498	3	12499		
	Total	38913	11			
IL-2	Treatment (between columns)	445	2	222.5	0.512	0.5358
	Individual (between rows)	65353	3	21784		
	Total	68405	11			
IL-4	Treatment (between columns)	300.5	2	150.2	2.061	0.2317
	Individual (between rows)	6299	3	2100		
	Total	7036	11			
IL-15	Treatment (between columns)	205.5	2	102.7	0.9884	0.3934
	Individual (between rows)	328.7	3	109.6		
	Total	1158	11			
IP-10	Treatment (between columns)	21530	2	10765	0.4337	0.6631
	Individual (between rows)	352426	3	117475		
	Total	522884	11			
MCP-1	Treatment (between columns)	300.8	2	150.4	1.17	0.3599
	Individual (between rows)	7613	3	2538		
	Total	8685	11			
MCP-2	Treatment (between columns)	345.6	2	172.8	0.1981	0.7041
	Individual (between rows)	2579	3	859.7		
	Total	8159	11			
MIG	Treatment (between columns)	12692	2	6346	0.7822	0.4528
	Individual (between rows)	21427	3	7142		
	Total	82795	11			
MIP-1β	Treatment (between columns)	343.6	2	171.8	0.4842	0.538
	Individual (between rows)	2159	3	719.8		
	Total	4632	11			
RANTES	Treatment (between columns)	37866	2	18933	0.08515	0.7902
	Individual (between rows)	3324360	3	1108120		
	Total	4696249	11			
G-CSF	Treatment (between columns)	0.5783	2	0.2891	3.778	0.0782
	Individual (between rows)	2.982	6	0.4969		
	Total	4.478	20			
TGF-β	Treatment (between columns)	31.2	2	15.6	0.09736	0.8646
	Individual (between rows)	11099	3	3700		
	Total	12092	11			

no fluctuations in levels of cytokines comparing levels during the three study visits corresponding to the three different phases of the menstrual cycle for each of the cytokines. Chemokine levels remained high throughout the menstrual cycle phases while levels of pro-inflammatory cytokines were low, contrary to CVF (*Figure 6.14*). In the highest eight cytokines in serum, 85% were chemokines, 6% were adaptive cytokines, 5% were pro-inflammatory cytokines and 4% were growth factors. Haematopoietics were not in the top eight cytokines. Majority of cytokines were down-regulated in serum while majority of cytokines were up-

regulated and mixed in the CVF of three women with CVF abnormalities, and the CVF of women without abnormalities, respectively. However, the profiles of cytokines in serum were similar throughout the menstrual cycle suggesting that cytokine levels in serum are not under hormonal control (*Table 6.6*). RANTES levels were the highest level of cytokines in this analysis and they were highest in serum at an average of 4000pg/mL versus CVF at an average level of 1pg/mL in women without abnormalities (*Figure 6.14 and Figure 6.15*). The only other high cytokine was IL-8, which was highest in women with CVF abnormalities in CVF.

DISCUSSION

From understanding the FGT as an immunohormonal system driven by alterations in both the endocrine and immune systems, we studied baseline levels of MIP-3α in CVF collected longitudinally over the three phases of the menstrual cycle in order to understand the impact that endogenous hormonal fluctuations have on the pattern of MIP-3α secretion. MIP-3α is a chemokine that belongs to the CC chemokine group of molecules [81]. It is the sole ligand for the receptor CCR6 which is expressed on immature dendritic cells and T lymphocytes, particularly memory T cells [84]. It tends to be distributed in mucosal and inflamed sites, being secreted by epithelial cells [86]. Its secretion and expression is induced by inflammation. Its functions range from chemoattraction to linking the innate and adaptive immune systems, and having antimicrobial activities [85]. It was shown in a landmark study in 2009 by Li *et al* to have a significant role in early SIV mucosal transmission events and establishment of productive infection in the FGT of macaques [96]. Wira *et al* suggested that there is a ‘window of vulnerability’ to HIV infection in the progesterone dominant phase of the menstrual cycle, some seven

to 10 days following ovulation, during which the potential for viral infectivity in the FGT is enhanced [203]. After the suggestion of a significant role of MIP-3α in early SIV transmission events in female macaques [96], we hypothesised that MIP-3α would also have a significant role to play in the early HIV infection in humans, and that this role would be particularly heightened in the progesterone dominant phase of the menstrual cycle. Particularly we hypothesised that MIP-3α will be high in the progesterone dominant phase of the menstrual cycle when it would then contribute towards the heightened HIV risk during this time.

MIP-3α was detectable at high levels at baseline in CVF secretions around a mean of 100pg/mL, however, levels of MIP-3α fluctuation did not reach significance in CVF collected over three time points of a single menstrual cycle. Levels of MIP-3α were quantified with the Luminex bead multiplex assay. The lack of fluctuation in MIP-3α levels over the three different menstrual cycle phases suggest that MIP-3α secretion is not under any influence of the endogenous hormones. Further, if indeed HIV vulnerability is heightened in any part of the menstrual cycle, then this heightened risk is unlikely to be mediated via levels of MIP-3α in the FGT. Again, the findings of lack of influence of endogenous hormone fluctuation on MIP-3α secretion confirm those of Patel *et al* [204]. Similarly to our study, Patel *et al* employed the ELISA immunoassay to quantify MIP-3α levels in CVF of seven women collected over the three different phases of the menstrual cycle and their data showed lack of significant fluctuation in MIP-3α levels. On the contrary, in a study of associations between contraceptive use and HIV infection, Morrison *et al* showed that MIP-3α levels were influenced by exogenous hormone use and pregnancy state [205]. There were significantly high levels of MIP-3α in combined oral contraceptive users while there were

significantly low levels in breastfeeding (a progesterone dominant state) women from Uganda and Zimbabwe with high background levels of MIP-3 α. [205]. In light of the window of vulnerability to HIV in the FGT in the luteal phase, it could be that normal steady state MIP-3α constitutive levels as seen under endogenous hormonal control are unlikely to mediate vulnerability to infection, however, in the presence of exogenous hormones, and therefore heightened hormonal exposure, MIP-3α possibly mediates this association. Data from Buckner *et al* showed that in endocervical explant tissues it was only in the presence of oestrogen and progesterone that poly I:C stimulation significantly influenced levels of cytokines, while administration of hormones alone or poly MIP-3α I:C alone either had no effect or had opposite effect to giving both simultaneously [206].

Of the 24 cytokines studied in CVF over the menstrual cycle, three (IL-12, IL-15 and MCP-2) were not detectable in the FGT with the Luminex assay. Of the 21 that were detectable, only four were significantly elevated in some phases of the menstrual cycle: IL-1β, G-CSF, and TGF-β were significantly elevated in the proliferative versus the mid-ovulatory and secretory phases while IFN-β was significantly elevated in the mid-ovulatory versus the proliferative and secretory phases. It is not surprising that IL-1β, G-CSF, and TGF-β would be significantly elevated in the proliferative phase of the menstrual cycle which is the period when the endometrial lining is shed as part of menstruation while also proliferating to repair the shed endometrial layer [172]. IL-1β is an apoptotic cytokine, which is a mediator of inflammation, while G-CSF and TGF-β are concerned with enhancing phagocytic neutrophil activity and proliferative cellular activity. While the majority of the rest of the cytokines showed a trend towards elevation in the proliferative phase, the changes in levels, however, did not reach statistical significance. The

FGT, and particularly its upper part (fallopian tubes, endometrium, and endocervix), is a dynamic system that is under heavy hormonal control in preparation for changes that enhance its main reproductive functions i.e. pregnancy and menstruation. Leucocytes which produce chemokines, growth factors and a range of proteases involved in tissue remodelling, proliferation and angiogenesis may vary over the menstrual cycle phases [207]. Accordingly, leucocytes which constitute 6-20% of cells in the FGT, appear at different densities and distribution patterns in different sub-compartments [56]. It has been shown on flow cytometric analysis that in the FGT leucocytes concentrate in the upper FGT, tapering down to lower numbers in the lower FGT, with CD3+ T cells being the most frequent leucocytes throughout the FGT [56]. Proportionately, levels of soluble proteins would hence vary with the variations in leucocyte densities throughout the FGT and would also vary between different sub-compartments in the FGT. For instance, neutrophils with phagocytic function, are constitutively present within the human FGT and dramatically increase in number at ovulation [208], while NK cells appear during the proliferative phase and increase in cell numbers thereafter [209]. However, some studies have shown that changes in leucocyte numbers remain static in the vagina subcompartment which is fraught with Langerhans cells throughout the menstrual cycle [210], while other studies have demonstrated slight increases, and changes in cell localisation within tissues, in the endometrium [56]. It could be that the limited fluctuations in cytokine levels over the menstrual cycle seen in this cohort reflect underestimation due to inappropriateness of the sub-compartment sampled. We sampled fluid in the vagina, which is in the lower FGT, whereas most of the leucocyte changes with associated cytokines changes take place in the upper FGT. Moreover fluid in the vagina is a collection of secretions from the entire FGT and it is thus difficult to

decipher precise contributions from the various sub-compartments. Boomsma *et al* sampled the endocervical sub-compartment at the same time that they sampled the endometrial sub-compartment and quantified the same soluble proteins in both these secretions [104]. Their data showed significantly unequal amounts of cytokines measured in these sub-compartments even though these sub-compartments are both in the upper FGT. Or it could be that the cytokines in our panel are those that are not affected by hormonal changes but are rather under paracrine and autocrine control from leucocytes.

There was no evidence that endogenous hormone levels in CVF modulated MIP-3α levels and those of 16 other cytokines. However, abnormalities of CVF caused drastic changes to the levels and profiles of cytokines in this analysis. CVF of three women had grossly abnormal looking CVF suggesting underlying pathology. CVF of these women appeared purulent, bloody, or abnormally mucoid, findings that are otherwise associated with an underlying cervicitis, an inflammatory condition of the cervix [114]. In these women, 10 cytokines including MIP-3α were significantly up-regulated, being two- to 100- fold higher in the CVF of women with these abnormalities than in the CVF of women without these abnormalities. These cytokines were mostly chemokine and pro-inflammatory cytokines and included IL-1α, IL-6, IL-16, IL-8, IP-10, MCP-1, RANTES, SDF-1β and IL-7. Moreover, three other cytokines, MIG, MIP-1β, and TNF-α, which were not detectable in women without these abnormalities in CVF, were suddenly detectable and at high levels in women with these abnormalities. These findings suggest that while there is minimal, if any, influence of endogenous hormones on most cytokines in this analysis, there however seems to be a dominant effect of possible underlying pathology on cytokine levels. Data from a study by Mlisana *et al* showed a profile

of elevated cytokines in CVF of women with reported symptoms of a sexually transmitted infection (STI) including an abnormal appearance of vaginal secretions [211] while that from Kyongo *et al* also showed cytokine signatures associated with the presence of leucocytes and/or altered Nugent scores in CVF [166, 167]. Pudney *et al* showed that the scant CD4 and CD8+ T cell numbers in the endocervix were suddenly numerous, often occurring as focal accumulations subepithelially in the presence of inflammation in the endocervical tissues. [58]. The suggested redistribution of target cells with associated superimposed cytokine changes may account for fluctuations in cytokine levels with abnormal CVF suggesting underlying pathology.

The blood compartment is a largely researched dynamic bodily fluid compartment in which a plethora of biomarkers are expressed. We accordingly studied the same range of cytokines in serum that we studied in CVF with the Luminex multiplex bead assay. We collected serum from the same women from whom we collected CVF and at the exact same time points that we collected CVF. We assessed correlations between CVF cytokines and serum cytokines and explored whether serum cytokines are under endogenous hormonal control. Half of the cytokines in our panel (IL-1α, IL-1β, IL-6, IL-12, TNF-α, IFN-γ, IL-8, MIP-3α, SDF-1β, IL-7, GM-CSF, and IFN-β) were below the level of quantitation in serum, as opposed to three that were below the level of quantitation in CVF. The volume of serum is substantial as compared to the volume of CVF and hence serum may underestimate levels of biomarkers due to over dilution. It may hence not be easy to discern whether the undetectable cytokines were not detectable in this analysis because they were either not present in blood *in vivo* or they were simply below detection levels for this assay. It is however interesting to note that other studies

have previously also found undetectable levels of IL-12 in CVF [166, 170]. Levels of RANTES in serum negatively correlated negatively with levels of RANTES in CVF. Similarly, levels of IL-2 in serum correlated positively with levels of IL-2 in CVF. Poor overlap in the detectability of most cytokines between the two compartments and the difference in the direction of correlation of RANTES and IL-2 confirm the unpredictability in the association between serum and genital tract biomarkers. It is therefore not adequate to use serum as a surrogate marker for understanding genital tract events in research. Further, the profile of cytokines was different between the two compartments. For instance pro-inflammatory cytokines occurred uncommonly in serum while they were prevalent in CVF. Perhaps this is to be expected given the fact that the FGT is the primary site for menstruation which is known to be characterised by inflammatory changes that are associated with progesterone withdrawal [172]. Further, bacterial vaginosis, a highly inflammatory condition of the FGT, occurs with high prevalence globally, with reports ranging from 7% to 51% depending on the patient population [212]. Also, levels of RANTES were less than 1pg/mL in CVF while they were highest in serum around 4000pg/mL, further confirming that these two compartments are distinct. Lastly, contrary to CVF, there was no evidence that there is hormonal regulation of cytokines in serum. Zegels *et al* previously reported that biomarkers found in CVF, being a " proximal" fluid, show more specificity and sensitivity for gynaecopathological conditions as compared to blood [112]. It is hence not appropriate to continue to study the one compartment to understand events in the other.

CONCLUSION

Our data has shown that MIP-3α levels are not hormonally regulated and hence they are unlikely to contribute to the heightened vulnerability to HIV infection. In contrast, MIP-3α levels, via a mediatory effect of underlying inflammation, which was evidently the predominant driver of its levels in the FGT, might contribute to the risk of HIV infection. However, our data confirmed endogenous hormonal and pathology regulation of other soluble proteins in the FGT of women at low risk for HIV infection with possible underlying pathology being more pronounced in its effect than endogenous hormones. These effects were not generalised in the FGT but rather occurred in a sporadic manner for some cytokines. Therefore the findings in this analysis that certain cytokines are hormonally regulated highlight the significance of timing of sample collection in the menstrual cycle and caution against interpretation of results based on samples collected randomly from the FGT. Similarly they make a strong case for identifying the presence of underlying inflammatory/pathologic condition, particularly in the research questions that answer the association between the immune system changes and HIV infection for instance. Further our data showed that the FGT has a distinct pro-inflammatory profile that is different from blood thus highlighting the inappropriateness of using serum as a surrogate marker for FGT events. Lastly our data suggested that serum cytokines are not under hormonal regulation, unlike CVF cytokines.

Rhesus Macaques. Source: [1]

CHAPTER SEVEN MIP-3α RESPONSES IN THE ENDOCERVIX OF MACAQUES

SUMMARY

Much of our understanding of the early events in HIV infection comes from landmark studies in female macaque monkeys exposed to Simian Immunodeficiency Virus (SIV), and yet history informs us that humans do not always respond and behave like macaques. The key study in this field, by Haase *et al*, suggested that exposure to SIV triggered sub-epithelial accumulation of MIP-3α in the endocervix of macaques, an event that preceded the recruitment of RNA SIV+ CD4+ T-cells and establishment of foci of infection in the submucosa. In view of our findings in humans, as discussed in the preceding chapters, that the endocervical explant tissues (EET), despite demonstrating high constitutive MIP-3α levels, do not secrete additional MIP-3α on exposure to HIV-1 preparations, we sought to replicate our MIP-3α studies in the endocervix of macaques. We studied constitutive and stimulated patterns of secretion of various soluble proteins: specifically we sought to determine whether or not viral preparations, and particularly SIV envelope preparations, trigger MIP-3α secretion in the genital tract of macaques. We prepared endocervical explant tissues (EET) from six macaques, three rhesus and three cynomolgus, which we exposed to 11 different stimulants including three SIV preparations and six Toll-like receptor (TLR) ligands over 24 hours prior to harvesting supernatants. We then measured 11 cytokines including MIP-3α in the generated supernatants with Luminex multiplex bead arrays. We studied down- and up- regulated cytokines, applying the one sample *t*-test to assess statistically significant fold-changes in stimulated tissues. It was shown that, similarly to the human EET, the macaque EET secreted MIP-3α

constitutively, albeit at much lower levels. Again, it was found that MIP-3α secretion was not triggered by either viral stimulation or TLR stimulation in the macaque EET, similarly to human EET. Based on these findings, there is no evidence that the macaque EET responds to viral stimulation by producing further levels of MIP-3α in the first 24 hours post viral exposure measured with the Luminex assay in these *in vitro* models.

INTRODUCTION

HIV-1 is a human-specific virus that does not replicate in many animal species. In particular, it does not readily infect non-human primates (NHP) including macaques. However not all studies aimed at understanding correlates of protection and responses to exogenous protective strategies to HIV-1 are feasible to conduct in humans. Consequently, macaques infected with SIV provide a useful - and to date - the best surrogate in HIV-1 pathogenesis and biomedical preventative studies.

NHP models have been used extensively in HIV/AIDS research from as early as the 1980's when HIV was first discovered in human beings [213]. They have been used with huge success in understanding disease pathogenesis [214]. Further, they have been employed with resounding success in informing the development of biomedical therapeutic and preventative strategies including vaccines, topical and oral pre exposure prophylaxis (PrEP) [215]. Lastly, in the female genital tract, they have been used extensively towards understanding the effects of hormones, both exogenous and endogenous, on the risk of HIV acquisition [216]. When in search of an NHP model best suited for studying HIV/AIDS in the mid 1980's,

Asian macaques of the genus macaca — Macaca mulatta (rhesus), Macaca nemestrina (pigtail), and Macaca fascicularis (cynomolgus) — which, although not natural hosts of SIV, were discovered to be susceptible to infection with SIV [217]. In particular, use of the SIV macaque model followed the accidental discovery of an Indian rhesus macaque, known to not be a natural host of SIV, that had become infected with SIV in the laboratory [218]. It was subsequently discovered that this infection led to a disease with striking similarities to human AIDS with regards to acute and chronic disease patterns. Consequently, this model has since been studied widely and also in the context of genital transmission of SIV infection [219].

However, these three species of macaques are not used interchangeably in HIV/AIDS research. Although they all belong to the *Cercopithecoidea* species, their evolutionary history shows that they separated from one another more than a few million years ago [220]. Inherently, though similar in many traits, they also differ in certain other traits, and as such research indications for their use differ [221]. The rhesus macaque (RM) model has previously been used in more than 80% of HIV vaccine pre-clinical trials and is hence widely accepted as a model for HIV infection in humans, being deemed a model of choice for such indications [217]. The widespread use of the RM species is due to familiarity with its genetic and physiological aspects; this is because they have very well characterised MHC allelic profiles with established dosing regimens tested for various viral isolates. Further, this species in particular is known to be highly susceptible to infection with a wide range of SIVmac and SHIV strains via various routes of infection: intravenous, intrarectal and intravaginal [96, 215]. The pigtail macaques (PM) on the other hand are more favoured for reproductive biological studies - they cycle

throughout the year, have vaginal ecology closely resembling that of a human and are reproducibly infected with S(H)IV without the need to use exogenous hormones [96, 216]. Then again the cynomolgus macaque (CM) species, while widely available, are much less popular for they are deemed to be less practical – they are much smaller in size, thereby restricting the amount of blood that can be collected from them, have low viral loads, requiring high infectious doses to achieve infection, thus making them unsuitable for vaccine studies, they display general resistance to infection with SIVs and SHIVs even though they are susceptible to infection with SIVmac251 [96, 220]. Moreover, they are less popular in reproductive biological studies on account of their small-sized FGT that is difficult to access.

In spite of all these differing traits between the species, the macaca genus is still said to be closely related to humans, sharing a last common ancestor ~25 million years ago [221]. There are documented differences between humans and macaques with regards to immunogenetic and immunological attributes. However, these have largely been studied in the context of responses to vaccines. Very limited research has been done in the area of innate immunity. Biophysiologically, the macaques are said to have a microflora profile similar to the bacterial vaginosis profile in the female genital tract (FGT) of humans [222], they seem to have a more basic pH than is demonstrated in humans [223], have varying menstrual cycle dynamics with regards to length and regularity [224], have more keratinised FGT walls than humans [225] and demonstrate dramatic epithelial thickness fluctuations in response to hormones compared to what is seen in humans [226]. Consequently, innate responses in humans are not necessarily similar to those in macaques and as such, we need to be careful in inferring

macaque-based research findings to human beings.

Besides the need for careful consideration in choosing the best suited macaque model for a specific research question at hand, choosing the virus stock to use deserves equal consideration - different macaque species are not equally susceptible to infection with the same virus stock, the same amount of virus/dose of infection, and the same route of infection. As a rough guide, RM succumb to SIVsm and its derivative isolates, while PM and CM succumb to SIVsm and SIVmac strains, and SIVmac251 respectively [215]. Most challenge experiments in macaques have been performed using either $SIV_{mac}251$, which is a swarm, or its pathogenic clone SIV_{mac} 239 derived through passaging from SIVmac251, or SIV_{sm} E660 [220]. SIVmac251, the first laboratory-discovered SIVmac strain, was identified when it accidentally infected a RM of Indian origin in the laboratory. It is typically highly pathogenic and therefore more representative of human HIV-1 infection. The vast majority of AIDS vaccine data generated in RM to date came from challenges using this pathogenic stock of SIVmac251.

Typically, preclinical studies involving the use of animals are conducted prior to human studies in order to answer a specific research question. However, literature makes a strong case for conducting macaque studies after human studies in certain instances, in order to answer mechanistic questions, amongst other things. We likewise embarked on doing a macaque tissue study after we had completed analyses on the human tissue study, in order to answer the question of the responses of the respective endocervices to incoming virus with regards to MIP-3α secretion. As already discussed, we found in our study using various FGT human

epithelial models including EET that levels of MIP-3α are not further elevated on exposure to HIV-1 preparations. We therefore went somewhat retrospectively to answer the question of whether macaque EET sense and respond to retroviral exposure differently from the way in which human EET appear to do with regards to MIP-3α.

Constitutive expression of MIP-3α in various macaque bodily compartments has previously been described in the literature. Firstly, similarly to human beings, it has been shown to be homeostatically detected in various haematopoietic sites [227-229]. Further, its association with SIV infection, and particularly its fluctuation patterns during different stages of infection has also been demonstrated. However, these studies have not yet been performed in the FGT. Choi *et al* showed, using *in situ* hybridization and immunohistochemical techniques, that MIP-3α and its receptor CCR6 are expressed differentially in tonsillar sites following SIV infection whereas they are not detectable in the spleen [228]. Haase's group, in two different publications but using the same animals from a single *in vivo* experiment, also showed, using immunohistochemical and image quantitative techniques, that levels of MIP-3α, which are expressed constitutively, are further elevated on exposure to high dose SIV in the FGT [96, 230]. However, this was a coincidental finding during a study designed to examine early events in SIV infection, and to date no one has designed a study specifically to evaluate the innate responses of endocervical epithelial cells to virus exposure. Moreover, no one has previously looked at this association employing a different quantitative immunological assay. Lastly, no one has done a side-by-side comparison of

epithelial responses to virus in macaques and humans with regards to MIP-3α secretion in the endocervix.

Given that our results using various genital epithelial cell models in humans were apparently contradictory to the findings in the literature derived from this single high profile study in macaques, we set out to replicate these studies in the genital tract of macaques using an *ex vivo* epithelial model to allow for a side by side comparison between the two. Further, given that the literature places significant emphasis on the role of MIP-3α in the initial events of SIV mucosal transmission and infection, and yet these findings are based on a single study using a single technique – RM challenged with SIVmac251 and studied using immunohistochemistry - we set out to answer the question of whether these results could be replicated using a different technique and a different macaque model.

MATERIALS and METHODS

Study cohort, setting, population, and size:

We received hysterectomy specimens from seven macaques and subsequently analysed data from only six macaques: three rhesus and three cynomolgus. The hysterectomy was performed immediately at the time of culling the macaques (i.e. *post mortem* hysterectomy) and the womb complete with uterus, endocervix and vagina was subsequently shipped intact within a few hours of womb resection to the University of Oxford laboratory. Sally Sharpe on behalf of Public Health England (PHE) in Porton Down kindly donated these samples to us. The RM had

been part of a BCG study but were TB uninfected. The CM were part of a simian retrovirus (SRV) study but we received only SRV-uninfected macaque tissues.

Sample handling and shipping:

Post resection, hysterectomy tissues were immediately immersed in cold RPMI-1640 medium (Sigma-Aldrich®, UK) complete with 10% heat inactivated foetal bovine serum (FBS) (Life Technologies, Gibco®, UK), 2 μM L-glutamine (Life Technologies, Gibco®, UK), and antibiotics (100 units/ml penicillin/streptomycin (Life Technologies, Gibco®, UK), 1μg/mL fungizone® (Life Technologies, Gibco®, UK), and 10μg/mL gentamycin (Life Technologies, Gibco®, UK). They were packaged and shipped to us on ice.

Experimental work:

We prepared explant tissues from the endocervix (EET) of *post mortem* hysterectomy specimens immediately on arrival of the tissue and hence on the same day of womb resection. Blocks of tissue from the macaques were hence used fresh within 8 hours of womb resection. The EET were exposed to various stimulants, which included Toll-like receptor (TLR) ligands one through to six, three viral preparations and interleukin 1 beta (IL-1β) as the positive control. Details of stimulants and viral preparations used appear below:

- IL-1β was used as positive control for activation at 10 ng/ml (R&D Systems, Bio-Techne, Abingdon, UK), Pam3CSK4 (TLR1/2) at 20 μg/ml (Tocris, Bio-Techne, Abingdon, UK), Zymosan (TLR2) at 10 μg/ml (Sigma-Aldrich®, UK), Poly I:C Polyinosinic–polycytidylic acid sodium salt (TLR3) at 25 μg/ml (Sigma-Aldrich®, UK), LPS (Lipopolysaccharides from *Escherichia coli* 0111:B40)

(TLR4) at 10 µg/ml (Sigma-Aldrich, UK), Flagellin (Flagellin from Salmonella typhimurium) (TLR5) at 20 ng/mL (Sigma-Aldrich®, UK), and FSL-1 (Pam2CGDPKHPKSF) (TLR2/6) at 2 µg/ml (Invivogen, UK).

- Virus preparations included pathogenic SIVmac251/CSH used at two concentrations: low dose and high dose i.e. 5*10 TCID50 and 5*10^3 TCID50, respectively (kindly donated by Professor Neil Berry at the National Institute for Biological Standards and Control (NIBSC), UK), recombinant SIVmac251 gp130 at 100 ng/mL (NIBSC, UK), and native SIVmac251 gp120 at 100 ng/mL (generously donated by Professor Marjorie Robert-Guroff at the National Institutes of Health, National Cancer Institute, US).

- Information on the pathogenic SIVmac251 virus stock: the *in vitro* titre of the stock was determined to be in the range of $4x10^4$ – $1.6*10^5$ TCID50/mL on C8166 cells, having previously been propagated in rhesus monkey peripheral blood mononuclear cells (PBMCs) (n=8). The PBMCs were stimulated with Staphylococcus Aureus and Staphylococcal enterotoxins A and B (SEB/SEA) for 24 hours and then infected with SIVmac251. Primary monkey cells were maintained in RPMI-1640 supplemented with 20% FBS, antibiotics (Penicillin and Streptomycin) and 100 U/mL of IL-2. Supernatants were pooled starting from 7 to 14 days post-infection. On Day 10, cultures were re-fed with fresh stimulated autologous PBMCs.

Culture conditions:

We cultured one EET per well of a 96 well tissue culture plate in 200µL of RPMI-1640 with supplements prepared as described above for shipping. Three EET

were cultured per test condition. EET were cultured with the various stimulants in the incubator at 37^0C in 5% CO_2 for 24 hours after which supernatants were harvested and stored for future analysis with the respective protein quantitative immunoassay.

Storage:

Supernatants were stored in 96 well tissue culture plates at -20^0C until assay performance.

Quantitative protein immunoassay: cytokine Measurements:

The concentrations of 11 cytokines including MIP-3α were measured in supernatants generated from EET using the Luminex multiplex bead assay. The cytokines measured fell in one of three functional groups: the pro-inflammatory, adaptive and chemokine groups. Supernatants collected from the three EET wells testing the same condition were pooled into polypropylene vials and centrifuged before being dispensed into duplicate wells of the Luminex assay plate. Supernatants were used undiluted in the assay. These cytokines were measured using the custom made MILLIPLEX MAP Non-Human Primate Cytokine/Chemokine - 11-Plex Premixed Immunology Multiplex Assay Kit (Merck-Millipore, France) according to the manufacturer's protocol. Data were collected using a Bio- Plex™ Suspension Array Reader (Bio-Rad Laboratories InC®). The lower limit of detection ranged between 1.7 and 266.6pg/mL for the cytokines measured. Specifically the cytokines with respective lower detection limits in pg/mL in this panel included: IL-1α (14.3), IL-6 (1.4), IL-16 (64.3), TNF-β (39.0), IL-2 (5.5), IL-4 (61.9), IL-17A (1.7), IL-17E/IL-25 (266.6), IP-10 (5.9), MIP-3α (3.6), and RANTES (1.7). Cytokine concentrations that were below the lower limit of

detection of the assay were reported as the mid-point between the lowest concentrations measured for each cytokine and zero.

Statistical analyses:

Statistical analyses were performed using GraphPad Prism version 7 for Mac OS X (Prism, GraphPad Software, La Jolla, California, USA). The 5 PL regression curve fitted formula was used to calculate cytokine concentrations from the standard curves on GraphPad Prism. Descriptive data were presented with schema prepared from GraphPad Prism. Median values were calculated and used to present data on pie diagrams. Results were also reported in bar graphs with bars representing the mean of three tests and error bars representing standard deviation. Floating bars showing the impact of each stimulant on each cytokine were presented with the horizontal line within the bar representing median values while the outer horizontal lines represent minimum and maximum values. Fold changes in analyte concentrations were calculated by dividing stimulated levels of analyte concentrations by the unstimulated levels of respective analyte concentrations. One sample t-test was used to assess statistical significance for down-/up-regulated analytes based on fold changes in analyte concentrations. For this analysis, we defined significantly up-/down-regulated cytokines as those that were at least 1.5 fold higher/lower than the unstimulated value plus a p-value of <0.05. Levels of MIP-3α were expressed in pg/mL throughout the study.

RESULTS

We included 6 adult macaques, three rhesus (RM) and three cynomolgus (CM), in this analysis and they were all negative for SIV and SRV. The mean age of the RM and CM were 14 and 10 years, respectively. On inspection, the FGT parts of the CM were much smaller in size compared with the RM. The vaginal walls of both species were different from those of the human beings – they were thick and wart-like in appearance. Moreover, the endocervical canal was much shorter with very thick mucoid yet copious secretions and the walls were thrown into deep folds.

The rhesus and cynomolgus macaque species differ from one another with regards to innate function of the endocervix

We prepared EET from fresh hysterectomy specimens and incubated them in RPMI-1640 at 37^0C 5% CO2 for 24 hours before harvesting supernatants in order

Table 7.1 Comparison of cytokine concentrations in supernatants of unstimulated EET of RM and CM

Function	Cytokine	Median Cytokine Concentration (IQR; pg/mL)		P-value
		Rhesus (n=3)	Cynomolgus (n=3)	
Pro-inflammatory	**IL-1α**	68.2 (67.2-69.0)	ND	
	IL-6	3557 (2955-3747)	3574 (2908-4084)	0.8176
	IL-16	496 (461-583)	348 (310-351)	0.01
	TNF-β	300 (282-313)	101 (94.7-135)	0.0002
Adaptive	**IL-2**	51.7 (50.8-56.6)	33.9 (32.9-34.8)	0.0005
	IL-4	500 (499-506)	0.66 (0.66-0.66)	<0.0001
	IL-17A	1.35 (0.94-1.46)	0.98 (0.79-1.75)	0.8251
	IL-25/IL-17E	ND	ND	
Chemokines	**IP-10**	50 (49.5-50.2)	37.8 (37.3-37.9)	<0.0001
	MIP-3α	27.1 (27-27.2)	6.84 (6.46-8.51)	<0.0001
	RANTES	33.3 (12-57.1)	31.3 (31.2-33.4)	0.8758

P-values < 0.05 were considered significant statistically. IQR: interquartile range, ND: not detectable

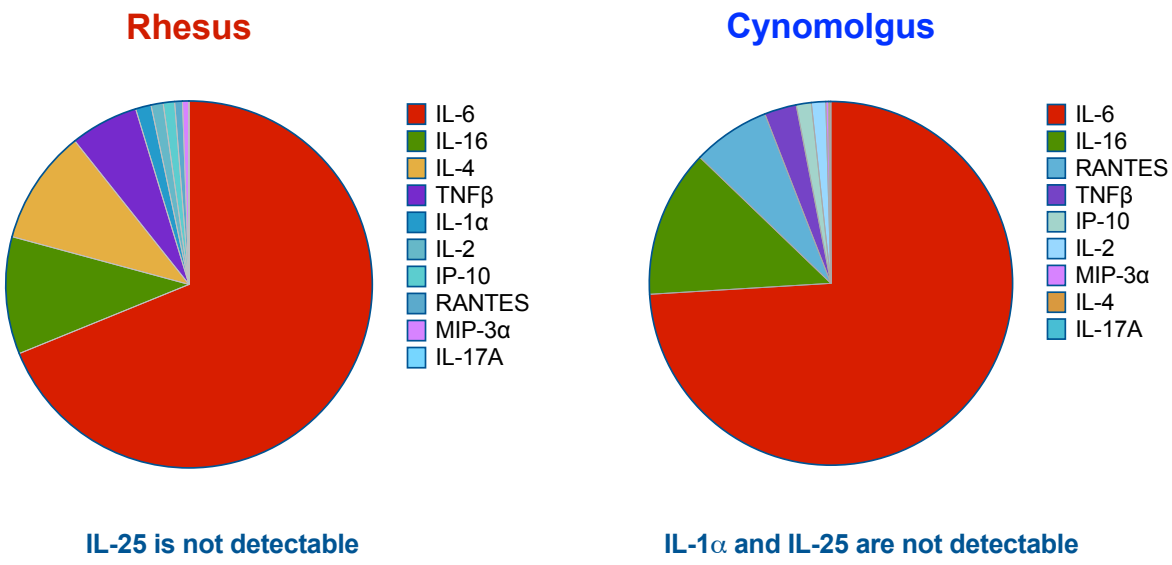

Figure 7.1 Pie curves showing the profiles of the frequency of eleven cytokines measured in unstimulated EET of the two macaque species studied (rhesus (RM) and cynomolgus (CM). Supernatants were harvested after 24 hours of incubation of EET and analyte levels (expressed in median pg/mL) were measured using the Luminex multiplex assay. The profiles of measured analytes were different between the two studied macaque species.

to evaluate cytokine baseline secretion patterns. We subsequently measured 11 cytokines in the supernatants of RM and CM with the Luminex assay platform: of these, two analytes were not detectable in CM (IL-1α and IL-25/IL-17E) while only one cytokine (IL-1α) was not detectable in RM (*Table 7.1* and *Figure 7.1*). Of note was that the kit used did not specify detection sensitivity based on different macaque species. Of the cytokines that were detectable in both macaque species, IL-16, TNF-β, IL-2, IL-4, IP-10 and MIP-3α were significantly higher in RM versus CM (*Table 7.1*). Within each species, the profiles of lowest to highest cytokine concentrations of various cytokines were different, thereby highlighting that there innate differences between these two species of macaques at the level of the cytokines at the level of the EET, we concluded that these two species differ, at

least with regards to innate immunity. We hence proceeded to analyse data from these two species separately throughout the rest of the analyses. We started off with evaluating differences in the secretion patterns of MIP-3α in the EET models, in both unstimulated and stimulated EET models, comparing the two macaque species and humans.

Macaque EET secrete MIP-3α constitutively albeit at lower levels compared to humans

In order to study the constitutive patterns of secretion of MIP-3α in the two species, comparing the EET of the two species with that of humans, we prepared EET from fresh hysterectomy specimens and incubated them in RPMI-1640 at 37^0C 5% CO2 for 24 hours before harvesting supernatants. We measured MIP-3α

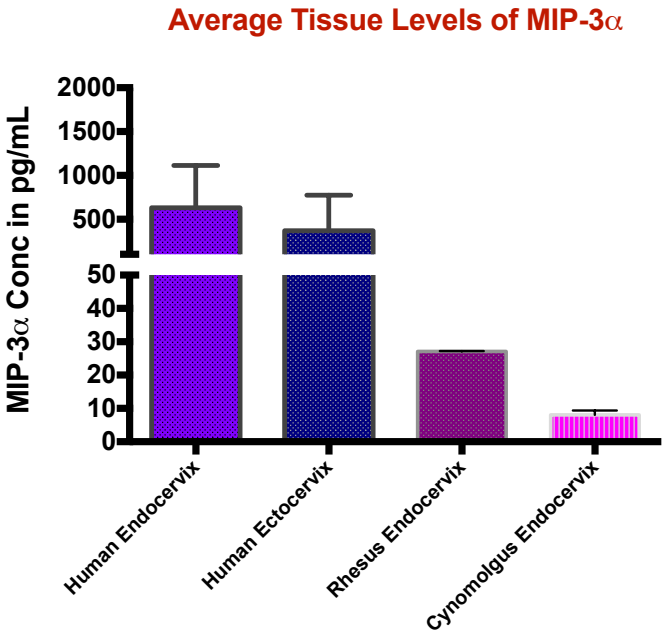

Figure 7.2 Bar graph showing mean constitutive levels with standard deviation of MIP-3α (pg/mL) measured in unstimulated EET of human beings (n=6) and 2 macaque species studied (RM and CM: n=3 each). We incubated EET in complete RPMI-1640 medium for 24 hours before harvesting supernatants. We seeded EET one per well; each test condition was tested in triplicate. MIP-3α levels were measured on Elisa and Luminex immunoassays. Human levels of MIP-3α were at least 100-fold higher than in macaques in the EET model.

in supernatants of RM and CM EET with the Luminex assay platform: MIP-3α constitutive secretion was demonstrated across both the macaque species studied. We had also previously studied constitutive secretion of MIP-3α in the human EET prepared in exactly the same manner as macaque EET and showed its constitutive secretion also in this model. We noted, however, that while both EET models demonstrated constitutive MIP-3α levels, they were lower in the macaque models. CM levels were lowest, followed by levels in RM and the humans with a mean of 7.2pg/mL, 27.1pg/mL, and 600pg/mL, respectively (*Figure 7.2*). These findings, that both humans and macaques secrete MIP-3α constitutively, suggest that MIP-3α has a homeostatic function in the endocervices of both species, however, the extent to which various exogenous stimuli trigger further secretion is not known. We therefore set out to study stimulated patterns of MIP-3α secretion, stimulating with various microbial preparations.

The Macaque EET do not secrete further MIP-3α in response to stimulation by either TLR ligands or various viral constructs.

In view of demonstrable constitutive baseline levels of MIP-3α, we proceeded to stimulate the macaque EET with various TLR ligands (one through to six) and relevant viral preparations (whole infectious SIVmac251 virus and two envelope preparations of SIVmac251) as studied previously in the human EET in order to determine the effect that stimulation has on levels of MIP-3α in the macaque EET. Specifically, we prepared EET on receiving hysterectomy specimens as described in the section above except that we also added various stimulants to a maximum volume of 200μL of media per well prior to incubation at 37^0C 5% CO_2. We harvested supernatants 24 hours post stimulation and incubation, and estimated

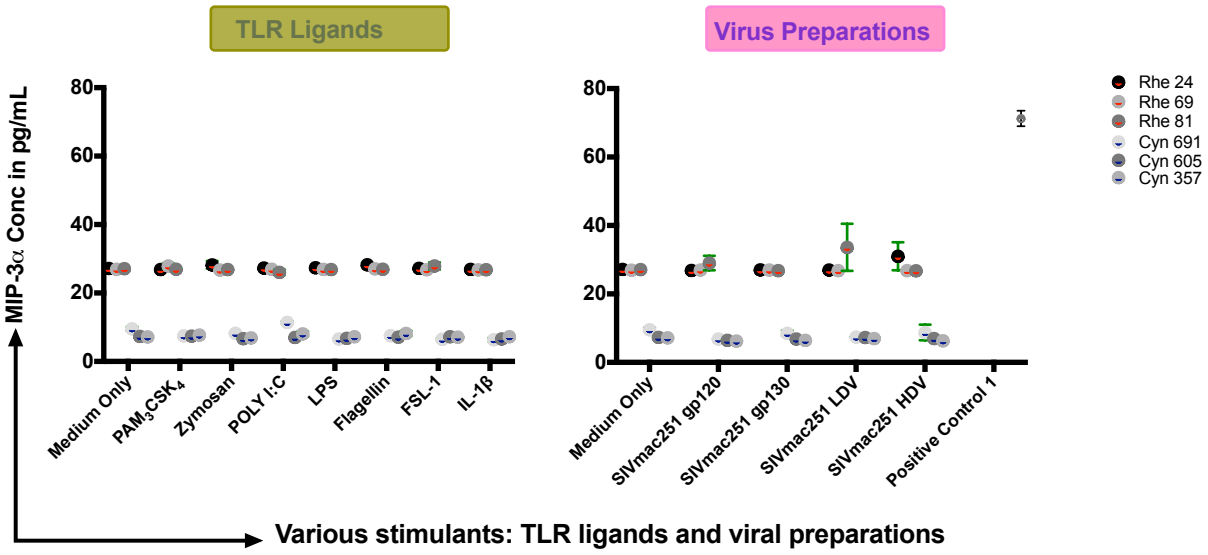

Figure 7.3 Dot schematic showing median levels of MIP-3α with range (pg/mL) measured in unstimulated (medium only) and stimulated EET in the two macaque species (RM and CM). We stimulated EET with various stimulants for 24 hours before harvesting supernatants. We seeded EET one per well; each test condition was tested in triplicate. Stimulants used included TLR ligands 1 through 6 and various viral preparations: whole infectious virus and envelope glycoproteins prepared from SIVmac251 (infectious SIVmac251 - LDV: 5*10 TCID50/mL, HDV: 5*10^5 TCID50/mL, recombinant SIVmac251 gp130 at 100ng/mL and native SIVmac251 gp120 at 100ng/mL). IL-1β was used as a positive control. MIP-3α levels were measured with the Luminex multiplex bead immunoassay. MIP-3α was secreted constitutively in both RM and CM. However, stimulating EET did not trigger further elevation of MIP-3α levels above constitutive levels in either species. Levels of MIP-3α were higher in RM versus RM, irrespective of stimulating agent.

MIP-3α levels by the Luminex multiplex bead assay. Neither TLR ligands nor viral preparations triggered further measurable levels of MIP-3α than those already detected constitutively in both the macaque species studied (*Figure 7.3*). Furthermore, levels of MIP-3α remained higher in RM than in CM, regardless of type and concentration of stimulant used. These findings were similar to findings in the human EET model, namely that after 24 hours of stimulation with various pathogen-associated molecular patterns (PAMPs) and viral preparations, this endocervical model is not responsive to microbial stimulation as far as MIP-3α

secretion is concerned. These data indicate that MIP-3α does not form part of the very first responses to incoming microbes in the EET. Neither the viral envelope nor the whole virus triggers its secretion in the first 24 hours post exposure to virus, and hence MIP-3α is unlikely to have any function beyond the homeostatic one in the first 24 hours post microbial exposure. The next question to answer was therefore that of whether this insensitivity of EET to stimulants was unique only to MIP-3α or whether it was the general response of the EET to microbial exposure with regards to the full range of cytokines in the panel.

Macaque EET do respond to stimulation by various viral preparations and TLR ligands with regards to secretion of other cytokines: whole infectious virus up-regulates IL-2 while viral envelope preparations and flagellin down-regulate IL-17A.

We studied a wide range of cytokines secreted by EET in response to stimulation with various viral preparations and TLR ligands. Studying a wide range of cytokines was particularly important, as we had learned in the human EET that contrary to other cytokines, the MIP-3α response pattern was relatively unique in this model in that MIP-3α secretion was not triggered by exposure to viral preparations and TLR ligands. Human EET on the other hand had responded significantly and differentially to other TLR ligands but not viral preparations with regards to the secretion of other cytokines in this model. We again prepared EET on receiving hysterectomy specimens and added various stimulants to a maximum volume of 200μL of media per well prior to overnight incubation at 37^0C 5% CO_2. We harvested supernatants 24 hours post stimulation and incubation, and measured levels of 10 other cytokines by the Luminex multiplex bead assay. Initial analysis of macaque EET identified constitutive secretion (medium only) of a wide

range of soluble proteins by the endocervices of both species (*Figures 7.4A. and B.*). Secondly, levels of most cytokines in the panel, comparing unstimulated levels (medium only) of cytokines to stimulated levels of cytokines, stimulating with various stimulants, were not further elevated above baseline on exposure to the stimulants. This was certainly the case with almost all stimulants in RM shown by data presented in stacked columns (*Figure 7.4A.)*. Thirdly, as already observed above with MIP-3α (*Figure 7.3*) and unstimulated cytokines (*Figure 7.1*), the levels of stimulated cytokines were higher in RM than in CM (*Figures 7.4A. and B.*). However, assessing the impact of individual stimulants on individual cytokines as presented in a dot schematic, IL-2 levels were elevated further above baseline when stimulated with the high dose of SIVmac251 infectious virus (*Figure 7.5*).

We then proceeded to study cytokines that were either up- or down-regulated following exposure to various viral and TLR ligand stimulants. We defined a significant fold change as a change of at least 1.5, dividing stimulated levels by those of unstimulated levels for respective cytokines in this analysis. Moreover, statistical significance was defined as a p-value of <0.005. Applying this definition in RM (*Figure 7.6A.*), IL-2 was up-regulated 2-fold (p-value=0.039) following exposure to high dose SIVmac251 whole virus while IL-17A was down-regulated 2-fold following exposure to SIVmac251 gp130 (p-value=0.0285) and SIVmac251 gp120 (p-value=0.0431), and all these fold changes reached statistical significance. Likewise in CM (*Figure 7.6B.*), IL-2 was up-regulated 2-fold (p-value=0.1324) following exposure to high dose SIVmac251 virus and IL-4 was up-regulated 2-fold (p-value=0.4208) following exposure to PAM_3CSK_4 but these fold changes did not reach statistical significance. Again in CM, IL-17A was

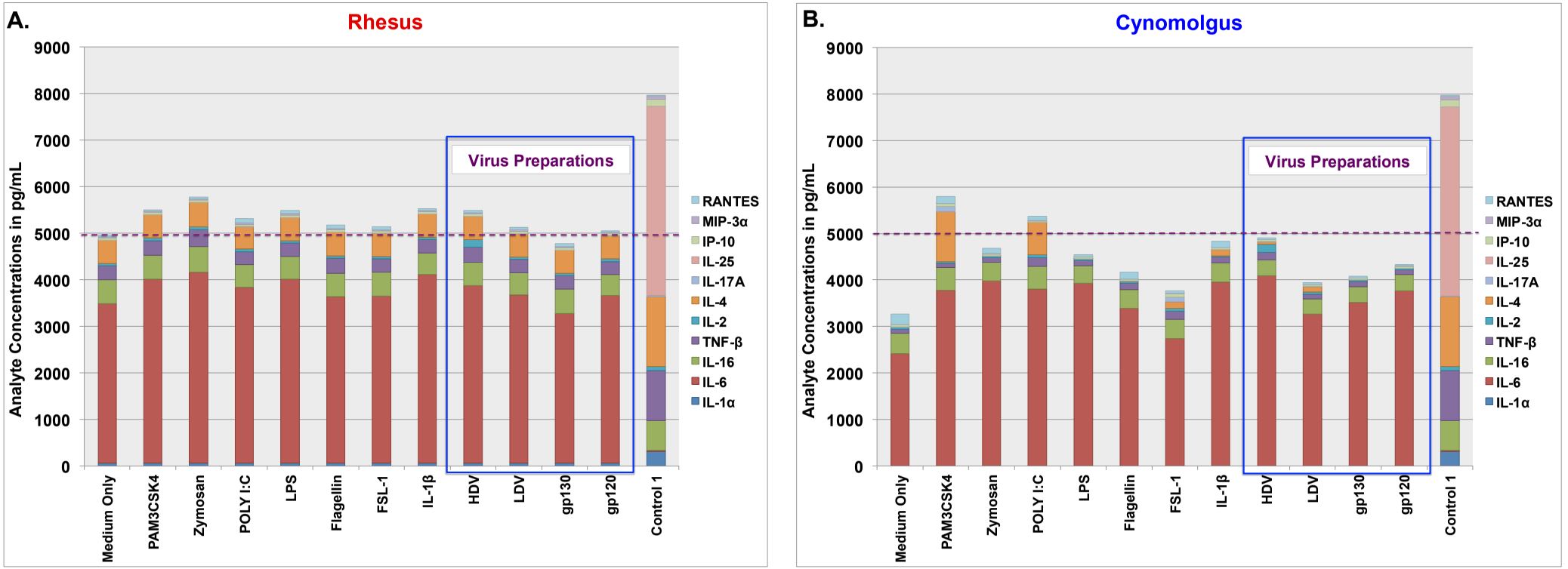

Figure 7.4: Stacked columns showing stimulated levels of 11 cytokines stimulating with TLR ligands 1 through 6, and whole and two envelope SIV preparations, RM: n=3 and CM: n=3. Specifically we stimulated with whole infectious virus and envelope glycoproteins prepared from SIVmac251 (infectious SIVmac251 - LDV: 5*10 TCID50/mL, HDV: 5*10^5 TCID50/mL, recombinant SIVmac251 gp130 at 100ng/mL and native SIVmac251 gp120 at 100ng/mL). IL-1β was used as a positive control. We prepared endocervical explant tissues from post mortem macaques. We plated one explant tissue block per well in a 96 well tissue culture plate in 200µL of medium. Conditions were tested in triplicate. Supernatants were harvested 24 hours post stimulation. Levels of all cytokines were quantified in supernatants with the Luminex multiplex bead immunoassay. Levels of cytokines secreted by EET, both stimulated and unstimulated, were higher in RM (A.) than in CM (B.).

significantly down-regulated 2-fold following exposure to SIVmac251 gp120 (p-value=0.0193) and flagellin (p-value=0.0219) and these fold changes reached statistical significance. These findings therefore suggest that IL-2 is up-regulated by exposure to high dose virus while IL-17A is down-regulated by exposure to flagellin and viral envelope preparations. These data provide evidence that the EET is not completely unresponsive to exogenous stimulation, but rather imply that the lack of response observed for MIP-3α is purely a reflection of the unique interaction between the various stimulants used and MIP-3α in the EET. These data further suggest that, while MIP-3α does not form part of the initial responses to microbial exposure in the first 24 hours in the EET, however IL -2 and IL-17A do form part of initial responses to different SIV preparations in this same period in the EET. IL-2 is the very first mucosal cytokine to respond to SIVmac251 whole virus exposure in the EET and viral constituents other than the envelope proteins appear to be responsible for triggering its secretion. Similarly to IL-2, IL-17A also responds to microbial exposure in the first 24 hours post microbial exposure but its response is opposite to that of IL-2. IL-17A responds by being down-regulated in the same period and this response is seen only in response to envelope proteins and not the whole virus. This same response is also seen in response to flagellin, a TLR5 ligand.

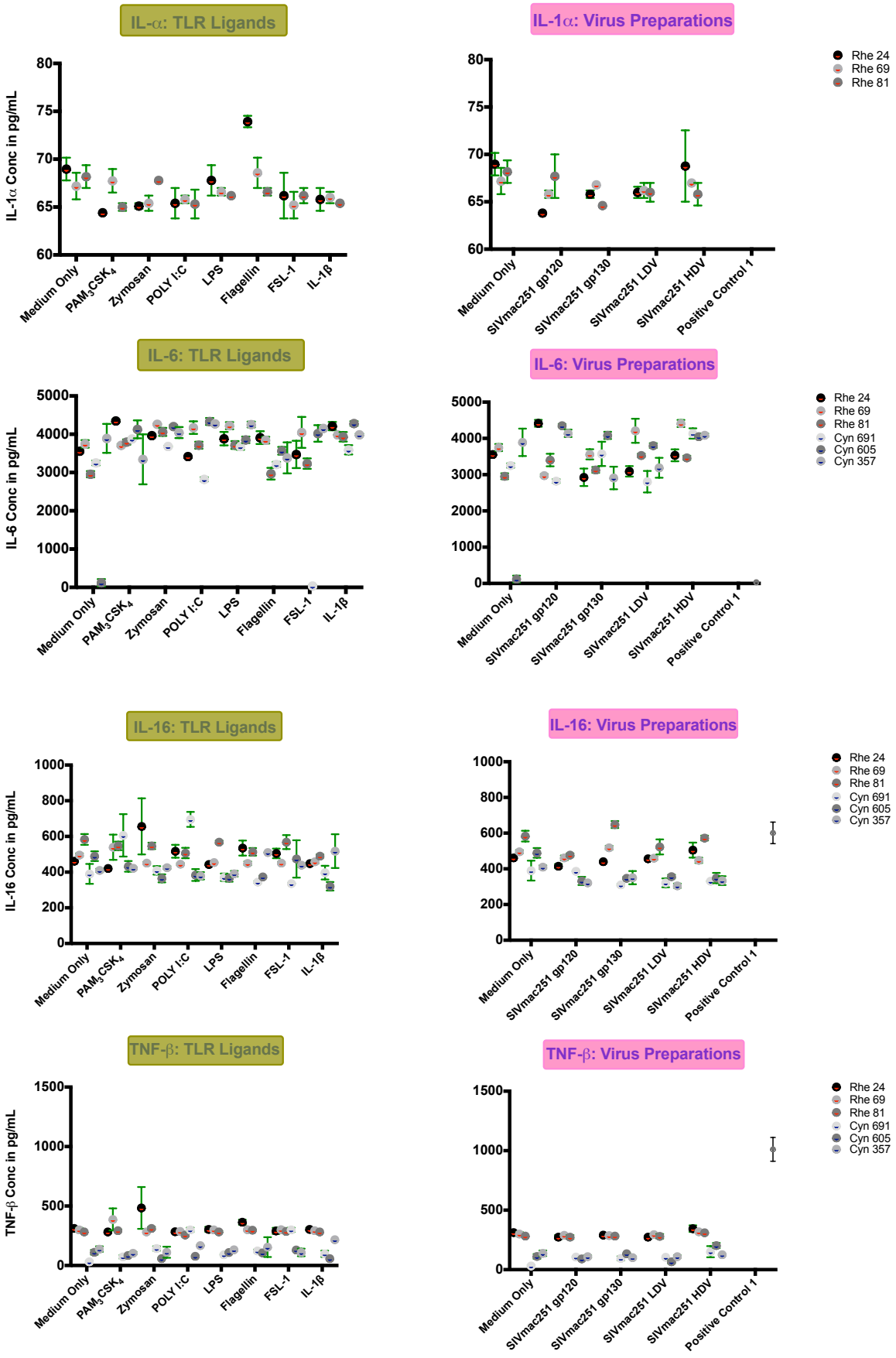
IL-α: TLR Ligands
IL-1α: Virus Preparations
IL-1α Conc in pg/mL
80
75
70
65
60
Medium Only
PAM3CSK4
Zymosan
POLY I:C
LPS
Flagellin
FSL-1
IL-1β
SIVmac251 gp120
SIVmac251 gp130
SIVmac251 LDV
SIVmac251 HDV
Positive Control 1
Rhe 24
Rhe 69
Rhe 81
IL-6: TLR Ligands
IL-6: Virus Preparations
IL-6 Conc in pg/mL
5000
4000
3000
2000
1000
0
Cyn 691
Cyn 605
Cyn 357
IL-16: TLR Ligands
IL-16: Virus Preparations
IL-16 Conc in pg/mL
1000
800
600
400
200
0
TNF-β: TLR Ligands
TNF-β: Virus Preparations
TNF-β Conc in pg/mL
1500
1000
500

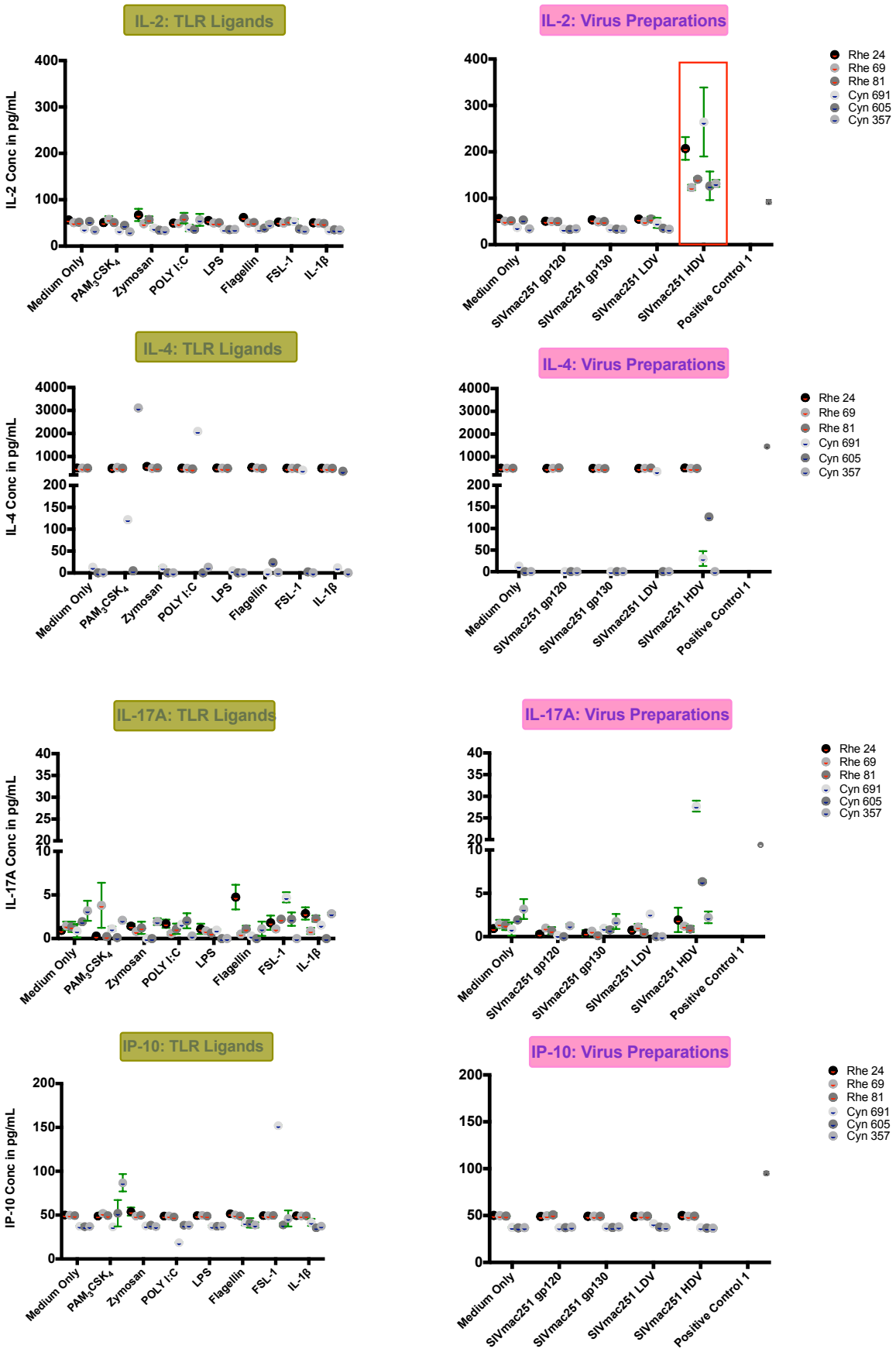
IL-2: TLR Ligands
IL-2 Conc in pg/mL
400
300
200
100
0
Medium Only
PAM3CSK4
Zymosan
POLY I:C
LPS
Flagellin
FSL-1
IL-1β
IL-2: Virus Preparations
SIVmac251 gp120
SIVmac251 gp130
SIVmac251 LDV
SIVmac251 HDV
Positive Control 1
Rhe 24
Rhe 69
Rhe 81
Cyn 691
Cyn 605
Cyn 357
IL-4: TLR Ligands
IL-4 Conc in pg/mL
4000
3000
2000
1000
200
150
100
50
0
IL-4: Virus Preparations
IL-17A: TLR Ligands
IL-17A Conc in pg/mL
40
35
30
25
20
10
5
0
IL-17A: Virus Preparations
IP-10: TLR Ligands
IP-10 Conc in pg/mL
IP-10: Virus Preparations

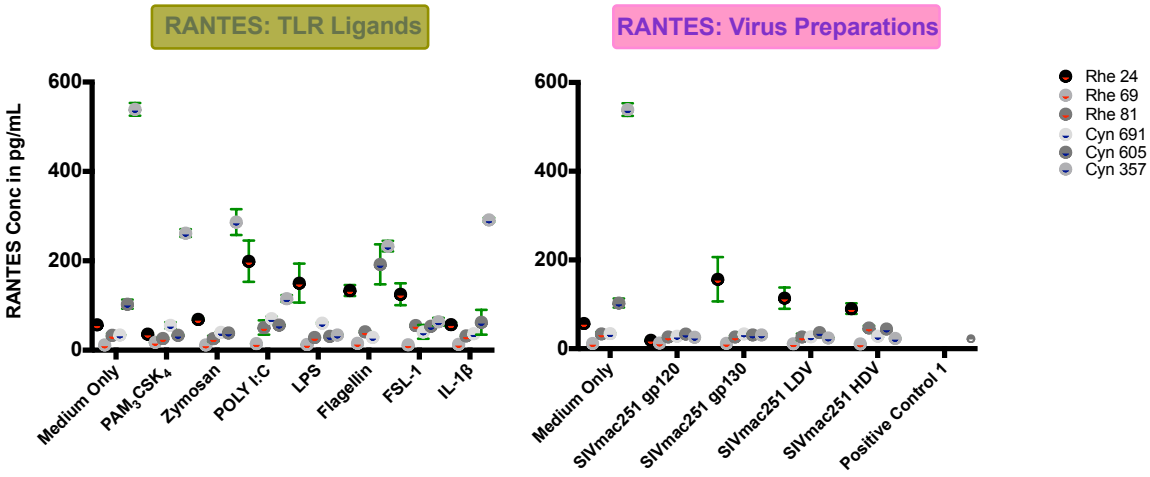

Figure 7.5 Dot plot schematic showing median levels of various cytokines with range (pg/mL) measured in unstimulated (medium only) and stimulated EET in the two macaque species (RM and CM) studied. We stimulated EET with various stimulants for 24 hours before harvesting supernatants. We seeded EET one per well; each test condition was tested in triplicate. Stimulants used included TLR ligands 1 through 6 and various viral preparations constructed from SIVmac251, whole virus and envelope glycoproteins (infectious SIVmac251 - LDV: 5*10 TCID50/mL, HDV: 5*10^5 TCID50/mL, gp130: recombinant SIVmac251, gp120: native SIVmac251). IL-1β was used as a positive control. Cytokine levels were measured with the Luminex multiplex bead immunoassay. Nine and eight cytokines were secreted constitutively in RM and CM, respectively. However, stimulating EET did not trigger further elevation of all measurable cytokines above constitutive levels in either species except for IL-2 in both species. Levels of TNF-β, IL-4, and IP-10 were higher in RM versus RM, irrespective of stimulating agent.

A.

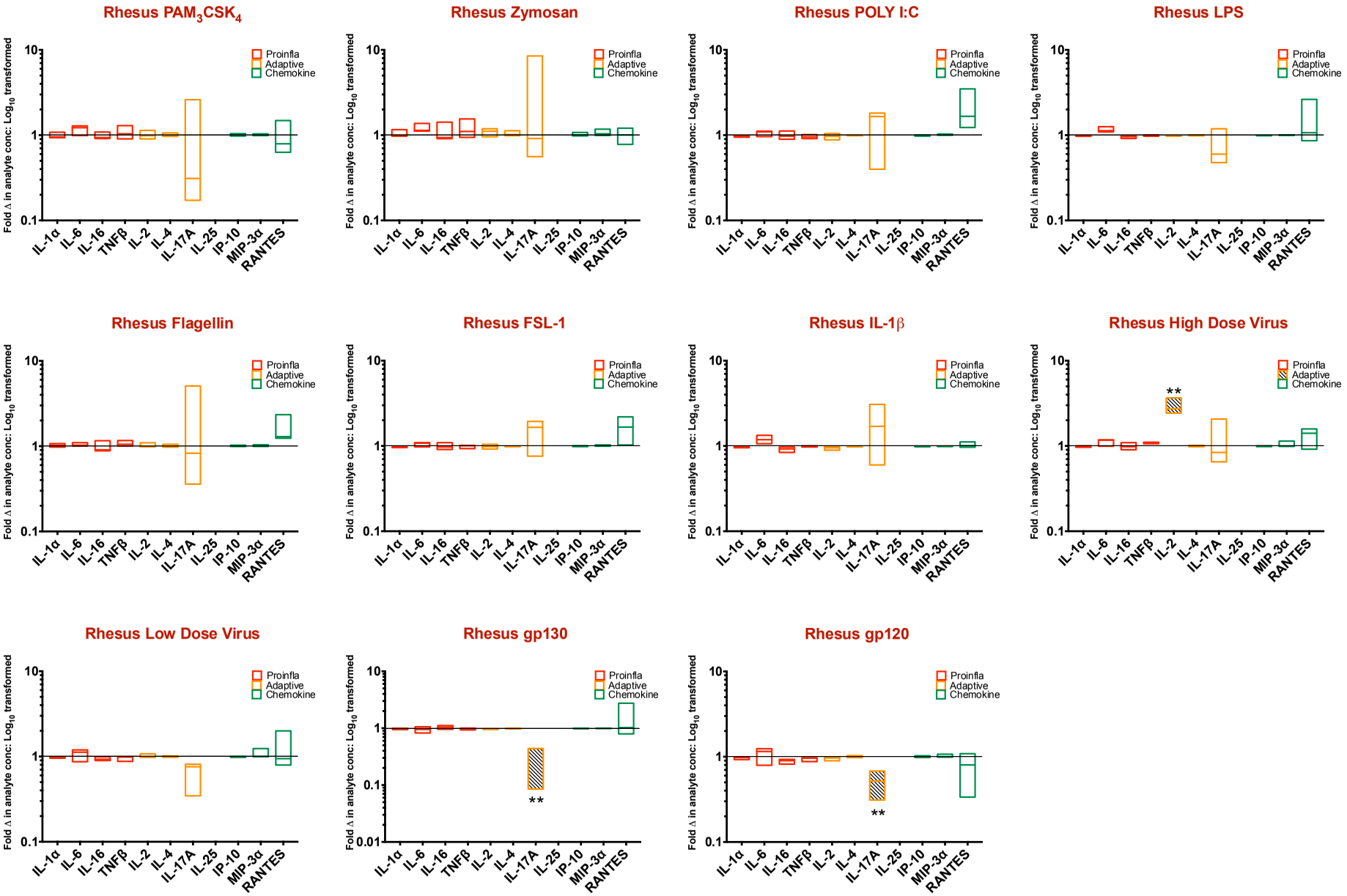
Rhesus PAM3CSK4
Rhesus Zymosan
Rhesus POLY I:C
Rhesus LPS
Rhesus Flagellin
Rhesus FSL-1
Rhesus IL-1β
Rhesus High Dose Virus
Rhesus Low Dose Virus
Rhesus gp130
Rhesus gp120
Proinfla
Adaptive
Chemokine
Fold Δ in analyte conc: Log10 transformed
IL-1α
IL-6
IL-16
TNFβ
IL-2
IL-4
IL-17A
IL-25
IP-10
MIP-3α
RANTES
**

B.

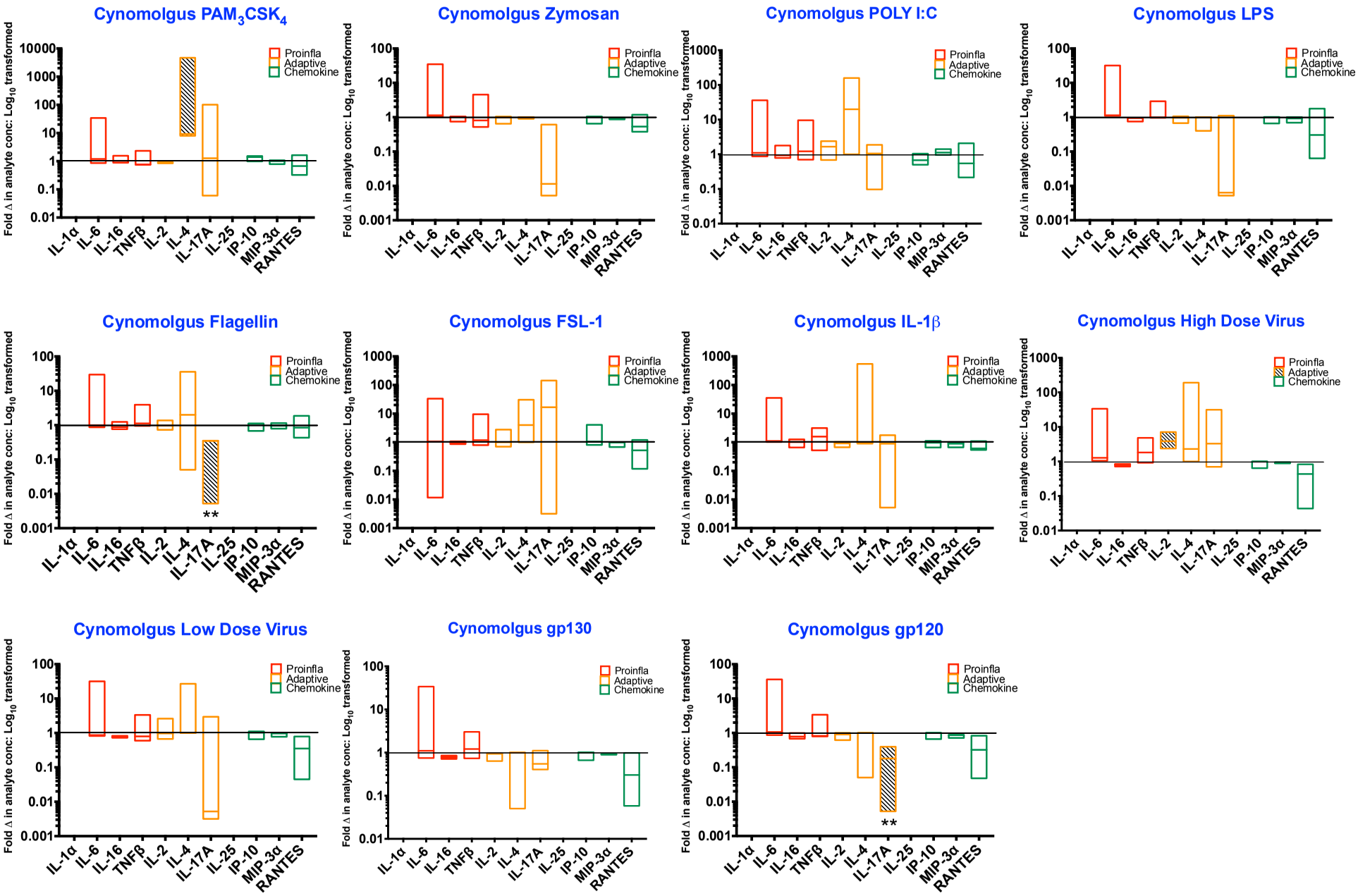
Cynomolgus PAM3CSK4
Cynomolgus Zymosan
Cynomolgus POLY I:C
Cynomolgus LPS
Cynomolgus Flagellin
Cynomolgus FSL-1
Cynomolgus IL-1β
Cynomolgus High Dose Virus
Cynomolgus Low Dose Virus
Cynomolgus gp130
Cynomolgus gp120
Proinfla
Adaptive
Chemokine
Fold Δ in analyte conc: Log10 transformed
IL-1α
IL-6
IL-16
TNFβ
IL-2
IL-4
IL-17A
IL-25
IP-10
MIP-3α
RANTES
**

Figure 7.6 Floating bars showing the impact of each stimulant on each cytokine – the horizontal line within the bar represents median while the outer horizontal lines represent minimum and maximum values. Cytokine levels were measured with the Luminex multiplex bead immunoassay. Cytokine fold changes were calculated by dividing the stimulated values by the unstimulated values. Significantly up- and/or down-regulated cytokines are defined by a fold change of at least 1.5 and are denoted by striked bars. One sample t test was employed to test the statistical significance of the fold change from one. Statistically significant fold changes as defined by a p-value < 0.05 are denoted with an asterisk. RM (n=3) (A.) are plotted separately from CM (n=3) (B.). IL-2 is up-regulated by exposure to high dose virus (infectious SIVmac251 5*10^5 TCID50/mL) in both the macaque species while IL-4 is up-regulated by exposure to PAM_3CSK_4 in CM. IL-17A is down-regulated by exposure to SIVmac251 gp120 in both the macaque species while it is also down-regulated by exposure to SIVmac251 gp130 in RM and flagellin in CM.

Table 7.2 Summary of up- and down-regulated cytokines in the macaque EET following stimulation with various stimulants: TLR ligands and virus preparations

Stimulant	Rhesus	Cynomolgus	Rhesus	Cynomolgus
	Upregulated		Downregulated	
Pam_3CSK_4 (TLR1/2)		↑ IL-4		
Zymosan (TLR2)				
Poly I:C (TLR3)				
LPS (TLR4)				
Flagellin (TLR5)				↓IL-17A*
FSL-1 (TLR2/6)				
IL-1β				
SIVmac251 HDV	↑ IL-2*	↑ IL-2		
SIVmac251 LDV				
SIVmac251 gp130			↓IL-17A*	
SIVmac251 gp120			↓IL-17A*	↓IL-17A*

* denotes statistically significant changes: p-values less than 0.05

DISCUSSION

We studied the pattern of secretion of MIP-3α, constitutive and stimulated, in the EET of macaques: three RM and three CM. We also studied the pattern of secretion of 10 other cytokines, constitutive and stimulated, in the EET of the same macaques. This followed on from our findings in the human EET which showed that levels of MIP-3α are not further elevated on exposure to HIV-1 preparations, a finding that was contrary to empirical reports in the literature based on previous findings in macaques [96, 230, 231]. The purpose of conducting these experiments was two-fold: to compare and contrast baseline and early epithelial responses in humans to those in macaques with regards to MIP-3α and to identify other factors that might be an equivalent of MIP-3α in the initial HIV infection events in humans. Identifying these factors and comparing responses in macaque and human tissues contributes towards understanding these important early events in SIV/HIV infection.

Constitutive MIP-3α levels were high in the EET of macaques according to the findings in our study. This was not the first time that high constitutive levels of MIP-3α have been demonstrated in the endocervix of macaques. Data from the study by Li *et al*. also demonstrated high constitutive MIP-3α levels in the macaque endocervix *in vivo* [96]. Moreover, their data suggested that levels of MIP-3α were even higher following exposure to SIV, which was not the case in our *in vitro* studies. Furthermore, in their study, over and above the epithelial response to virus involving the MIP-3α secretion, there were also concurrent innate and inflammatory responses in the tissues evoked by exposure to the virus preparation. However, treating tissues with glycerol-monolaurate (GML), an anti-

inflammatory compound, quenched all these responses i.e. MIP-3α secretion, inflammation and the other innate responses, *in vitro* [96]. Thus over and above the secretion of MIP-3α as an initiation step to productive infection, the role of inflammation in promoting productive infection was also highlighted. After reviewing the original report and our own data, we propose that it is likely that the high levels of sub-epithelial MIP-3α seen in the Li *et al* study were due to inflammation rather than simply to viral exposure. The original paper does not provide details of how the SIV preparation used to infect the macaques was prepared, but we speculate that it may have contained inflammatory ingredients that led to the reported results. Contrary to the findings in the Li *et al* study, we did not see any evidence of inflammation in the tissues we studied, which might account for the lack of elevated levels of MIP-3α.

MIP-3α, a chemokine, is a small pro-inflammatory peptide, which functions to attract leucocyte populations to sites of inflammation, and hence its levels are highest in the presence of inflammation. Following its discovery in the 1990's, MIP-3α was mapped to inflamed tonsillar sites [87]. Later, MIP-3α was shown to be inducible *in vitro* by mediators of inflammation such as ionomycin, TNF-α, and IL-1β while being down-regulated by the anti-inflammatory cytokine IL-10 [90]. Research in this thesis showed in an earlier chapter that MIP-3α levels were elevated five-fold in the presence of abnormalities suggesting underlying inflammation in cervicovaginal fluid (CVF). Furthermore, in the context of HIV-1 infection in Africa where the prevalence of inflammatory vaginal conditions and HIV-1 are highest, the presence of high MIP-3α levels were associated with an increased risk of HIV-1 infection in two landmark studies [232, 233]. Evidently then, based on macaque and human studies, inflammation is as much a

necessary accompaniment to productive infection as it is to enhancing tissue MIP-3α levels - this is assuming that high levels of MIP-3α are necessary in the pathway to infection, as discussed in the previous studies. It is hence likely that viral exposure, in the absence of inflammation, does not elicit further secretion of MIP-3α. This is particularly important as the tissues we studied did not have any overt inflammation and could thus explain the absence of response of EET to viral exposure. This study did not study the pathogenesis of infection but it investigated whether MIP-3α levels are elevated after viral exposure, which we have shown is not the case. Interestingly, though, data in our study showed that IL-17A, a cytokine known to be pro-inflammatory and hence up-regulated in the presence of inflammation following microbial invasion, was down-regulated in our analysis [234]. This could be further of evidence that there was no inflammation in the tissues we studied, accounting for the lack of elevation of MIP-3α levels in the EET.

Our experiments indicate that viral exposure, to either envelope glycoproteins or whole virus, does not induce further MIP-3α secretion in the EET of macaques: at least this is the case during the first 24 hours post viral exposure, measuring MIP-3α levels with the quantitative Luminex multiplex bead assay. This is in contrast to the findings in the one other study to date that looked at MIP-3α in the context of SIV infection in the FGT, the landmark study conducted by Lie *et al* [96] and recently confirmed by the same group in another publication [230]. The findings of this group employing the use of immunohistochemical techniques and quantitative image analysis methods suggested that exposure of epithelium to SIV preparations triggered secretion of further MIP-3α in the macaque endocervix *in vivo*. Of note, however, is that these findings were coincidental to the primary

questions of their study. In contrast to our study, which was designed to answer the question of MIP-3α response on epithelial exposure to oncoming virus, their study had not been designed primarily to answer the question of epithelial response to viral exposure in the context of MIP-3α. Secondly, these two authors used the same samples that had originally been collected and stored down for later use from a single experiment, and hence the results of the second analysis can hardly be considered as being confirmatory of the initial analysis. Furthermore, they conducted only imaging techniques, immunohistochemical and tissue quantitative image analytical techniques, to identify and estimate levels of MIP-3α in tissue, which is not the same as conducting Luminex protein quantitative assays which are likely to be more sensitive to changes in protein quantities. Our study was broader, being inclusive of EET exposure to different viral constituents and concentrations, while theirs looked at responses following exposure to at least two inoculations of the same high dose preparation (10^5 TCID50/mL) of pathogenic SIVmac251. Hence, having evaluated the association between MIP-3α secretion and viral exposure from different angles, we conclude that exposure to pure viral constituents does not trigger MIP-3α secretion in the endocervix of either macaques or humans.

Constitutive MIP-3α levels in humans were 100-fold higher versus those of macaques in our analyses. While humans differed from macaques in this one regard, on the other hand, they were similar in that none of the viral preparations employed elicited further levels of MIP-3α by EET in samples from both species. Performing the analyses of MIP-3α responses side by side in humans and in macaques in this analysis was therefore highly informative in understanding the role of MIP-3α - or the lack thereof - in the initial infection events in the endocervix.

If the endocervix was at all sensitive to viral exposure with regards to MIP-3α secretion, it would have at least responded by increasing MIP-3α levels in macaque tissue, where the starting levels were very low. We could not expect the same for human beings as the human EET already secreted very high constitutive MIP-3α levels. If we assumed, therefore, that pre-viral exposure levels needed to be low in order to be ignited into secreting higher levels of MIP-3α by viral exposure, then we would argue that we would have observed a response to viral exposure in the macaque EET, which was not the case. Further, using varying doses and varying preparations of virus did not make a difference. This highlights once again that an additional factor (or factors) is probably required for increased levels of MIP-3α to be secreted in response to viral exposure which would fuel productive infection.

While analysing human data alongside macaque data was informative in our understanding of the lack of a role for MIP-3α in the initial infection events in the endocervix, analysis of a wide range of cytokines simultaneously was helpful in pointing us towards identifying the cytokine(s) that might be relevant in the initial infection events in the endocervix of macaques. While the EET of macaques did not respond to virus by secreting further MIP-3α, it did however respond by secreting further IL-2 on exposure to whole pathogenic virus, even though this reached statistical significance only in the RM model. This further suggests that, if there was ever going to be any MIP-3α response to viral exposure i.e. if a biological relationship existed between virus exposure and MIP-3α secretion in the epithelium of the endocervix, then we would have seen it with the various stimulants studied. The endocervix in itself is not entirely unresponsive to viral exposure, and neither are the stimulants used completely inactive with regards to

the EET. This suggests that the EET itself is not problematic as a model but rather that MIP-3α is simply not secreted on exposure to a pure virus preparation in the endocervix.

CD4+ T cells are the primary target of both HIV and SIV in the FGT [156, 235]. In the study by Li *et al*, accumulation of SIV RNA+ CD4+ T cells in the infected foci was larger than could be explained on pure recruitment of CD4+ T cells by virus alone [96]. Hence they documented the growth of clusters by accretion of new infections in influxes of CD4+ T cell targets secondary to innate immune and inflammatory responses involving the MIP-3α "outside-in" signaling cascade, believed to be triggered by exposure of epithelium to SIV. In our study MIP-3α was not up-regulated but instead IL-2 was. IL-2 was one of the first cytokines to be discovered and is produced mainly by activated T cells, particularly CD4+ T-helper (Th) cells [236]. It has a potent capacity to enhance *in vitro* T-cell proliferation and differentiation, and is also reported to aid differentiation of naive T cells into effector and memory cells. Together with interferon gamma (IFN-γ) and lymphotoxin- alpha (LT- α), they are secreted by Th1 lymphocytes and stimulate type 1 responses. Hence it could be that rather than MIP-3α ultimately leading to the recruitment of CD4+ T cells, IL-2, the secretion of which is evidently triggered by SIV exposure in our study, contributes to the high density of CD4+ T cells in the endocervix at the time of exposure to virus instead of MIP-3α.

Conversely, IL-17A was down-regulated by viral envelope preparations. IL-17A is a potent pro-inflammatory cytokine mainly produced by specialised T cells, the IL-17A-producing CD4+ T cells called Th17 [237]. IL-2 forms part of the T helper type 1 (Th1) response while IL-17A forms part of the T helper type 17 (Th17) response.

The Th17 lineage constitutes a branch of the immune system which has a function in the clearance of specific types of pathogens that require a massive inflammatory response and are not adequately dealt with by Th1 or Th2 immunity [238]. The suppression of the Th17 response, hence reflecting reduced inflammation, would probably be the reason that MIP-3α levels were not high in these experiments. Type 1 responses include activation of other cell types such as endothelial cells, keratinocytes and fibroblasts to secrete pro-inflammatory cytokines [239]. It is interesting therefore that in this study the EET would secrete higher levels of IL-2 (we did not measure IFN-γ and LT-α) in the first 24 hours post viral exposure. This response might be regarded as helpful in order to enhance T cell activity, while also enhancing the rest of the environment for productive infection by boosting the inflammatory response. However, in the first 24 hours post viral exposure there was no detectable inflammatory response elicited, as already mentioned above which could reflect the absence of the more potent pro-inflammatory effect of the Th17 response.

One might argue that these results are due to the model we studied i.e. the explant tissue model, but it is not always practical and feasible to do *in vivo* studies. Explants are more representative of *in vivo* conditions, in that they allow for studies on morphology and function as normal interactions of all immune cells with each other, where the extracellular matrix of the tissue is preserved. They are hence a bridge between *in vitro* and *in vivo* situations and they have proved to be useful models to identify early targets of infection and to address potential mechanisms by which infectious virus traverses the mucosal surfaces [109].Their greatest strength is that they do not disrupt the natural organisation of the tissues, and they preserve the interactions between the epithelial cells and the underlying

stromal cells. They are the best model for studies aiming to identify existing biological associations (if they exist), and consequently, predictions for situations in living tissues can be inferred [240]. As much as it is not feasible always to study macaques alongside human beings, we should by all means strive towards doing this, as there are differences between macaques and human beings and it is not always easy to predict where there will be differences and what will be the extent of the differences where they exist.

CONCLUSION

We conclude that, while MIP-3α levels are readily detectable constitutively in macaque endocervix, they are however not triggered further by viral exposure alone in the first 24 hours after exposure to pure viral stocks. These data suggest that while MIP-3α has a homeostatic role to play in the macaque endocervix, as its constitutive secretion is readily detectable, it does not however have a significant role to play in the first 24 hours of SIV/HIV infection in the mucosa. IL-2 was up-regulated while IL-17A was down-regulated which suggests the dominance of the Th1 responses over the Th17 responses on exposure to SIV in the macaque endocervix.

CHAPTER EIGHT DISCUSSION and SUMMARY

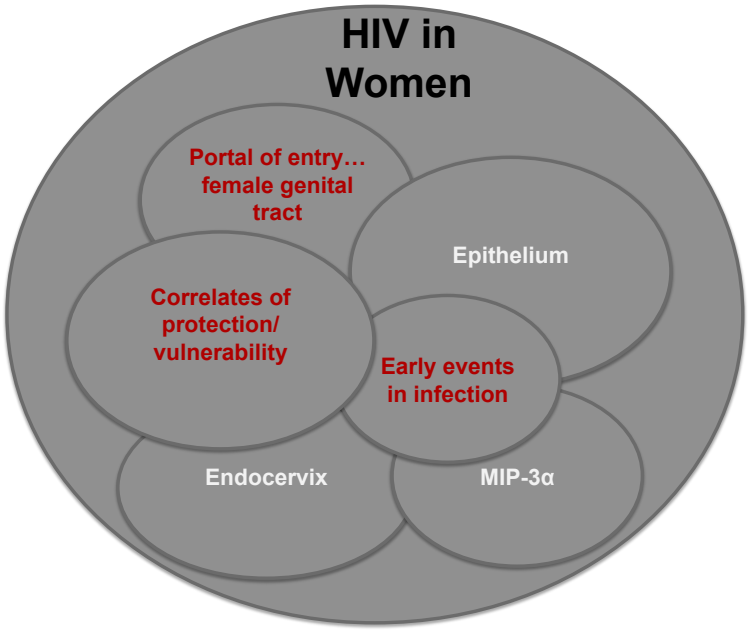

Figure 8.1: Schematic of the background concepts in the field of HIV infection that this thesis has brought together

This thesis has attempted to address one of the pressing challenges in the field of infectious diseases in the 21st century: the issue of Human Immunodeficiency Virus (HIV) infection in women. Women continue to bear the brunt of the disease yet there are hardly any biomedical preventive strategies that they can use to protect themselves against HIV acquisition. Whereas globally an estimated 50% of new HIV infections were in women in 2015, in sub-Saharan Africa alone an estimated 57% new HIV infections were in women, with 25% being in young girls between the ages of 15 and 24 years [2, 103]. Sub-Saharan Africa is known to be home to the overwhelming majority of both incident and prevalent HIV infections worldwide. From the early 2000s there have been calls to focus on and prioritise three research areas within the HIV field: (i) to design research aimed at

understanding reasons for increased vulnerability to HIV infection in women, (ii) to focus research on studying correlates of protection at the portal of viral entry where there are initial HIV-host defence interactions, and to (iii) study innate immunity at the mucosal epithelial frontline as this surface has emerged as a significant mediator of the body's defences against microbes early in infection. This was with the understanding that prioritising these areas will enhance and inform development of appropriate biomedical HIV preventive strategies and thereby reducing HIV incident rates. Consequently this thesis responds to these background concepts and needs of the HIV field as recently identified.

SECTION A: THESIS BACKGROUND CONCEPTS

A.1 Women bear the brunt of HIV infection:

Heterosexual transmission is understood to be the most common risk factor for acquisition of HIV-1 in women, overtaking other modes of transmission such as injection drug use. There has been a steady escalation of HIV-1 incident infections in women from the early 1980s, when only a few women were infected with HIV to the early 2000s when women came to bear the brunt of the HIV epidemic [37]. Hence the literature describes the "feminisation" of the acquired immune deficiency syndrome (AIDS) pandemic referring to the dominance of HIV infection proportions in women over men [38]. Increased vulnerability in women is multifactorial ranging from behavioural to biological causes. Stein argued that women in sub-Saharan Africa, where feminisation of HIV-1 is at its worst, are not able to negotiate safer sexual practices and hence biomedical preventive strategies that women can control might hold better hope for this group [39]. However, development has been hindered by poor understanding of correlates of

protection in the female genital tract (FGT). In view of the burden of HIV infection in women in the 21st century, this thesis has therefore focused solely on addressing issues around HIV infection in this risk group. The biological samples we used in this thesis all came from women.

A.2 Portal of HIV entry: mucosal surfaces:

Mucosal surfaces constitute the major portal of entry and transmission route for HIV. Of the estimated 33 million infections, more than 90% gain entry into the body through gastrointestinal and genital tracts with the FGT alone comprising almost 40% [63]. Understanding the overview of mucosal transmission and acute infection based on *in vivo* macaque studies early in the 2000s, and considering the great difficulties that host defences encounter once the lymphatic reservoir is established, Pope *et al* proposed that the focus of studies on HIV prevention should focus primarily at the beginning of transmission i.e. at the mucosal barriers during the initial interaction between virus and the host [241]. Further, in view of the challenges posed by the rapid rate of mutation of HIV that escapes cytotoxic lymphocytes (CTL) and the problems in induction of neutralising antibodies to wild strains of HIV, Lehner concluded that in the context of sexually transmitted HIV infection and the development of its prevention strategies, understanding genital tract mucosal immune responses is as important as understanding peripheral immune responses [242]. This thesis has hence focused on studying mucosal surfaces at the genital tract level, which is the portal of entry in the context of heterosexually transmitted HIV infection in women. Specifically, we have studied biological samples taken from the different sub-compartments of the FGT including the endometrium, endocervix, ectocervix, and cervicovaginal fluid secretions.

A.3 Correlates of protection and innate immunity:

The Global HIV Vaccine Enterprise Working Group declared that understanding natural correlates of mucosal protection and defining the earliest events in mucosally transmitted HIV-1 infection are of central importance for characterisation of the precise virus–host interactions that must be altered by vaccine-induced immune responses [40]. Haynes *et al,* in their publication discussing critical issues in mucosal immunity in the context of HIV-1 vaccine development, expressed the need to define the sequence of events required to establish infection and to elucidate acute mucosal events that need to be prevented by HIV biomedical preventive strategies [44]. This thesis has thus attempted to understand natural correlates of protection and/or vulnerability, particularly focusing on innate immunity to HIV infection at this site. In the different chapters of this thesis we have sought to delineate constitutive secretion patterns of 33 soluble proteins (SPs and antimicrobial peptides (AMPs), secreted by epithelia and stromal cells prior to exposure to HIV infection. Further, the FGT being an immunohormonal system heavily influenced by hormonal fluctuations during the menstrual cycle, we have also investigated the influence of the endocrine system on the innate secretion patterns of the same analytes.

A.4 Early HIV infection: best chance to intervene to prevent HIV infection:

Studies into acute HIV-1 infection in animal models revealed potential viral vulnerabilities at the mucosal portal of entry in the earliest stages of infection that might be most effectively targeted by vaccines and microbicides, thereby preventing acquisition and averting systemic infection [110]. From non-human primate (NHP) studies the critical events following mucosal exposure to high doses of Simian Immunodeficiency Virus (SIV) are as follows: virus can cross the

mucosal epithelial barrier within hours to establish a small founder population of infected cells. This founder population then undergoes a necessary local expansion during the first week of infection to generate sufficient virus and infected cells to disseminate and establish a self-propagating systemic infection throughout the secondary lymphoid organs. Beginning in the second week of infection, replication explodes in the lymphatic tissues where virus has access to many more susceptible target cells in close spatial proximity. Virus levels in blood and tissues peak near the end of this second week of infection, before declining towards relatively stable lower levels by four weeks after exposure. At this time, these infected lymphatic tissues comprise a reservoir where virus is produced and stored and where proviruses are harbored in latently infected cells in SIV-infected rhesus macaques, just as in HIV-1 infected humans. According to the findings of these studies, prevention strategies should therefore target the first week of infection both to take advantage of viral vulnerabilities and to avert the ill effects of systemic infection in the second week and beyond. The first viral vulnerability and opportunity for prevention is related to prevention of the establishment of the small founder population, while the second opportunity is preventing local expansion so that insufficient virus and infected cells are produced to disseminate and establish systemic infection. In accordance with this, we conducted studies on mucosal tissue within the first few hours of viral exposure, thereby exploiting the first proposed opportunity in the first week of infection. Specifically, we studied mucosal responses in the first 24 hours post viral exposure for most experiments, while extending this period to 72 hours post viral exposure for some experiments.

SECTION B: BACKGROUND RESEARCH AND CONCEPTS THIS THESIS HAS BUILT UPON

A recent landmark study looking at the SIV/Rhesus macaque model highlighted the role of the endocervix, the epithelium, and MIP-3α simultaneously in early SIV infection. In this study they noted that the accumulation of SIV RNA+ CD4+ T cells post exposure to virus in a SIV/Rhesus macaque model was preceded by a subepithelial influx of plasmacytoid dendritic cells (pDCs) in the endocervix one day post inoculation (d.p.i.), an effect that was not replicated in the vagina and transformation zone sub compartments [96]. They subsequently showed that this accumulation of pDCs was associated with increased expression of MIP-3α, a molecule which had earlier been shown to be a strong chemoattractant for pDCs [103]. Through a series of experiments they concluded that the exposure and binding of SIV to epithelial cells in the FGT induced an “outside-in” signalling cascade i.e. exposure of endocervical epithelium to the viral inoculum increases the expression of MIP-3α, which in turn recruits pDCs, thereby commencing the sequence of events leading to productive infection. Because these findings had not been replicated in humans and the secretion of MIP-3α by the endocervix on exposure to virus had not been investigated in humans, we embarked on a project that looks at the role of MIP-3α in early HIV infection in humans.

B.1 The endocervix:

To date, there is no agreement about what the primary site of infection of HIV-1 is. In a series of transmission studies and publications Miller *et al* showed that vagina was the primary site of SIV transmission in the SIV/Rhesus macaque model [154, 155]. In their study, the lack of the cervix and uterus did not affect establishment of

SIV infection, a finding strongly suggesting that target cells for SIV were present in the vaginal mucosa. In humans, a woman born without a cervix and uterine body was found to have established HIV infection following heterosexual intercourse through a very short vagina, thus providing further evidence for vaginal HIV transmission [182]. Again in humans, HIV incidence was not lowered in women wearing a diaphragm for HIV prevention in Africa, thus providing further evidence for vaginal transmission of HIV [183]. Evidence that the primary site of infection post exposure to SIV inoculum in animals is the cervix, and particularly the endocervix and transformation zone is fairly recent [96, 110]. Furthermore, Pudney et al showed that the cervix, especially the transformation zone, is the major inductive and effector site for cell-mediated immunity in the lower FGT. Furthermore they showed that the endocervix had a high concentration of intraepithelial lymphocytes and concluded that this provided evidence that the cervix is a primary infection site for HIV-1 (Pudney, Quayle, & Anderson, 2005). In accordance with recent studies suggesting endocervix as the primary site of infection, we focused our studies on the endocervix.

B.2 The epithelium:

Whereas previously the epithelium was thought to function solely as a physical barrier to the passage of microorganisms, it has now become understood that it also has a range of immune functions that regulate infection across the genital epithelium [71, 107]. The distinctive role of the epithelium includes the detection of harmful stimuli through pattern recognition receptors (PRRs) and then to relay this information to the adaptive immune system through secretion and up-regulation of various cytokines and chemokines. Mucosal epithelial cells also have the ability to

modulate the recruitment and activity of immune cells of both the innate and adaptive immune systems. By secreting antimicrobial factors, such as SLPI and human β-defensins, epithelial cells are able to eliminate potential pathogens [75]. By secreting chemokines such as interleukin-8 (IL-8), monocyte chemoattractant protein (MCP-1), and RANTES (regulated upon activation, normal, T-cell-expressed and secreted), epithelial cells are able to recruit immune cells to the sites of infection [76-78]. In addition, by secreting cytokines such as IL-6 and IL-1β epithelial cells are able to activate and regulate the inflammatory and immune responses of both the innate and adaptive immune systems [79, 80]. In view of all these functions of the epithelium, which are over and above the function of a simple physical barrier, we sought to study the innate role of the epithelium in the early HIV infection events. Particularly, we studied various epithelial cell models from the genital tract: the cell lines, the primary epithelial cells and the explant tissues.

B.3 MIP-3α:

MIP-3α was first discovered through bioinformatics in 1997 [90] after which it was studied widely for its association with dermatological and gastrointestinal diseases [91, 92]. From thence MIP-3α was studied in the FGT. Data from *Sun et al* demonstrated for the first time that cells of the FGT secrete MIP-3α [102]. Their findings revealed that an endometrial epithelial cell line (ECL), (HHUA1[9]), secreted MIP-3α both constitutively and on stimulation with the inflammatory mediators tumor necrosis factor alpha (TNF-α) and interleukin 1 beta (IL-1β). Subsequently,

[9] HHUA is an endometrial epithelial cell line shown to secrete MIP-3α on stimulation by TNF-α and IL-1β and not by LPS

Cremel *et al* showed that the vagina ECL (SiHa[10]) and primary epithelial cells of the vagina equally secreted MIP-3α and that this secretion was both constitutive and up regulated by the inflammatory mediator IL-1β [93]. Data from Wira *et al* subsequently showed that primary epithelial cells of the endometrium secrete MIP-3α constitutively and on exposure to pathogen associated molecular patterns (PAMPs) poly I:C, a TLR 3 agonist [85]. However, none of these or other groups studied the secretion of MIP-3α by the human cervix, in the form of either the ECL, primary epithelial cells or the cervical explant models. We therefore designed a study that primarily focused on the secretion of this molecule, MIP-3α, by the endocervical epithelial models. Furthermore, except for a study by Berlier *et al*, none of these groups studied the role of MIP-3α in HIV infection. In the context of heterosexual transmission, MIP-3α expression was shown to be significantly stimulated by seminal plasma in the SiHa cell line, regardless of whether the seminal plasma donor was HIV infected or uninfected [135]. We hence studied the stimulated pattern of MIP-3α secretion in endocervical epithelial cell and tissue models, stimulating with various HIV-1 preparations.

SECTION C: EXPERIMENTAL METHOD CONCEPTS

Studying mucosal immunity to HIV infection at the portal of entry being a relatively recent concept, techniques we have adopted in this thesis are novel:

C.1 Explant tissues:

Most studies into the pathogenesis of HIV using human tissue in the FGT have utitlised *in vitro* assays, employing the use of cell lines rather than explant tissues

[10] SiHa is a vaginal epithelial cell line shown to behave like primary vaginal cells with regards to epithelial cell differentiation and proliferative functions

(ET). The technique of culturing cells grown under controlled laboratory conditions was developed long before that of *ex vivo* ET and this was in the US by Ross Harrison [243, 244]. Later the method was significantly improved by Alexis Carrel [245]. On the other hand the first idea of a tissue matrix came out in the early 1950's with the study of a sponge matrix method for formation of cell aggregates in tissue culture [246]. This was subsequently adopted in the HIV field in the study of human tonsil by Glushakova *et al* [247]. More recently, the *ex vivo* ET studies were conducted for the first time in the cervicovaginal compartment in the context of HIV infection in the early 1990's [248]. ET models are a form of *ex vivo* culture models designed as a bridge between cell cultures and *in vivo* models. They comprise epithelium suspended on the rest of the mucosa (epithelium and lamina propria) and stroma. Cells in the lamina propria, and particularly the fibroblasts, have been shown to have paracrine effects that contribute to the functioning of the cells of the epithelium and hence studying epithelial cells in a model where they are embedded on the underlying stroma has added benefits to studying epithelial cells alone. Their greatest strength is that they do not disrupt the natural organisation of the tissues, and they preserve the interactions between the epithelial cells and the underlying stromal cells (Merbah et al., 2011). Although cell-based assays yield more reliable results in that they are reproducible and can be standardised with regards to uniformity in the numbers of cells studied, ET nevertheless remain a valuable method of study: they are more representative of *in vivo* conditions in that they allow for studies on morphology and function, as normal interactions of immune cells with each other and with the extracellular matrix in this tissue are preserved (Richardson-Harman et al., 2009). In this thesis, for biological reasons as elucidated, we therefore studied ET as one of the

epithelial models. More importantly, we are not aware of any study answering the questions on MIP-3α and its role in HIV infection using the ET model.

C.2 Primary epithelial cells:

For ethical reasons, most research questions into HIV acute infection events cannot be answered *in vivo* in humans and hence we made use of primary epithelial cellular models and ET models in this thesis, which were both prepared from hysterectomy samples. While explant tissues are more ideal to study as they are closest to *in vivo* situations as discussed above, primary cells are also an important model to study as the data they provide is complementary to that of ET. Following preparation and utilisation of epidermal suspensions from embryonic animal skin, Medawar *et a*l isolated epidermal cells from human skin using tryptic digestion in the 1940s [249]. Serial studies were subsequently conducted to refine methodology and optimise conditions using keratinocytes in various body sites [250-252]. Keratinocytes are pluripotent epithelial cells derived from the basal layers of the epithelial layer. In the context of MIP-3α keratinocytes were studied by various groups looking at the vaginal and endometrial sub-compartments [85, 93]. Advantages of using primary epithelial cell preparations include the following: (i) properties of epithelial cells can be studied in the absence of influence from the underlying basement membrane and cells of the lamina propria, thereby focusing purely on epithelial function, (ii) direct cell counts can be done, thus facilitating quantitative studies, and (iii) biological, metabolic, and malignant alterations resulting from prolonged sub-culture *in vitro* as seen with the use of immortalised cell lines are avoided by use of freshly obtained *ex vivo* cells [253]. In this thesis we hence used keratinocytes to confirm the epithelial source of MIP-3α in the endocervix while also quantifying levels of MIP-3α by the same cells. More

importantly, no group had previously studied the secretion of MIP-3α in the endocervical primary epithelial cells.

C.3 Transwell® inserts:

Epithelial cells have a structural polarised orientation with a distinct apical surface to the lumen and a basolateral surface to the basement membrane and underlying cells that is crucial to their functioning in the mucosal lumen. Each pole has a distinct protein and lipid composition as well as distinct receptors, ion transporters and channels, signal transduction proteins, and cytoskeletal proteins maintained by different intracellular trafficking. Hence epithelial cellular models were grown and studied with the aid of the Transwell® insert system in order to encourage polarisation in this thesis. The Transwell® insert system is a permeable support system in which a plastic insert that comprises a microporous membrane in the middle is inserted into each dome of the tissue culture plate in order to divide the dome into the apical and basal compartments. For epithelial cells, the use of permeable supports *in vitro* allows cells to be grown and studied in a polarised state under more natural conditions. Further, these permeable supports permit cells to uptake and secrete molecules on both their basal and apical surfaces and thereby carry out metabolic activities in a more natural fashion. Hence Transwell® inserts provide independent access to both sides of a monolayer, thus enhancing the ability to study transport, absorption, secretion, electrophysiological and other metabolic activities *in vitro*. Consequently, for our analyses, epithelial cellular models were grown on the microporous membrane of the apical compartment of the Transwell® insert system to encourage epithelial monolayer formation and its physiological function. Polarised epithelial cell culture systems exhibit many of the phenotypic and functional characteristics of columnar epithelium, which is

characteristic of the endometrium and endocervix. Because we wanted to establish the polarisation pattern of constitutive MIP-3α secretion, we accordingly studied primary epithelial cells in a polarised culture system. Further, because it has been shown that cells grown on plastic culture plates behave differently to those grown on membranes in a polarised system [254], we studied polarised cells.

C.4 Cervicovaginal fluid concentrate (CVF) versus cervicovaginal lavage (CVL):

One of the previous common practices in HIV biomedical prevention studies was to blindly collect and store CVL in order to run assays to address various scientific questions pertaining to the mucosal status in the FGT at a later date. This was regardless of what the assay for running these samples would be and what the scientific question that needed to be answered would be. As the field evolved, it became apparent that CVL was not always the most appropriate specimen for answering various scientific questions [255]. CVL is merely a representation of cervicovaginal secretions containing few desquamated cells presented in a dilute solution. Diluted samples are obtained by washing the vaginal tract in a cervicovaginal lavage. Samples can be diluted with normal saline or by phosphate-buffered saline [256]. Depending on volume of samples needed for testing, researchers have used 3, 5 and 10 mL lavages; however, each volume will result in different recovered volume depending on clinician technique and the amount of secretions already in the vaginal vault. Further, there is a large difference in how much of the infused lavage fluid is absorbed vaginally. Thus, the large variation in volume recovered will have an impact on the quantification of the biological marker, thus CVL has the intrinsic disadvantage of having to account for

differences in absorption of the infused sample making it more complicated to calculate a dilution factor. Another disadvantage with CVL is that the infused liquid dilutes the samples and assessments of certain cytokines may fall below the limit of detection. Hence for all these reasons work within the microbicide field has been ongoing to evaluate the collection of samples for soluble factor (e.g. cytokines) estimation that can be recovered undiluted [257]. More recently there has also been a drive to use devices that women can self-sample while also collecting undiluted fluid [258]. Hence, in accordance with this evolution in the field, we opted to use the Instead™ softcup, a menstrual cup, to collect undiluted samples of CVF in order to estimate the levels of MIP-3α and other cytokines in this sub-compartment. This method, which women self-inserted, is novel, having been used only rarely in this field.

C.5 Macaque alongside human studies:

Most of our recent understanding of the process of HIV mucosal transmission comes from animal models and *in vitro* studies. NHP models have been used extensively in HIV/AIDS research from as early as the 1980s when HIV was first discovered in human beings [213]. They have been used with huge success in understanding disease pathogenesis [214]. The SIV/Rhesus macaque model of HIV transmission has led to an increased understanding of the interactions between virus and host during the sexual transmission of HIV. The macaca genus is said to be closely related to humans, sharing a last common ancestor ~25 million years ago [221]. However, there are documented differences between humans and macaques with regards to immunogenetic and immunological attributes, and these have largely been studied in the context of responses to vaccines. Very limited research has been done in the area of innate immunity.

Biophysiologically, the macaques are said to have a microflora profile similar to the bacterial vaginosis profile in the female genital tract (FGT) of humans [222], they seem to have a more basic pH than is demonstrated in humans [223], have varying menstrual cycle dynamics with regards to length and regularity [224], have more keratinised FGT walls than humans [225] and demonstrate dramatic epithelial thickness fluctuations in response to hormones compared to what is seen in humans [226]. Consequently, innate responses in humans are not necessarily similar to those in macaques and as such, we need to be careful in inferring macaque-based research findings to human beings. Because of our awareness that there are differences between humans and macaques in the FGT with regards to innate immunity, yet there being limited research into the extent of these differences with regards to MIP-3α secretion and its role in early infection, we studied macaque tissues alongside human tissues in order to answer this question. This was particularly important as there has been a generalisation in the field about the role of MIP-3α in ealy HIV infection in humans, even though there is currently no evidence that humans respond to viral exposure in the same manner as macaques.

C.6 Viral preparations:

We conducted studies in this thesis using various viral preparations that are known to be particularly highly immunogenic for human samples and highly infectious for macaque samples.

- *Human studies*

We studied four HIV-1 preparations including soluble CN54gp140 trimeric protein,

CN54gp120 virus-like particles (VLPs), R5 tropic whole virus, HIV-1 strain BaL, and envelope-deleted HIV-1, NL4-3 deleted. The first two are pure envelope preparations. HIV-1 envelope preparations are considered the principal target for preventative vaccines and hence we studied envelope preparations that are highly immunogenic, trimeric gp140 and gp120 VLPs. Heterodimers of the transmembrane glycoprotein (gp41) and a surface glycoprotein (gp120) are used to generate trimeric envelope glycoproteins (Env) similar to those that are displayed on HIV virions. The development of soluble versions of trimeric Env, such as gp140, that display biochemical and structural properties similar to those observed on infectious viruses, is of considerable interest in the context of designing vaccines against HIV/AIDS. gp140 has been shown in different preclinical studies to be highly immunogenic [140], which may offer improvements over monomeric gp120. gp140 is considered to be particularly superior to the corresponding gp120 as an immunogen, with regards to inducing more potent and cross-reactive neutralising responses. In the context of mucosal studies, gp140 has been studied as a form of mucosal immunisation where it has been shown to induce local antibody responses [141-143]. We hence studied gp140 in the context of triggering innate epithelial responses in this thesis. We also prepared and studied gp120 in a highly immunogenic preparation as well, using VLPs. VLPs are formed from the assembly of envelope and/or capsid proteins from many viruses and hence because of their repetitive, high-density display of epitopes, they are often effective in eliciting strong immune responses [259]. In many cases such VLPs have structural characteristics and antigenicity similar to the parental virus. They have also been studied in the context of HIV preventive strategies. We hence used them in this thesis for their quality of being highly immunogenic.

- *Macaque studies*

We studied rhesus macaques and cynomolgus macaques. Besides the need for careful consideration in choosing the best suited macaque model for a specific research question at hand, choosing the virus stock to use deserves equal consideration as different macaque species are not equally susceptible to infection with the same virus stock, the same amount of virus/dose of infection, and the same route of infection. Most challenge experiments in macaques have been performed using either $SIV_{mac}251$, which is a swarm, or its pathogenic clone SIV_{mac} 239 derived through passaging from SIVmac251, or SIV_{sm} E660 [220]. SIVmac251, the first laboratory-discovered SIVmac strain, was identified when it accidentally infected a RM of Indian origin in the laboratory. It is typically highly pathogenic and therefore more representative of human HIV-1 infection. The vast majority of AIDS vaccine data generated in RM to date came from challenges using this pathogenic stock of SIVmac251. We hence used this highly pathogenic preparation of SIV for our studies, comparing its envelope preparations to its whole infectious preparation.

SECTION D: CONTEXT OF RESULTS AND THEMES THAT EMERGED FROM THIS THESIS

The work presented in this thesis has aimed to characterise baseline secretion patterns and FGT factors that influence the pattern of secretion of MIP-3α in the FGT, and particularly in the endocervix, and the impact that HIV/SIV exposure might have on MIP-3α secretion patterns in early infection. The principal findings of our research that have extended knowledge in the field were the following:

D.1 Compartmentalisation: MIP-3α levels are high in the endocervix:

The literature describes the concept of compartmentalisation in the FGT [260]. Compartmentalisation refers to the distinct structural and functional architecture of the different sub-compartments of the FGT, which are differentially influenced by hormones, thus in turn influencing the immune responses of the different sub-compartments of the FGT. The FGT is divided into the upper and lower parts with the upper genital tract comprising endocervix, uterus and fallopian tubes, while the lower part comprises the ectocervix and vagina. We hence evaluated secretory patterns of MIP-3α in the various sub-compartments of the FGT in order to compare and contrast secretion patterns in these various sub-compartments. Our results demonstrated that constitutive MIP-3α secretion is indeed compartmentalised in the FGT with its levels being highest in the endocervix compared with the other sub-compartments.

D.2 Polarisation: constitutive MIP-3α secretion is apically polarised in the endocervix:

Epithelial cells structurally comprise two poles, the apical and the basal, that are crucial to their functioning in the mucosal lumen. Each pole has a distinct protein and lipid composition as well as different receptors, ion transporters and channels, signal transduction proteins, and cytoskeletal proteins that are maintained by different intracellular trafficking [254]. Accordingly, chemokine secretion by epithelial cells occurs in either an apical or a basal polarised manner, thereby influencing gradient diffusion patterns and chemokine functions across body sites. MIP-3α secretion itself has been shown by others to be basally secreted in Caco-2 cells, the colorectal cell line [250, 251] while being apically polarised in SiHa cells, the vaginal cell line [93] and uterine primary epithelial cells [85]. Our data in

endocervical primary epithelial cells showed that MIP-3α constitutive secretion is apically polarised in the endocervix while it also confirmed that it is also apically polarised in the endometrial cell line. MIP-3α has been shown by others to be a kinocidin i.e. a chemokine that possesses antimicrobial functions as well. It particularly has been shown to possess anti-HIV-1 activity. Hence MIP-3α secretion being high in the endocervix while also being apically polarised in the same sub-compartment is significant. It might be responsible for the lack of response to HIV-1 preparations in the endocervix that our results demonstrated.

D.3 The FGT is a compartment characterised by high inflammation even in women at low risk for HIV infection:

We measured cytokines with various functions in the CVF of women uninfected with HIV infection and at low risk of HIV infection. Of the 24 SPs measured in these analyses, the chemokine class of cytokines were in the highest concentrations in both the FGT (CVF) and blood compartments. However, unlike in blood, pro-inflammatory cytokines were also present at high levels in CVF. Serum hardly had any pro-inflammatory cytokines amongst the top eight cytokines, unlike CVF, which had high levels of IL-1α, IL-1β and IL-6. This is perhaps not surprising in view of the fact that the FGT experiences frequent inflammatory insults due to prevalent and frequent reproductive tract challenges including infections, intravaginal insertions, and sexual intercourse. Menstruation itself has been described as an inflammatory event [172]. MIP-3α, a chemokine whose levels have previously been described as higher in inflamed sites, was amongst the SPs and AMPs in high concentrations in the endocervix in our study [103]. We concede therefore that the reason MIP-3α levels are high in the human

FGT, unlike in the macaque FGT, is because the human FGT is an inflammatory environment.

D.4 MIP-3α constitutive levels are amongst the levels of soluble proteins known to be in the highest concentrations in the FGT:

Before the advent of the study highlighting the significant role of MIP-3α in the context of HIV infection, the microbicide field delineated cytokines that were deemed important to study in the FGT in the context of inflammation as follows: IL-1α, IL-1β, IL-1-receptor antagonist, IL-6, IL-8, TNF-α and SLPI [169]. Of a total of 33 analytes in our study, MIP-3α levels were amongst the levels of 8 highest analytes including IL-1α, SLPI and IL-8 appearing in the list above. The findings of constitutive levels of MIP-3α being high in the FGT further substantiates the bullet point above that the FGT is a compartment characterised by high inflammation even in the absence of overt infection. Further, in the CVF of women with purulent, bloody or thick mucoid clumps, MIP-3α levels were significantly higher than in women without those abnormalities, thereby further confirming that MIP-3α is high in sites of inflammation and suggesting that inflammation may be the primary driver of MIP-3α levels.

D.5 Endogenous hormonal fluctuations during the menstrual cycle do not drive levels of MIP-3α in the FGT

The mucosal immune system of the FGT is under hormonal control that regulates the distribution of various cell populations, the levels of cytokines, the transport of immunoglobulins, and antigen presentation in the genital tissues during the various stages of the menstrual cycle [108]. Hence we investigated the influence

of endogenous hormonal fluctuations on the levels of MIP-3α and those of 23 other SPs in the CVF of women at low risk of HIV infection. While some cytokine levels (IL-1β, G-CSF, TGF-β and IFN-β) were significantly driven by hormonal changes, MIP-3α levels were not, thereby excluding hormonal changes as the primary driver of MIP-3α levels in the FGT.

D.6 MIP-3α secretion does not form part of initial responses to HIV-1 and SIV in the human and simian endocervices, respectively

Evidence exists that SIV and HIV-1 do interact with the epithelium within the first few hours of viral exposure. In studies *in vivo* of mucosal transmission of SIV in the FGT, MIP-3α secretion was shown to form part of the earliest epithelial response to SIV exposure [96]. SIV crosses the epithelial barrier within the first few hours of SIV exposure, thus providing evidence that SIV is able to interact with the epithelial barrier within the first few hours of deposition into the vaginal lumen [110]. The epithelium was triggered to increase its membrane permeability and to secrete some cytokines in the first few hours of viral exposure *in vitro*, thus providing further evidence of activation of innate function early in HIV infection [136, 137]. In this thesis, our data showed that MIP-3α could be secreted within 4 hours of microbial exposure, stimulating with Poly I:C, a TLR3 ligand. However, in our *ex vivo* studies using EPECs and EET, MIP-3α levels were not elevated on exposure to either SIV or HIV-1 in the endocervix in the first 24 hours post viral exposure, thus confirming that MIP-3α is not part of the initial viral responses in the endocervices of both humans and macaques. Elevation of MIP-3α levels following viral exposure in the Li *et al* study could be due to the presence of a stimulant of inflammation in the viral inoculum.

D.7 The human endocervix does not respond to stimulation by HIV-1 preparations

We investigated constitutive secretion patterns of 33 analytes including 25 SPs and 8 AMPs in the human EET model. We also investigated stimulated secretion patterns of the same analytes in the first 24 hours post stimulation stimulating with various HIV-1 preparations. Whereas the EET constitutively secreted varying levels of all 33 analytes studied, it however did not secrete any further analytes in response to stimulation with all HIV-1 preparations. Thus in this study, there was no evidence that HIV-1 triggers secretion of any analytes studied in the EET. Instead levels of AMPS, known to have anti-HIV-1 activity, were high which could contribute to the lack of response by the endocervix.

D.8 MIP-3α secretion is probably stimulated through TLR1/2 in human epithelial models, while it may also be stimulated through TLR3 and TLR5 in the human endocervix and endometrium

We had set out to test the hypothesis that the human endocervical epithelium secretes MIP-3α when the viral envelope interacts with its apical pole and to test the signalling pathway for MIP-3α secretion in epithelial cells following exposure to HIV-1 preparations. However, the latter part was negated when the first part of the hypothesis showed lack of response of the human endocervix to HIV-1 stimulation. Our results instead showed that MIP-3α levels are significantly elevated in response to stimulation with Pam_3CSK_4, a TLR1/2 ligand, in all epithelial cell models studied i.e. Caco-2 cells, HEC-1A cells and EPECs. Further, Poly I:C, a TLR3 ligand, and Flagellin, A TLR5 ligand, also triggered significant MIP-3α secretion in both HEC-1A cells and EPECs, thus suggesting that additionally in these epithelial models, MIP-3α secretion might be stimulated through TLR 3 and

TLR5. However, we did not perform further neutralisation assays (for instance) to confirm or refute this.

D.9 The macaque endocervix responds to SIV stimulation by secreting further IL-2 while IL-17 is down-regulated

We investigated constitutive secretion patterns of 11 analytes in the macaque EET model. Whereas the EET constitutively secreted varying levels of some analytes studied, only IL-2 was significantly up-regulated in response to whole infectious SIVmac251 in rhesus macaques while IL-17A was down-regulated in response to stimulation with SIVmac251 gp120 and SIVmac251 gp130 in both macaque species, thus confirming that SIV does interact with the epithelium early in SIV infection. However, responses are differential, depending on whether the virus is whole and infectious or not. IL-2 forms part of the T helper type 1 (Th1) response while IL-17A forms part of the T helper type 17 (Th17) response. The Th17 lineage constitutes a branch of the adaptive immune system which has a function in the clearance of specific types of pathogens that require a massive inflammatory response and are not adequately dealt with by Th1 or Th2 immunity [238]. The suppression of the Th17 response, hence reflecting reduced inflammation, would probably be the reason that MIP-3α levels were not high in these experiments.

SECTION E: LIMITATIONS AND FUTURE PERSPECTIVES

1. As already discussed, HIV incidence and prevalence are highest in sub-Saharan Africa where the prevalence and incidence of inflammatory sexually transmitted diseases are also high. Here we have recruited and studied

samples from women residing in the United Kingdom where the risk of HIV infection is low. Our results are therefore not generalisable to the sub-Saharan African population. It might hence be more appropriate to extend these studies to women at high risk of HIV infection, as pathogenic processes might differ between these two populations.

2. Inflammation was a recurring theme throughout this thesis, yet we did not conduct microbiological tests to confirm/refute presence of underlying infection as the cause of the inflammatory picture. We would need to collect appropriate samples, and process and store samples appropriately in order to incorporate microbiological studies in the future.
3. We have described MIP-3α secretion patterns in the FGT mostly in the first 24 hours post stimulation, as we were interested in the earliest responses. However, the founder virus has been shown to be established on Day 4 post inoculation in the SIV/Rhesus macaque model which has been taken to provide an opportunity to intervene to prevent SIV infection up to that point. It would hence be beneficial to extend these studies to look at MIP-3α secretion patterns up to Day 4 post stimulation.
4. We have established that MIP-3α levels are high in the FGT but we have not studied the precise role/s of the same in the FGT. MIP-3α has been shown in the literature to possess various functions. Specifically, it might add value to study anti-HIV-1 activity of MIP-3α in the endocervical secretions.

REFERENCES

1. University Emory, *Rhesus Macaque*, R. macaque, Editor. 2017: http://www.yerkes.emory.edu/animals/rhesus_macaque.html.

2. UNAIDS, *Global AIDS Update 2016*. 2016: http://www.unaids.org/sites/default/files/media_asset/global-AIDS-update-2016_en.pdf.

3. UNAIDS, *Get on the Fast-Track: the life-cycle approach to HIV*, in *UNAIDS 2016*. 2016: http://www.unaids.org/sites/default/files/media_asset/Get-on-the-Fast-Track_en.pdf.

4. WHO, *Global Health Observatory Data*, in *Global Health Observatory Data*, WHO, Editor. 2016, World Health Organisation: http://gamapserver.who.int/mapLibrary/app/searchResults.aspx.

5. Roser, M., *HIV/AIDS*, in *OurWorldInData.org*. 2016, OurWorldInData.org: https://ourworldindata.org/hiv-aids/.

6. Introini, A., et al., *An ex vivo model of HIV-1 infection in human lymphoid tissue and cervico-vaginal tissue.* Bio-protocol, 2014. **4**(4).

7. Johnston, M.I. and A.S. Fauci, *An HIV vaccine--challenges and prospects.* N Engl J Med, 2008. **359**(9): p. 888-90.

8. Matter, K. and M.S. Balda, *Signalling to and from tight junctions.* Nat Rev Mol Cell Biol, 2003. **4**(3): p. 225-36.

9. Nasu, K. and H. Narahara, *Pattern recognition via the toll-like receptor system in the human female genital tract.* Mediators Inflamm, 2010. **2010**: p. 976024.

10. Haase, A.T., *Targeting early infection to prevent HIV-1 mucosal transmission.* Nature, 2010. **464**(7286): p. 217-23.

11. Barré-Sinoussi, F., et al., *Isolation of a T-lymphotropic retrovirus from a patient at risk for acquired immune deficiency syndrome (AIDS).* Science, 1983. **220**(4599): p. 868-871.

12. Centers for Disease Control (CDC), *Task Force on Kaposi's Sarcoma and Opportunistic Infections. Epidemiologic aspects of the current outbreak of Kaposi's sarcoma and opportunistic infection.* N Engl J Med, 1982. **306**: p. 248-52.

13. Gao, F., et al., *Origin of HIV-1 in the chimpanzee Pan troglodytes troglodytes.* Nature, 1999. **397**(6718): p. 436-441.

14. Gao, F., et al., *Human infection by genetically diverse SIVSM-related HIV-2 in west Africa.* 1992.

15. Sharp, P.M., D.L. Robertson, and B.H. Hahn, *Cross-species transmission and recombination of'AIDS'viruses.* Philosophical Transactions of the Royal Society of London B: Biological Sciences, 1995. **349**(1327): p. 41-47.

16. Hirsch, V.M., et al., *An African primate lentivirus (SIVsmclosely related to HIV-2.* 1989.

17. Barin, F., et al., *Serological evidence for virus related to simian T-lymphotropic retrovirus III in residents of west Africa.* Lancet, 1985. **2**(8469-70): p. 1387-9.

18. Clavel, F., et al., *Isolation of a new human retrovirus from West African patients with AIDS.* Science, 1986. **233**(4761): p. 343-6.

19. Brennan, R. and D. Durack, *Gay compromise syndrome.* The Lancet, 1981. **318**(8259): p. 1338-1339.

20. Gottlieb, M.S., et al., *Pneumocystis carinii pneumonia and mucosal candidiasis in previously healthy homosexual men: evidence of a new acquired cellular immunodeficiency.* New England Journal of Medicine, 1981. **305**(24): p. 1425-1431.

21. Hymes, K., et al., *Kaposi's sarcoma in homosexual men—a report of eight cases.* The Lancet, 1981. **318**(8247): p. 598-600.

22. Hunt, R., *Humman Immunodeficinecy Virus and AIDS: types, sub-types and co-receptors*. Microbiology and Immunology On-line, ed. U.o.N.C.S.o. Medicine. 2016, http://www.microbiologybook.org/lecture/hiv6.htm.

23. Freed, E.O., *HIV-1 assembly, release and maturation.* Nat Rev Microbiol, 2015. **13**(8): p. 484-96.

24. Friedman-Kien, A., et al., *Kaposis sarcoma and Pneumocystis pneumonia among homosexual men--New York City and California.* MMWR. Morbidity and mortality weekly report, 1981. **30**(25): p. 305-8.

25. Centers for Disease Control (CDC), *Current trends update on Acquired Immune Deficiency Syndrome (AIDS)-United States.* Morbidity and mortality weekly report 1982. **31**(37): p. 507-508.

26. Francioli, P., et al., *[Acquired immunologic deficiency syndrome, opportunistic infections and homosexuality. Presentation of 3 cases studied in Switzerland].* Schweizerische medizinische Wochenschrift, 1982. **112**(47): p. 1682-1687.

27. Rozenbaum, W., et al., *Multiple opportunistic infection in a male homosexual in France.* The Lancet, 1982. **319**(8271): p. 572-573.

28. Vilaseca, J., et al., *Kaposi's sarcoma and Toxoplasma gondii brain abscess in a Spanish homosexual.* The Lancet, 1982. **319**(8271): p. 572.

29. Serwadda, D., et al., *Slim disease: a new disease in Uganda and its association with HTLV-III infection.* The Lancet, 1985. **326**(8460): p. 849-852.

30. Ehrenkranz, N., et al., *Pneumocystis carinii pneumonia among persons with hemophilia A.* MMWR. Morbidity and mortality weekly report, 1982. **31**(2): p. 365-7.

31. Masur, H., et al., *An outbreak of community-acquired Pneumocystis carinii pneumonia: initial manifestation of cellular immune dysfunction.* New England Journal of Medicine, 1981. **305**(24): p. 1431-1438.

32. Centers for Disease Control (CDC), *A cluster of Kaposi's sarcoma and Pneumocystis carinii pneumonia among homosexual male residents of Los*

Angeles and Orange Counties, California. MMWR. Morbidity and mortality weekly report, 1982. **31**(23): p. 305-307.

33. Centers for Disease Control (CDC), *Current trends Acquired Immunodeficiency Syndrome (AIDS) update--United States.* MMWR-Morbidity & Mortality Weekly Report, 1983. **32**(24): p. 309-311.

34. Centers for Disease Control (CDC), *Immunodeficiency among female sexual partners of males with acquired immune deficiency syndrome (AIDS)-New York.* MMWR. Morbidity and mortality weekly report, 1983. **31**(52): p. 697.

35. UNAIDS, *The Gap Report*. 2014: http://www.unaids.org/sites/default/files/media_asset/UNAIDS_Gap_report_en.pdf.

36. CDC, *Pneumocystis pneumonia---Los Angeles.* MMWR, 1981. **30**: p. 250-252.

37. Quinn, T.C. and J. Overbaugh, *HIV/AIDS in women: an expanding epidemic.* Science, 2005. **308**(5728): p. 1582-1583.

38. UNAIDS, *Report on the Global AIDS Epidemic*, in *UNAIDS 2004*. 2004: http://files.unaids.org/en/media/unaids/contentassets/documents/unaidspublication/2004/GAR2004_en.pdf.

39. Stein, Z.A., *HIV prevention: the need for methods women can use.* Am J Public Health, 1990. **80**(4): p. 460-2.

40. Shattock, R.J., et al., *Improving defences at the portal of HIV entry: mucosal and innate immunity.* PLoS Med, 2008. **5**(4): p. e81.

41. WHO, *WHO expands recommendation on oral pre- exposure prophylaxis of HIV infection*, in *Policy Brief*, WHO, Editor. 2015: http://apps.who.int/iris/bitstream/10665/197906/1/WHO_HIV_2015.48_eng.pdf?ua=1.

42. Thomson, K.A., et al., *Tenofovir-based oral preexposure prophylaxis prevents HIV infection among women.* Curr Opin HIV AIDS, 2016. **11**(1): p. 18-26.

43. Hope, T.J. and J.M. Marrazzo, *A Shot in the Arm for HIV Prevention? Recent Successes and Critical Thresholds.* AIDS Res Hum Retroviruses, 2015. **31**(11): p. 1055-9.

44. Haynes, B.F. and R.J. Shattock, *Critical issues in mucosal immunity for HIV-1 vaccine development.* J Allergy Clin Immunol, 2008. **122**(1): p. 3-9; quiz 10-1.

45. Hwang, L.Y., et al., *Higher levels of cervicovaginal inflammatory and regulatory cytokines and chemokines in healthy young women with immature cervical epithelium.* J Reprod Immunol, 2011. **88**(1): p. 66-71.

46. Shattock, R.J. and J.P. Moore, *Inhibiting sexual transmission of HIV-1 infection.* Nature Reviews Microbiology, 2003. **1**(1): p. 25-34.

47. Fahey, J.V., et al., *Estradiol selectively regulates innate immune function by polarized human uterine epithelial cells in culture.* Mucosal Immunol, 2008. **1**(4): p. 317-25.

48. Morrison, C.S., et al., *Hormonal contraception and the risk of HIV acquisition.* Aids, 2007. **21**(1): p. 85-95.

49. Fleming, D.T. and J.N. Wasserheit, *From epidemiological synergy to public health policy and practice: the contribution of other sexually transmitted diseases to sexual transmission of HIV infection.* Sexually transmitted infections, 1999. **75**(1): p. 3-17.

50. Wira, C.R., et al., *Innate and adaptive immunity in female genital tract: cellular responses and interactions.* Immunological reviews, 2005. **206**(1): p. 306-335.

51. Yeaman, G.R., et al., *Unique CD8+ T cell-rich lymphoid aggregates in human uterine endometrium.* J Leukoc Biol, 1997. **61**(4): p. 427-35.

52. Perry, L.L., et al., *Distinct homing pathways direct T lymphocytes to the genital and intestinal mucosae in Chlamydia-infected mice.* The Journal of Immunology, 1998. **160**(6): p. 2905-2914.

53. Mestecky, J., et al., *Mucosal immunology of the genital and gastrointestinal tracts and HIV-1 infection.* J Reprod Immunol, 2009. **83**(1-2): p. 196-200.

54. Mestecky, J., Z. Moldoveanu, and M.W. Russell, *Immunologic uniqueness of the genital tract: challenge for vaccine development.* Am J Reprod Immunol, 2005. **53**(5): p. 208-14.

55. Kutteh, W.H. and J. Mestecky, *Secretory immunity in the female reproductive tract.* Am J Reprod Immunol, 1994. **31**(1): p. 40-6.

56. Givan, A.L., et al., *Flow cytometric analysis of leukocytes in the human female reproductive tract: comparison of fallopian tube, uterus, cervix, and vagina.* American journal of reproductive immunology, 1997. **38**(5): p. 350-359.

57. Wira, C.R., M. Rodriguez-Garcia, and M.V. Patel, *The role of sex hormones in immune protection of the female reproductive tract.* Nat Rev Immunol, 2015. **15**(4): p. 217-30.

58. Pudney, J., A.J. Quayle, and D.J. Anderson, *Immunological microenvironments in the human vagina and cervix: mediators of cellular immunity are concentrated in the cervical transformation zone.* Biol Reprod, 2005. **73**(6): p. 1253-63.

59. Wira, C.R. and J.V. Fahey, *A new strategy to understand how HIV infects women: identification of a window of vulnerability during the menstrual cycle.* AIDS (London, England), 2008. **22**(15): p. 1909.

60. Vishwanathan, S.A., et al., *High susceptibility to repeated, low-dose, vaginal SHIV exposure late in the luteal phase of the menstrual cycle of pigtail macaques.* J Acquir Immune Defic Syndr, 2011. **57**(4): p. 261-4.

61. Saba, E., et al., *Productive HIV-1 infection of human cervical tissue ex vivo is associated with the secretory phase of the menstrual cycle.* Mucosal Immunol, 2013. **6**(6): p. 1081-90.

62. Kersh, E.N., et al., *SHIV susceptibility changes during the menstrual cycle of pigtail macaques.* Journal of medical primatology, 2014. **43**(5): p. 310-316.

63. Hladik, F. and M.J. McElrath, *Setting the stage: host invasion by HIV.* Nat Rev Immunol, 2008. **8**(6): p. 447-57.

64. Bomsel, M. and A. Alfsen, *Entry of viruses through the epithelial barrier: pathogenic trickery.* Nat Rev Mol Cell Biol, 2003. **4**(1): p. 57-68.

65. Hickey, D.K., et al., *Innate and adaptive immunity at mucosal surfaces of the female reproductive tract: stratification and integration of immune protection against the transmission of sexually transmitted infections.* Journal of reproductive immunology, 2011. **88**(2): p. 185-194.

66. Miller, C.J., et al., *Propagation and dissemination of infection after vaginal transmission of simian immunodeficiency virus.* J Virol, 2005. **79**(14): p. 9217-27.

67. Carias, A.M., et al., *Defining the interaction of HIV-1 with the mucosal barriers of the female reproductive tract.* J Virol, 2013. **87**(21): p. 11388-400.

68. Dezzutti, C.S., et al., *Cervical and prostate primary epithelial cells are not productively infected but sequester human immunodeficiency virus type 1.* J Infect Dis, 2001. **183**(8): p. 1204-13.

69. Bobardt, M.D., et al., *Cell-free human immunodeficiency virus type 1 transcytosis through primary genital epithelial cells.* J Virol, 2007. **81**(1): p. 395-405.

70. Herbst-Kralovetz, M.M., et al., *Quantification and comparison of toll-like receptor expression and responsiveness in primary and immortalized human female lower genital tract epithelia.* Am J Reprod Immunol, 2008. **59**(3): p. 212-24.

71. Wira, C.R., K.S. Grant-Tschudy, and M.A. Crane-Godreau, *Epithelial cells in the female reproductive tract: a central role as sentinels of immune protection.* Am J Reprod Immunol, 2005. **53**(2): p. 65-76.

72. Hein, M., et al., *Antimicrobial factors in the cervical mucus plug.* American journal of obstetrics and gynecology, 2002. **187**(1): p. 137-144.

73. Helmig, R., N. Uldbjerg, and K. Ohlsson, *Secretory leukocyte protease inhibitor in the cervical mucus and in the fetal membranes.* European Journal of Obstetrics & Gynecology and Reproductive Biology, 1995. **59**(1): p. 95-101.

74. Chimura, T., T. Hirayama, and M. Takase, *Lysozyme in cervical mucus of patients with chorioamnionitis.* Jpn J Antibiot, 1993. **46**(8): p. 726-9.

75. King, A.E., et al., *Differential expression of the natural antimicrobials, beta-defensins 3 and 4, in human endometrium.* Journal of reproductive immunology, 2003. **59**(1): p. 1-16.

76. Hornung, D., et al., *Immunolocalization and Regulation of the Chemokine RANTES in Human Endometrial and Endometriosis Tissues and Cells 1.* The Journal of Clinical Endocrinology & Metabolism, 1997. **82**(5): p. 1621-1628.

77. Arici, A., P.C. MacDonald, and M.L. Casey, *Regulation of monocyte chemotactic protein-1 gene expression in human endometrial cells in cultures.* Molecular and cellular endocrinology, 1995. **107**(2): p. 189-197.

78. Arici, A., et al., *Regulation of interleukin-8 gene expression in human endometrial cells in culture.* Molecular and cellular endocrinology, 1993. **94**(2): p. 195-204.

79. Simón, C., et al., *Interleukin-1 type I receptor messenger ribonucleic acid expression in human endometrium throughout the menstrual cycle.* Fertility and sterility, 1993. **59**(4): p. 791-796.

80. Laird, S., T. Li, and A. Bolton, *The production of placental protein 14 and interleukin 6 by human endometrial cells in culture.* Human Reproduction, 1993. **8**(6): p. 793-798.

81. Zlotnik, A. and O. Yoshie, *Chemokines: a new classification system and their role in immunity.* Immunity, 2000. **12**(2): p. 121-7.

82. Hieshima, K., et al., *Molecular cloning of a novel human CC chemokine liver and activation-regulated chemokine (LARC) expressed in liver. Chemotactic activity for lymphocytes and gene localization on chromosome 2.* J Biol Chem, 1997. **272**(9): p. 5846-53.

83. Hromas, R., et al., *Cloning and characterization of exodus, a novel beta-chemokine.* Blood, 1997. **89**(9): p. 3315-22.

84. Greaves, D.R., et al., *CCR6, a CC chemokine receptor that interacts with macrophage inflammatory protein 3α and is highly expressed in human dendritic cells.* The Journal of experimental medicine, 1997. **186**(6): p. 837-844.

85. Ghosh, M., et al., *CCL20/MIP3alpha is a novel anti-HIV-1 molecule of the human female reproductive tract.* Am J Reprod Immunol, 2009. **62**(1): p. 60-71.

86. Dieu, M.-C., et al., *Selective recruitment of immature and mature dendritic cells by distinct chemokines expressed in different anatomic sites.* The Journal of experimental medicine, 1998. **188**(2): p. 373-386.

87. Dieu-Nosjean, M.C., et al., *Regulation of dendritic cell trafficking: a process that involves the participation of selective chemokines.* Journal of Leukocyte Biology, 1999. **66**(2): p. 252-262.

88. Mantovani, A., *The chemokine system: redundancy for robust outputs.* Immunology today, 1999. **20**(6): p. 254-257.

89. Schutyser, E., et al., *Regulated production and molecular diversity of human liver and activation-regulated chemokine/macrophage inflammatory protein-3α from normal and transformed cells.* The Journal of Immunology, 2000. **165**(8): p. 4470-4477.

90. Rossi, D.L., et al., *Identification through bioinformatics of two new macrophage proinflammatory human chemokines: MIP-3alpha and MIP-3beta.* J Immunol, 1997. **158**(3): p. 1033-6.

91. Homey, B., et al., *Up-regulation of macrophage inflammatory protein-3α/CCL20 and CC chemokine receptor 6 in psoriasis.* The Journal of Immunology, 2000. **164**(12): p. 6621-6632.

92. Sierro, F., et al., *Flagellin stimulation of intestinal epithelial cells triggers CCL20-mediated migration of dendritic cells.* Proceedings of the National Academy of Sciences, 2001. **98**(24): p. 13722-13727.

93. Cremel, M., et al., *Characterization of CCL20 secretion by human epithelial vaginal cells: involvement in Langerhans cell precursor attraction.* J Leukoc Biol, 2005. **78**(1): p. 158-66.

94. Cremel, M., et al., *Female genital tract immunization: evaluation of candidate immunoadjuvants on epithelial cell secretion of CCL20 and dendritic/Langerhans cell maturation.* Vaccine, 2006. **24**(29): p. 5744-5754.

95. Sun, B., et al., *Expression of macrophage inflammatory protein-3α in an endometrial epithelial cell line, HHUA, and cultured human endometrial stromal cells.* Molecular human reproduction, 2002. **8**(10): p. 930-933.

96. Li, Q., et al., *Glycerol monolaurate prevents mucosal SIV transmission.* Nature, 2009.

97. Haase, A.T., et al., *Glycerol Monolaurate Microbicide Protection against Repeat High-Dose SIV Vaginal Challenge.* PLoS One, 2015. **10**(6): p. e0129465.

98. Kaushic, C., et al., *Primary human epithelial cell culture system for studying interactions between female upper genital tract and sexually transmitted viruses, HSV-2 and HIV-1.* Methods, 2011. **55**(2): p. 114-21.

99. Ma, J.M. and H.X. Yang, *Role of Toll-like receptor 4 and human defensin 5 in primary endocervical epithelial cells.* Chin Med J (Engl), 2010. **123**(13): p. 1762-7.

100. Radtke, A.L., A.J. Quayle, and M.M. Herbst-Kralovetz, *Microbial products alter the expression of membrane-associated mucin and antimicrobial peptides in a three-dimensional human endocervical epithelial cell model.* Biol Reprod, 2012. **87**(6): p. 132.

101. Ghosh, M., et al., *CCL20/MIP3α is a Novel Anti‐HIV‐1 Molecule of the Human Female Reproductive Tract.* American Journal of Reproductive Immunology, 2009. **62**(1): p. 60-71.

102. Sun, B., et al., *Expression of macrophage inflammatory protein-3alpha in an endometrial epithelial cell line, HHUA, and cultured human endometrial stromal cells.* Mol Hum Reprod, 2002. **8**(10): p. 930-3.

103. Dieu-Nosjean, M.-C., et al., *Regulation of dendritic cell trafficking: a process that involves the participation of selective chemokines.* Journal of leukocyte biology, 1999. **66**(2): p. 252-262.

104. Boomsma, C., et al., *Cytokine profiling in endometrial secretions: a non-invasive window on endometrial receptivity.* Reproductive biomedicine online, 2009. **18**(1): p. 85-94.

105. Wira, C.R., et al., *Innate immunity in the human female reproductive tract: endocrine regulation of endogenous antimicrobial protection against HIV and other sexually transmitted infections.* American journal of reproductive immunology, 2011. **65**(3): p. 196-211.

106. Fahey, J.V., et al., *Secretion of cytokines and chemokines by polarized human epithelial cells from the female reproductive tract.* Hum Reprod, 2005. **20**(6): p. 1439-46.

107. Kaushic, C., *HIV-1 infection in the female reproductive tract: role of interactions between HIV-1 and genital epithelial cells.* Am J Reprod Immunol, 2011. **65**(3): p. 253-60.

108. Wira, C.R., K.S. Grant-Tschudy, and M.A. Crane-Godreau, *Epithelial cells in the female reproductive tract: A central role as sentinels of immune protection.* American Journal of Reproductive Immunology, 2005. **53**(2): p. 65-76.

109. Asin, S.N., et al., *HIV type 1 infection in women: increased transcription of HIV type 1 in ectocervical tissue explants.* J Infect Dis, 2009. **200**(6): p. 965-72.

110. Haase, A.T., *Early events in sexual transmission of HIV and SIV and opportunities for interventions.* Annu Rev Med, 2011. **62**: p. 127-39.

111. Kumar, R., et al., *Compartmentalized secretory leukocyte protease inhibitor expression and hormone responses along the reproductive tract of postmenopausal women.* J Reprod Immunol, 2011. **92**(1-2): p. 88-96.

112. Zegels, G., et al., *Use of cervicovaginal fluid for the identification of biomarkers for pathologies of the female genital tract.* Proteome science, 2010. **8**(1): p. 1.

113. Shaw, J.L., C.R. Smith, and E.P. Diamandis, *Proteomic analysis of human cervico-vaginal fluid.* Journal of proteome research, 2007. **6**(7): p. 2859-2865.

114. Clark, L.R. and M. Atendido, *Group B streptococcal vaginitis in postpubertal adolescent girls.* Journal of adolescent health, 2005. **36**(5): p. 437-440.

115. Hirota, K., et al., *Preferential recruitment of CCR6-expressing Th17 cells to inflamed joints via CCL20 in rheumatoid arthritis and its animal model.* The Journal of experimental medicine, 2007. **204**(12): p. 2803-2812.

116. Kaser, A., et al., *Increased expression of CCL20 in human inflammatory bowel disease.* Journal of clinical immunology, 2004. **24**(1): p. 74-85.

117. Tanaka, Y., et al., *Selective expression of liver and activation-regulated chemokine (LARC) in intestinal epithelium in mice and humans.* European journal of immunology, 1999. **29**(2): p. 633-642.

118. Yang, D., et al., *Many chemokines including CCL20/MIP-3α display antimicrobial activity.* Journal of leukocyte biology, 2003. **74**(3): p. 448-455.

119. Baba, M., et al., *Identification of CCR6, the specific receptor for a novel lymphocyte-directed CC chemokine LARC.* Journal of Biological Chemistry, 1997. **272**(23): p. 14893-14898.

120. Power, C.A., et al., *Cloning and characterization of a specific receptor for the novel CC chemokine MIP-3alpha from lung dendritic cells.* J Exp Med, 1997. **186**(6): p. 825-35.

121. Izadpanah, A., et al., *Regulated MIP-3α/CCL20 production by human intestinal epithelium: mechanism for modulating mucosal immunity.* American Journal of Physiology-Gastrointestinal and Liver Physiology, 2001. **280**(4): p. G710-G719.

122. Shattock, R.J. and J.P. Moore, *Inhibiting sexual transmission of HIV-1 infection.* Nat Rev Microbiol, 2003. **1**(1): p. 25-34.

123. Kanneganti, T.D., M. Lamkanfi, and G. Nunez, *Intracellular NOD-like receptors in host defense and disease.* Immunity, 2007. **27**(4): p. 549-59.

124. Muir, A., et al., *Toll-like receptors in normal and cystic fibrosis airway epithelial cells.* American journal of respiratory cell and molecular biology, 2004. **30**(6): p. 777-783.

125. Melmed, G., et al., *Human intestinal epithelial cells are broadly unresponsive to Toll-like receptor 2-dependent bacterial ligands: implications for host-microbial interactions in the gut.* The Journal of Immunology, 2003. **170**(3): p. 1406-1415.

126. Smith, M.F., et al., *Toll-like receptor (TLR) 2 and TLR5, but not TLR4, are required for Helicobacter pylori-induced NF-κB activation and chemokine expression by epithelial cells.* Journal of Biological Chemistry, 2003. **278**(35): p. 32552-32560.

127. Schaefer, T.M., et al., *Innate immunity in the human female reproductive tract: antiviral response of uterine epithelial cells to the TLR3 agonist poly (I: C).* The Journal of Immunology, 2005. **174**(2): p. 992-1002.

128. Fichorova, R.N., et al., *Response to Neisseria gonorrhoeae by cervicovaginal epithelial cells occurs in the absence of toll-like receptor 4-mediated signaling.* J Immunol, 2002. **168**(5): p. 2424-32.

129. Miyake, K., *Endotoxin recognition molecules, Toll-like receptor 4-MD-2.* Semin Immunol, 2004. **16**(1): p. 11-6.

130. Smith, K.D., et al., *Toll-like receptor 5 recognizes a conserved site on flagellin required for protofilament formation and bacterial motility.* Nat Immunol, 2003. **4**(12): p. 1247-53.

131. Edelmann, K.H., et al., *Does Toll-like receptor 3 play a biological role in virus infections?* Virology, 2004. **322**(2): p. 231-8.

132. Jurk, M., et al., *Human TLR7 or TLR8 independently confer responsiveness to the antiviral compound R-848.* Nat Immunol, 2002. **3**(6): p. 499.

133. Hemmi, H., et al., *A Toll-like receptor recognizes bacterial DNA.* Nature, 2000. **408**(6813): p. 740-5.

134. Sun, B., et al., *Expression of macrophage inflammatory protein-3 α in an endometrial epithelial cell line , HHUA , and cultured human endometrial stromal cells.* Mol Hum Reprod, 2002. **8**(10): p. 930-933.

135. Berlier, W., et al., *Seminal plasma promotes the attraction of Langerhans cells via the secretion of CCL20 by vaginal epithelial cells: involvement in the sexual transmission of HIV.* Hum Reprod, 2006. **21**(5): p. 1135-42.

136. Nazli, A., et al., *Exposure to HIV-1 directly impairs mucosal epithelial barrier integrity allowing microbial translocation.* PLoS Pathog, 2010. **6**(4): p. e1000852.

137. Nazli, A., et al., *HIV-1 gp120 induces TLR2- and TLR4-mediated innate immune activation in human female genital epithelium.* J Immunol, 2013. **191**(8): p. 4246-58.

138. Rossi, D.L., et al., *Identification through bioinformatics of two new macrophage proinflammatory human chemokines: MIP-3alpha and MIP-3beta.* The Journal of Immunology, 1997. **158**(3): p. 1033-1036.

139. Zhu, J. and W.E. Paul, *Peripheral CD4+ T-cell differentiation regulated by networks of cytokines and transcription factors.* Immunol Rev, 2010. **238**(1): p. 247-62.

140. Katinger, D., et al., *CN54gp140: product characteristics, peclinical and clinical use-recombinant glycoprotein for HIV immunization.* Retrovirology, 2012. **9**(2): p. 1.

141. Donnelly, L., et al., *Intravaginal immunization using the recombinant HIV-1 clade-C trimeric envelope glycoprotein CN54gp140 formulated within lyophilized solid dosage forms.* Vaccine, 2011. **29**(27): p. 4512-20.

142. Mann, J.F., et al., *Mucosal application of gp140 encoding DNA polyplexes to different tissues results in altered immunological outcomes in mice.* PLoS One, 2013. **8**(6): p. e67412.

143. Arias, M.A., et al., *Glucopyranosyl Lipid Adjuvant (GLA), a Synthetic TLR4 agonist, promotes potent systemic and mucosal responses to intranasal immunization with HIVgp140.* PLoS One, 2012. **7**(7): p. e41144.

144. Rossio, J., et al., *Inactivation of human immunodeficiency virus type 1 infectivity with preservation of conformational and functional integrity of virion surface proteins.* Journal of virology, 1998. **72**(10): p. 7992-8001.

145. Sankapal, S., et al., *HIV exposure to epithelial cells in ectocervical and colon tissues induces inflammatory cytokines without tight junction disruption.* AIDS research and human retroviruses, 2016(ja).

146. Fontenot, D., et al., *TSLP production by epithelial cells exposed to immunodeficiency virus triggers DC-mediated mucosal infection of CD4+ T cells.* Proceedings of the National Academy of Sciences, 2009. **106**(39): p. 16776-16781.

147. Fazeli, A., C. Bruce, and D. Anumba, *Characterization of Toll-like receptors in the female reproductive tract in humans.* Human Reproduction, 2005. **20**(5): p. 1372-1378.

148. Cremel, M., et al., *Female genital tract immunization: evaluation of candidate immunoadjuvants on epithelial cell secretion of CCL20 and dendritic/Langerhans cell maturation.* Vaccine, 2006. **24**(29-30): p. 5744-54.

149. Abreu, M.T., et al., *TLR signaling at the intestinal epithelial interface.* Journal of endotoxin research, 2003. **9**(5): p. 322-330.

150. Nagai, Y., et al., *Essential role of MD-2 in LPS responsiveness and TLR4 distribution.* Nature immunology, 2002. **3**(7): p. 667-672.

151. McGettrick, A.F. and L.A. O'Neill, *Toll‐like receptors: key activators of leucocytes and regulator of haematopoiesis.* British journal of haematology, 2007. **139**(2): p. 185-193.

152. Wang, J., et al., *The functional effects of physical interactions among Toll-like receptors 7, 8, and 9.* Journal of Biological Chemistry, 2006. **281**(49): p. 37427-37434.

153. Blaskewicz, C.D., J. Pudney, and D.J. Anderson, *Structure and function of intercellular junctions in human cervical and vaginal mucosal epithelia.* Biology of reproduction, 2011. **85**(1): p. 97-104.

154. Miller, C.J., *Localization of Simian immunodeficiency virus-infected cells in the genital tract of male and female Rhesus macaques.* J Reprod Immunol, 1998. **41**(1-2): p. 331-9.

155. Miller, C.J., et al., *Mechanism of genital transmission of SIV: a hypothesis based on transmission studies and the location of SIV in the genital tract of chronically infected female rhesus macaques.* J Med Primatol, 1992. **21**(2-3): p. 64-8.

156. Gupta, P., et al., *Memory CD4(+) T cells are the earliest detectable human immunodeficiency virus type 1 (HIV-1)-infected cells in the female genital mucosal tissue during HIV-1 transmission in an organ culture system.* J Virol, 2002. **76**(19): p. 9868-76.

157. Saidi, H., et al., *R5- and X4-HIV-1 use differentially the endometrial epithelial cells HEC-1A to ensure their own spread: implication for mechanisms of sexual transmission.* Virology, 2007. **358**(1): p. 55-68.

158. Iqbal, S.M., et al., *Elevated elafin/trappin-2 in the female genital tract is associated with protection against HIV acquisition.* AIDS, 2009. **23**(13): p. 1669-77.

159. Drannik, A.G., et al., *Anti-HIV-1 activity of elafin depends on its nuclear localization and altered innate immune activation in female genital epithelial cells.* PLoS One, 2012. **7**(12): p. e52738.

160. Burgener, A., et al., *Identification of differentially expressed proteins in the cervical mucosa of HIV-1-resistant sex workers.* J Proteome Res, 2008. **7**(10): p. 4446-54.

161. Buckner, L.R., et al., *Innate immune mediator profiles and their regulation in a novel polarized immortalized epithelial cell model derived from human endocervix.* J Reprod Immunol, 2011. **92**(1-2): p. 8-20.

162. Quiñones-Mateu, M.E., et al., *Human epithelial β-defensins 2 and 3 inhibit HIV-1 replication.* Aids, 2003. **17**(16): p. F39-F48.

163. Moriuchi, M. and H. Moriuchi, *A milk protein lactoferrin enhances human T cell leukemia virus type I and suppresses HIV-1 infection.* The Journal of Immunology, 2001. **166**(6): p. 4231-4236.

164. McNeely, T.B., et al., *Inhibition of human immunodeficiency virus type 1 infectivity by secretory leukocyte protease inhibitor occurs prior to viral reverse transcription.* Blood, 1997. **90**(3): p. 1141-1149.

165. Fichorova, R.N., L.D. Tucker, and D.J. Anderson, *The molecular basis of nonoxynol-9-induced vaginal inflammation and its possible relevance to human immunodeficiency virus type 1 transmission.* J Infect Dis, 2001. **184**(4): p. 418-28.

166. Kyongo, J.K., et al., *Searching for lower female genital tract soluble and cellular biomarkers: defining levels and predictors in a cohort of healthy Caucasian women.* PLoS One, 2012. **7**(8): p. e43951.

167. Francis, S.C., et al., *Immune Activation in the Female Genital Tract: Expression Profiles of Soluble Proteins in Women at High Risk for HIV Infection.* PLoS One, 2016. **11**(1): p. e0143109.

168. Fichorova, R.N. and D.J. Anderson, *Differential expression of immunobiological mediators by immortalized human cervical and vaginal epithelial cells.* Biol Reprod, 1999. **60**(2): p. 508-14.

169. Fichorova, R.N., *Guiding the vaginal microbicide trials with biomarkers of inflammation.* J Acquir Immune Defic Syndr, 2004. **37 Suppl 3**: p. S184-93.

170. Dezzutti, C.S., et al., *Performance of swabs, lavage, and diluents to quantify biomarkers of female genital tract soluble mucosal mediators.* PLoS One, 2011. **6**(8): p. e23136.

171. Lieberman, J.A., et al., *Determination of cytokine protein levels in cervical mucus samples from young women by a multiplex immunoassay method and assessment of correlates.* Clin Vaccine Immunol, 2008. **15**(1): p. 49-54.

172. Evans, J. and L.A. Salamonsen, *Inflammation, leukocytes and menstruation.* Rev Endocr Metab Disord, 2012. **13**(4): p. 277-88.

173. Elstein, M., *Functions and physical properties of mucus in the female genital tract.* Br Med Bull, 1978. **34**(1): p. 83-8.

174. Boomsma, C.M., et al., *Cytokine profiling in endometrial secretions: a non-invasive window on endometrial receptivity.* Reprod Biomed Online, 2009. **18**(1): p. 85-94.

175. Kutteh, W.H., et al., *Variations in immunoglobulins and IgA subclasses of human uterine cervical secretions around the time of ovulation.* Clin Exp Immunol, 1996. **104**(3): p. 538-42.

176. Ferreira, V.H., J.K. Kafka, and C. Kaushic, *Influence of common mucosal co-factors on HIV infection in the female genital tract.* Am J Reprod Immunol, 2014. **71**(6): p. 543-54.

177. Aboud, L., et al., *The role of serpin and cystatin antiproteases in mucosal innate immunity and their defense against HIV.* Am J Reprod Immunol, 2014. **71**(1): p. 12-23.

178. Yarbrough, V.L., S. Winkle, and M.M. Herbst-Kralovetz, *Antimicrobial peptides in the female reproductive tract: a critical component of the mucosal immune barrier with physiological and clinical implications.* Hum Reprod Update, 2015. **21**(3): p. 353-77.

179. Yang, D., et al., *Many chemokines including CCL20/MIP-3alpha display antimicrobial activity.* J Leukoc Biol, 2003. **74**(3): p. 448-55.

180. Yeaman, M.R. and N.Y. Yount, *Unifying themes in host defence effector polypeptides.* Nat Rev Microbiol, 2007. **5**(9): p. 727-40.

181. Lentsch, A.B., et al., *Inhibition of NF-kappaB activation and augmentation of IkappaBbeta by secretory leukocyte protease inhibitor during lung inflammation.* Am J Pathol, 1999. **154**(1): p. 239-47.

182. Kell, P.D., et al., *HIV infection in a patient with Meyer-Rokitansky-Kuster-Hauser syndrome.* J R Soc Med, 1992. **85**(11): p. 706-7.

183. Ramjee, G., et al., *The diaphragm and lubricant gel for prevention of cervical sexually transmitted infections: results of a randomized controlled trial.* PLoS One, 2008. **3**(10): p. e3488.

184. Yeaman, G.R., et al., *Human immunodeficiency virus receptor and coreceptor expression on human uterine epithelial cells: regulation of expression during the menstrual cycle and implications for human immunodeficiency virus infection.* Immunology, 2003. **109**(1): p. 137-46.

185. Lü, F., et al., *The strength of B cell immunity in female rhesus macaques is controlled by CD8+ T cells under the influence of ovarian steroid hormones.* Clinical & Experimental Immunology, 2002. **128**(1): p. 10-20.

186. Lü, F.X., et al., *Immunoglobulin concentrations and antigen-specific antibody levels in cervicovaginal lavages of rhesus macaques are influenced by the stage of the menstrual cycle.* Infection and immunity, 1999. **67**(12): p. 6321-6328.

187. White, H.D., et al., *CD3+ CD8+ CTL activity within the human female reproductive tract: influence of stage of the menstrual cycle and menopause.* The Journal of Immunology, 1997. **158**(6): p. 3017-3027.

188. McNeely, T., et al., *Secretory leukocyte protease inhibitor: a human saliva protein exhibiting anti-human immunodeficiency virus 1 activity in vitro.* Journal of Clinical Investigation, 1995. **96**(1): p. 456.

189. Wira, C.R. and J.V. Fahey, *The innate immune system: gatekeeper to the female reproductive tract.* Immunology, 2004. **111**(1): p. 13-15.

190. Moriyama, A., et al., *Secretory leukocyte protease inhibitor (SLPI) concentrations in cervical mucus of women with normal menstrual cycle.* Mol Hum Reprod, 1999. **5**(7): p. 656-61.

191. Keller, M.J., et al., *PRO 2000 elicits a decline in genital tract immune mediators without compromising intrinsic antimicrobial activity.* AIDS, 2007. **21**(4): p. 467-76.

192. Drake, A.L., et al., *Incident HIV during pregnancy and postpartum and risk of mother-to-child HIV transmission: a systematic review and meta-analysis.* PLoS Med, 2014. **11**(2): p. e1001608.

193. Miller, L., et al., *Depomedroxyprogesterone-induced hypoestrogenism and changes in vaginal flora and epithelium.* Obstetrics & Gynecology, 2000. **96**(3): p. 431.

194. Ghanem, K.G., et al., *Influence of sex hormones, HIV status, and concomitant sexually transmitted infection on cervicovaginal inflammation.* 2005. **191**(3).

195. Marx, P.A., et al., *Progesterone implants enhance SIV vaginal transmission and early virus load.* Nature Medicine, 1996. **2**(10): p. 1084-1089.

196. Morrison, C.S., et al., *Hormonal contraception and HIV acquisition: reanalysis using marginal structural modeling.* AIDS, 2010. **24**(11): p. 1778-81.

197. Polis, C.B., et al., *Update on hormonal contraceptive methods and risk of HIV acquisition in women.* AIDS, 2016.

198. Smith, S.M., G.B. Baskin, and P.A. Marx, *Estrogen protects against vaginal transmission of simian immunodeficiency virus.* J Infect Dis, 2000. **182**(3): p. 708-15.

199. Molander, U., et al., *Effect of oral oestriol on vaginal flora and cytology and urogenital symptoms in the post-menopause.* Maturitas, 1990. **12**(2): p. 113-20.

200. Felding, C., et al., *Preoperative treatment with oestradiol in women scheduled for vaginal operation for genital prolapse. A randomised, double-blind trial.* Maturitas, 1992. **15**(3): p. 241-9.

201. Nilsson, K., B. Risberg, and G. Heimer, *The vaginal epithelium in the postmenopause--cytology, histology and pH as methods of assessment.* Maturitas, 1995. **21**(1): p. 51-6.

202. Castelo-Branco, C., et al., *Management of post-menopausal vaginal atrophy and atrophic vaginitis.* Maturitas, 2005. **52 Suppl 1**: p. S46-52.

203. Wira, C.R. and J.V. Fahey, *A new strategy to understand how HIV infects women: identification of a window of vulnerability during the menstrual cycle.* AIDS, 2008. **22**(15): p. 1909-17.

204. Patel, M.V., et al., *Innate Immunity in the Vagina (Part II): Anti‐HIV Activity and Antiviral Content of Human Vaginal Secretions.* American Journal of Reproductive Immunology, 2014. **72**(1): p. 22-33.

205. Morrison, C., et al., *Cervical inflammation and immunity associated with hormonal contraception, pregnancy, and HIV-1 seroconversion.* JAIDS Journal of Acquired Immune Deficiency Syndromes, 2014. **66**(2): p. 109-117.

206. Buckner, L.R., et al., *Innate immune mediator profiles and their regulation in a novel polarized immortalized epithelial cell model derived from human endocervix.* Journal of reproductive immunology, 2011. **92**(1): p. 8-20.

207. Kayisli, U.A., N.G. Mahutte, and A. Arici, *Uterine chemokines in reproductive physiology and pathology.* Am J Reprod Immunol, 2002. **47**(4): p. 213-21.

208. Smith, J.M., et al., *Human fallopian tube neutrophils–a distinct phenotype from blood neutrophils.* American Journal of Reproductive Immunology, 2006. **56**(4): p. 218-229.

209. Sentman, C.L., et al., *Recruitment of uterine NK cells: induction of CXC chemokine ligands 10 and 11 in human endometrium by estradiol and progesterone.* The Journal of Immunology, 2004. **173**(11): p. 6760-6766.

210. Patton, D.L., et al., *Epithelial cell layer thickness and immune cell populations in the normal human vagina at different stages of the menstrual cycle.* American journal of obstetrics and gynecology, 2000. **183**(4): p. 967-973.

211. Mlisana, K., et al., *Symptomatic vaginal discharge is a poor predictor of sexually transmitted infections and genital tract inflammation in high-risk women in South Africa.* J Infect Dis, 2012. **206**(1): p. 6-14.

212. Taylor, B.D., T. Darville, and C.L. Haggerty, *Does bacterial vaginosis cause pelvic inflammatory disease?* Sex Transm Dis, 2013. **40**(2): p. 117-22.

213. Heeney, J.L., *Primate models for AIDS vaccine development.* AIDS, 1996. **10 Suppl A**: p. S115-22.

214. ten Haaft, P., et al., *Comparison of early plasma RNA loads in different macaque species and the impact of different routes of exposure on SIV/SHIV infection.* J Med Primatol, 2001. **30**(4): p. 207-14.

215. Pereira, L.E., *Simian-Human Immunodeficiency Viruses and Their Impact on Non-Human Primate Models for AIDS*. 2012.

216. McNicholl, J.M., et al., *Non-human primate models of hormonal contraception and HIV.* Am J Reprod Immunol, 2014. **71**(6): p. 513-22.

217. Baroncelli, S., et al., *Macaca mulatta, fascicularis and nemestrina in AIDS vaccine development.* Expert Rev Vaccines, 2008. **7**(9): p. 1419-34.

218. Murphey-Corb, M., et al., *Isolation of an HTLV-III-related retrovirus from macaques with simian AIDS and its possible origin in asymptomatic mangabeys.* Nature, 1986. **321**(6068): p. 435-7.

219. Lifson, J.D. and N.L. Haigwood, *Lessons in nonhuman primate models for AIDS vaccine research: from minefields to milestones.* Cold Spring Harb Perspect Med, 2012. **2**(6): p. a007310.

220. Antony, J.M. and K.S. MacDonald, *A critical analysis of the cynomolgus macaque, Macaca fascicularis, as a model to test HIV-1/SIV vaccine efficacy.* Vaccine, 2015. **33**(27): p. 3073-83.

221. Yan, G., et al., *Genome sequencing and comparison of two nonhuman primate animal models, the cynomolgus and Chinese rhesus macaques.* Nat Biotechnol, 2011. **29**(11): p. 1019-23.

222. Spear, G.T., et al., *Identification of rhesus macaque genital microbiota by 16S pyrosequencing shows similarities to human bacterial vaginosis: implications for use as an animal model for HIV vaginal infection.* AIDS research and human retroviruses, 2010. **26**(2): p. 193-200.

223. Hanna, N., et al., *The relation between vaginal pH and the microbiological status in vaginitis.* BJOG: An International Journal of Obstetrics & Gynaecology, 1985. **92**(12): p. 1267-1271.

224. Riesen, J., R. Meyer, and R. Wolf, *The effect of season on occurrence of ovulation in the rhesus monkey.* Biology of reproduction, 1971. **5**(2): p. 111-114.

225. Poonia, B., et al., *Cyclic changes in the vaginal epithelium of normal rhesus macaques.* Journal of endocrinology, 2006. **190**(3): p. 829-835.

226. Hadzic, S.V., et al., *Comparison of the vaginal environment of Macaca mulatta and Macaca nemestrina throughout the menstrual cycle.* Am J Reprod Immunol, 2014. **71**(4): p. 322-9.

227. Pegu, A., J.L. Flynn, and T.A. Reinhart, *Afferent and efferent interfaces of lymph nodes are distinguished by expression of lymphatic endothelial markers and chemokines.* Lymphatic research and biology, 2007. **5**(2): p. 91-104.

228. Choi, Y.K., et al., *Simian immunodeficiency virus dramatically alters expression of homeostatic chemokines and dendritic cell markers during infection in vivo.* Blood, 2003. **101**(5): p. 1684-91.

229. Qin, S., et al., *Simian immunodeficiency virus infection alters chemokine networks in lung tissues of cynomolgus macaques: association with Pneumocystis carinii infection.* The American journal of pathology, 2010. **177**(3): p. 1274-1285.

230. Shang, L., et al., *Epithelium-innate immune cell axis in mucosal responses to SIV.* Mucosal Immunol, 2016.

231. Broliden, K., et al., *Functional HIV-1 specific IgA antibodies in HIV-1 exposed, persistently IgG seronegative female sex workers.* Immunol Lett, 2001. **79**(1-2): p. 29-36.

232. Arnold, K.B., et al., *Increased levels of inflammatory cytokines in the female reproductive tract are associated with altered expression of proteases, mucosal barrier proteins, and an influx of HIV-susceptible target cells.* Mucosal Immunol, 2016. **9**(1): p. 194-205.

233. Masson, L., et al., *Genital inflammation and the risk of HIV acquisition in women.* Clin Infect Dis, 2015. **61**(2): p. 260-9.

234. Gu, C., L. Wu, and X. Li, *IL-17 family: cytokines, receptors and signaling.* Cytokine, 2013. **64**(2): p. 477-85.

235. Zhang, Z., *Sexual Transmission and Propagation of SIV and HIV in Resting and Activated CD4+ T Cells.* Science, 1999. **286**(5443): p. 1353-1357.

236. Bachmann, M.F. and A. Oxenius, *Interleukin 2: from immunostimulation to immunoregulation and back again.* EMBO Rep, 2007. **8**(12): p. 1142-8.

237. Ley, K., E. Smith, and M.A. Stark, *IL-17A-producing neutrophil-regulatory Tn lymphocytes.* Immunol Res, 2006. **34**(3): p. 229-42.

238. Korn, T., et al., *IL-17 and Th17 Cells.* Annual review of immunology, 2009. **27**: p. 485-517.

239. Spellberg, B. and J.E. Edwards, Jr., *Type 1/Type 2 immunity in infectious diseases.* Clin Infect Dis, 2001. **32**(1): p. 76-102.

240. Merbah, M., et al., *Cervico-vaginal tissue ex vivo as a model to study early events in HIV-1 infection.* Am J Reprod Immunol, 2011. **65**(3): p. 268-78.

241. Pope, M. and A.T. Haase, *Transmission, acute HIV-1 infection and the quest for strategies to prevent infection.* Nat Med, 2003. **9**(7): p. 847-52.

242. Lehner, T., *Innate and adaptive mucosal immunity in protection against HIV infection.* Vaccine, 2003. **21**: p. S68-S76.

243. Harrison, R.G., *The outgrowth of the nerve fiber as a mode of protoplasmic movement.* Journal of Experimental Zoology, 1910. **9**(4): p. 787-846.

244. Harrison, R.G., et al., *Observations of the living developing nerve fiber.* The Anatomical Record, 1907. **1**(5): p. 116-128.

245. Carrel, A., *On the permanent life of tissues outside of the organism.* The Journal of experimental medicine, 1912. **15**(5): p. 516-528.

246. Leighton, J., *A sponge matrix method for tissue culture. Formation of organized aggregates of cells in vitro.* Journal of the National Cancer Institute, 1951. **12**(3): p. 545-561.

247. Glushakova, S., et al., *Infection of human tonsil histocultures: a model for HIV pathogenesis.* Nature medicine, 1995. **1**(12): p. 1320-1322.

248. Palacio, J., et al., *In vitro HIV1 infection of human cervical tissue.* Research in virology, 1994. **145**: p. 155-161.

249. Medawar, P., *Sheets of pure epidermal epithelium from human skin.* Nature, 1941. **148**(Dec 27): p. 783.

250. Wheeler, C.E., C.M. Canby, and E.P. Cawley, *Long-term tissue culture of epithelial-like cells from human skin.* J Invest Dermatol, 1957. **29**(5): p. 383-91; discussion 391-2.

251. Perry, V.P., et al., *Long-term tissue culture of human skin.* Am J Hyg, 1956. **63**(1): p. 52-8.

252. Furukawa, F., et al., *Characterization and practical benefits of keratinocytes cultured in strontium-containing serum-free medium.* Journal of Investigative Dermatology, 1988. **90**(5): p. 690-696.

253. Briggaman, R.A., et al., *Preparation and characterization of a viable suspension of postembryonic human epidermal cells.* J Invest Dermatol, 1967. **48**(2): p. 159-68.

254. Wyrick, P., *Polarized epithelial cell culture for Chlamydia trachomatis.* Wymondham, Norfolk, UK: Horizon Bioscience, 2006.

255. Sibeko, S. and S. Makvandi-Nejad, *From the laboratory to clinical trials and back again: lessons learned from HIV prevention trials.* Am J Reprod Immunol, 2013. **69 Suppl 1**: p. 106-15.

256. Jespers, V., et al., *Methodological issues in sampling the local immune system of the female genital tract in the context of HIV prevention trials.* Am J Reprod Immunol, 2011. **65**(3): p. 368-76.

257. Jespers, V., et al., *Assessment of mucosal immunity to HIV-1.* Expert Rev Vaccines, 2010. **9**(4): p. 381-94.

258. Boskey, E.R., et al., *A self-sampling method to obtain large volumes of undiluted cervicovaginal secretions.* Sexually transmitted diseases, 2003. **30**(2): p. 107-109.

259. Grgacic, E.V. and D.A. Anderson, *Virus-like particles: passport to immune recognition.* Methods, 2006. **40**(1): p. 60-5.

260. Kumar, R., et al., *Compartmentalized secretory leukocyte protease inhibitor expression and hormone responses along the reproductive tract of postmenopausal women.* Journal of reproductive immunology, 2011. **92**(1): p. 88-96.